

**Joint Investigation Report**

**On the Attack  
Against ROK Ship  
Cheonan**

## Joint Investigation Report



# On the Attack Against ROK Ship Cheonan



Ministry of National Defense  
Republic of Korea

## Preface

On March 26, 2010, an unprecedented incident in which ROKS Cheonan was sunk by a surprise torpedo attack by a North Korean submarine occurred, resulting in the death of 46 crew members.

The Ministry of National Defense organized the Civilian-Military Joint Investigation Group on March 31 in order to clearly identify the cause of the sinking as well as the entity responsible for the incident. The Civilian-Military Joint Investigation Group proceeded with the investigation with the participation of civilian and foreign experts to ensure objectivity and credibility.

The Civilian-Military Joint Investigation Group conducted its investigation while the whole group was lodging near the incident site in the West Sea facing unfavorable conditions such as harsh climates and currents. Despite these difficulties, its objective and scientific investigation found that ROKS Cheonan was sunk due to a torpedo launched by a North Korean midget submarine. The final investigation results were announced on May 20.

The Civilian-Military Joint Investigation Group reported the investigation results to the UN Security Council on June 14. As a result, UN Security Council Presidential Statement that acknowledges and condemns North Korea's culpability in the incident was unanimously adopted.

Nonetheless, North Korea continues to deny the facts and has heightened its threats of military provocations, claiming that the Republic of Korea fabricated the investigation results. Even within the Republic of Korea, the reality is that there are individuals who raise doubts against the investigation results based on their own interests, and they are taking irresponsible actions such as spreading groundless assertions.

Thus, the Ministry of National Defense has published the *Joint Investigation Report on the Attack Against ROK Ship Cheonan*, which contains the findings of the Civilian-Military Joint Investigation Group and the evidence data in both Korean and English in order to inform Koreans and the international community of the truth, and to resolve unnecessary misunderstandings and suspicions.

The report presents the overview, analysis on possible causes of the sinking, detailed

analysis results by team, conclusion, and appendix in order. Detailed contents of the analysis and assessment result are in appendix. The Civilian-Military Joint Investigation Group took into consideration every single possible cause of sinking in order to eliminate any preconception that may exist in finding the actual cause of the sinking. The report encompasses the whole process of the joint investigation and utilizes more than 300 pictures and diagrams to facilitate the readers' understanding.

In particular, a total of 73 experts from 4 different nations, 12 domestic civilian institutions, and military personnel actively participated in investigations on various fields such as scientific investigation, ship structure, explosives, and intelligence analysis. The experts also participated extensively in writing of the report. Every participant and expert concurred with the content, indicating that the report is internationally verified.

This is one of the world's first reports on an investigation of a salvaged hull of a warship that was sunk by a torpedo. The finding of the propulsion motor of a torpedo (the smoking gun) and the detection of explosive components illustrated to the North and the international community that even the most covert of attacks will leave evidence behind. Most importantly, all this entails a solemn warning to the North not to engage in further military provocations.

This report is a pledge that the Republic of Korea will reflect upon this incident and not let the North exercise further military provocations. We are confident that it will contribute to the understanding that the security awareness of the people of the Republic of Korea and the security issues that we face cannot be compromised by any personal and group interests.

Please understand that this report is subject to limitations in release of confidential military information, and since the report focused on the task of demonstrating the findings in a scientific and objective manner, the expression of certain information by using technical terminologies was unavoidable.

It is our sincere hope that *Joint Investigation Report on the Attack Against ROK Ship Cheonan* delivers the truth, and provides grounds to solve the misunderstandings and doubts raised thus far, becoming useful information to interested civilians, domestic and foreign scholars, as well as the press media.

September 2010

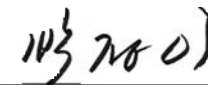
Civilian-Military Joint Investigation Group

다국적 민·군 합동조사단은 2010년 3월 26일 21:22경 대한민국 백령도 근해에서 발생한 천안함 피격사건의 원인을 조사하였다. 아래 서명자들은 조사에 참여한 각국 조사팀의 대표로서 이 보고서의 내용에 동의하며 아래와 같이 서명하다.

The multinational Civilian-Military Joint Investigation Group examined the cause of the attack against Republic of Korea Ship Cheonan occurred in vicinity of Baekryong Island at 2122, March 26, 2010. The undersigned are the chief representatives of each investigation team, concurring with the contents in this report.



공동단장 박사 윤덕용  
Co-Chairman Dr. Yoon, Duk-Yong



공동단장 육군대장 박정이  
Co-Chairman ROK Army GEN Park, Jung-I

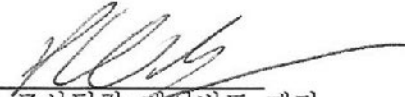


미국 조사팀장 해군소장(진) 토마스 에클스  
US Investigation Team Leader RADM(S) Thomas J. Eccles, USN

*As Senior US Representative to the Republic of Korea Joint Investigation Group, I concur with the finding and conclusions of this report.*



호주 조사팀장 해군중령 안토니 파월  
Australian/Investigation Team Leader CDR Anthony R. Powell, RAN  
*As Senior Australian Representative to the Republic of Korea Joint Investigation Group, I concur  
with the finding and conclusions of this report.*



영국 조사팀장 데이비드 맨리

UK Investigation Team Leader Mr. David W. Manley, RCNC

*As the Senior British Representative to the Republic of Korea Joint Investigation Group, I concur with the findings and conclusions of this report.*



스웨덴 조사팀장 에그니 위드홀름

Swedish Investigation Team Leader Mr. Agne Widholm

*As Senior Swedish Representative in support of the Republic of Korea Joint Investigation Group, I concur with the finding and conclusions of this report relevant to the Swedish team's participation.*

## Index

Preface	4
Summary	26
Part I. Overview	34
1. Situation Overview	36
2. Situation Development	37
3. Investigation Activities	41
4. Overall Shape and Structures of ROKS Cheonan	50
Part II. Analysis on Possible Causes of the Sinking	52
1. Non-explosion	54
2. Internal Explosion	65
3. External Explosion	79
Part III. Detailed Analysis Results by Team	104
1. Shape and Trace Analysis	106
2. Evidence Analysis	113
3. Testimony Analysis	132
4. Results of Postmortem and Surviving Patient Examinations	142
5. Explosion Type Analysis	146
6. Analysis on Shock Response to Underwater Explosion	155
7. Analysis on Sea Area of the Incident	191
8. Propulsion Motor System of Torpedo	206
Part IV. Conclusion	218
Appendix I. CCTV Recovery and Analysis Result	226
II. Underwater Explosion Phenomenon	230
III. Analysis Result on Direction and Location of the Explosion	245
IV. Analysis Result on Charge Size and Depth	254
V. Analysis Result on Adhered Materials	261
VI. Stability Analysis Result	289
VII. Basic Hull Strength Analysis Result	306

## Table Index

〈Table I-3-1〉	CCTV The organizational structure of the Joint Investigation Group(JIG)	41
〈Table II-1-1〉	Ultrasonic test results on the hull(April 30, 2010)	64
〈Table II-2-1〉	Analysis result on the possibility of diesel engine explosion	71
〈Table II-2-2〉	Diesel engine operation & maintenance records	72
〈Table II-2-3〉	Diesel engine maintenance records for past 3 years	72
〈Table II-2-4〉	Cause of damage to gas turbine & characteristics	75
〈Table II-2-5〉	Analysis on possibility of gas turbine explosion	76
〈Table II-2-6〉	Gas turbine maintenance records for past 3 years	76
〈Table II-3-1〉	Detection method and characteristics of torpedoes	90
〈Table II-3-2〉	Types and operating mechanisms of fuses	91
〈Table III-2-1〉	Evidence status	122
〈Table III-2-2〉	Examination status	122
〈Table III-2-3〉	Status of the evidence collection, recovery and examination by stages	123
〈Table III-2-4〉	Explosive composition analysis procedure	124
〈Table III-2-5〉	Molecular structure of the explosives	127
〈Table III-2-6〉	Explosive components of major marine weapons	127
〈Table III-2-7〉	Explosive component by friendly ammunition types	128
〈Table III-4-1〉	Patients status	143
〈Table III-4-2〉	Results of postmortem examination and X-ray on 36 bodies	144
〈Table III-6-1〉	Main specifications of ROKS Cheonan	157
〈Table III-6-2〉	Natural frequency analysis in a fully-loaded condition	160
〈Table III-6-3〉	Ultimate bending moment, for each frame	163
〈Table III-7-1〉	All available charts for waters near Baekryong Island	193
〈Table III-7-2〉	Objects found in the sinking site by Navy Search and Rescue Group	194
〈Table III-7-3〉	Objects found in the sinking site by the KORDI	195
〈Table III-8-1〉	Recovery and collection status applying special net	209
〈Table III-8-2〉	Recovery operation status applying special net	211
〈Table Appendix I-3-1〉	CCTV recovered contents	228
〈Table Appendix II-1-1〉	Energy partition of a bulk warhead fired underwater	231
〈Table Appendix II-1-2〉	Shockwave constants for various explosives	233
〈Table Appendix II-1-3〉	Conversion factors between shockwave and bubble	233
〈Table Appendix II-1-4〉	Bubble constants for selected explosives	235
〈Table Appendix IV-2-1〉	Simulation conditions(3m to port)	257
〈Table Appendix IV-2-2〉	Comparison of shockwave pressure	257
〈Table Appendix IV-4-1〉	Summary of simulation results	260
〈Table Appendix V-2-1〉	Sampling locations	263
〈Table Appendix V-2-2〉	CHNS elemental analysis results	266
〈Table Appendix V-2-3〉	Composition of the adhered material	269
〈Table Appendix V-3-1〉	Sampling locations	269
〈Table Appendix V-3-2〉	CHNS elemental analysis results	272
〈Table Appendix V-3-3〉	Composition of the adhered material (bow and stack)	273

〈Table Appendix V-4-1〉	Sampling locations	274
〈Table Appendix V-4-2〉	Composition of the adhered material (propulsion section and motor)	277
〈Table Appendix V-6-1〉	Change of O/Al composition ratio in EDS analysis with different heat treatment	283
〈Table Appendix VI-3-1〉	Static stability analysis result of ROKS Cheonan before the damage	292
〈Table Appendix VI-3-2〉	Dynamic stability analysis result prior to the damage	293
〈Table Appendix VI-4-1〉	Damage stability standards in different types of ships	294
〈Table Appendix VI-4-2〉	Stability analysis results of Case 1	296
〈Table Appendix VI-4-3〉	Stability analysis results of Case 2	297
〈Table Appendix VI-4-4〉	Stability analysis results of Case 3	298
〈Table Appendix VI-4-5〉	Stability analysis results of Case 4	299
〈Table Appendix VI-4-6〉	Stability analysis results of Case 5	300
〈Table Appendix VI-4-7〉	Stability analysis results of Case 6	300
〈Table Appendix VI-5-1〉	Initial stabilities of the bow and stern after the separation	301
〈Table Appendix VII-3-1〉	Design wave estimation results of ROKS Cheonan to conduct the direct strength analysis	308
〈Table Appendix VII-4-1〉	Allowable stress of main hull structure	309
〈Table Appendix VII-4-2〉	Allowable strength of superstructure	309
〈Table Appendix VII-4-3〉	Stress evaluation of each structural member	311

## Figure Index

〈Figure Summary-1〉	3D laser scan image of the fractured bow and stern	29
〈Figure Summary-2〉	Traces of shockwave and bubble effect	29
〈Figure Summary-3〉	Schematic of torpedo and recovered rear section of torpedo	31
〈Figure Summary-4〉	Rear section of torpedo	31
〈Figure Summary-5〉	Marking on North Korean test torpedo	31
〈Figure Summary-6〉	Anticipated infiltration route of North Korean midget submarine	33
〈Figure Summary-7〉	CHT-02D torpedo manufactured by North Korea	33
〈Figure I-1-1〉	The location of ROKS Cheonan incident	36
〈Figure I-4-1〉	Overall shape and structures of ROKS Cheonan	51
〈Figure II-1-1〉	The sonar dome at the time of bow salvage	55
〈Figure II-1-2〉	ROKS Cheonan propellers upon the recovery of the stern	56
〈Figure II-1-3〉	Dishing on the shell plating panels on the bottom of the hull	56
〈Figure II-1-4〉	3D laser scanning images on breakplanes of bow and stern	57
〈Figure II-1-5〉	Shell plates of ROKS Cheonan gas turbine room	57
〈Figure II-1-6〉	Analysis result on the damage characteristics of the fractured surface seen on ROKS Cheonan	58
〈Figure II-1-7〉	The deformation of starboard propellers	58
〈Figure II-1-8〉	Probing result of seafloor geography in incident site	59
〈Figure II-1-9〉	Fractured areas of ROKS Cheonan	61

〈Figure II-1-10〉	Breakplane of the bow and stern	63	〈Figure III-2-1〉	Soil with explosive substance near the explosion point and the collected location	113
〈Figure II-2-1〉	Shape of damage on ROKS Cheonan	65	〈Figure III-2-2〉	Collection activities on the barge when the hull was salvaged	114
〈Figure II-2-2〉	Conditions of the bottom of bow and stern	66	〈Figure III-2-3〉	Evidence collection at the stern	115
〈Figure II-2-3〉	Conditions of magazines after the hull recovery	66	〈Figure III-2-4〉	Evidence collection at the bow	116
〈Figure II-2-4〉	Ammunitions layout on ROKS Cheonan	67	〈Figure III-2-5〉	Evidence collection at the stack	117
〈Figure II-2-5〉	Location of fuel tank of ROKS Cheonan	69	〈Figure III-2-6〉	Sector 1 hull identification and salvaging status	118
〈Figure II-2-6〉	Location of the diesel engine room of ROKS Cheonan	71	〈Figure III-2-7〉	Sector 2 hull identification and salvaging status	119
〈Figure II-2-7〉	Location of the gas turbine of ROKS Cheonan	74	〈Figure III-2-8〉	The gas turbine room layout and gas turbine configuration	119
〈Figure II-2-8〉	The positions of ROKS Cheonan gas turbine, diesel engine, and shaft	75	〈Figure III-2-9〉	Salvaged bottom shell portion of gas turbine room	120
〈Figure II-2-9〉	Gas turbine protective box	77	〈Figure III-2-10〉	Salvaged gas turbine	121
〈Figure II-2-10〉	Bulkhead between gas turbine room and diesel engine room	78	〈Figure III-2-11〉	Detected explosives in bow area	124
〈Figure II-2-11〉	Gas turbine room just before the incident(CCTV)	78	〈Figure III-2-12〉	Detected explosives in stack area	125
〈Figure II-3-1〉	Classification of external explosion by detonation point	79	〈Figure III-2-13〉	Detected explosives in gas turbine room	125
〈Figure II-3-2〉	Breakplane of bow and stern	80	〈Figure III-2-14〉	Detected explosives from seabed evidences	126
〈Figure II-3-3〉	Direction of the deformation, PORT-bottom → STBD-top	81	〈Figure III-2-15〉	ROKS Cheonan hull composition	130
〈Figure II-3-4〉	Shape of the split section	81	〈Figure III-2-16〉	Composition of North Korean light weight torpedo samples	131
〈Figure II-3-5〉	Structural diagram of a mine	83	〈Figure III-2-17〉	Composition of evidences	131
〈Figure II-3-6〉	Mine types categorized by laying position and method	84	〈Figure III-4-1〉	Location of crew members in ROKS Cheonan at the time of the incident	142
〈Figure II-3-7〉	Seabed geography and water depth of incident site	86	〈Figure III-5-1〉	The progress of physical effects by bubble formed below the hull	146
〈Figure II-3-8〉	Seabed geography and water depth of incident site	86	〈Figure III-5-2〉	Detection results of seismic and air acoustic wave on the incident day	147
〈Figure II-3-9〉	Drifting level of moored mines by current speed	87	〈Figure III-5-3〉	Charge size and depth of explosion according to bubble periods	148
〈Figure II-3-10〉	General structure of a torpedo	88	〈Figure III-5-4〉	Explosion type similar to dishing of ROKS Cheonan hull bottom	149
〈Figure II-3-11〉	Operating concept of heavy and light weight torpedoes	89	〈Figure III-5-5〉	Result of examination on explosion type of ROKS Cheonan	149
〈Figure II-3-12〉	Wake produced by surface vessel	91	〈Figure III-5-6〉	Sample collection locations at fractured surface	151
〈Figure II-3-13〉	Mechanism to track wake produced by surface vessel	91	〈Figure III-5-7〉	Possible range of explosion	151
〈Figure II-3-14〉	Operating mechanism of magnetic influence fuses	92	〈Figure III-5-8〉	Damage from the explosion seen on ROKS Cheonan	152
〈Figure II-3-15〉	Operating mechanism of acoustic influence fuses	92	〈Figure III-5-9〉	Three comparison criteria	152
〈Figure II-3-16〉	3D laser scan image on the split section of ROKS Cheonan	94	〈Figure III-5-10〉	SEM image of adhered materials	153
〈Figure II-3-17〉	Emplacement of the land control mine	99	〈Figure III-5-11〉	EDS analysis result of adhered materials	154
〈Figure II-3-18〉	Design and specification of the land control mine	99	〈Figure III-5-12〉	XRD analysis result of adhered materials	154
〈Figure II-3-19〉	Detonation cable and metal stand	100	〈Figure III-6-1〉	Underwater explosion conditions for whipping analysis	158
〈Figure II-3-20〉	Detonation cable in detail	100	〈Figure III-6-2〉	Beam whipping analysis model	158
〈Figure II-3-21〉	Detonation process of MK-6 depth charge	101	〈Figure III-6-3〉	Weight distribution along the ship in fully-loaded condition	159
〈Figure II-3-22〉	Detonation process of land control mine	101	〈Figure III-6-4〉	Calculated whipping bending moments for different charge weights and standoff distances	161
〈Figure III-1-1〉	Overall shape	106	〈Figure III-6-5〉	Frame locations calculated in ultimate bending moments	162
〈Figure III-1-2〉	Shape analysis	107	〈Figure III-6-6〉	Curvature-bending moments for each frame	162
〈Figure III-1-3〉	Starboard breakplane & CVK deformation	108	〈Figure III-6-7〉	Comparison of whipping bending moments and ultimate bending moments for various charges	163
〈Figure III-1-4〉	Starboard fracture	109	〈Figure III-6-8〉	Condition for close-in underwater explosion analysis	164
〈Figure III-1-5〉	Portside fracture	109	〈Figure III-6-9〉	Comprehensive finite element analysis model	165
〈Figure III-1-6〉	Stern breakplane deformation	110	〈Figure III-6-10〉	Finite element analysis on the hull	166
〈Figure III-1-7〉	Bow fractured surface deformation	110	〈Figure III-6-11〉	Detailed modeling through Frame 50 to Frame 106	167
〈Figure III-1-8〉	Main deck deformation	111	〈Figure III-6-12〉	Modeling for gas turbine and generator	167
〈Figure III-1-9〉	Fractured surface of portside bottom	111			
〈Figure III-1-10〉	Trace analysis	112			

〈Figure III-6-13〉 Modeling for charge, seawater, and air	168	〈Figure III-7-18〉 Anticipated infiltration route and current speed when submarine or midget submarine from the anticipated North Korea infiltration base infiltrates through the shortest route	203
〈Figure III-6-14〉 Analysis result(TNT 360kg at 9m depth): damage in gas turbine room	170, 171	〈Figure III-7-19〉 Current at time of incident & expected attack staging site	204
〈Figure III-6-15〉 Side view of analysis result(TNT 360kg at 9m depth) on bubble migration and shock response	172, 173	〈Figure III-7-20〉 Current speed at various depths near Baekryong Island and tactics for torpedo employment by North Korean submarine	205
〈Figure III-6-16〉 Side view of analysis result(TNT 360kg at 7m depth)	174, 175	〈Figure III-7-21〉 Current direction & speed at slack tide during March 23~26	205
〈Figure III-6-17〉 Side view(closed-in) of analysis result(TNT 360kg at 7m depth)	176, 177	〈Figure III-8-1〉 Conceptual diagram of the special net and bull trawler	208
〈Figure III-6-18〉 Section view of analysis result(TNT 360kg at 7m depth)	178, 179	〈Figure III-8-2〉 Propulsion device location	211
〈Figure III-6-19〉 Internal view of analysis result(TNT 360kg at 7m depth)	180, 181	〈Figure III-8-3〉 Recovery and collection of the evidence	213
〈Figure III-6-20〉 Internal top view of analysis result(TNT 360kg at 7m depth)	182, 183	〈Figure III-8-4〉 Blueprint of CHT-02D	213
〈Figure III-6-21〉 Internal side view of analysis result(TNT 360kg at 7m depth)	184, 185	〈Figure III-8-5〉 Size comparison between the blueprint of CHT-02D and the evidence	214
〈Figure III-6-22〉 Deck view of analysis result(TNT 360kg at 7m depth)	186, 187	〈Figure III-8-6〉 Shape comparison between the blueprint of CHT-02D and the evidence	214
〈Figure III-6-23〉 Comparison between modelled damage and actual damage of ROKS Cheonan (side view of bow)	188	〈Figure III-8-7〉 The Korean inscriptions on torpedo propulsion motor and North Korean light torpedo	215
〈Figure III-6-24〉 Comparison between modelled damage and actual damage of ROKS Cheonan (front view of bow)	188	〈Figure III-8-8〉 CHT-02D Torpedo	217
〈Figure III-6-25〉 Comparison between modelled damage and actual damage of ROKS Cheonan (bottom view of bow)	189	〈Figure Appendix I-1-1〉 ROKS Cheonan CCTV location	226
〈Figure III-6-26〉 Comparison between modelled damage and actual damage of ROKS Cheonan (side view of stern)	189	〈Figure Appendix I-2-1〉 CCTV recovery process	227
〈Figure III-6-27〉 Comparison between modelled damage and actual damage of ROKS Cheonan (front view of stern)	190	〈Figure Appendix I-3-1〉 CCTV recorded footage	229
〈Figure III-6-28〉 Comparison between modelled damage and actual damage of ROKS Cheonan (bottom view of stern)	190	〈Figure Appendix II-1-1〉 Shockwave & bubble pressure-time graph	230
〈Figure III-7-1〉 The sinking site of ROKS Cheonan	192	〈Figure Appendix II-1-2〉 Shockwave parameters	232
〈Figure III-7-2〉 Anticipated infiltration routes of North Korean submarine or midget submarine	192	〈Figure Appendix II-1-3〉 Shockwave peak overpressure of various weights of TNT	234
〈Figure III-7-3〉 Area of underwater terrain search operation at the sinking site by the KORDI	195	〈Figure Appendix II-1-4〉 Shockwave peak overpressure at several distances from underwater explosion of 250kg TNT	234
〈Figure III-7-4〉 Result of underwater terrain search in the sinking site	196	〈Figure Appendix II-1-5〉 Time constant( $\theta$ ) for different charge weights	234
〈Figure III-7-5〉 Metal structure found near unknown sunken vessel	196	〈Figure Appendix II-1-6〉 Shockwave impulse vs. TNT charge size	234
〈Figure III-7-6〉 Underwater terrain around the unknown sunken vessel	197	〈Figure Appendix II-1-7〉 Bubble period(T) of the bubble formed by TNT at different depths	236
〈Figure III-7-7〉 Depression at the seabed near the incident site	197	〈Figure Appendix II-1-8〉 Maximum bubble radius( $A_m$ ) of the bubble formed by TNT at different depths	236
〈Figure III-7-8〉 Reef(Honghapyeo) near Baekryong Island shown on a chart	198	〈Figure Appendix II-1-9〉 Maximum jet height vs. scaled depth for TNT	237
〈Figure III-7-9〉 Locations of observation buoys of the NORI near Baekryong Island	199	〈Figure Appendix II-1-10〉 Max. column diameter vs. Scaled depth	237
〈Figure III-7-10〉 Comparison between 「Military Operational tidal movement and tidal current forecasting system」 and the actual current speed measurement data of buoys	199	〈Figure Appendix II-1-11〉 The effect of aluminum on underwater explosion properties	238
〈Figure III-7-11〉 Tidal current at ebb and flood tide near Baekryong Islands	200	〈Figure Appendix II-2-1〉 Bubble collapse and formation of water jet	239
〈Figure III-7-12〉 Tidal current and height in March (↖: direction and speed of tidal current,  : height of flood and ebb tide)	200	〈Figure Appendix II-2-2〉 Physical effects of bubble formed below hull as time elapses	240
〈Figure III-7-13〉 Tidal current and height on the incident date(March 26)	201	〈Figure Appendix II-3-1〉 Explosive train used in the experiment	241
〈Figure III-7-14〉 Maneuvering course of ROKS Cheonan on the incident day(March 26)	201	〈Figure Appendix II-3-2〉 Small water tank used in the UNDEX test	241
〈Figure III-7-15〉 Direction and speed of current on the incident day(March 26)	202	〈Figure Appendix II-3-3〉 Images obtained through the experiment(5,000 frames/sec)	242
〈Figure III-7-16〉 Result of simulation on the tidal current from March 23 until 2120 March 26 between the Anticipated infiltration base and Baekryong Island	202	〈Figure Appendix II-3-4〉 White substance obtained from the small-scale UNDEX experiment	243
〈Figure III-7-17〉 Anticipated infiltration route and current speed when submarine or midget submarine from the anticipated North Korea infiltration base infiltrates through the open sea	203	〈Figure Appendix II-4-1〉 Maximum bubble radius vs. slant distance	243
		〈Figure Appendix III-1〉 Types of fractures	245
		〈Figure Appendix III-1-1〉 Sample collection locations at breakplane	246
		〈Figure Appendix III-2-1〉 Fracture surfaces of collected samples	247
		〈Figure Appendix III-2-2〉 The pattern of fracture on the stern	247
		〈Figure Appendix III-2-3〉 Overall fracture pattern of the stern part	248
		〈Figure Appendix III-2-4〉 Shape of fracture on the hull	249

〈Figure Appendix III-2-5〉	Analysis of cutting shape of upper and lower hull	249	〈Figure Appendix VI-3-1〉	The righting arm curve of ROKS Cheonan prior to the damage	292
〈Figure Appendix III-3-1〉	Thickness measurement of collected samples	250	〈Figure Appendix VI-3-2〉	The righting arm curve and the heeling arm curve	293
〈Figure Appendix III-3-2〉	Microstructures of collected samples	251	〈Figure Appendix VI-4-1〉	Buoyancy level with 2 compartments flooded(Case 1)	295
〈Figure Appendix III-3-3〉	Typical microstructure change due to heat influence (example)	252	〈Figure Appendix VI-4-2〉	Dynamic stability curve with the damage	295
〈Figure Appendix III-3-4〉	A microstructure of fractured surface	252	〈Figure Appendix VI-4-3〉	Buoyancy level with 2 compartments flooded(Case 2)	296
〈Figure Appendix III-4-1〉	Possible range of torpedo explosion	253	〈Figure Appendix VI-4-4〉	Buoyancy level with three compartments flooded(Case 3)	297
〈Figure Appendix IV-1-1〉	Simulation range for explosive analysis	255	〈Figure Appendix VI-4-5〉	Buoyancy level with 3 compartments flooded(Case 4)	298
〈Figure Appendix IV-1-2〉	Modeling shape	255	〈Figure Appendix VI-4-6〉	Buoyancy level with four compartments flooded(Case 5)	299
〈Figure Appendix IV-1-3〉	Mesh shape	255	〈Figure Appendix VI-4-7〉	Buoyancy level with four compartments flooded(Case 6)	300
〈Figure Appendix IV-1-4〉	Initial analysis model	256	〈Figure Appendix VI-5-1〉	Estimation of the bow buoyancy level immediately after the separation	302
〈Figure Appendix IV-2-1〉	Comparison of bubble behavior	258	〈Figure Appendix VI-5-2〉	Estimation of the stern buoyancy level immediately after the separation	303
〈Figure Appendix IV-3-1〉	Three comparison criteria	259	〈Figure Appendix VI-5-3〉	Buoyancy level estimations with each flooding condition in the diesel engine room	303
〈Figure Appendix V-1-1〉	SEM Images	262	〈Figure Appendix VI-5-4〉	Crater on the stern breakplane & the main deck hatch	304
〈Figure Appendix V-1-2〉	EDS result	262	〈Figure Appendix VI-5-5〉	Sinking time estimation of the stern	304
〈Figure Appendix V-1-3〉	X-ray diffraction result	262	〈Figure Appendix VII-2-1〉	Direct strength analysis flow chart	307
〈Figure Appendix V-2-1〉	Sampling locations	264	〈Figure Appendix VII-3-1〉	3D hydrodynamic analysis model and load condition	307
〈Figure Appendix V-2-2〉	SEM images of the adhered material(stern)	264	〈Figure Appendix VII-4-1〉	3D structural analysis model	309
〈Figure Appendix V-2-3〉	EDS results of the adhered material(stern)	265	〈Figure Appendix VII-4-2〉	Structural analysis result of the shell plates	310
〈Figure Appendix V-2-4〉	XRD results of the adhered material(stern)	266	〈Figure Appendix VII-4-3〉	Structural analysis of the main deck	310
〈Figure Appendix V-2-5〉	TGA results of the adhered material(stern)	268	〈Figure Appendix VII-4-4〉	Buckling strength assessment result: FR.27~FR.67	311
〈Figure Appendix V-3-1〉	SEM images of the adhered material(bow and stack)	269	〈Figure Appendix VII-4-5〉	Buckling strength assessment result: FR.106~FR.130	312
〈Figure Appendix V-3-2〉	EDS results of the adhered material(bow and stack)	270	〈Figure Appendix VII-4-6〉	Location and shape of partial longitudinal bulkhead(example)	312
〈Figure Appendix V-3-3〉	XRD results of the adhered material(bow and stack)	271			
〈Figure Appendix V-3-4〉	TGA results of the adhered material(bow and stack)	273			
〈Figure Appendix V-4-1〉	SEM images of the adhered material(propulsion section and motor)	274			
〈Figure Appendix V-4-2〉	EDS results of the adhered material(propulsion section and motor)	274			
〈Figure Appendix V-4-3〉	XRD results of the adhered material(propulsion section and motor)	275			
〈Figure Appendix V-4-4〉	TGA results of the adhered material(propulsion section and motor)	276			
〈Figure Appendix V-5-1〉	SEM images of the explosion products	278			
〈Figure Appendix V-5-2〉	EDS analysis of UNDEX sample	278			
〈Figure Appendix V-5-3〉	XRD results of the explosion products	280			
〈Figure Appendix V-6-1〉	Change of elemental composition of adhered materials in EDS area analysis with different heat treatment	281			
〈Figure Appendix V-6-2〉	Change of elemental composition of adhered materials in EDS spot analysis with different heat treatment	282			
〈Figure Appendix V-6-3〉	Microstructure of adhered material	283			
〈Figure Appendix V-7-1〉	AL-O Binary Phase Diagram	284			
〈Figure Appendix V-7-2〉	Analysis of amorphous Al <sub>2</sub> O <sub>3</sub> content	286			
〈Figure Appendix V-7-3〉	XRD results of adhered material before and after heat treatment	287			
〈Figure Appendix VI-2-1〉	Stability factors	289			
〈Figure Appendix VI-2-2〉	Positive(+) stability	290			
〈Figure Appendix VI-2-3〉	Negative(-) stability	291			
〈Figure Appendix VI-2-4〉	The righting arm curve overlapped with the heeling arm curve, displaying a dynamic stability of a vessel	291			

# *Summary*

Republic of Korea Ship(ROKS) Cheonan(PCC) of the 2nd Fleet, ROK Navy sank by a North Korean torpedo attack while conducting a normal mission in the vicinity of Baekryong Island on Friday, March 26, 2010 at 2122. This attack resulted in the death of 46 out of 104 crew members, and 58 crew members survived the incident.



## 1. Overview

In the wake of the sinking of Republic of Korea Ship(ROKS) Cheonan on March 26, 2010, the Ministry of National Defense organized a Civilian-Military Joint Investigation Group(JIG) and commenced an investigation in order to find the cause of the sinking.

In order to ensure the transparency and credibility of the investigation process, the investigation was conducted with 25 experts from 12 Korean civilian agencies, 22 military experts, 3 advisors recommended by the National Assembly, and 24 foreign experts from the United States, Australia, the United Kingdom, and Sweden. The JIG organized the experts into four teams in order to conduct a scientific and systematic investigation. The four teams were as follows: Scientific Investigation Team, Explosive Analysis Team, Ship Structure Team, and Intelligence Analysis Team.

The JIG conducted its investigation in phases with the recovery of the ship as the dividing point. The final investigation results were announced on May 20.

In addition, the Ministry of National Defense operated a “Multinational Combined Intelligence TF” with participations of the United States, Australia, Canada, and the United Kingdom starting from May 4 to verify the perpetrator of this incident.

## 2. Investigation Result on the Cause of the Sinking

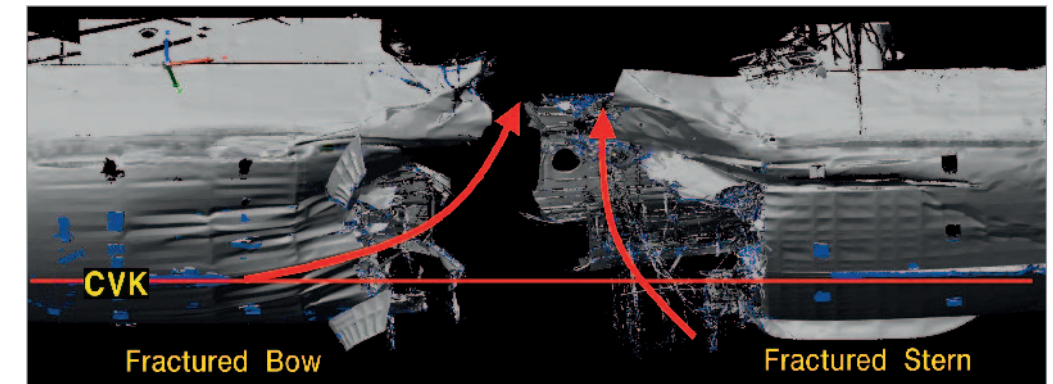
Based on the investigation of the collected evidence and the deformed shape of the recovered bow and stern, the JIG assessed that ROKS Cheonan was split and sunk due to a strong underwater explosion(UNDEX) of an influence torpedo manufactured by **North Korea(nK)**.

The reasonings behind the assessment are as follows.

First, a precise measurement and analysis of the damaged hull showed that a shockwave and bubble effects caused significant upward bending of the CVK(Center Vertical Keel) compared to its original state. The shell plating was steeply bent, with parts of the ship fragmented. On the main deck, fracture occurred along the large openings used for the maintenance of equipment in the gas turbine room, and the portside was deformed significantly in an upward direction. The bulkhead of the gas turbine room was significantly

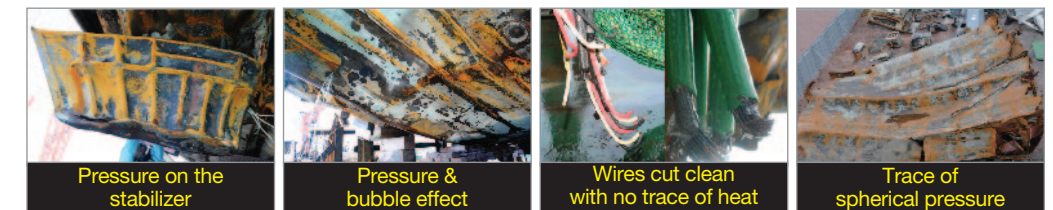
damaged and deformed.

As seen in <Figure Summary-1>, the upward bending of the bottom of the stern and bow indicates that an underwater explosion took place.



<Figure Summary-1> 3D laser scan image of the fractured bow and stern

Second, as seen in <Figure Summary-2>, through a thorough investigation of the interior and exterior of the ship, the JIG had found evidence of extreme pressure on the fin stabilizer, which prevents significant rolling of the ship; traces of high water pressure and bubble effect on the hull bottom; wires cut with no traces of heat; and traces of spherical pressure on the gas turbine room. The above indicate that strong shockwave and bubble effects caused the splitting and sinking of the ship.



<Figure Summary-2> Traces of shockwave and bubble effect

Third, statements made by the survivors were collected, including that they heard a nearly simultaneous explosion once or twice and that water was splashed on the face of the port lookout who fell by the impact. Furthermore, statements made by the coastal sentries on Baekryong Island testified that they saw a 100-meter high pillar of white flash for 2~3

seconds, consistent with the occurrence of a water plume resulting from shockwave and bubble effect. Also, no traces of fragmentation or burn injury were found from the examination of the wounded survivors and the deceased service members, while fractures and lacerations were observed. These observations are consistent with phenomena resulting from shockwave and bubble effect.

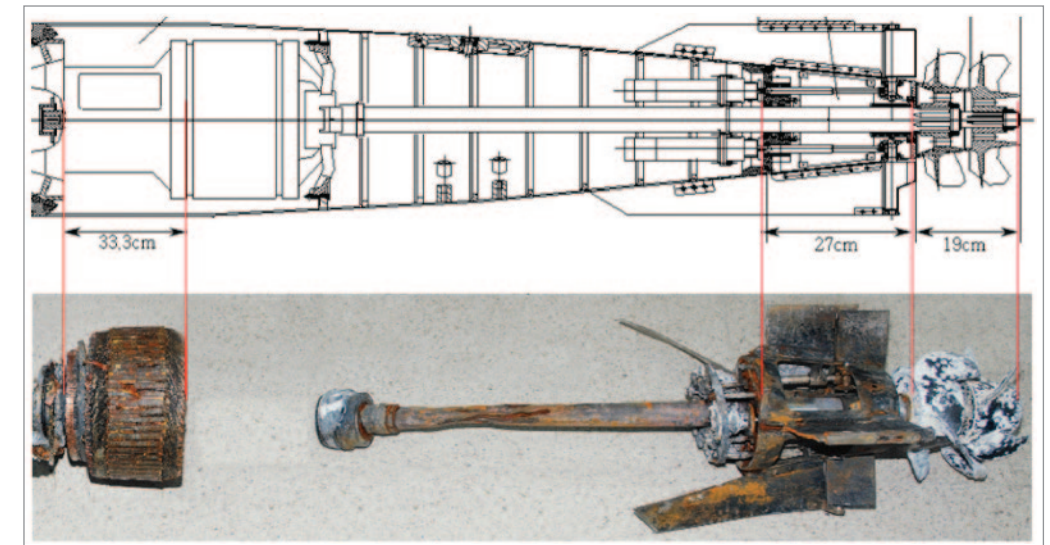
Fourth, the seismic and air acoustic wave analysis conducted by the Korea Institute of Geoscience and Mineral Resources(KIGAM) showed the following. A seismic wave of magnitude 1.5 was detected at 4 stations. Two air acoustic waves with a 1.1 second interval were detected at 11 stations. The analysis of seismic and air acoustic waves verified that they originated from an identical location. All these are consistent with the phenomena that arise from a shockwave and bubble effect produced by an underwater explosion.

Fifth, the 1st analysis result by the US team, from the hull deformation showed that the possible explosion type is an explosion of TNT equivalent of 200~300kg charge size at a point of 3m to the port from the central bottom of gas turbine room, and at a depth of 6~9m. The 2nd analysis result on simulation, by the ROK resulted in the identical location, with TNT equivalent of 250~360kg charge size. The efforts on this were also participated by the UK Investigation Team.

Sixth, based on the analysis of tidal currents in the vicinity of Baekryong Island, the JIG determined that although the currents would not significantly influence the launch of a torpedo, they were strong enough to limit the emplacement of mines.

Seventh, the analysis of the explosive residue found HMX from 28 locations including the stack and fractured surface; RDX from 6 locations including the stack and seabed; and traces of TNT from 2 locations including the fin stabilizer. Based on this analysis, the JIG confirmed the use of an explosive compound containing HMX, RDX, and TNT.

Lastly, on May 15, the JIG recovered the conclusive evidence that confirmed the use of a torpedo during a detailed search in the vicinity of the incident location using special nets. The conclusive evidence was a torpedo propulsion motor system including propellers, a propulsion motor, and steering section. The evidence is consistent with the drawing shown in <Figure Summary-3> in its size and design. The figure was a part of an introductory brochure produced by **North Korea** for an export purpose.



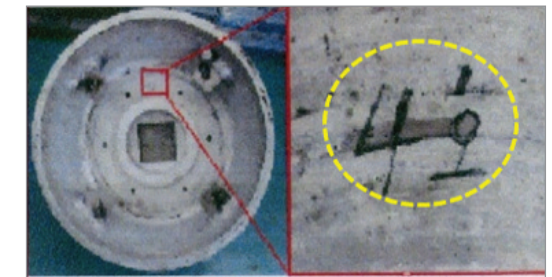
<Figure Summary-3> Schematic of torpedo and recovered rear section of torpedo

A composition analysis of the adhered materials from ROKS Cheonan showed that the materials are consistent with those found on the rear section of the torpedo.

As shown on <Figure Summary-4> and <Figure Summary-5>, the Korean marking “1번(No. 1 in English)” inside the rear section of the propulsion system is similar to the marking of a **North Korean** test torpedo obtained in 2003.



<Figure Summary-4> Rear section of torpedo



<Figure Summary-5> Marking on **North Korean** test torpedo

These evidences confirmed that the recovered torpedo parts were manufactured in **North Korea**.

In conclusion, after taking the entirety of the analysis results of Korean and foreign ex-

perts on the following factors into consideration – the torpedo propulsion system recovered from the incident location, deformation of the hull, statements by related personnel, medical examination of the deceased and wounded service members, seismic and infrasound waves, simulations of underwater explosions, tidal currents in the vicinity of Baekryong Island, analysis of explosive components and recovered torpedo parts – the JIG concluded the following:

**ROKS Cheonan was split and sunk due to shockwave and bubble effects generated by the underwater explosion of a torpedo. The detonation location was 3m to the port from the center of the gas turbine room and at a depth of 6~9m. The weapon system used was a CHT-02D torpedo with approximately 250kg of explosives manufactured by North Korea.**

### 3. Identification of Perpetrator

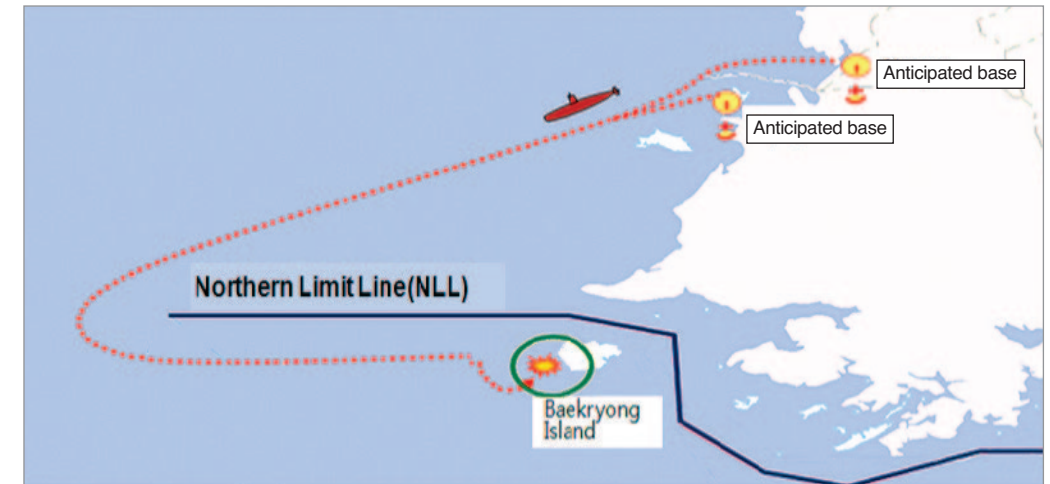
The Multinational Combined Intelligence Task Force(MCITF, and comprised of 5 states including the US, Australia, Canada, and the UK) reached the following conclusion after analyzing relevant intelligence:

The **North Korean** military possesses about 70 submarines and midget submarines in total, with its submarine fleet consisting of approximately 20 Romeo class submarines, 40 Sango class submarines, and 10 midget submarines including the Yono class. Also, it possesses torpedoes of various capabilities, including straight running, acoustic and wake homing torpedoes.

Moreover, it was confirmed that a few midget submarines from **North Korean** naval bases in the West Sea left their bases 2~3 days before the day of the incident and returned 2~3 days after the day of the attack.

Furthermore, it was confirmed that all submarines from neighboring countries were either in or near their respective home bases at the time of the incident.

The torpedo parts, recovered at the incident location by bull trawlers on May 15(they include 5-bladed/contra-rotating propellers, propulsion motor and steering section), perfectly match the schematics of the CHT-02D torpedo displayed in the introductory brochure produced by North Korea for export purposes.



〈Figure Summary-6〉 Anticipated infiltration route of **North Korean** midget submarine

The CHT-02D torpedo manufactured by **North Korea** utilizes acoustic/wake homing and passive acoustic tracking methods. It is a heavyweight torpedo with a diameter of 21 inches, a weight of 1.7 tons, and a net explosive weight of up to 250kg.



〈Figure Summary-7〉 CHT-02D torpedo manufactured by **North Korea**

Based on all the relevant facts and analyses of the classified information, the JIG and MCITF reached the following conclusion: **ROKS Cheonan was sunk due to an underwater explosion caused by an attack of a CHT-02D torpedo manufactured and used by North Korea.** The evidence points overwhelmingly to the conclusion that the torpedo was fired by a **North Korean** submarine. There is no other plausible explanation.

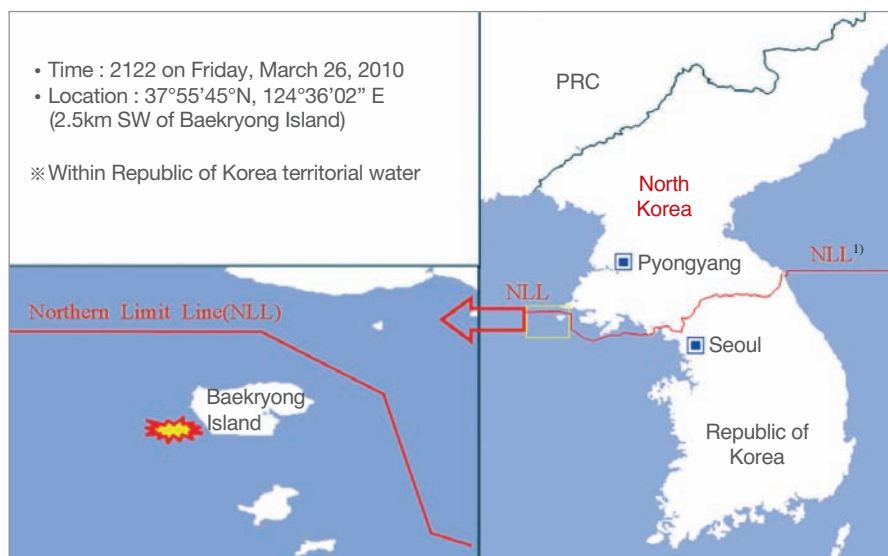
Part I

*Overview*



## 1. Situation Overview

Republic of Korea Ship(ROKS) Cheonan(PCC) of the 2nd Fleet, ROK Navy sank by a North Korean torpedo attack while conducting a normal mission in the vicinity of Baekryong Island on Friday, March 26, 2010 at 2122. This attack resulted in the death of 46 out of 104 crew members, and 58 crew members survived the incident.



〈Figure I-1-1〉 The location of ROKS Cheonan incident

### ■ ROKS Cheonan's mission

- Tuesday, March 16. Left Pyeongtaek, deployed to Western Baekryong Island Patrol Zone.
- Thursday, March 25. Heavy seas warning activated in the West Sea. Left Western Baekryong Island Patrol Zone. Averted to SE of Daechung Island.
- Approximately at 0600 on Friday, March 26, started to return back to the patrol zone due to good weather. Arrived at the patrol zone at about 0830 and began normal operations. At 2000, there was a duty shift(29 personnel), with others taking a rest or involved in maintenance.

.....  
1) NLL: The maritime boundary set by UN force immediately after the armistice in 1953.

## 2. Situation Development

### 1) Before the Incident

Before the incident, there were 7 personnel on the bridge; 7 personnel at the Combat Situation Center; 2 personnel at the communication cell; 3 personnel at the bow gun R/S; 7 personnel at the machinery control room; 1 at the guiding control room; and 2 personnel at the diesel engine room. A total of 29 personnel were on duty while others were on break or sleeping at the mess hall or their berthing. The Commanding Officer of the ship finished his patrol at about 2105, returned to the CO's cabin and was checking e-mails, message boards and KNTDS<sup>2)</sup>.

At the time of the incident(2122 on March 26), ROKS Cheonan was in its normal operating conditions.

### 2) After the Incident

- 2122 ROKS Cheonan began to sink(the time of the incident)
- 2128 Second FLT receives situation report on the sinking of ROKS Cheonan
- 2130 Second FLT orders the immediate departure of 5 PKMs sub-squadrons in Daechung Island to incident location
- 2131 Second FLT instructs ROKS Sokcho to sail to the incident location at full speed
- 2132 Second FLT requests emergency support to Incheon maritime police(ships 501, 1002) and government ships
- 2134 Second FLT activates crisis response element
- 2140 Second FLT activates crisis action team and deploys all operation elements for combat
- 2147 Second FLT orders deployment of LYNX helicopter in Dukjuk Isl. to Baekryong Island
- 2156 Arrival of 3 PKMs, commencement of rescue operations
- 2157 Second FLT declares anti-submarine alert posture
- 2159 Second FLT requests Air Force search and rescue support
- 2207 Second FLT requests Incheon maritime police RIBs<sup>3)</sup>(501, 1002) support

.....  
2) KNTDS: Korea Naval Tactical Data System.

3) RIB: The bottom section is consisted of glass-fiber stiffened plastic, and the upper section is composed of expandable tube. RIB is light and rigid, allowing for operation in long distance maneuver and high waves in comparison to other small vessels.

- 2210 Additional arrival of 2 PKMs, commencement of rescue operations
- 2228 Rescue of 1 sailor(Operations officer of ROKS Cheonan) by Chamsoori 322
- 2241 Arrival of Maritime Police Ship 501 and 2 RIBs, commencement of rescue operations
- 2250 Commencement of rescue operations by GOV ships(214, 227)
- 2313 Rescue operations completed, 58 survivors rescued
- 2313~0435 March 27 Night search of incident location, transportation of patients

The 58 survivors stated that they heard ‘Kwang! Ku-wang’ (for 1~2 seconds) sounds as they felt an impact in the rear, and a blackout occurred. The influx of seawater to sections of the ship suddenly tilted the ship to the starboard side by 90 degrees. The impact caused the Commanding Officer to be locked inside the CO’s cabin. He strapped a fire hose that 4 or 5 crew members had lowered to his waist and escaped to the portside deck. At this time, about 20 crew members had gathered at the deck.

When the Commanding Officer looked towards the aft side standing from the bow section of the separated ship, the stack and the stern part aft of the stack were not visible (he also sensed a slight smell of fuel). Seeing that the bow side, where the surviving crew members had gathered, was tilted by 90 degrees to starboard, he took necessary measures. The Commanding Officer first instructed the executive officer(LCDR) to rescue the crew members locked inside the ship and the operations officer(LT) to count the number of crew members and check for a suitable disembarking location once the rescue ships arrived and approached the ship. 6 personnel including a LTJG were instructed to help or carry on their backs the injured personnel, including a PO1(lumbar fracture), PO1(fracture of the femoral region), SCPO(bruise on thigh), SCPO(shoulder injury), and SCPO(rib fracture). Following the rescue of all the survivors in the bow, the Commanding Officer confirmed that a total of 58 personnel were present and instructed them to wait for PKMs.

The Commanding Officer had a cell phone conversation with the Squadron Commander, second Fleet between 2232 and 2242. The key points of the conversation included the following: “It seems that we are hit by something,” “What do you think it is?” “It seems like a torpedo, the stern is completely invisible,” “Stern? From which part of the stern?” “The stack is not visible. Please send PKMs or RIBs quickly,” “What about survivors?” “A total of 58 survivors. Many are bleeding. Two of them are severely wounded and not able

to stand up.”

### 3) Situation Report and Dissemination

At approximately 2128, the gunnery officer of ROKS Cheonan called the watch officer of second Fleet by his cell phone to request rescue(the communication method within the ship was limited from the power outage). The call was forwarded to the chief of the second Fleet situation cell, who had heard the content of the conversation. He was told that “the ship is tilted to the right, and we need to be rescued.” He utilized a text message information network at 2130 to order the PKM sub-squadron at Daechung Island to depart immediately to the incident location.

At approximately 2130, the duty officer at second Fleet situation room received a phone call from the combat intelligence officer of ROKS Cheonan with the information that “ROKS Cheonan ‘ran aground’ in the vicinity of Baekryong Island and is sinking. Send help immediately.” The duty officer reported the situation to the chief of the situation room. Then, he made a phone call to an Inspector, the deputy chief of the Incheon Maritime Police and said, “I got a phone call that a ROK ship ran aground west of Baekryong Island. The situation is urgent. Please send Maritime Police Ships 501 and 1002 to the west of Baekryong Island.”<sup>4)</sup>

The deputy chief instantly instructed the 501, which was located south of Daechung Island, and the 1002, which was located south of Sochung Island, to depart for the incident location immediately.

At approximately 2132, the 2nd Fleet liaison officer called the captain of Ship 214, fishery guide ship of Ongjin county, with his cell phone and said, “ROKS Cheonan is sinking west of Baekryong Island. Please send help to support rescue efforts.” The captain of the fishery guide ship notified an official at Ongjin county of the incident and set sail at approximately 2150.

.....  
4) Upon the occurrence of the incident, the urgency of the situation led some survivors to use words such as grounding instead of using precise terms.

#### 4) Rescue of Crew Members

All operational elements including ROKN PKMs, maritime police ships, and GOV ships were mobilized to rescue a total of 58 survivors. Around 2156, 3 PKMs from Sub-squadron arrived at the incident location and started personnel recovery accompanied by 2 additional PKMs at 2210. PKM Sub-squadron connected a wire(3 inches) to ROKS Cheonan. The operation officer of ROKS Cheonan fell into the sea while he was moving between ships and was rescued by PKM.

Considering the possibility that the use of a PKM may increase the rolling of the ship and increase the risk of missteps during the rescue, the Commanding Officer of ROKS Cheonan decided to use maritime police RIBs. Due to the high waves, the wire connected between PKM sub-squadron and ROKS Cheonan was untied around 2238 in order to prevent crew members aboard the bow section of ROKS Cheonan from falling. Two RIBs from Maritime Police Ship 501(500tons) arrived around 2241, approached ROKS Cheonan, and rescued 19 crew members. Ship Incheon 227, a fishery guide ship, rescued 2 wounded crew members and transported them to Baekryong Island around 2308. The remaining 36 survivors were rescued by Maritime Police Ship 501.

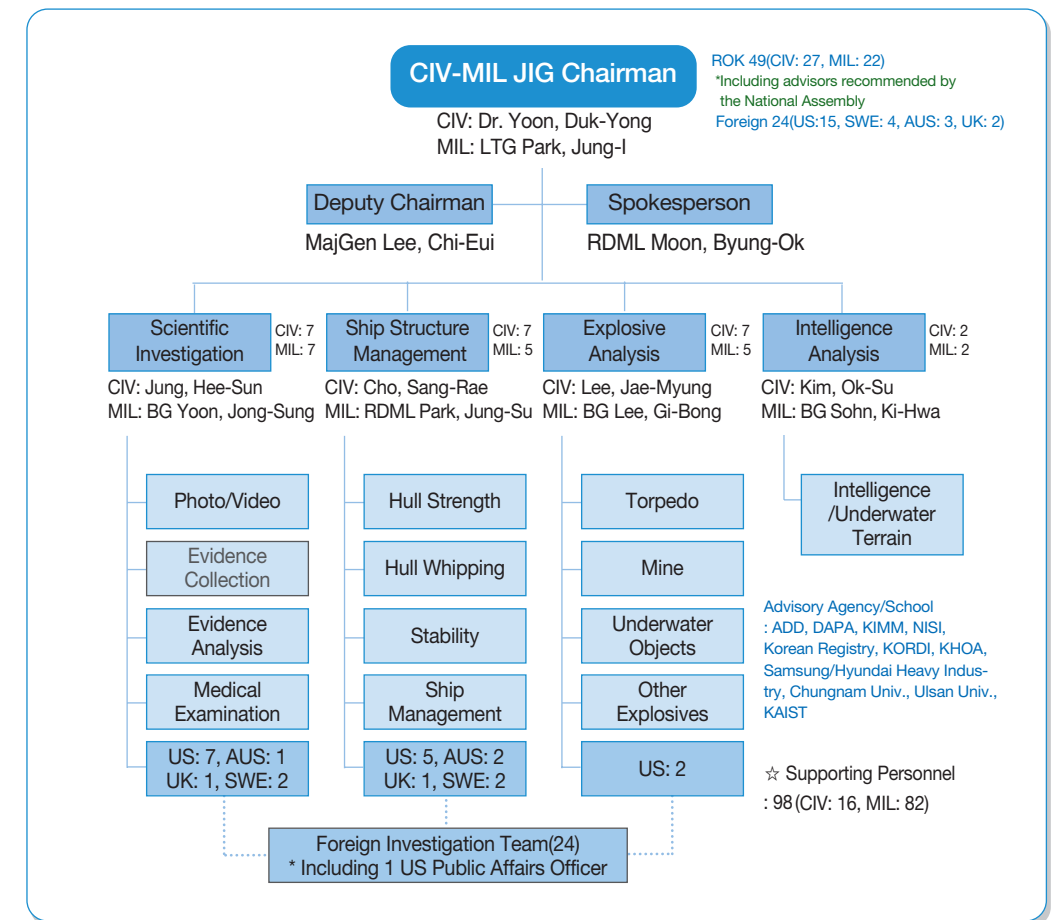
Following the arrival of RIBs, the Commanding Officer of ROKS Cheonan ordered personnel gathered by the aft gun to be transported first and ordered that “the wounded go first and help the severely wounded.” In accordance with the Commanding Officer’s orders, the wounded and seaman apprentices were rescued first and moved to Maritime Police Ship 501 with RIBs and rescue boards. The Commanding Officer, executive officer, and communication officer were the last to leave ROKS Cheonan. Between 2313 March 26 and 0435 March 27, the incident location was searched, and the 51 survivors aboard Maritime Police Ship 501 were transported to PKM Sub-squadrons and then moved to PCC. They arrived at Pyeongtaek port at approximately 1400 March 27.

### 3. Investigation Activities

#### 1) JIG Operations

The CIV-MIL JIG was initially organized on March 31 and included 82 personnel(59 active service members, 17 government personnel, and 6 civilians). It was then reorganized as the Civilian-Military Joint Investigation Group on April 12 and included 73 personnel (49 ROK, 24 Foreign experts), to initiate investigation activities.

The JIG was in operation for a total of 92 days until June 30. During this time, it held press conferences on its investigation activities on four different occasions(April 7, 15, 25,



<Table I-3-1> The organizational structure of the Joint Investigation Group(JIG)

and May 20) and also attended a UN Security Council meeting for 9 days from June 9 through June 17 to explain the investigation results.

The objective of the JIG was to find the exact cause of the sinking through a detailed investigation conducted in a scientific and objective manner. The focus was first, to form a civilian and military joint investigation group in order to improve the transparency and credibility of the investigation process; second, to secure international credibility through the participation of foreign experts from the US and other nations; third, to conduct the investigation in phases, with the recovery of the ship as the dividing point; and fourth, to conduct the investigation in a scientific and systematic manner.

## 2) Activities of Teams

### (1) Scientific Investigation Team

The Scientific Investigation Team was composed of 25 research personnel<sup>5)</sup> in total (7 military personnel / 7 civilian / 11 foreign experts) from MND Criminal Investigation Command(CIC), ROK Army Investigation Group, National Institute of Scientific Investigation(NISI), Defense Media Agency, and foreign experts. The participating personnel were divided into 4 sub-teams of photo/video analysis, evidence collection, evidence analysis, and medical examination team(responsible for postmortem examination and autopsy). Their investigation was conducted aboard ships(ROKS Dokdo, ROKS Chunghaejin, ROKS Sunginbong, etc.), at Baekryong Island, 2nd Fleet Command, MND, CIC, and NISI.

During a period spanning the occurrence of the incident to the recovery of the stern, the Scientific Investigation Team collected and analyzed statements of the 58 survivors over four periods(1st: March 27, 2nd: March 28, 3rd: March 31, 4th: April 1). Based on these statements, the individuals' locations and status of their injury at the time of the incident were identified and incorporated into a compartmental diagram of ROKS Cheonan, which was then reflected in the investigation for the cause of the sinking.

From April 2 to 5, the JIG clearly identified the circumstances surrounding the incident by confirming that ROKS Cheonan was conducting its normal operation and that the

incident occurred at 2122 hours by analyzing the TOD<sup>6)</sup> (DVR) recording around incident time, and the cell phone call records of 96 crew members from 1700 to 2400, March 26. This excluded 8 of 104 members who did not possess a cell phone.

The Scientific Investigation Team divided the area in the vicinity of the incident location into section 1(the stern) and section 2(the bow). The photo/video analysis team photographed the entire recovery process beginning from the salvaging of the hull. Together with the evidence collection team, they photographed and analyzed the fractured surfaces, internal and external traces to verify the cause of the incident including factors such as non-explosion, internal explosion, and external explosion. In addition, they conducted digital forensics<sup>7)</sup> on the CCTVs.

The evidence collection team divided its efforts into sea evidence collection, bow and stern evidence collection, and seabed evidence collection. During the search and rescue operations, the sea evidence collection team extracted all possible evidence, including the soil at the incident location seabed, metal pieces suspected to be fragments of the incident, and materials that are conducive to the adherence of explosive residue. The bow and stern evidence collection efforts initially focused on the on-site examination of evidence collected every time the bow, stern, and stack aboard the barge ship were salvaged. After the recovered ship was transported to the 2nd Fleet Command at Pyeongtaek, a precise examination was conducted on three occasions for the stern, and on two occasions for the bow. These investigations were focused on the collection of evidences necessary for explosive residue and metallic content analysis.

Lastly, the seabed evidence collection efforts gathered the missing gas turbine protective cover, generator armature and parts, fiber and metallic fragments of the motor. In particular, explosive residue and metallic fragments were collected using a gauze along the hull bottom, mud, and breakplane of the gas turbine room, which had directly received the pressure resulting from the explosion.

In addition, seabed materials collected with the use of a special net were initially sorted out on the deck and moved to a separate site at the Battalion from the 6th Brigade, ROKMC where they were further classified manually and through the use of a mine(metal) detector.

.....  
6) TOD(Thermal Observation Device): A device that detects the infrared rays of an object or creature, and converts them into a video imagery. TOD is mainly used for surveillance and reconnaissance purposes.

7) Digital Forensics: A digital investigation process which analyzes data acquired from electric evidences such as a cell phone, PDA, PC, and server.

.....  
5) Total number of ROK investigators was 83(14 ROK military & civilian, and 69 supporting personnel).

The evidence analysis team considered the recovered locations and features of the collected evidence to prioritize its evidence analysis. In case of the chemical analysis, the liquid-chromatography mass analysis method<sup>8)</sup> was utilized to detect the explosive components such as HMX, RDX, and TNT.

For the physical analysis, the composition ratios of 3 North Korean test torpedo samples, hull samples from various locations on ROKS Cheonan and various parts of the gas turbine room, which was close to the point of explosion, were contrasted for a comparison analysis.

Afterwards, a composition analysis of collected metals was conducted through the use of an electron microscope and energy dispersion X-ray analysis<sup>9)</sup>. By comparing the composition of extracted samples, irrelevant metals were excluded, and further evaluation was conducted on the metals containing aluminum and aluminum alloy, which are metals used in torpedoes.

The medical examination team, comprised jointly of civilian and military forensics personnel, was located aboard the barge ship and ROKS Dokdo. They guided the recovery process of the deceased service members, identified the bodies of the deceased, performed medical examinations, found the causes of death, and analyzed the causes of death in connection with the cause of the sinking.

## (2) Ship Structure/Management Team

The Ship Structure/Management Team consisted of personnel from ROK Joint Chiefs of Staff(JCS), ROKN HQ, Defense Acquisition and Procurement Agency(DAPA), academia (Ulsan and Chungnam National University), the ship building industry(Hyundai and Samsung Heavy Industries), research institutes(Agency for Defense Development, Korea Institute of Machinery and Materials and Korean Register of Shipping), and foreign experts. A total of 22 research personnel, including 7 civilian, 5 military and 10 foreign experts as well as 3 additional supporting personnel, was included in the team. The investigation activities of the Ship Structure/Management Team were divided into ship management, basic hull strength analysis, stability analysis, and analysis of the impact on the hull due to an un-

.....  
8) An analysis method to confirm the composition of a material by using a device that analyzes the mass of an element after separating everything except vapor by various means such as ion exchange, and high-speed liquidation.

9) A method of analyzing the content and components of a sample, and the electron's wavelength released after injecting electron into a target sample.

derwater explosion.

In the area of ship management, the team analyzed the possibility of ROKS Cheonan sinking due to non-explosion factors such as fatigue fracture, grounding, and collision by referring to ship maintenance records and the damage seen on ROKS Cheonan.

In the area of basic hull strength analysis, the latest structural analysis methods were used to analyze the stability of ROKS Cheonan in extreme sea conditions(wave height 10.06m) that can occur during 25~30 years of operation.

In the area of stability analysis, the design standard and capability of ROKS Cheonan's stability were analyzed. This analysis confirmed that ROKS Cheonan would not have any issue in stability under normal conditions. Further stability analysis of the fractured bow and stern was conducted.

In the area of analysis on the impact to the hull due to an underwater explosion, experts and measuring devices from the Defense Agency for Technology and Quality(DTaQ) were employed prior to the underwater explosion analysis to precisely measure and analyze the size and shape of the damage seen on the bow and stern. In order to evaluate the nature of the explosion(size of explosive and detonation location), a one-dimensional whipping<sup>10)</sup> analysis was conducted on the ship structure. Afterwards, a three-dimensional underwater explosion analysis was conducted for describing the destruction of ROKS Cheonan by using the explosion type that had been deduced by the Explosive Analysis Team.

## (3) Explosive Analysis Team

The Explosive Analysis Team consisted of 14 personnel(7 civilian, 5 military, 2 foreign) from ROK JCS, ADD as well as civilian and foreign experts. The Explosive Analysis Team divided its activities into sub-categories of torpedoes, mines, fluid analysis, and other explosives.

In order to analyze the cause of the sinking, a detailed analysis on the possibility of an internal explosion such as a magazine explosion, fuel tank explosion, diesel engine explosion or gas turbine explosion was conducted prior to the recovery of the ship. Following the recovery of the ship, an analysis on the possibility of an explosion on or above the sur-

.....  
10) Whipping: A phenomenon where an abrupt bending on the hull (interpreted as the beam) occurs by the effects from the expansion and contraction of the bubble.

face due to a cruise(anti-surface) missile or ballistic missile, as well as an analysis on the possibility of an underwater explosion due to a torpedo, mine, land-controlled mine or improvised explosive device(IED) was conducted. An on-site examination and investigation were conducted in parallel with the above analysis to find the cause of the sinking.

This process allowed the team to narrow down the possible weapon systems to torpedoes and mines. Following the recovery of the ship, it was scientifically proven that ROKS Cheonan was sunk due to a non-contact underwater explosion through analysis of the fractured surface, analysis of adhered materials, and simulations of the splitting of the ship.

In addition, the team came up with the most likely size of the explosive charge and explosion location through various underwater explosion simulations that took into account varying charge sizes and water depths.

#### **(4) Intelligence Analysis Team**

The Intelligence Analysis Team consisted of 4 investigation personnel(2 civilian, 2 military) from the Korea Defense Intelligence Agency(KDIA), National Oceanographic Research Institute(NORI), and Korea Ocean Research and Development Institute(KORDI), as well as 12 supporting personnel. The Intelligence Analysis Team was composed of 4 sub-teams focusing in maritime conditions, North Korea provocation analysis, technical intelligence, and TOD footage analysis.

In order to determine the cause of the sinking, the Intelligence Analysis Team analyzed the underwater obstacles(reefs) and characteristics of currents in the vicinity of Baekryong Island. The analysis of the underwater terrain was conducted in 5 phases for sequential verification. The analysis of the tidal current was done through analysis and verification using the tidal movement and current forecast system for military operations. A detailed analysis of the TOD imagery before and after the incident was conducted. For types of possible North Korean provocations, an analysis was conducted through categorization by types of infiltration assets and armaments. The technical intelligence analysis focused on supporting the Scientific Investigation Team with evidence collection in an attempt to identify the cause of the sinking.

### **3) Investigation Activities**

#### **(1) Prior to the Recovery of the Ship: March 31~April 14**

Prior to the recovery of the ship, each team of the JIG closely reviewed the operational timeline and actions of ROKS Cheonan. The JIG recruited personnel from the private sector and concurrently held discussions with relevant experts. Internal and external factors were both considered as a possible cause of the sinking. As for internal factors of the sinking, the analysis conducted by the ADD indicated that fatigue fracture was highly unlikely. The summary of the maintenance records also indicated that the possibility of maintenance failure causing the sinking was highly unlikely as well. In addition, a fuel tank explosion was assessed to be highly unlikely, because such an explosion would not satisfy the necessary conditions for the splitting of the ship.

As for the external factors of the sinking, the possibility of friendly mines was found to be limited according to the expert opinions and assessment by the JIG. An explosion of North Korean torpedoes and mines, on the other hand, was assessed to be possible by experts. There were no reefs on the sea charts of the incident location, and according to expert opinions, chopping waves would be highly unlikely to cause the sinking. In addition, radar records and TOD imagery of the incident location vicinity showed no other ships, indicating that sinking by a collision is highly unlikely as well.

An examination of key materials such as the clothing and recovered items resulted in no explosive residue being detected from the clothes of the survivors(9 items including service uniforms). The recovered items(3 items including MCR floor plate) from the surface and coast of Baekryong Island also showed no trace of fire.

#### **(2) After the Recovery of the Stern: April 15 ~ April 23**

During the recovery of the stern, the JIG organized an on-site investigation team of 57 personnel, which was deployed to ROKS Dokdo on April 14. The stern was recovered on April 15, and the on-site investigation results following the recovery of the stern were announced on April 16.

The preliminary on-site investigation led to the assessment that an internal explosion causing the sinking was highly unlikely. This assessment was based on the lack of burn damage on the interior structure, the good condition of the wires, and the upward defor-

mation of the hull bottom plating.

Grounding was also assessed to be highly unlikely given that the hull bottom was found in relatively good condition and that the fractured surface on the bottom of the stern was bent in an upward direction.

Fatigue fracture was assessed to be highly unlikely given that the fractured surface of the hull bottom was bent upward with an 80° angle and that the stiffeners located at the aft bulkhead of the gas turbine room were rolled up.

Therefore, it was assessed that an external explosion was the most likely possibility given that the hull fracture occurred from the port bottom toward the starboard side in an upward direction; no trace of fragments was found at the fractured surface; the bending of the hull was caused by external pressure; and the wires were cut and not melted by heat. An examination of the collected evidence from the scene, which consisted of 10 samples including interior materials from the fractured surface, was conducted to detect explosive residue and aluminum components.

A detailed examination of the stern was conducted on April 18. At this time, 147 samples of 29 types were collected. A 3-dimensional laser scan of the fractured stern was performed on April 21. The DTaQ took precise measurements of the damaged parts of the stern and conducted an investigation of the damaged locations and deformations. The on-site investigation during the recovery of the stern, and the detailed investigation following the recovery of the stern, which was conducted from April 15 to 25, led to the assessment that an external explosion was more likely than an internal explosion.

### (3) After the Recovery of the Bow: April 24 ~ May 19

The JIG sent an on-site investigation team of 50 personnel to Baekryong Island on April 23 for investigative activities following the recovery of the bow. The bow was recovered on April 24, and the investigation results following the recovery of the bow were announced on April 25. The second on-site investigation led to the assessment that the possibility of an internal explosion was highly unlikely given the intact magazines and fuel tanks, inward bending of the hull at the fractured surface, upward rolling of ribs and upward bending of the CVK.

A grounding was confirmed to be highly unlikely given that the hull bottom was found in good condition and the sonar dome<sup>11)</sup> located at the hull bottom did not show any damage.

11) Sonar dome: The cover for the sonar, and consists of special material to allow the transmission of the sound waves

Fatigue fracture was confirmed to be highly unlikely given the nature of the deformation: the fractured surface was significantly deformed in an upward direction due to external pressure, and complicated damage was delivered to ROKS Cheonan.

Among the factors of an external explosion, a contact explosion was assessed to be unlikely given the lack of soot within and outside the hull. Furthermore, there were no holes or traces of melting due to heat on the wires and interior materials at the fractured surface.

Therefore, the possibility of a non-contact external explosion was assessed to be highly likely based on the severe inward bending and severance of the hull due to shockwave and bubble effect generated by an underwater explosion.

The on-site investigation results indicated that the explosion occurred at the port of the gas turbine room centerline with pressure being exerted upward toward the starboard side. The size of the explosive charge was estimated through a simulation that took into account the size and shape of the damage seen.

A three-dimensional laser scanning was conducted on the fractured surface of the bow. A discussion on an underwater explosion hull whipping analysis by the US team was conducted on April 26. The on-site investigation during the recovery of the bow and the detailed investigation following the recovery of the bow, which was conducted from April 23 to May 19, led to the assessment that an underwater explosion occurred and that a non-contact explosion was more likely than a contact explosion.

### (4) The Recovery of the Torpedo Propulsion Motor: May 15

The propulsion motor and propellers of a torpedo propulsion system were recovered on May 15, during a detailed search of the seabed using a special net that began on May 10.

An analysis of the torpedo propulsion section confirmed that the recovered evidence was identical in size and shape to the schematics of a North Korean torpedo. Furthermore, the JIG was able to confirm through composition analysis that the adhered materials found on the torpedo propulsion section and ROKS Cheonan were identical. In addition, the Korean alphabet inscription in the rear of the propulsion section (“1번”, Number 1 in English) is similar in style with the Korean alphabet inscription method on a North Korean torpedo (“4호”, unit 4 in English) obtained in 2003 near waters in the vicinity of Pohang.

### (5) Press Conference on Investigation Result: May 20

During a press conference at the MND conference room with members of the local and foreign press corps in presence, Dr. Yoon Duk Yong(Civilian Co-chairman) announced the investigation result.

After taking the entirety of the analysis results of Korean and foreign experts on the following factors into consideration – the torpedo propulsion system recovered from the incident location, deformation of the hull, statements by related personnel, medical examination of the deceased and wounded service members, seismic and air acoustic waves, simulations of underwater explosions, tidal currents in the vicinity of Baekryong Island, and analysis of explosive components – the JIG confirmed the following:

ROKS Cheonan was split and sunk due to shockwave and bubble effect generated by the underwater explosion of a torpedo. The detonation location was 3m to the port from the center of the gas turbine room and at a depth of 6~9m. The weapon system used was a CHT-02D torpedo with roughly 250kg of explosives made by North Korea.

## 4. Overall Shape and Structures of ROKS Cheonan

ROKS Cheonan was constructed by Korea TACOMA Marine Ind.(merged with Hanjin Heavy Ind. & Construction Holdings co. in 1999), and after its acquisition to ROK Navy in 1988, it had been in operation for approximately 22 years before the incident.

ROKS Cheonan consisted of O-1 deck and O-2 deck above the main deck, and of 1st Platform and 2nd Platform below the main deck. On the main deck, from the bow-side to stern-side there were a ward room, officers' berthing, CPOs' mess, machinery control room and crew's mess. The CO's cabin, Combat Information Center, communication room, demist<sup>12)</sup>, and stack<sup>13)</sup> are located on the O-1 deck. The bridge and mast<sup>14)</sup> are located on the O-2 deck. On the bow-side of the 1st Platform, there are a deck admin room, sail/gunnery/operation crews' berthing, and CPOs' berthing. The machinery crews' berthing, CPOs' lounge, aft head, decontamination room, machinery storage, stern gun R/S, and steering

.....  
12) A demist is a device which inhales air that the engine needs and excludes moisture and dust.

13) A stack is a chimney which acts as an exhaust part of an engine.

14) A mast is located at the center of a ship.

gear room are located on the stern-side. On the 2nd Platform, firearms admin room, elec. maintenance room, and gyro room are located on the bow-side, and the gas turbine room and diesel engine room are on the stern-side. On the ship bottom, a sonar dome, fin stabilizer, and bilge keel<sup>15)</sup> are located.



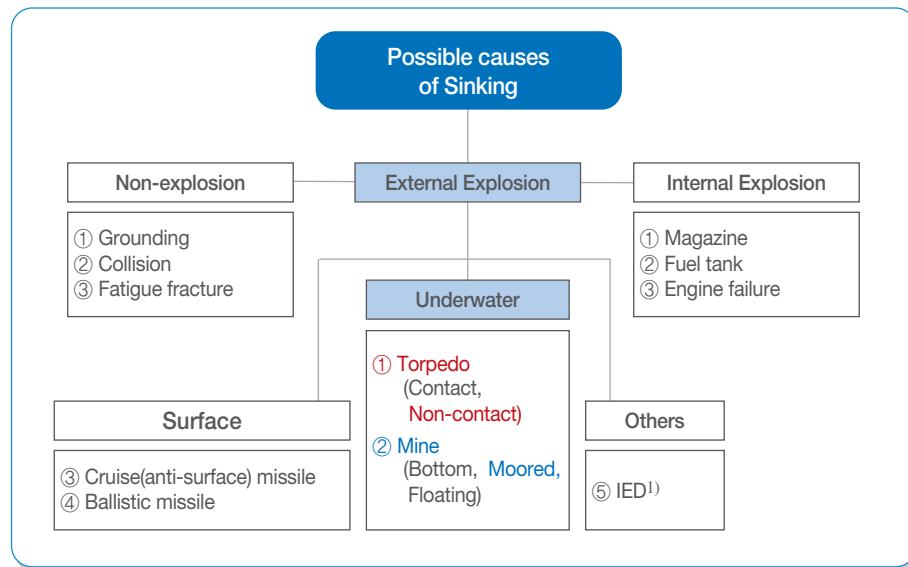
〈Figure I-4-1〉 Overall shape and structures of ROKS Cheonan

.....  
15) A bilge keel is located on the left and right side of a ship bottom mitigating blurring of a ship.

P a r t II

*Analysis on Possible  
Causes of the Sinking*





All possible causes of the sinking were analyzed after defining these factors in 3 categories: non-explosion, external explosion, and internal explosion. The evaluations were conducted under the review standards employed by IMO(International Maritime Organization) to assess the likelihood of each possible cause to the incident.

## 1. Non-explosion

### 1) Grounding

A damage inflicted on a ship by a grounding would typically result in lengthwise cutting on the bottom of the hull. Especially for vessels with a sonar dome on the bow(such as ROKS Cheonan), normally the sonar dome would be damaged prior to the hull in case of a grounding.

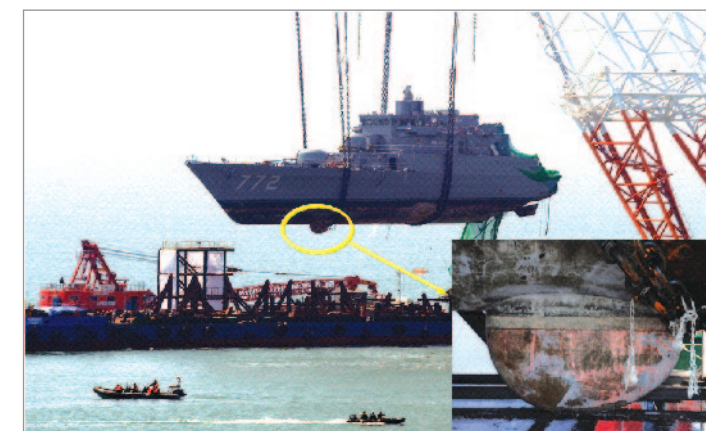
.....  
1) IED: Improvised Explosive Device.

### (1) Damage Indicators

Damage patterns	Investigation result
• Cutting effect in longitudinal direction on the bottom hull	None
• Scratch marks in longitudinal direction	None
• Damage on sonar dome and propellers	None
• Damage condition indicating grounding (damage caused by large plastic deformation <sup>2)</sup> )	None
• Possibility of grounding by depth and unknown reef	None
• Indications, warnings, and testimonies	None

### (2) Visual Inspection

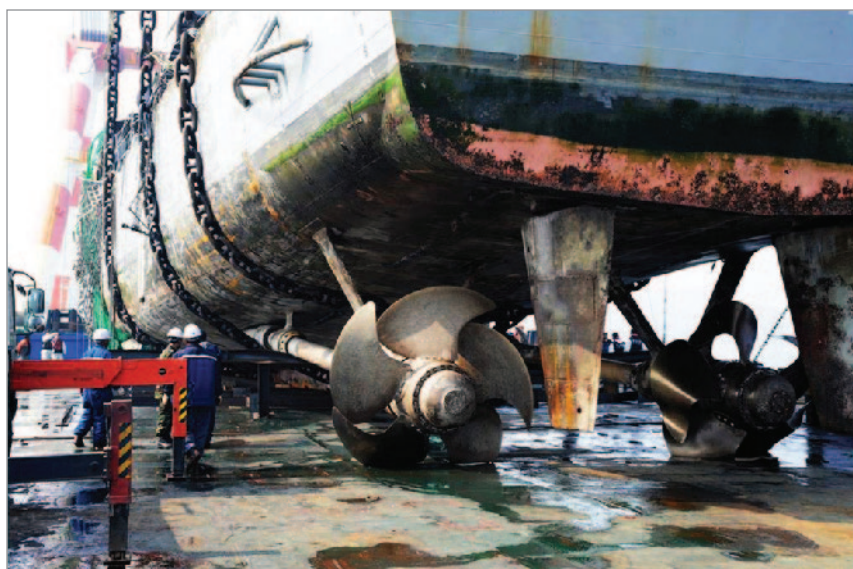
No scratch or cutting consistent with a grounding was found on ROKS Cheonan on the bottom of the hull along the longitudinal direction. In addition, the sonar dome, and propellers located on the very bottom of the ship, were observed with no grounding damages as displayed in <Figure II-1-1> and <Figure II-1-2>. Furthermore, two types of hull deformations, impossible to occur in a grounding event, were observed.



<Figure II-1-1> The sonar dome at the time of bow salvage

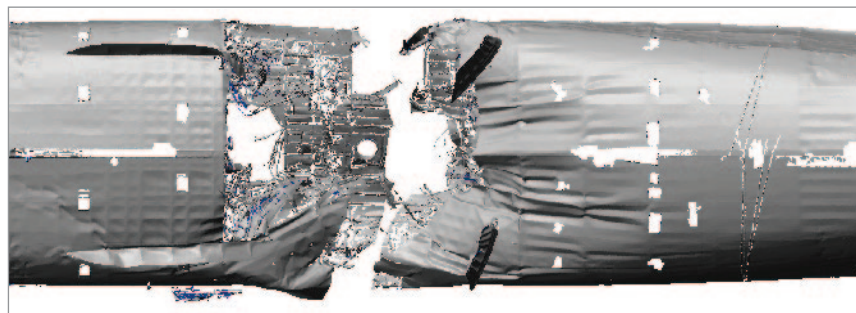
First, severe dishing(concave deformation of outer panels between stiffeners) was present on the bottom shell plates of the forward and aft sections of the gas turbine room

.....  
2) Plastic deformation: Permanent deformation by the force exceeding elastic limit of a material.



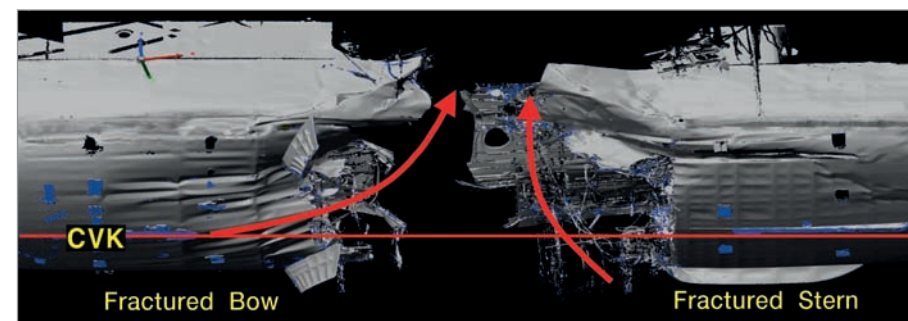
〈Figure II-1-2〉 ROKS Cheonan propellers upon the recovery of the stern

(See 〈Figure II-1-3〉). This is a result of extreme pressure impacting broadly on the shell plates due to shockwave and bubble effect, and cannot be explained with grounding as a cause.



〈Figure II-1-3〉 Dishing on the shell plating panels on the bottom of the hull

Secondly, shell plates on the bottom of the fractured area bent significantly inward. On the stern side of the fractured areas, shell plates were deformed in an upward direction, from the bottom of the hull to the main deck level(See 〈Figure II-1-4〉). The shell plates on the bow portside of the fractured areas also suffered an equivalent level of inward deformation. The shell plates on the portside of the bow were deformed in concave curvature with the



〈Figure II-1-4〉 3D laser scanning images on breakplanes of bow and stern

center located outside of the ship. The CVK below the gas turbine room, as shown in 〈Figure II-1-5〉, had also been severely deformed in an arc-shape by spherical pressure. These cannot occur in case of a grounding.

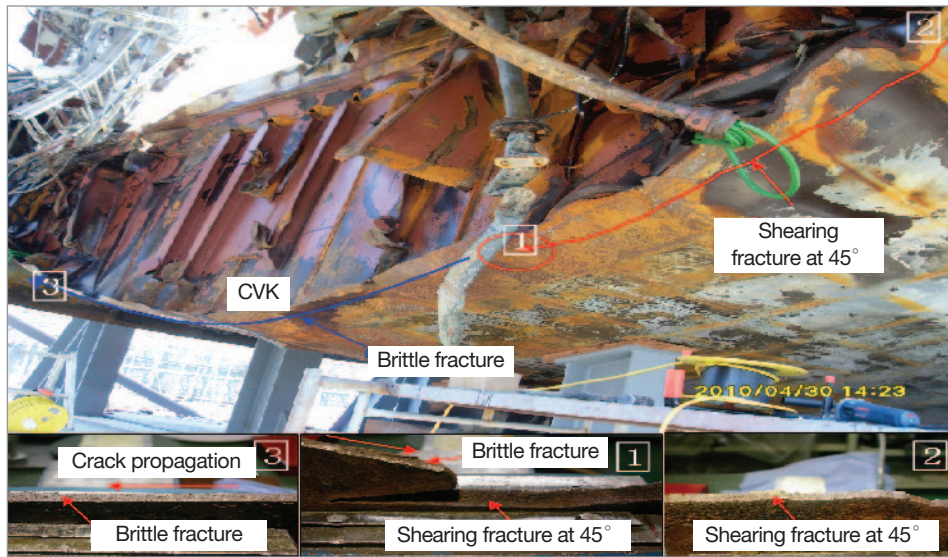


〈Figure II-1-5〉 Shell plates of ROKS Cheonan gas turbine room

On the other hand, the damage characterization of the fractured surface did not reveal traces of large plastic deformation caused by loss of longitudinal strength<sup>3)</sup> after a grounding, but shearing fracture<sup>4)</sup>, which results from instantaneous pressure on shell plating along the direction of plating thickness, and brittle fracture<sup>5)</sup> by a rapid deformation(See 〈Figure II-1-6〉).

Also, after examining the deformation of the starboard propellers, it was assessed that

3) Longitudinal strength: The strength to endure the loading or any other pressure on the longitudinal direction of the hull.  
 4) Shear fracture: Instantaneous force severs an object plane in shear direction.  
 5) Brittle fracture: An object fractured by external force without expansion in size(length, width, etc.).



〈Figure II-1-6〉 Analysis result on the damage characteristics of the fractured surface seen on ROKS Cheonan

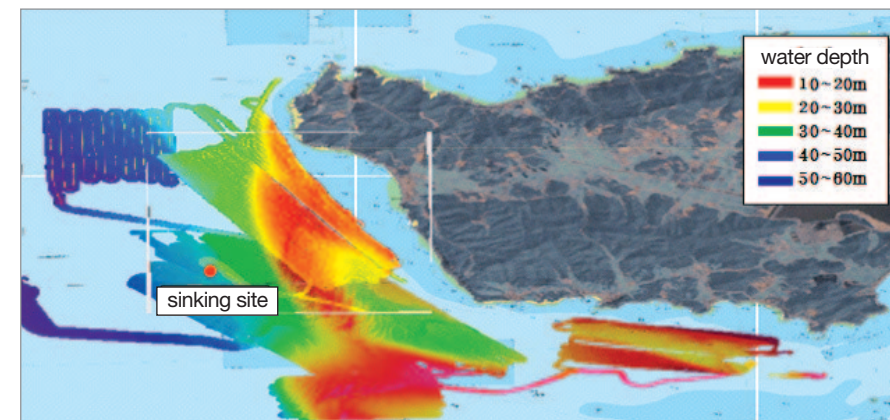
the break of the blades or global scratch marks were absent, which would have occurred in case of grounding, but no such traces were found. Instead, 5 blades were bent toward the bow side in a symmetric manner(See 〈Figure II-1-7〉). The Swedish Investigation Team assessed that this type of deformation cannot occur due to a grounding event, and concluded the possible cause as the mass force of inertia, which was created from the sudden halt of the propeller rotation, and propulsion shaft being pushed severely.



〈Figure II-1-7〉 The deformation of starboard propellers

### (3) Environmental Conditions

According to the data of ROKS Cheonan, the draft of the ship is 2.88m. Judging from the growth of seaweed remaining on the hull, operational draft is estimated to be an average of less than 3.1m. The water depth of the incident site is 47m. It is known that the depth at the shallowest point around the operational area is 8.6m, thus leaving no possibility for ROKS Cheonan to make contact with the seabed. In addition, there were no obstacles identified in the water after thorough probing on the incident site from March 28 to May 8 with 4 Navy mine sweeping vessels and 2 investigation vessels from KORDI(See 〈Figure II-1-8〉). It was also discovered that artificial reefs were placed at depths of around 17~34m. This also leaves no possibility of contact with the seafloor. These facts were verified by the Australian Investigation Team.



〈Figure II-1-8〉 Probing result of seafloor geography in incident site

### (4) Modeling and Simulation(M&S)

M&S were not conducted due to no possibility of a grounding with little practical significance expected.

### (5) Indication and Warning

There were no indication and warning that can support a grounding as the cause of the sinking of ROKS Cheonan.

**(6) Statement from Relevant Personnel**

There is no statement that can support a grounding.

**(7) Conclusion: No Possibility**

The damage conditions that would be present in case of a grounding such as longitudinal cutting effects, hull scratch, sonar dome and propeller damage(located under hull bottom), and others were not present. In addition, it is confirmed that there are no known reefs in the incident sea area. Furthermore, since dishing effect(normally generated from underwater explosion) was apparent on the bottom shell plating, the possibility of damage from reefs or other grounding events was rejected.

**2) Collision**

When an incoming ship collides into a victim ship during navigation, the side shell plates of the victim ship are torn apart, and the fracture shape normally appears in a form almost identical to the head of the incoming ship.

Additionally, the trace of an incoming vessel such as paint will remain at the collided(victim) vessel.

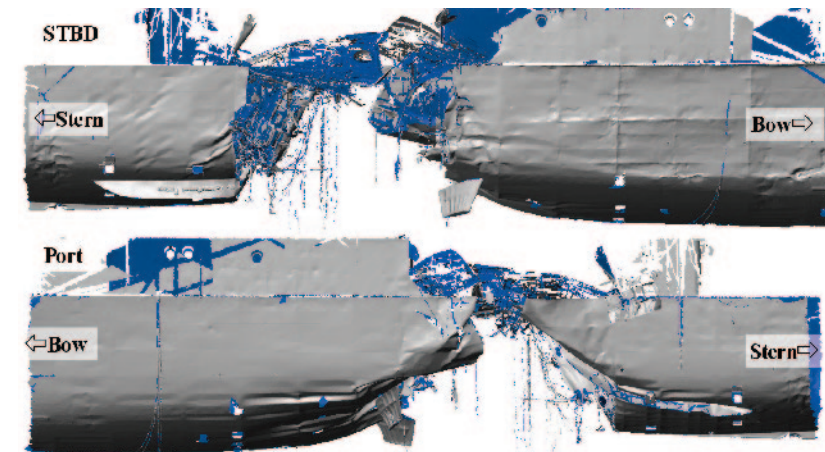
**(1) Damage Indicators**

Damage patterns	Investigation result
• Damage condition indicating collision(head shape of incoming ship)	None
• Traces and debris left by incoming ship on victim ship	None
• Vessels operated in nearby area at the time of incident	None
• Indications, warnings, and testimonies	None

**(2) Visual Inspection**

When observing the fracture shape of ROKS Cheonan on the sides(See <Figure II-1-9>), there are no apparent fractures and debris that resemble a bow of an incoming ship. Furthermore, the overall fracture status indicates a massive upward force originated from the bottom. Additionally, the dishing effect apparent on the bottom plate of the ship, shown in

<Figure II-1-3>, is a deformation that cannot occur through a collision but can be seen as a result of intense shock pressure from underwater.



<Figure II-1-9> Fractured areas of ROKS Cheonan

**(3) Environmental Condition**

There is no possibility of a collision since KNTDS(Korea Naval Tactics Data System) and AIS(Automatic Identification System) data confirmed that there were no vessels within 5.5 miles of ROKS Cheonan at the time of the incident. Furthermore, no vessels were confirmed to be operating near ROKS Cheonan on the TOD imagery.

**(4) Modeling and Simulation**

Since there is no possibility of a collision, M&S were not conducted with little practical significance expected.

**(5) Indication and Warning**

At the time of the incident, there were no indication and warning relating to a collision.

**(6) Statement from Relevant Personnel**

There was no testimony made by the survivors and the rescuers relating to a collision, and rescue operation footage captured no vessels involved in a collision.

**(7) Conclusion: No Possibility**

The damage status that correlates to a collision, such as the shape of a bow of an incoming ship, traces, debris indicating a collision, and nearby vessels in the area at the time of the incident were not present. Additionally, there are no survivor testimonies related to a collision. Furthermore, since dishing effect, which can occur through a non-contact underwater explosion, was apparent on the bottom plate, the possibility of a collision was disregarded.

**3) Fatigue Fracture**

Fatigue fracture, where fracture occurs at a lower level of stress<sup>6)</sup> than the yield stress of the material, can take place when a structure is exposed to a repeated load. The crack (which begins when the stress cycle reaches limit) gradually expands and may result in unstable breakdown if it reaches the critical size, and it usually initiates from the surface rather than in the interior. At the initiating phase of a crack, a complete destruction of the hull is almost impossible.

If repeated load is applied to the crack, it expands and propagates. Generally, this phase also does not develop rapidly, and is detected and repaired through a periodic inspection. These minute cracks are kept at a level that can only create local damage on structural members<sup>7)</sup>, so it is nearly impossible for them to result in a catastrophic accident such as the hull breaking down in half.

The fractured surfaces due to fatigue fracture would leave beach marks as a trace. Also, the clean cut split on each surface would allow the exact match between the fractured surfaces when fitted together.

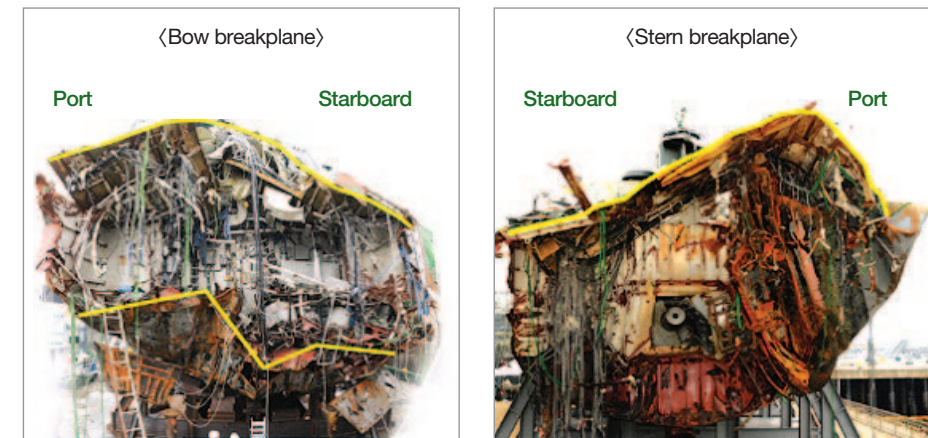
**(1) Damage Indicators**

Damage patterns	Investigation result
• Crack in the hull	None
• Damage cutting indicating fatigue fracture (beach mark on fractured surface, clean-cut fractured surface)	None
• Hull aging	Insufficient to fail
• Indications, warnings, and testimonies	None

6) Stress: The counter force created within an object as a reaction when the object is affected with the external force.  
 7) Structural members: The materials consisting the ship.

**(2) Visual Inspection**

A close inspection on the breakplane of ROKS Cheonan reveals that the bottom of the bow was bent upward, while the stern portside bottom was deformed extremely upward to the main deck level, to the point that it is almost not recognizable(See <Figure II-1-10>). The fractured surface on the bottom of the stern is cut clean at in front of the transverse bulkhead.



<Figure II-1-10> Breakplane of the bow and stern

After examining the damages seen in <Figure II-1-6>, it was verified that an enormous force exerted in an upward direction from the bottom resulted in instantaneous shearing around bulkheads and external breakdown accompanied by a large plastic deformation. Also, the rigid foundation of the gas turbine and the side structure of the starboard side were fallen apart, and the bottom of starboard side of the bow breakplane has also been torn out because of intense tensile force.

**(3) Environmental Conditions**

ROKS Cheonan had been in service for 22 years since its commission and had not reached the end of its service life(25 years). For the last 5 years, ROKS Cheonan had been under maintenance for a total of 14 times over 69 weeks. Extensive maintenance in the fleet was conducted a total of 5 times over 9 weeks with safety maintenance done on the hull such as anti-fouling coating and ultrasonic tests. Especially, no cracks or indicative evidences were discovered in the previous maintenance.

Also, after the hull was recovered, ultrasonic tests were conducted on April 30, 2010 to check

the condition of the hull. Since the average hull thickness reduction(See <Table II-1-1>) was 3.22%, significantly below the reserve thickness reduction of 20%, the condition of the hull was confirmed to be sufficient(for the design standard) to render no possibility of fatigue damage.

CAT	Port (avg. thickness: mm)			Starboard (avg. thickness: mm)			Overall
	Initial thickness	Measured thickness	Avg. corrosion(%)	Initial thickness	Measured thickness	Avg. corrosion(%)	Avg. corrosion(%)
Diesel engine room	9	8.75	2.77	9	8.67	3.66	3.215
	11	10.59	3.72	11	10.63	3.36	3.54
	11	10.68	2.90	11	10.55	4.09	3.495
	15	14.59	2.73	15	14.61	2.60	2.665
			3.03			3.42	3.22

<Table II-1-1> Ultrasonic test results on the hull(April 30, 2010)

#### (4) Modeling and Simulation

M&S were not conducted because there is no possibility of fatigue fracture with little practical significance expected.

#### (5) Indication and Warning

There were no indication and warning of hull cracking or fatigue fracture.

#### (6) Statement from Relevant Personnel

After interviewing one of the survivors responsible for maintenance and repair of the ship, he reiterated that there were no cracks throughout ROKS Cheonan. There were no other testimonies that could support the possibility of fatigue fracture.

#### (7) Conclusion: No Possibility

No hull cracking was discovered in ROKS Cheonan prior to the incident. Also, beach marks which are normally found in fatigue fractures, were not present on the structures and fractured surface of the hull. The ultrasonic tests also revealed the thickness reduction of the hull plates at 3.22% on average, which indicates a good condition for operation. Additionally, the dishing effect on the shell plates and observed damage shapes were consistent with the effects of a non-contact underwater explosion. Thus, the JIG rejected the possibility of fatigue fracture as a cause of the incident.

## 2. Internal Explosion

### 1) Magazine Explosion

ROKS Cheonan mostly conducts patrol missions with an installment of 40 and 76mm naval guns, anti-surface Harpoon missiles, anti-submarine depth charges, and other various types of explosives.

#### (1) Damage Indicators

Damage patterns	Investigation result
• Completely broken apart or damaged bulkhead of magazine and upper deck from the center of detonation	None
• Outward bending of deck and sideshells	None
• Trace of fire / soot	None
• Fragment marks and damage holes created by fragments on the bulkhead and upper deck of magazine	None
• Damage on the gun in case of R/S room explosion	None
• Internal damage in magazine and damaged ammo inside	None
• Numerous burn injuries from heat and hearing damage	None

#### (2) Visual Inspection

TOD footage showed that ROKS Cheonan was sunk and broken in half. It was confirmed following the recovery of the ship that it had been split up in the middle.



<Figure II-2-1> Shape of damage on ROKS Cheonan



〈Figure II-2-2〉 Conditions of the bottom of bow and stern

Investigation on the exterior of the stern and the bow, where 40 and 76mm magazines are located, showed that no upper iron plates of the waterline had undergone bending effects. In addition, the magazines showed no trace of internal damages, and there was no deformation in an outwardly direction on the magazine bulkhead and no damages resulting from fragments. Furthermore, no leftover fragments were found.

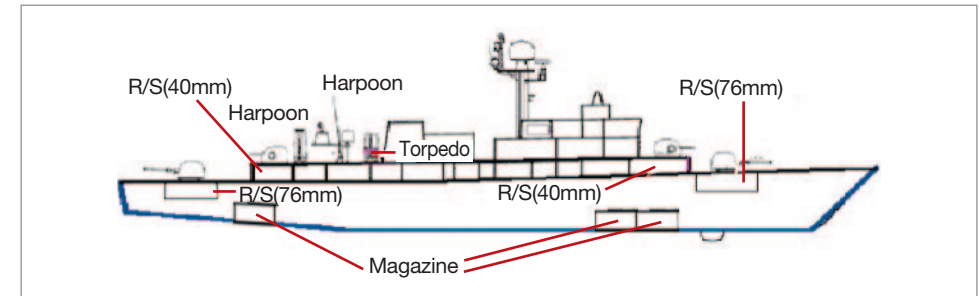
In addition, the salvaged ammunition cases were only bent as a result of the water pressure without traces of an explosion(See 〈Figure II-2-3〉).



〈Figure II-2-3〉 Conditions of magazines after the hull recovery

### (3) Environmental Condition

〈Figure II-2-4〉 below depicts specific locations of the major ammunition storage area(excluding small arms, etc.). Harpoon missiles, Mistral missiles, torpedoes, depth charges, and small depth charges are located on board and 40 and 76mm ammunitions are stored inside the ship.



〈Figure II-2-4〉 Ammunitions layout on ROKS Cheonan

### (4) Indication and Warning

There were no unusual indication and warning regarding an ammunition explosion prior to the incident.

### (5) Modeling and Simulation

No magazine explosion modeling and simulation were performed due to no possibility of a magazine explosion with little practical significance expected.

### (6) Statement from Relevant Personnel

Most survivors heard one explosion noise but one heard a “wham” and a “bang” noise(another crew heard “gwang”, “gwa~ang”). At the time of the incident, hull and crew members’ bodies were lifted up to the air approximately 30~100cm and dropped back onto the surface. All crew members testified that they did not witness any fire or smell explosives.

### (7) Conclusion: No Possibility

After the hull recovery, counting of the installed ammunitions from ROKS Cheonan showed

that a few 5.56mm ammunitions, small depth charge fuses, and R-BOC<sup>8)</sup> were lost.

All the munitions stored in the upper deck were installed with full consideration of their safety. Regarding the operation mechanisms of these munitions, there is no possibility of a self-detonation. In case of the self-detonation, these munitions would have only caused local damages; the self-detonation of these ammunition can not cause a comprehensive damage to the hull. The gun rounds stored in the bottom of the ship could have caused a significant damage to the hull given their net explosive weight. However, since these ammunitions are stored at the bow and stern, they cannot cause the splitting of the ship's center.

Additionally, there were no traces of an explosion in the bottom of the ship and magazines. Also, the entirety of 76 and 40mm ammunition was recovered further proving that the magazine explosion did not occur.

## 2) Fuel Tank Explosion

### (1) Damage Indicators

Damage patterns	Investigation result
<ul style="list-style-type: none"> <li>Broken apart or damaged bulkhead of fuel tank and upper deck from the center of detonation</li> </ul>	None
<ul style="list-style-type: none"> <li>Outward bending of side plating of fuel tank</li> </ul>	None
<ul style="list-style-type: none"> <li>Trace of fire occurrence, and soot from fuel vapor</li> </ul>	None
<ul style="list-style-type: none"> <li>Damaged fuel pipe</li> </ul>	None
<ul style="list-style-type: none"> <li>Weakened fuel tank material due to explosion</li> </ul>	None
<ul style="list-style-type: none"> <li>Outward bending of hull shell plating</li> </ul>	None
<ul style="list-style-type: none"> <li>Damaged fuel tank in the bow and stern</li> </ul>	None

### (2) Visual Inspection

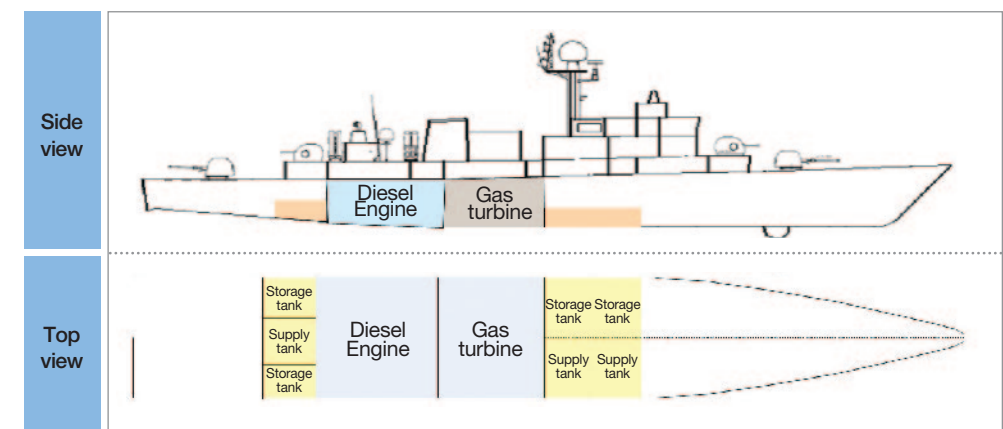
Damage on the hull is not at the fuel tank and is not consistent with that of a fuel tank explosion. After recovering the hull, it was confirmed that the two fuel tanks behind the diesel engine room and in front of the gas turbine room were not damaged. The fuel, mixed with

.....  
8) A device that spreads aluminum pieces near the enemy's guided missile in order to induce the missile towards another direction.

seawater, remained in a relatively good condition and was recovered and disposed of. The side plating and bottom hull were intact. In other words, there was no trace of a fuel tank explosion.

### (3) Environmental Condition

〈Figure II-2-5〉 illustrates the fuel tank locations of ROKS Cheonan. No damaged conditions were found after the inspection on these tanks, the remaining fuel was preserved, with no traces of fire or an explosion observed.



〈Figure II-2-5〉 Location of fuel tank of ROKS Cheonan

### (4) Modeling and Simulation

No fuel tank explosion modeling and simulation were performed due to no possibility of a fuel tank explosion with little practical significance expected.

### (5) Indication and Warning

There were no unusual indication and warning regarding a fuel tank explosion prior to the incident.

### (6) Statements from Relevant Personnel

There were no relevant statements to support that a fuel tank explosion was the cause of the sinking.

### (7) Conclusion: No possibility

Although there was an ambiguity of statements from the survivors, there were no crews that witnessed fire, or fire column. After recovering ROKS Cheonan, no traces of fire, soot or an internal explosion of the fuel tank were found. The stern fuel tank was in a good condition and with the exception of 2 bow supply tanks, which had moved upwards, there were no significant changes in structure. Therefore, the assessment is that a fuel explosion did not occur. The investigation of the fuel tanks showed that the 2 bow storage tanks were not damaged, and 2 supply tanks were moved upwards due to the damage to the gas turbine room. The 3 tanks in the stern were in a good condition. In conclusion, it was confirmed that ROKS Cheonan did not sink due to a fuel tank explosion.

### 3) Diesel Engine Defect

There were two MTU 12V 956 TB 82 diesel engines on ROKS Cheonan, with each engine connected to the right and left shaft respectively. Normally, both engines are used during the ship's maneuver.

#### (1) Damage Indicators

Damage patterns	Investigation result
<ul style="list-style-type: none"> <li>Broken apart or ripped apart bulkhead of diesel engine room and upper deck from the center of detonation</li> </ul>	None
<ul style="list-style-type: none"> <li>Outward bending of side shell plate of diesel engine room above waterline</li> </ul>	None
<ul style="list-style-type: none"> <li>Trace of fire occurrence and soot</li> </ul>	None
<ul style="list-style-type: none"> <li>Damage holes due to fragmentation from an explosion</li> </ul>	None
<ul style="list-style-type: none"> <li>Damaged diesel engine room</li> </ul>	None
<ul style="list-style-type: none"> <li>Outward bending of hull shell plating</li> </ul>	None

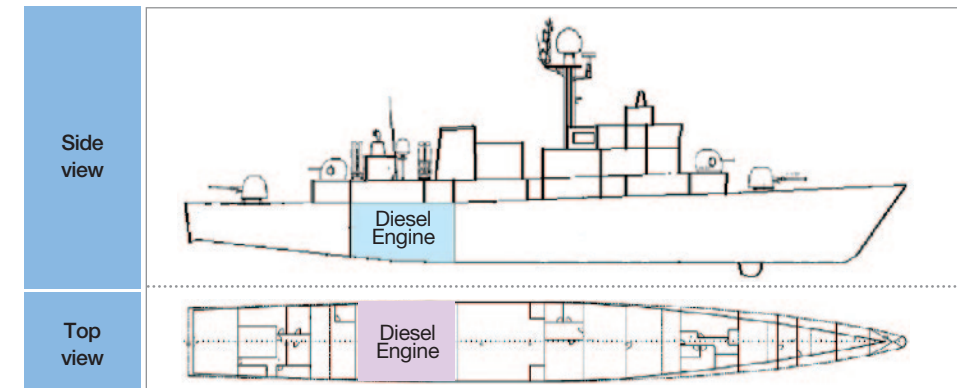
#### (2) Visual Inspection

The front bulkhead of diesel engine room was damaged towards the stern direction. The gear box and shafts were found bent upwards and toward the starboard, with the starboard shaft bent more than the port. The two diesel engines did not show any damage that would result from an internal explosion and remained in a relatively good condition.

### (3) Environmental condition

#### ① Location of the Diesel Engine

The location of the diesel engine is in the stern side on the bottom of the ship as shown in <Figure II-2-6>.



<Figure II-2-6> Location of the diesel engine room of ROKS Cheonan

#### ② Possibility and Checklist for the Possibility of Diesel Engine Explosion

The following <Table II-2-1> lists the result of the analysis on the possibility of a diesel engine explosion. The analysis referred to an up-to-date investigation and analysis, documents regarding the maintenance and operation of ROKS Cheonan and inspection following the recovery of the ship.

Category	Check-list	Analysis Result	
Related Documents	<ul style="list-style-type: none"> <li>Engine records and operation records(life cycle, etc.)</li> <li>Anything special during "operations"</li> <li>Check on regular maintenance schedule and implementation</li> </ul>	Although the life cycle was over, regular maintenance was done and no problem was found with operation	
Survivor statements	<ul style="list-style-type: none"> <li>Explosion sound</li> <li>Check on sound of engine</li> <li>Sound of metal breaking, internal shock sound</li> <li>Check on fire alarm in engine room</li> </ul>	<ul style="list-style-type: none"> <li>None Heard</li> <li>None Heard</li> <li>Not activated</li> </ul>	
Condition During Recovery	Engine	<ul style="list-style-type: none"> <li>Damage of exhaust such as engine cylinder.</li> <li>Damage (pressure, temperature) to engine gauges</li> </ul>	<ul style="list-style-type: none"> <li>No damage</li> <li>No trace of explosive</li> </ul>
	Engine Room	<ul style="list-style-type: none"> <li>Leaking of fuel or lubricants in the engine room</li> <li>Are there any secondary damages due to engine explosion</li> <li>Equipment damage in engine area, fire, soot</li> <li>Damage to the ENG' BED, etc.</li> </ul>	No signs of fire and soot in engine room. Engine was in proper spot
	Engine Room Wall	<ul style="list-style-type: none"> <li>Hole, scratch to the side bulkhead of engine room</li> <li>Soot on side bulkhead and ceiling of the engine room</li> </ul>	No signs of hole to bulkheads or scratches

<Table II-2-1> Analysis result on the possibility of diesel engine explosion

After checking the maintenance and operations records of ROKS Cheonan with the ROK Navy maintenance information system at ROK 2nd Fleet N4, it was found that the diesel engine has been in operation since 1988. Although this exceeds the life cycle(2008), regular maintenance was conducted internally and through outsourcing. The summary of maintenance records for total operated hours is shown in <Table II-2-2> . As displayed, the maintenance period for both internal and outsourcing were never reached at the time of the incident.

Category	First operated	Maintenance		Total operated hours since maintenance	
		W-5 maint.	W-6 maint.	W-5 maint.	W-6 maint.
No.1 D/E	'88. 12. 29	'07. 4. 30 '09. 5. 13	'08. 2. 22	2,288	5,434
No.2 D/E	'88. 12. 29	'07. 4. 30 '09. 5. 13	'08. 2. 22	2,288	5,434
Maintenance cycle	<ul style="list-style-type: none"> <li>• Life cycle(years) : 20 years</li> <li>• W-5 (internal maintenance) : Operates 3,000 hours</li> <li>• W-6 (outsourced maintenance) : Operates 9,000 hours</li> </ul>				

<Table II-2-2> Diesel engine operation & maintenance records

The summary of the maintenance record in the ROK Navy maintenance information system for the past 3 years is listed in <Table II-2-3> below(detailed information can be accessed in Navy Maintenance Information System).

Year	Maintenance record
2007	• Cylinder head inspection and repair etc. 28 cases
2008	• Circulation pump motor repair etc. 15 cases
2009	• Air isolation equipment repair etc. 50 cases

<Table II-2-3> Diesel engine maintenance records for past 3 years

In addition, after checking with national agencies, manufacturers, and Navy engine operators for manuals and technical materials, it was found that the diesel engine explosion is highly unlikely. Even in case of an explosion, it will be limited to the engine components, and given the size of the diesel engine room(10m × 10m), any form of an explosion would not result in the fracture of the hull. In theory, an explosion of the diesel engine would cause a massive fire. However, there are fire detectors and extinguishers equipped to put out the fire. Therefore, fire would not lead to an explosion of the ship. No traces of fire were

found in the ship after the recovery of the ship.

There is no possibility of an engine explosion by overload because the fuel and exhaust supply line are automatically isolated in the occurrence of overload. Even in case of an overload of oil pen vapor, the possibility of fire is extremely limited due to the automatic safety measures that are installed.

In order to check the condition of the engine at the time of the incident, survivors' statements were used as a reference. At the time of the incident, ROKS Cheonan was operating at a low speed of 6.7kts, which indicates that the possibility of the engine overheating is very low to almost nonexistent. The survivors did not report witnessing any fire or hearing anything resembling a metallic explosion sound that would have resulted from an engine explosion.

#### (4) Modeling and Simulation

No diesel engine explosion modeling and simulation were performed due to no possibility of a diesel engine explosion with little practical significance expected.

#### (5) Indication and Warning

There were no unusual indication and warning regarding a diesel engine explosion prior to the incident.

#### (6) Statement from Relevant Personnel

There was no relevant statement to support that a diesel engine explosion was the cause of the sinking.

#### (7) Conclusion: No Possibility

Although the ROKS Cheonan diesel engine had exceeded its life cycle, no operational problems were ever identified from the normal depot maintenance(W-5 or W-6). Fundamentally, a diesel engine explosion is highly unlikely by nature. While the destruction of the main components can scatter debris as a result of overloading the diesel engine, this would be restricted to the interior of the engine room and would not lead to an explosion. Furthermore, since the ROKS Cheonan was operating at a low speed at the time of the incident, there could not have been an overloading of the engine. Therefore, it was assessed that an engine explosion was not the cause of the incident.

## 4) Gas Turbine Defect

ROKS Cheonan has one LM-2500 gas turbine, and it is used mainly for high speed maneuvers.

### (1) Damage Indicators

Damage patterns	Investigation result
<ul style="list-style-type: none"> <li>Broken apart or ripped apart bulkhead of gas turbine room and upper deck from the center of detonation</li> </ul>	Observed
<ul style="list-style-type: none"> <li>Outward bending of side shell plate of gas turbine room above waterline</li> </ul>	Observed
<ul style="list-style-type: none"> <li>Trace of fire occurrence and soot</li> </ul>	None
<ul style="list-style-type: none"> <li>Damage holes due to fragmentation from an explosion</li> </ul>	None
<ul style="list-style-type: none"> <li>Damaged gas turbine room</li> </ul>	Observed
<ul style="list-style-type: none"> <li>Outward bending of hull shell plating</li> </ul>	None

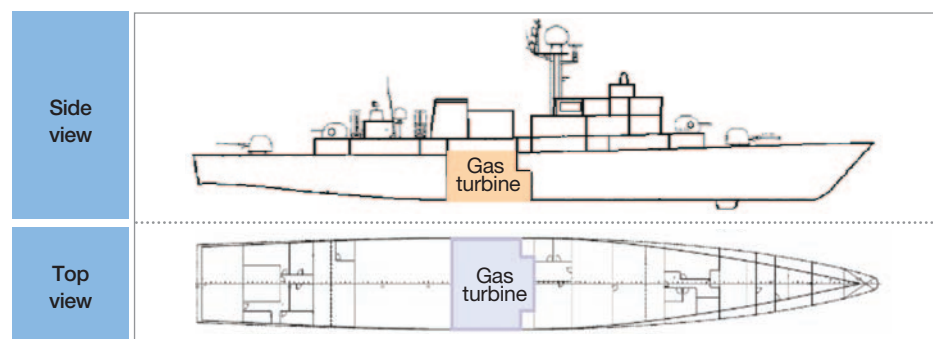
### (2) Visual Inspection

The starboard shell plating and upper deck were blown off in an outward direction from the gas turbine room by explosion. An inward deformation of the hull occurred and no traces of fire, soot or damage holes due to fragmentation were found.

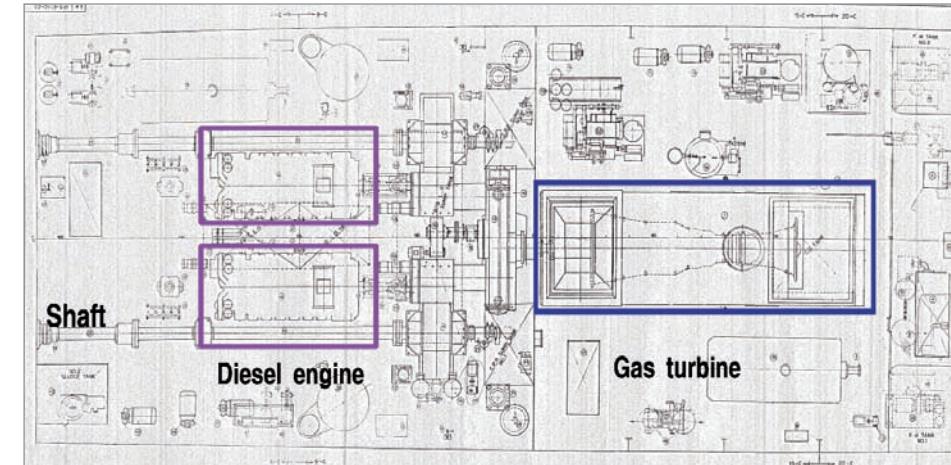
### (3) Environmental Condition

#### ① Location of the Gas Turbine

The gas turbine room is located in the middle of the ship and in front of the diesel engine room. The drawings of the gas turbine, shaft, and screw are shown in <Figure II-2-8>.



<Figure II-2-7> Location of the gas turbine of ROKS Cheonan



<Figure II-2-8> The positions of ROKS Cheonan gas turbine, diesel engine, and shaft

#### ② Phenomenon and Checklist of Gas Turbine Explosion

In a gas turbine, the compressor compresses the air and the diesel fuel is burned to generate gas in the G/G(Gas Generator) in order to operate the PT(Power Turbine) which then generates propulsion force. By nature, the gas turbine explosion is highly unlikely. Although fires can occur, there is a fire resistant wall that prevents the spread of fire. The characteristics and causes of damage for the gas turbine are listed in <Table II-2-4>.

Cause of damage	Characteristics
<ul style="list-style-type: none"> <li>Defective gas turbine components</li> <li>- Fracture between Gas turbine HSFCS and reduction gear</li> </ul>	<ul style="list-style-type: none"> <li>Damage to key components of gas turbine</li> <li>• Fire within the protective box</li> </ul>

<Table II-2-4> Cause of damage to gas turbine & characteristics

In regards to the gas turbine damage, key components of the gas turbine can be damaged. However, since these components are within a protective box, the possibility of this damage causing further damage to the whole ship is very low. In addition, if fire starts due to the damaged components within the protective box, the automated alarms and extinguishing system within the box immediately put the fire out.

The following <Table II-2-5> lists the result of the analysis on the possibility of the gas turbine explosion. The analysis referred to documents regarding maintenance and operation of ROKS Cheonan, testimony of the survivors, and inspection after the recovery of the ship.

Category		Checklist	Analysis Result
Check related documents		<ul style="list-style-type: none"> <li>• Engine records and operation records(life cycle, etc.)</li> <li>• Anything unusual during “operations”</li> <li>• Regular maintenance schedule and implementation</li> </ul>	Although the life cycle was over, regular maintenance was done and no problem operating it
Survivor statements	Sounds	• Too much noise from the gas turbine	None Heard
		• Sound of metal breaking, internal shock sound	None Heard
Condition during recovery	Gas turbine	• Damage to exhaust, compressor or turbine <sup>9)</sup>	Partially damaged
		• Damage to protective box and evidence of soot	Bow side lost, stern side intact
		• Physical damage to connective device of gas turbine(reduction gear)	Partially damaged
		• Activation of fire alarm in gas turbine room	Not activated
	• Damage to key components such as exhaust	Not damaged	
Protective wall	<ul style="list-style-type: none"> <li>• Evidence of fire or soot on walls</li> <li>• Damage to gas turbine armrest bold, etc.</li> </ul>	Detached away but recovered	

〈Table II-2-5〉 Analysis on possibility of gas turbine explosion

After checking the maintenance and operations records of ROKS Cheonan with the ROK Navy maintenance information systems at ROK 2nd Fleet N4 to confirm the gas turbine condition before the incident, it was found that the gas turbine had been in operation since 1988. Although 20 years had passed, the gas turbine had been in operation for a total of 5,213 hours, had only reached a quarter of its dismantle maintenance cycle, and maintenance was conducted regularly. The summary of maintenance records for the past 3 years is shown in 〈Table II-2-6〉 below.

Year	Maintenance records
2007	• Turbine frame, turbine fins, and converter etc. 17 cases
2008	• Vibration detecting circuit inspection etc. 15 cases
2009	• Fixed side fin inspection and repair etc. 36 cases

〈Table II-2-6〉 Gas turbine maintenance records for past 3 years

In addition, after checking with national agencies, manufacturers, and Navy engine operators for manuals and technical materials, it was confirmed that since the gas turbine

9) Gas turbine was initially lost, but was recovered on May 9th, with no heavy damage.

uses diesel fuel by design, its explosion is highly unlikely. There is a slight possibility of fire(almost none), but the gas turbine is inside a protective box, and thus the possibility of fire spreading to the rest of the ship is next to none. Even if fire occurs, there are fire detectors and extinguishers equipped in the protective box to put the fire out. Therefore, fire from the gas turbine would not lead to an explosion of the ship.



〈Figure II-2-9〉 Gas turbine protective box

After recovering the bow and stern of ROKS Cheonan, it was found that the gas turbine room had been lost. However, after an extensive search, components of the gas turbine were recovered. There was no trace of damage holes to the bulkhead between the gas turbine room and the diesel engine room which would have been produced by an engine damage. In case of the gas turbine damage, the turbine blades would disperse and create damage holes on the nearby walls. The CCTV footage recorded up to the incident also shows no indication of damage to the gas turbine or fire. Also, the survivor statements indicate that ROKS Cheonan was maneuvering at a speed of 6.7kts and therefore was not operating the gas turbine.

#### (4) Modeling and Simulation

No gas turbine explosion modeling and simulation were performed due to no possibility of a gas turbine explosion with little practical significance expected.

#### (5) Indication and Warning

There were no unusual indication and warning regarding a gas turbine explosion prior to

the incident.

### (6) Statement from Relevant Personnel

There was no relevant statement to support that a gas turbine explosion was the cause of the sinking.

### (7) Conclusion: No possibility

Although the life cycle of the gas turbine had been exceeded, regular maintenance had been conducted, and the gas turbine had been in operation for only 25% of the hours set for dismantle maintenance under fine condition of continuing operation. Based on the structural characteristics of the gas turbine, the possibility of an explosion is highly unlikely, not to mention how the ship operated safety measures that would have prevented a large scale fire from the gas turbine room spreading to other areas of the ship. In addition, the gas turbine was not in operation at the time of the incident. Therefore, it was concluded that a gas turbine defect is not the cause of the incident.



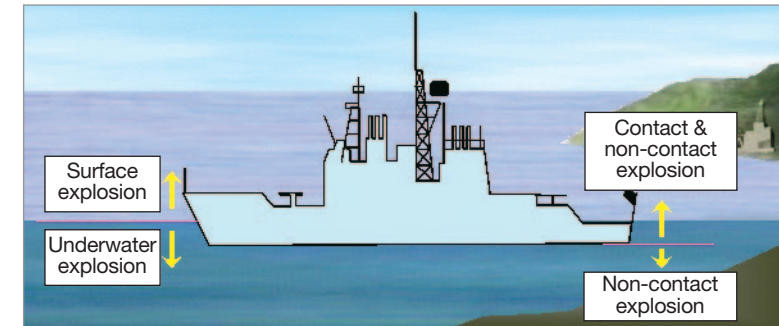
〈Figure II-2-10〉 Bulkhead between gas turbine room and diesel engine room



〈Figure II-2-11〉 Gas turbine room just before the incident(CCTV)

## 3. External Explosion

External explosion refers to the possibility that ROKS Cheonan was sunk by an explosion generated by an external force. The possibilities were categorized by detonation points (surface/underwater) and contact types(contact/non-contact) as shown in 〈Figure II-3-1〉.



〈Figure II-3-1〉 Classification of external explosion by detonation point

The agents involved in a surface explosion include a cruise(anti-surface) missile, ballistic missile, and naval gun/coastal defense artillery. Those that could have caused an underwater explosion include straight running torpedoes and buoyant mines, which detonate upon a contact with the hull(contact explosion); moored mines and bottom mines, which utilize acoustic and magnetic influence methods to detonate under the ship; and acoustic and magnetic influence torpedoes, which are normally delivered from submarines and subsmersibles(non-contact explosion).

In this investigation, for the purposes of promptness, effectiveness, and efficiency, the JIG first attempted to identify whether the explosion was contact or non-contact through a damage observation. Then, a more profound analysis was conducted with emphasis on a non-contact explosion, excluding contact explosion scenarios based on the observation result. The team formulated the report in the following order: surface explosions, focused on missiles such as cruise(anti-surface) missile and ballistic missile(excluding the attacks of naval gun and coastal defense artillery due to improbability); torpedoes and mines including contact and non-contact explosions; followed by land control mines(MK-6) that had been used by ROK in the past(a variant of depth charge).

## 1) Surface Explosion(Cruise Missile and Ballistic Missile)

A surface explosion refers to an explosion due to an external attack occurring above and at the sea surface. The attack can include naval guns from ships, coastal artillery fire from the surface, and cruise(anti-surface) missiles and ballistic missiles.

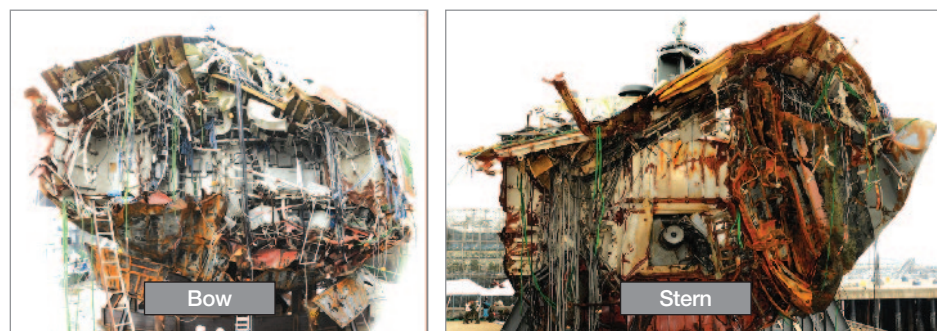
It was assessed North Korea to possess enhanced surface strike capability with longer range of targeting based on its production of new missiles and the continued test launches of improved versions of these missiles since the 1990s.

### (1) Damage Indicators

Damage patterns	Investigation result
• Petal-shaped crater at the detonation location	None
• Local shell dishing	Observed
• Trace or soot from heat or fire on electric line, various cables and structure, caused by explosion	None
• Fragments and holes created by fragments on the shell plating and upper deck	None
• Mass hearing loss and burned patients by shock wave and explosion sound	None
• Round hole(jagged) impact on superstructure	None

### (2) Visual Inspection

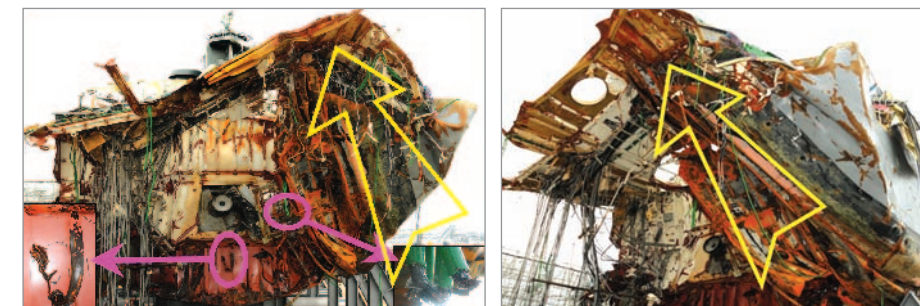
A summary of our investigation following the salvage of ROKS Cheonan is shown in <Figure II-3-2>. The hull was severed through the gas turbine room and approximately 7.8m



<Figure II-3-2> Breakplane of bow and stern

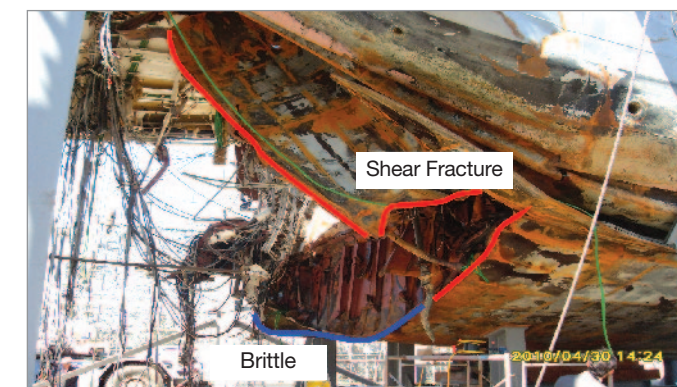
of the starboard was lost. The port was ruptured and severed with no loss besides small portions of the bottom. The CVK was bent upward, 680mm for the stern section and 1,475mm for the bow section.

Concerning the fractures of the breakplane as shown in <Figure II-3-3>, the lower part of the port was severed(shear fracture) by an instantaneous upward force; the bottom part was torn(brittle fracture) by a strong force in a short time; and other parts showed fractures due to large tensile force. Therefore, the shape of the damaged structure indicated typical bubble effect, where the explosion occurred below the port side of the gas turbine room and caused the ship to sever as the explosion power was exerted in an upward and starboard side direction.



<Figure II-3-3> Direction of the deformation, PORT-bottom → STBD-top

In addition, there were no craters observed on the top part of the salvaged hull, with no heat damage in the breakplane and no evidence of fire in any part of the ship. The electric and other wires did not show signs of melting or any other heat damage. Rather, they



<Figure II-3-4> Shape of the split section

were cut by the exertion of a large force in a short period of time. Also, there were no indications of chain explosions either in the magazines or fuel tanks that can be caused by a surface explosion or other explosions in any part of the ship other than the lost section.

### (3) Environmental Condition

A surface explosion occurs upon contact with or nearby detonation of an explosive on the surface or in the air, and should result in a petal-shaped crater at the detonation point, local dishing, shock damage, and remains of the weapon system. In particular, the plating around the point of explosion can be fragmented or lost due to the explosion pressure in case of a massive explosion. In addition, heat damage, fire, and evidence of heat or flame on the electric cables and other structures will appear. In this case, an external explosion leading to an internal explosion is highly probable and can cause hearing injury and burnt skin due to an explosion sound and shockwave. Also, unlike an underwater explosion, the superstructure of the ship is damaged in case of a surface explosion. A rapid sinking is unlikely and the ship can stay afloat for a significant amount of time considering the stability, since the explosion energy is mostly dispersed through the atmosphere.

### (4) Modeling and Simulation

No surface explosion modeling and simulation were performed due to no possibility of a surface explosion with little practical significance expected.

### (5) Indication and Warning

There were no indication and warning about a guided missile attack that could have caused a surface explosion. The radar around the incident site detected no flying objects.

### (6) Statement from Relevant Personnel

Although all the survivors heard a blast, none of them smelled explosives or saw fire. The marine sentries from the 6th Brigade stated that they observed a white flash light.

### (7) Conclusion: No Possibility

The analysis of the hull, which provides the most reliable evidence, indicates that the shell dishing was caused by a non-contact underwater explosion. No crater or fragmentation

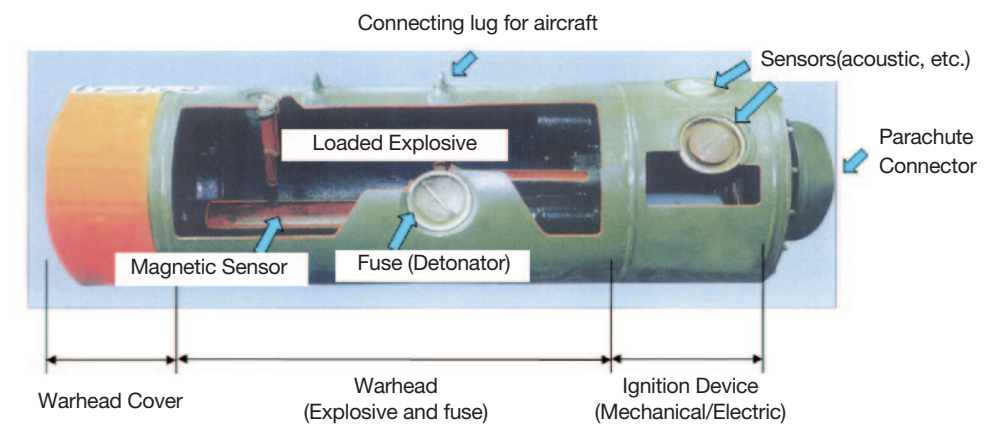
from a surface explosion above the waterline was observed, nor were traces of fire and remains of any weapon fragment present. Combining the lack of evidence and other additional testimonies that can support the possibility of a surface explosion, it was concluded that there is no possibility of a surface explosion.

## 2) Mines(Floating, Moored, Bottom)

Mines are one of the most effective naval weapon systems for port or naval blockade/defense and can be defined as a “weapon system that detonates below or around the waterline of an enemy ship in order to inflict damage.”

Mines target below ship's waterline, the most vulnerable part of a ship, and differentiate themselves from other weapon systems in that they do not pursue the enemy but wait for it to approach. The difficulty of detection allows a mine field to pose a direct threat to enemy naval forces and restricts naval advances or transportations over the sea, with the risk of serious loss and danger, once installed.

A mine is consisted of a warhead cover, warhead, and ignition device as shown in <Figure II-3-5>.



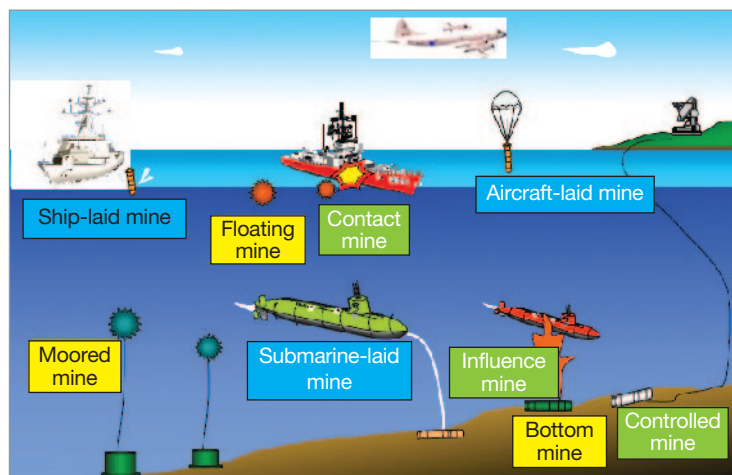
<Figure II-3-5> Structural diagram of a mine

The warhead cover serves following functions: diminishing air resistance when dropped from an aircraft, mitigating the impact to the warhead upon the contact with sea surface, and enhancing integrity on the seabed.

The warhead portion is composed of a warhead and fuse. The warhead is loaded with the main explosives, and the fuse contains a safety load device and a triggering device, which operates above a certain water pressure value and detonates the mine after receiving the signal from the ignition device in the controlling portion. When storing and handling a mine on the ground, a safety pin/rod prevents activation. A detonation power source is attached to the water pressure switch, and the ignition signal is relayed to the fuse through a cable. The explosion occurs through a series of chemical-mechanical parts that relay and amplify the detonation energy inside the fuse. The chemical-mechanical parts are composed of an electric detonation tube, connecting tube, secondary explosives, main detonation tube and main explosives.

The ignition device is comprised of an ignition device, sensor, water pressure switch and batteries. The ignition device is the “brain” of the mine that controls the mine, sorts the target according to the target detection algorithm and ignites the mine. It contains a signal amplifier, signal processor and function controller. The water pressure switch connects the operation and detonation power sources after installation.

A mine can be laid by a variety of means such as an aircraft, submarine or ship and is categorized accordingly. A mine can be employed in a broad range of depth, from shallow sea to deep-sea. Also, as shown in <Figure II-3-6> below, mines are categorized into bottom, moored, and floating mines according to its position. When classifying according to triggering method, a contact mine is ignited by impact; an influence mine is ignited by a



<Figure II-3-6> Mine types categorized by laying position and method

change in the general physical surroundings such as the magnetic field generated by the ship, underwater acoustic signature or pressure; and a controlled mine is ignited by an artificial decision. In recent years, the majority of mines are combined mines laid on the seabed which operate upon the change of the magnetic field, acoustic signature and pressure generated by the passing target.

### (1) Damage Indicators

Damage patterns	Investigation result
• Holes on shell plating	None
• Damage due to fragmentation	None
• Inward bending of hull at the detonation point	Observed
• Heat damage or occurrence of fire at damaged sections	None
• Contact from the bow direction, causing explosion	None
• Multiple fragments exist within hull in case of nearby explosion	None
• Shock wave and bubble effect by UNDEX	Observed
• Rapid tilting or lifting of hull by shock wave produced by UNDEX	Observed

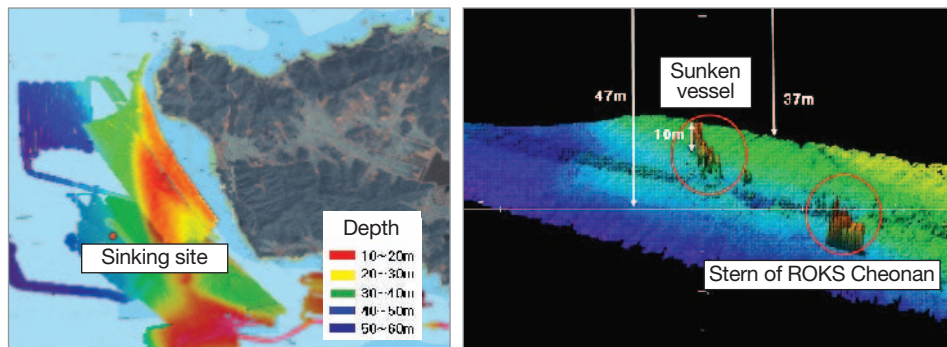
### (2) Visual Inspection

As addressed in the surface explosion investigation and analysis result, explosion observations of ROKS Cheonan correspond to a classic case of hull separation due to a shock-wave and bubble effect generated by an underwater explosion. Therefore, there is no possibility of contact explosion by surface or moored mine. Although non-contact underwater explosion of moored mine cannot be excluded considering the damage patterns observed, the operable environment of moored mine was severely limited, and with extreme vulnerability of moored mine to be affected in the underwater environment, its employment was assessed highly unlikely.

### (3) Environmental Condition

An examination of incident site showed that it is 2.5km SW (37° 55' 45"N, 124° 36' 02"E) of Baekryong Island. The water depth in this area is 47m and the seabed geography is as displayed in <Figure II-3-7>.

At the time of the incident, a SW wind was blowing relatively strongly at 20kts, as



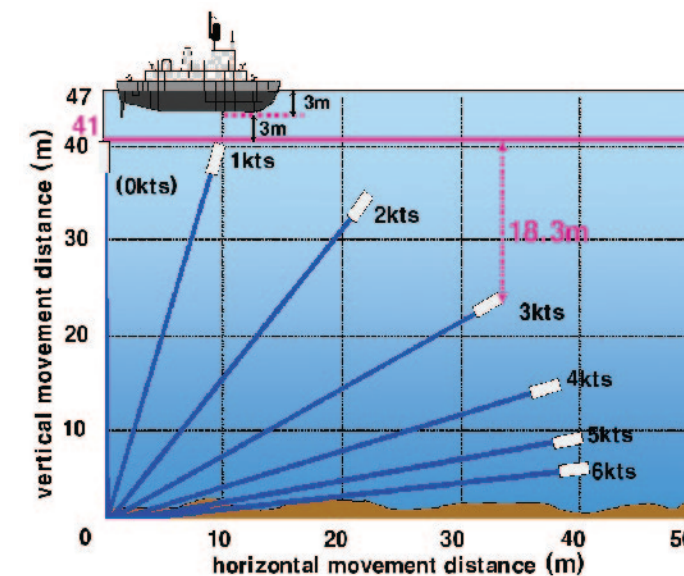
〈Figure II-3-7〉 Seabed geography and water depth of incident site

shown in 〈Figure II-3-8〉. Wave height was 2.5m, current was 161°-2.89kts, and the visibility was 2.5nm. In particular, on the day of the incident, flood tide(high water) was at 0225 (2.3m) / 1515(2.7m), and ebb tide(low water) was at 0843(0.7m) / 2147(0.8m). The average tidal current speed in the region is 3~5kts, and the tide difference is 4m at maximum, which poses severe limitations to the installation of moored mines.



〈Figure II-3-8〉 Seabed geography and water depth of incident site

Therefore, since strong current(3~5kts) and depth(47m), as well as large tide difference(max 4m) and wave height(2.5m) pose significant challenges to moored mine fixation and optimum depth maintenance, employment of moored mine would have been highly unlikely. Drifting level of moored mines by current speed is displayed in 〈Figure II-3-9〉. At current speeds of 3kts, the location of a moored mine will be 18.3m below its original position, and the effects generated by its influence and explosion will be sharply reduced.



〈Figure II-3-9〉 Drifting level of moored mines by current speed

#### (4) Modeling and Simulation

While conducting modeling and simulation on the possibility of a heavyweight torpedo, the hull whipping analysis and advanced mathematical analysis were conducted with different charge sizes and explosion depths. Same charge size and explosion depth scenarios can be applied in assessing the possibility of a mine.

#### (5) Indication and Warning

In the vicinity of Baekryong Island, the industry concentrates its activities during the blue crab season from August to October as well as the blue crab and san eel season from April to June. Even during the slack season from November to March, 40~50 fishing vessels per day engage in fishing.

Moreover, after examining ROKS Cheonan's track on the day of the incident, it was found that it departed from Daechung Island base at 06:00, March 26th, entered its patrol area at 08:30 and conducted its patrol operation in a zig-zag manner irregularly once or twice per hour in the identical region, thus resulting in patrol near the incident site at least more than 10 times(At the time of the incident ROKS Cheonan was moving in 327° , 6.7kts). This indicates that there were no prior mine installations.

In addition, the operational installation of a single mine results in a very low success

rate; therefore, multiple number of mines should be laid at the same time in order to raise the possibility of success. However, no mines have been discovered. There are numerous surface vessels such as fishing and merchant vessels operating in the vicinity of Baekryong Island. Targeting a warship would result in a very low likelihood of success.

### (6) Statement from Relevant Personnel

According to statements of survivors, they experienced and observed lifting of the hull and explosion sound once or twice by shock wave and bubble effect.

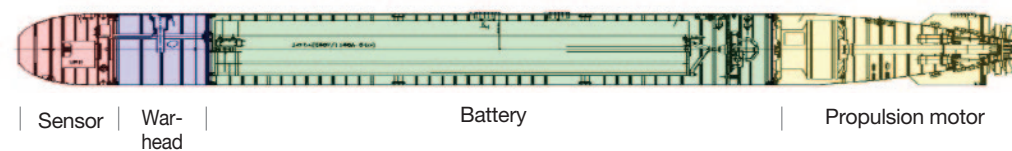
### (7) Conclusion: No Possibility

The rapid current speeds of 3~5kts, tidal difference of 4m, and depth of 47m pose difficulties for effective mine operation. Also, given that ROKS Cheonan had taken an irregular route around the incident location over 10 times on the day of the incident, and that no anchors or mooring devices that are parts of moored mines were found during the search of the seabed, it is assessed that an explosion of moored mines is impossible.

## 3) Torpedo

Torpedoes can be installed on vessels, aircraft, and submarines to attack enemy submarines or vessels. The torpedoes are categorized as lightweight and heavyweight torpedoes.

Torpedoes are assembled in the following structure: the sensor section, warhead section, battery section, and propulsion motor section.



〈Figure II-3-10〉 General structure of a torpedo

The sensor section uses sound signals to locate targets. This device has two modes: a passive mode that tracks sounds from targets, and an active mode that sends out sound signals to locate targets once the signals bounce back from a target.

The warhead section carries main explosives that cause damage to the target. There are two detonation methods: a proximity and acoustic fuse that uses magnetic sensors, and an impact fuse that detonates upon contact.

The battery(fuel) and propulsion section provides propulsion power to a torpedo. Either electric or combustion propulsion method is selected depending on the strategic situation, operating concept, and sound volume level. The engine propulsion is capable of high-speed propulsion; however, this method generates too much noise, making the torpedo vulnerable to enemy detection. Other electric propulsion problems include decrease of power depending on the depth of water. However, these issues have been recently resolved with the development of a closed-cycle engine<sup>10</sup>.

Surface vessels and submarines use sonar or towed array sonar<sup>11</sup>), and in other instances, they use dipping sonars<sup>12</sup>) or sonobuoys<sup>13</sup>) to detect targets and guide torpedoes. The following 〈Figure II -3-11〉 illustrates the basic operating concept of torpedoes.



〈Figure II-3-11〉 Operating concept of heavy and light weight torpedoes

Torpedoes that operate underwater use acoustic sensors installed on the front end to analyze sound specifications of targets to detect them, and estimate target information(azimuth, distance, speed, etc.). As the following table shows, torpedoes can employ straight

10) Closed-cycle engine: An engine that, unlike ordinary diesel engine, functions by burning reprocessed exhaust gas and stored oxygen without the help of air from the outside. Used in ships and submarines.  
 11) Towed array sonar: The system of naval assets to insert the cable underwater equipped with sound detecting device. This device detects underwater targets, and is mainly used for a long range target detection.  
 12) Dipping sonar: A device that is dipped in the surface by helicopters or surface vessels to detect underwater targets. This device is equipped with a cable and the helicopter or surface vessel can control the sonar's degree of depth.  
 13) Sonobuoy: A device in which a sound detector is attached to a buoy to float on the surface to detect underwater targets or search seabed geography.

running method, as well as acoustic homing and wake homing methods by using sonar. The detection mechanisms are as follows:

Detection method		Characteristics
Straight running method		<ul style="list-style-type: none"> <li>No detection ability</li> <li>Straight and zig-zag method of cruising</li> </ul>
Acoustic homing	Passive mode	<ul style="list-style-type: none"> <li>Detects by analyzing noise generated in the propulsion section of the targeted vessel</li> <li>Mainly used for detecting surface vessels</li> </ul>
	Active mode	<ul style="list-style-type: none"> <li>Detects by transmitting signals from torpedoes and analyzing the reflected signals from the bodies of targeted vessels</li> <li>Mainly used for detecting submarines</li> </ul>
Wake homing		<ul style="list-style-type: none"> <li>Detect by using navigation tracks generated by operation of targeted vessels</li> <li>Navigation sensors installed on top of torpedoes detect targets by transmitting and receiving sound signals, and analyzing the signals that correlate to navigation of vessels</li> <li>Used for detecting navigation of surface vessels</li> </ul>

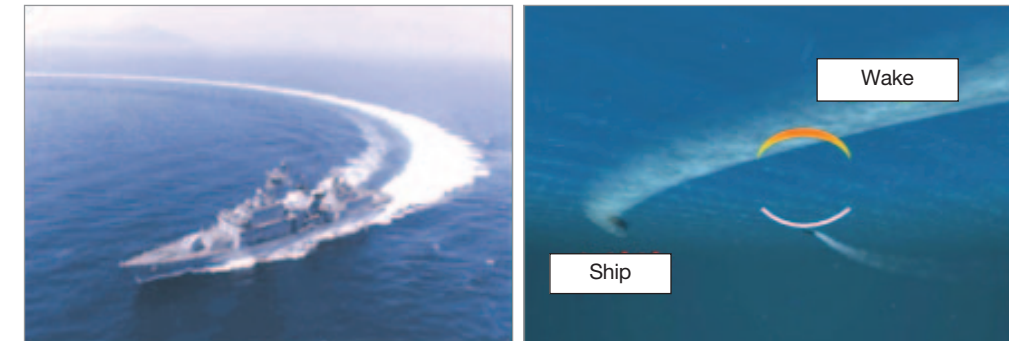
〈Table II-3-1〉 Detection method and characteristics of torpedoes

A straight running torpedo does not have detecting abilities and is normally used with impact fuses. The cruising methods are direct and zig-zag cruising. The following settings are inputted on this type of torpedo: first cruising distance, rotating degree and second cruising distance. Once this torpedo is launched, it first cruises the distance set by the first cruising distance, then rotates according to the rotating degree and cruises up to the second cruising distance. The torpedo detonates upon a successful contact with the target.

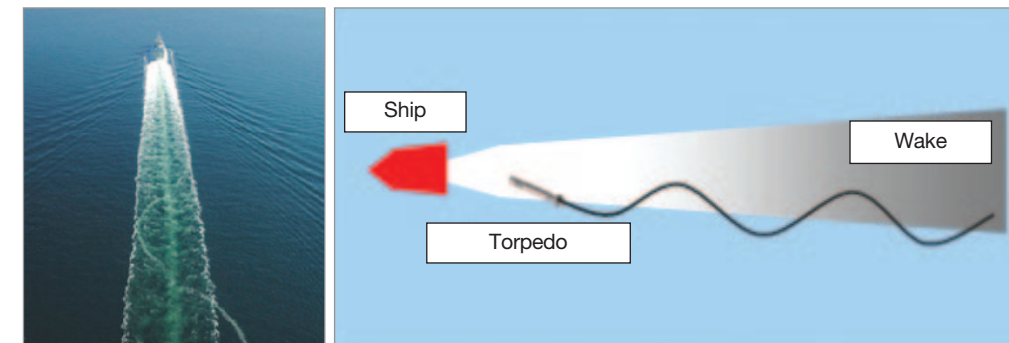
A passive acoustic homing torpedo detects the target by analyzing the noise generated from the propulsion section of the target vessel and tracks the target by analyzing its azimuth. This method is mainly used for detecting surface vessels. An active acoustic homing method transmits signals from torpedoes and analyzes the reflected signals from the hull of the targeted vessel. This method is mainly used to detect submarines.

Wake homing is a method that tracks navigation signals generated from propellers and hull of surface vessels. Navigation signals vary depending on the shape of hull and cruising speed. Small bubbles (couple of ten  $\mu\text{m}$  in diameter) remain on the surface for more than 10 minutes following the passing of a surface vessel. In order to detect these signals, a navigation sensor is installed on the top of torpedoes to analyze the signals correlated to vessel wake

using transmitted and received sound signals. This detection method is used for detecting wake signals of surface vessels and involves tracking the boundary of the created wakes.



〈Figure II-3-12〉 Wake produced by surface vessel



〈Figure II-3-13〉 Mechanism to track wake produced by surface vessel

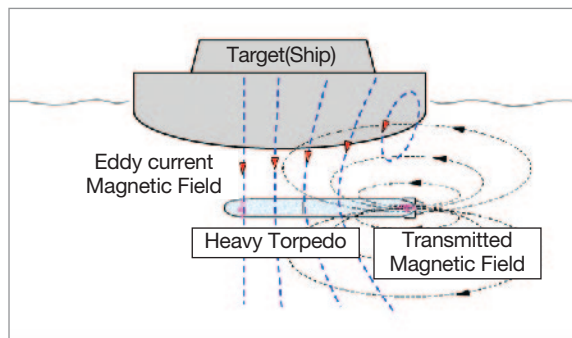
A fuse is an influence equipment used to detonate warheads of torpedoes when they are guided to their targets. The types and operating mechanisms of fuses used in torpedoes are shown in 〈Table II-3-2〉.

Fuse		Operating mechanism
Impact fuse		<ul style="list-style-type: none"> <li>Detonates by detecting the impact during hull contact</li> <li>⇒ Explodes at the side of vessels</li> </ul>
Proximity fuse	Magnetic influence fuse	<ul style="list-style-type: none"> <li>Detonates by detecting the reflected signals from the Eddy current of hull while cruising through hull bottom</li> <li>⇒ Explodes at the bottom of hull</li> </ul>
	Acoustic influence fuse	<ul style="list-style-type: none"> <li>Detonates by detecting the reflected sound signals from the hull while cruising through hull bottom</li> <li>⇒ Explodes at the bottom of hull</li> </ul>

〈Table II-3-2〉 Types and operating mechanisms of fuses

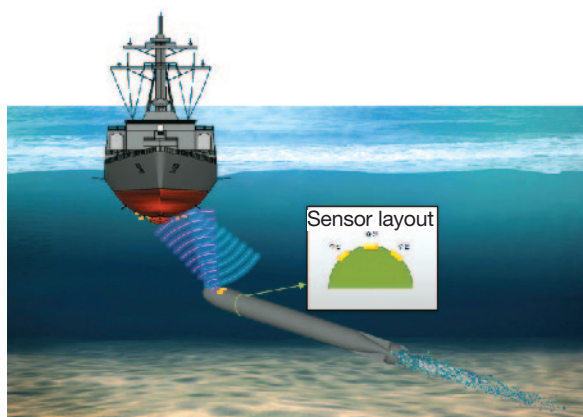
Impact fuses are installed with firing switches that detect the impact during a contact and trigger detonation. Firing switches react against all impacts that happen from all angles and at a low acceleration. This method causes an explosion at the sides of vessels.

Magnetic proximity fuses detonate by generating currents at specific frequencies and detecting eddy currents formed on the surfaces of targets. This kind of fuse usually causes an explosion at the central areas of vessels.



〈Figure II-3-14〉 Operating mechanism of magnetic influence fuses

Acoustic proximity fuses transmit acoustic signals from the high frequency (several hundred kHz) transmitting sensors installed on the center upper area of torpedoes. Two high frequency receiving sensors detect the receiving signals and assess the existence of a nearby target, and detonate. This method also normally causes explosion at the central areas of vessels.



〈Figure II-3-15〉 Operating mechanism of acoustic influence fuses

### (1) Damage Indicators

Damage patterns	Investigation result
• Holes on shell plating	None
• Local dishing of hull	Observed
• Inward bending of hull at the explosion point	Observed
• Heat damage or occurrence of fire at damaged sections	None
• Multiple fragments exist within hull in case of proximity explosion	None
• Damage by shock wave and bubble produced by UNDEX	Observed
• Rapid tilting or lifting of hull by shockwave produced by UNDEX	Observed
• Holes and debris	None
• Torpedo debris	Observed

Torpedo is a weapon system capable of contact and non-contact detonation. A contact torpedo detonation causes identical damage as a contact mine detonation while a non-contact torpedo detonation causes identical damage as a non-contact mine detonation.

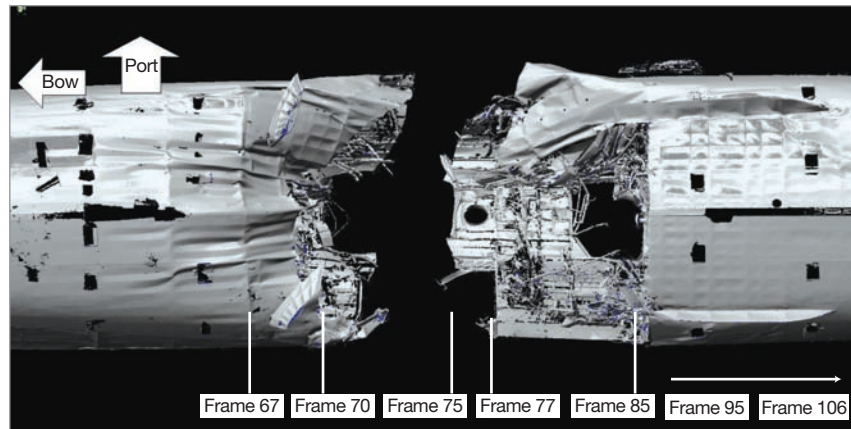
### (2) Visual Inspection

ROKS Cheonan was broken in half by a whipping effect and upward bubble pressure on the port side bottom area of the gas turbine room towards the starboard side. The CVK and the fractured surface were twisted and ripped upwards. The CVK area is where the gas turbine engine was installed and the parts of the ship bottom were blasted away while the stiffeners and the ship structure reinforcements were crushed inward and on top of each other towards the starboard due to pressure. Wires on the port side and the starboard side were cut from tensile force. No traces of fire, soot, and laceration that would indicate internal fire were found. Additionally, sectional paint jobs on the bottom of the hull were scratched off in a wide range.

After Frame 106, no traces of damages from impact were found. In regards to the port side shell plating, local bending of plating appeared from the severed area to Frame 95. As for the starboard plating, local bending of plating appeared from the severed area to Frame 90. Additionally, areas from Frames 67 to 70 were significantly bent in an upward direction.

There were significant deformations on the external plating of the stern section between Frames 75 and 85 on the port side, and significant deformations were observed be-

tween Frames 70 and 71 on the bow section. The platings were bent severely in a round shape towards the inside. The stern CVK was deformed towards port in the main deck direction of the stern(upward direction). Furthermore, a significant bending appeared on the severed CVK from Frames 70 and 85. This effect is highly likely to have taken place during the initial sagging of the hull which would have been generated by the tensile force.



〈Figure II-3-16〉 3D laser scan image on the split section of ROKS Cheonan

### (3) Environmental Condition

The sea conditions and currents were identical to those mentioned on the mine section and these environmental conditions were not severe enough to limit torpedoes from detecting and tracking ROKS Cheonan.

The water depth at the sinking site poses significant limitations on the installation of normal mines. However, it does not limit the employment of heavy/midget class submarines. The tidal difference, water speed, and wave height are not limiting factors for a torpedo attacks by a submarine.

### (4) Modeling and Simulation

The US investigation team presented the result of “ROKS Cheonan modeling by US Navy” on April 26, 2010. The presentation stated that there is the highest possibility for a torpedo explosion to have occurred under the CVK of the hull. It also indicated that an explosion of an explosive weight of 250kg occurred at a location below Frame 75, 3m to the port from the centerline and at a depth of 6~9m. The ADD investigation team assessed based on ex-

amination of material deformation that the hull suffered an instant severance by a strong force from the port side of the hull and the propagation of brittle fracture towards the starboard direction led to the separation of the hull. The Joint Investigation Group modelled a part of the hull, focusing on the site of separation, and conducted simulations with different depths and explosive charge sizes and obtained a similar result. The simulation result of the UK team was also similar to those from the US and ROK teams.

### (5) Indications and Warning

The incident site is deep enough for an employment of a torpedo against a surface vessel, and an acoustic guided torpedo can be guided to the center of a ship. Therefore, it is very likely that a submarine targeted and attacked ROKS Cheonan from a location northwest of the incident site. A light torpedo(45kg of TNT or less) does not have sufficient explosives to break a hull apart, and the use of a straight running contact torpedo(impact inertia method) leaves many traces. All these assessments lead to the unlikelihood of these weapons' employments.

### (6) Statement from Relevant Personnel

The survivors from ROKS Cheonan heard 1~2 explosion sounds. The port watchout, who fell down as the bow tilted to the starboard, was splashed in the face with water. The post sentries of the 6th Brigade, Marine Corps. witnessed a flash of white light<sup>14)</sup>(20~30m in width, 100m in height).

### (7) Conclusion: High Possibility

The ROK ADD, UK, and US investigation teams made the assessment that the explosive was precisely guided to the center of the ship where it exploded in the proximity of below the gas turbine room 3m to the portside from the center, where the shockwave and bubble effect generated by the explosion caused the separation of the ship.

Therefore, there is a high possibility of a torpedo attack. An acoustic guided torpedo which can be launched from a submarine is assessed to be the likely weapon system used.

<sup>14)</sup> Testimony from the LCM technical expert who participated in the land control mine emplacement project.

#### 4) Explosion of Land Control Mine(modified MK-6)

As the analysis on the cause of the sinking of ROKS Cheonan continued, the media engaged in persistent speculation regarding the various possibilities. One possibility raised involved land control mines (modified MK-6) that the ROK Navy had installed in the late 1970s near Baekryong Island and removed at a later date.

Investigation on the land control mines commenced immediately after the Joint Investigation Group was established in late March. The investigation group proceeded based on the statements from the LCM<sup>15)</sup> technical expert who had participated in the emplacement of the land controlled mines at the shore of Yeonhwari, Baekryong Island in the late 1970s.

The technical expert participated in the initial research at Je-il Precision Engineering located in Changwon, Kyungnam Province and in the emplacement of the mines in the waters off Yeonhwari. In his explanation on the design of the land control mine (LCM) and the structure of the detonation cable, he argued that the detonation cable, when cut and exposed to seawater, can induce voltage in accordance with the volta battery principle<sup>16)</sup>, which then can ignite the electric detonator. His argument was based on the fact that 1 layer of the detonation cable consisted of net-shaped metal lines plated with zinc and the electric wire in the core that delivers power was made out of copper<sup>17)</sup>.

On April 3, experts from the ADD as well as the technical expert were invited for a joint discussion. He emphasized that there is enough possibility, based on the volta battery principle and the experiment in which he found the detonator to be sensitive enough to explode when he measured the electric current with a measuring device. He presented that he had seen measurements of approximately 1V and 5~10mA. However, the explosive experts from ADD assessed that there is low possibility for the explosion of a mine due to naturally induced electric power because most electric power is discharged into the seawater even if it is induced and because there were doubts whether the zinc and copper wire together can produce enough electric power for the detonation.

.....  
15) LCM: Land Control Mine.

16) A battery made by connecting wires after putting in two metal boards of different ionization inclination in electrolysis such as diluted acid.

17) At this period, media also raised possibility of explosion of unrecovered mine off the Yeonhwari.

Upon the establishment of the Joint Investigation Group office in Pyeongtaek, a detailed investigation on the issue commenced. The group obtained a 50cm-long detonation cable on April 19 and tested on April 21 in Pyeongtaek harbor whether electric power can be generated from the detonation cable in seawater. The experiment found 0.47V but no electric currents. The Joint Investigation Group consulted<sup>18)</sup> Hanhwa Co. on April 23 to seek opinions from the expert agency on whether the generated electric power in seawater would be sufficient for detonation. In response to the request to review “the possibility of the underwater explosion of the military KM6 detonator,” Hanhwa Co. stated that detonation is not possible because at least 0.45A is required to detonate the military standard KM6 detonator and the voltage and current generated by the Galvanic action between two different metals underwater are only  $\mu$ A or mA local electric current(corrosion reaction).

##### (1) Damage Indicators

Damage patterns	Investigation result
• Damage by weak shock	None
• Global dishing of shell plating	Observed
• Overall hull deformation	None
• Mine debris	None

##### (2) Visual Inspection

Localized damage by shock is shown around the gas turbine room, but no global dishing was found on the hull. Also, no dishing was found near the screw and around the bottom of the magazine.

##### (3) Environmental Condition

###### ① Emplacement of Land Control Mine

The emplacement of land control mines was carried out by ROKN HQ. It was conducted to prevent the landing of North Korean amphibious forces on Baekryong Island. The major content involved removing the safety pin, safety cover, fulminating mercury(igni-

.....  
18) Hosted by a CPT(R), recommended from the National Assembly.

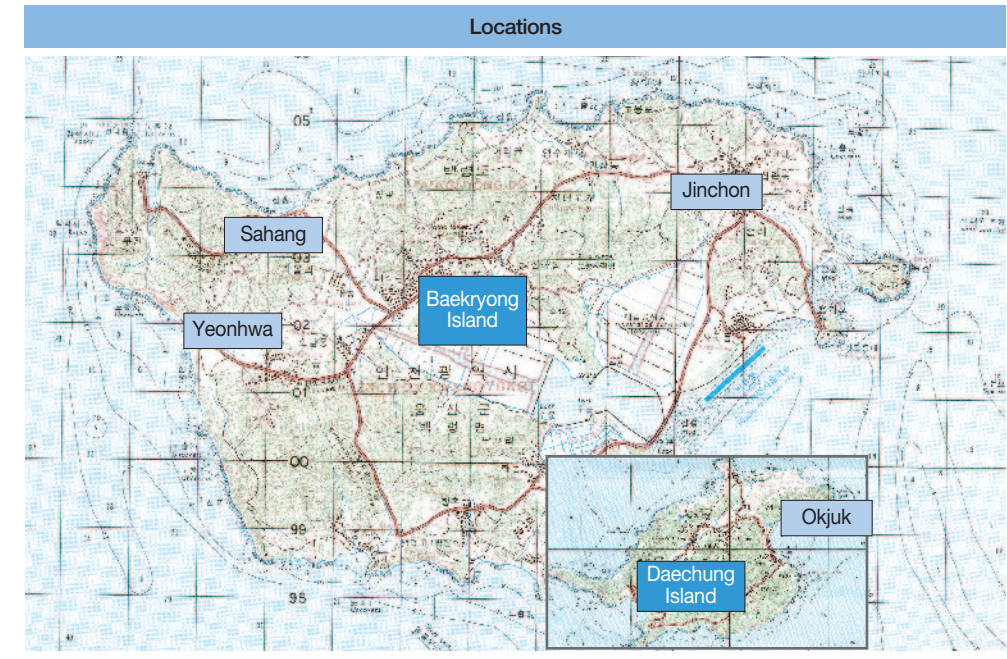
tion explosive), and pistol from MK-6 depth charges and equipping the MK-6s with electric detonators(US electrical detonator<sup>19)</sup>, M6 series<sup>20)</sup> and detonation cables.

On November 14, 1975, modified MK-6s were approved for emplacement. Technical review and test on the modified MK-6s were completed by ADD in July 1976. Contracts were established with Je-il Precision Engineering(which supervised the overall modification project) and Geumsung Wires(which supplied cables) by December 1976 for the project. The land control mines were all assembled by April 1977 and transported to the northwest of the island using LST 816 in June 1977. Emplacement and test fire were conducted between July and October 1977.

After the mines were assessed to be unnecessary they were neutralized by removing<sup>21)</sup> the detonation cable(from the land control group to the shore) and the control box(detonation cable connected to each mine) in late 1985. However, the main bodies of the mines were left unrecovered at the seabed. After about 16 years, fishers in Baekryong Island requested to recover the main bodies of the mines from the seabed in June 2001, and the ROK JCS assessed the recovery operation to be unnecessary in November of the same year, but in July 2008, JCS reviewed the operation again and decided to remove the mines. From August 11 to September 26, 2008, the Navy Special Operations Squadron and the Marine Search and Rescue team were committed with equipments (RIB, etc.), and resulted in successful recovery of 00 munitions. The average depth of the water was 6m, and the distance from the shore was 200~400m for the location of the mine sweeping operation.

The detonator and booster were removed from the recovered land controlled mines and were disposed of in the detonation training field of the 6th brigade from September 22~24, 2008. The main bodies of the mines were transported using a periodic transport vessel to the ordinance and ammunition depot in the Logistics Command and were retained until July 2009 when they were disposed.

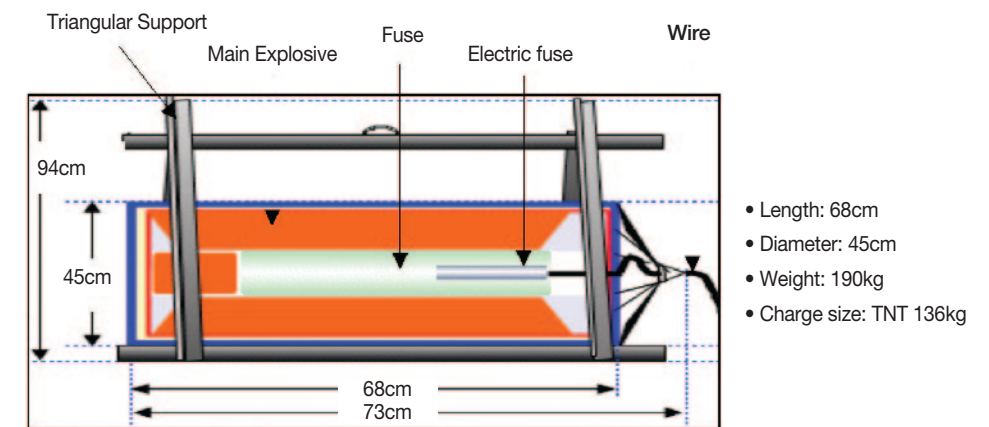
The emplacement status is shown in <Figure II-3-17>.



<Figure II-3-17> Emplacement of the land control mine

### ② Structure and Operating Principle of the Land Control Mine

The land control mine is a modification of the hydrostatic pressure MK-6 depth charge. The design and specification are shown in <Figure II-3-18>.



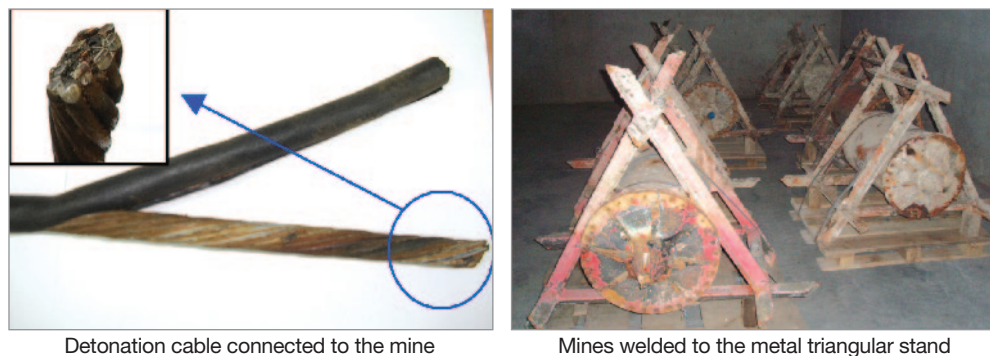
<Figure II-3-18> Design and specification of the land control mine

19) Testimony from the LCM technical expert who participated in the land control mine emplacement project.

20) Result of ADD investigation on US battery blasting cap which was extensively used in 70s.

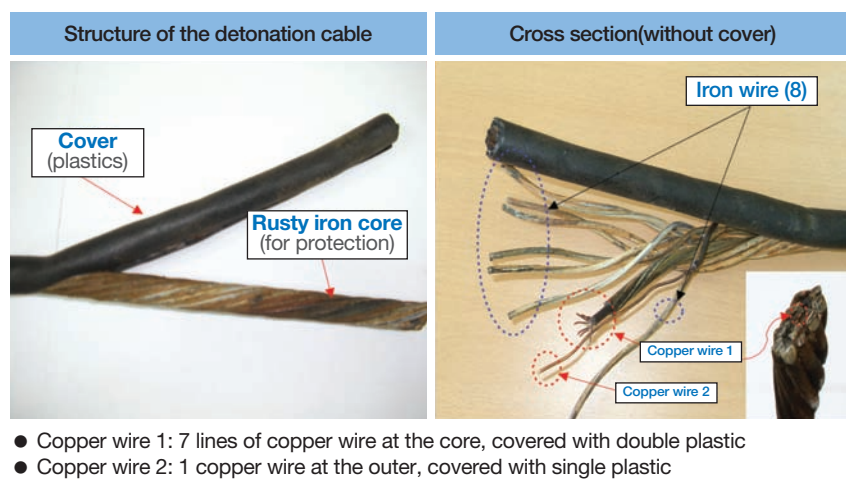
21) Testimony from a military contractor who participated in the work at the time.

The land control mines were laid 400~450m away from the shore at a depth of 7~10m, being fixed in metal triangular stands. Detonation cables connecting the mines to the ground control group allow individual detonation of the mines(See <Figure II-3-19>). A generator was installed separately as the power source for the ignition.



<Figure II-3-19> Detonation cable and metal stand

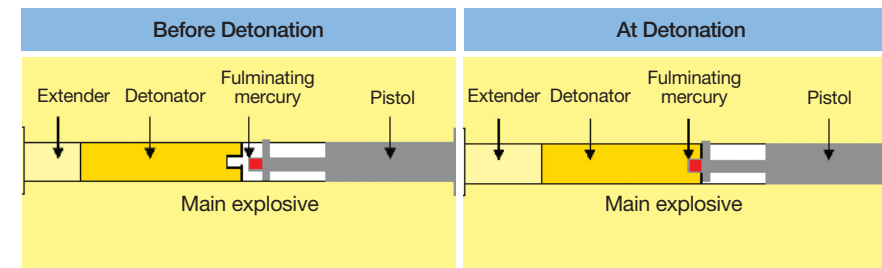
The detonation cables supplied by Geumsung Wires had a diameter of approximately 1.6cm and were covered with plastic. 2 lines of copper wires covered with plastic were combined with 8 lines of tensile strength reinforced wires, and therefore the cable was not easy to bend. The cable was designed to lie at the seabed due to its weight(6kg per 10m). The detonation cable is shown in <Figure II-3-20>.



- Copper wire 1: 7 lines of copper wire at the core, covered with double plastic
- Copper wire 2: 1 copper wire at the outer, covered with single plastic

<Figure II-3-20> Detonation cable in detail

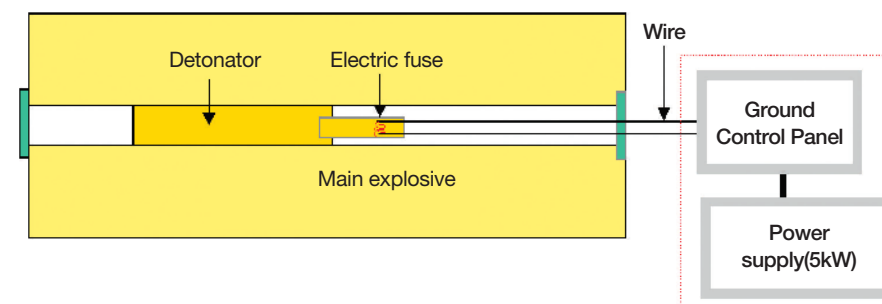
MK-6 depth charges were modified by removing an extender, pistol, and fulminating mercury. Afterwards, an electric detonator was installed and sealed with silicon. A detonation cable was connected to allow for remote control from the shore(See <Figure II-3-21>).



- ① Extender and pistol are actuated by water pressure exerted when dropped
  - Extender: Water pressure exerted between 11~22ft below surface push priming powder toward fulminating mercury, making it ready to detonate
  - Pistol: When reaching a pre-set water depth, water pressure makes a firing pin hit fulminating mercury and detonates the mine
- ② With the detonation of fulminating mercury(explosive), priming powder and the main explosive detonates

<Figure II-3-21> Detonation process of MK-6 depth charge

A modified MK-6 works in the similar manner to the ROK Army's claymore. The process is as shown on <Figure II-3-22>.



- ① Detonator ignites when power is supplied to electric detonator from the outside.
- ② With a detonator ignited, priming powder and then main explosive explode.

<Figure II-3-22> Detonation process of land control mine

The water depth at the incident site is 47m. Also, the land control mine had been underwater for approximately 30 years and thus would have lost its ignition function. The mine was installed so that it would not move. Therefore, it is not possible for the mine to have moved from its original location to the incident site.

#### **(4) Modeling and Simulation**

The simulation of a torpedo was applied for the underwater explosion of a land controlled mine. Given the charge size and water depth, it was assessed that hull separation is not possible. The UK Investigation Team concluded that the damage of ROKS Cheonan would require the explosive charge 20 times larger than the land control mine(MK-6).

#### **(5) Indication and Warning**

Information regarding indication and warning was not collected due to no possibility of explosion of land control mine.

#### **(6) Statement from Relevant Personnel**

There was no testimony that could indicate an explosion of land control mine.

#### **(7) Conclusion: No Possibility**

Referring to the modeling and simulation of the hull whipping caused by an underwater explosion, which was conducted by the US investigation team and the Ship Structure Management Team, the Joint Investigation Group assessed that a land controlled mine with a charge size of 136kg at a depth of 47m cannot break ROKS Cheonan in half.

Another possibility suggested involved the power supply detonation cable on the seafloor being tangled with propeller blades and detonating. The detonation cable consists of a rigid steel and copper line which poses difficulty in clinging. In addition, its weight (6kg in 10m) would not provide enough buoyancy for the mine to float from a depth of 40m. The condition of the stern, which was found intact, also eliminates the possibility of an explosion occurring nearby the propeller section.

In conclusion, there is no possibility of a land control mine(MK-6) detonating by itself at the time of the incident, 30 years after its installation. Even if such an explosion occurred, there would have been insufficient explosive power to separate the hull at a depth

of 47m with its small charge size(136kg). In addition, given the weight of the detonation cable, a mine would not be tangled with propeller blades. The above indicate that there is no possibility of a land control mine detonation.

P a r t III

*Detailed  
Analysis Results  
by Team*



## 1. Shape and Trace Analysis

Shape analysis of the hull's shell was conducted in the following three areas: first, the salvaged bow and hull's overall form, second, the deformation of hull's structure and the shape of the rupture, and third, microscopic traces such as pressures, pushes, cuts, and scratches. Through these analyses, the location of the explosion, and the size and direction of the explosion's pathway were assessed as well as how it influenced the hull.

### 1) Overall Shape

The overall length of ROKS Cheonan is 88.32 meters. The 3D precision measurements using a 3D scanned image of the ruptured bow and stern and the actual measurements of the hull indicate that the breakplane was located at the center of the gas turbine room(47.6m from the portside, and 45.4m from the starboard side).

When the ruptured parts were fitted together, the portside had resulted in an outer shell length of 50.32m in the bow and 38m in the stern, and hence experienced no loss except for the parts of the stern hull bottom. However, the starboard side had experienced a 7.8m loss with the bow part being 47.2m and the stern part being 33.32m long. The degaussing room on the main deck, CPO mess hall, machine control room, construction storage, crews'



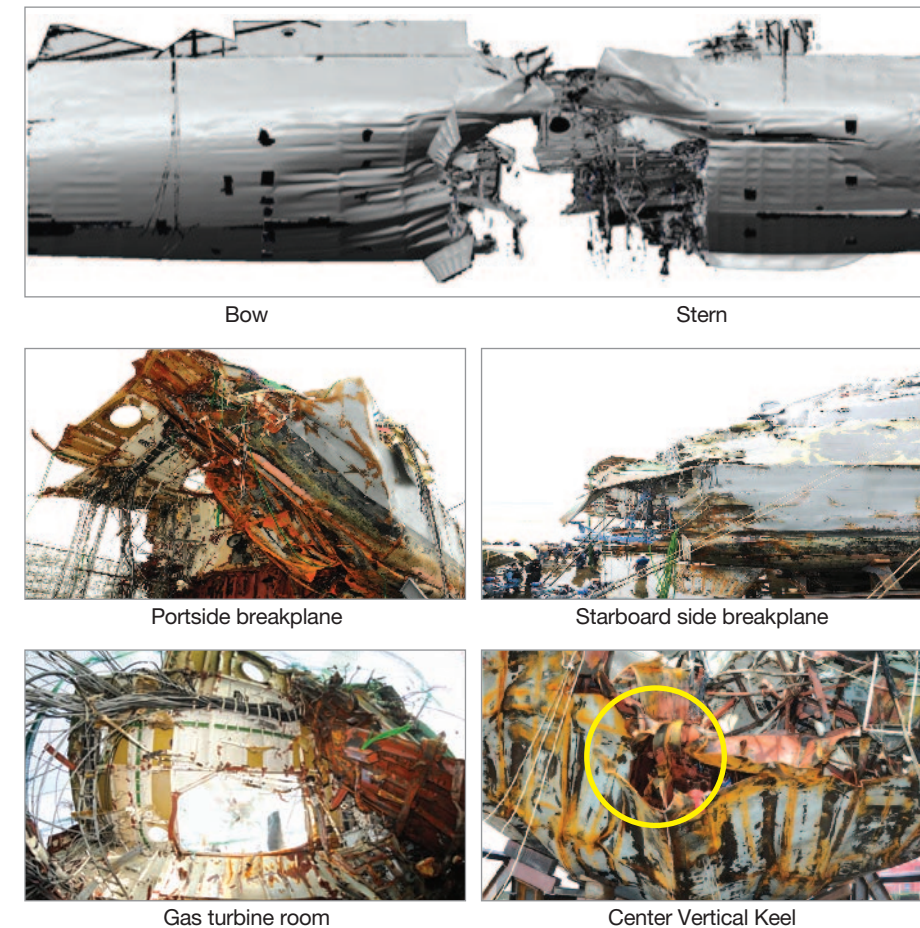
〈Figure III-1-1〉 Overall shape

galley, demist and stack on the O-1 deck, and harpoon missiles were lost. These losses were localized at the upper and lower parts of the gas turbine room.

### 2) Shape Analysis

Shape analysis was conducted with the emphasis on structural deformations, the shape of the breakplane, the detached structures, and the shape of the damage. These analyses allowed for the assessment on the starting point and traveling direction of the external force (such as explosion or shock) that influenced ROKS Cheonan.

〈Figure III-1-2〉 indicates that the bow and stern's hull bottom are bent upward due to water pressure; the portside breakplane is bent and pushed upward; and 7.8m of the star-



〈Figure III-1-2〉 Shape analysis

board side is fallen off at the gas turbine room's fore and aft.

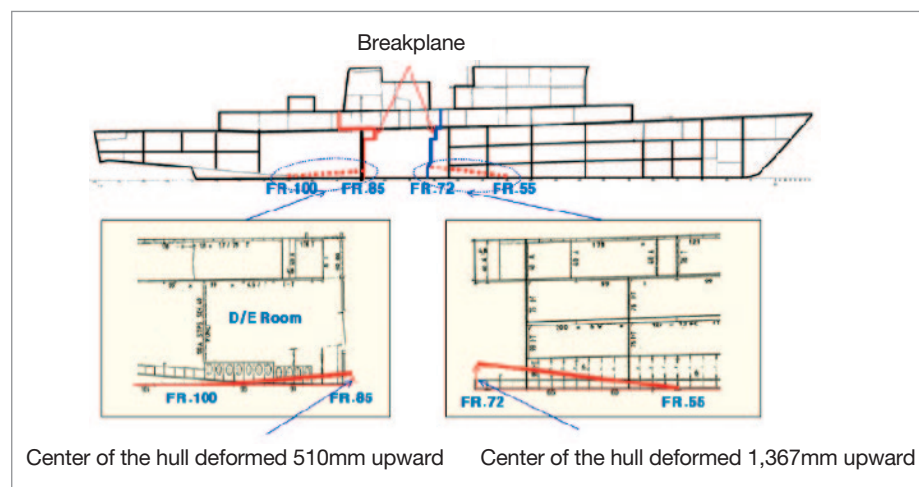
Also the portside ceiling of the gas turbine room is bulged up, while the exhaust opening has fallen off due to water pressure. Also, the bow side CVK is severely rolled upward and twisted to the starboard side.

The upward bending of the bow and stern's hull bottom indicates that an underwater explosion had occurred. The portside breakplane was bent upward; the starboard side breakplane was partially ripped out; and the keel was twisted towards the starboard side.

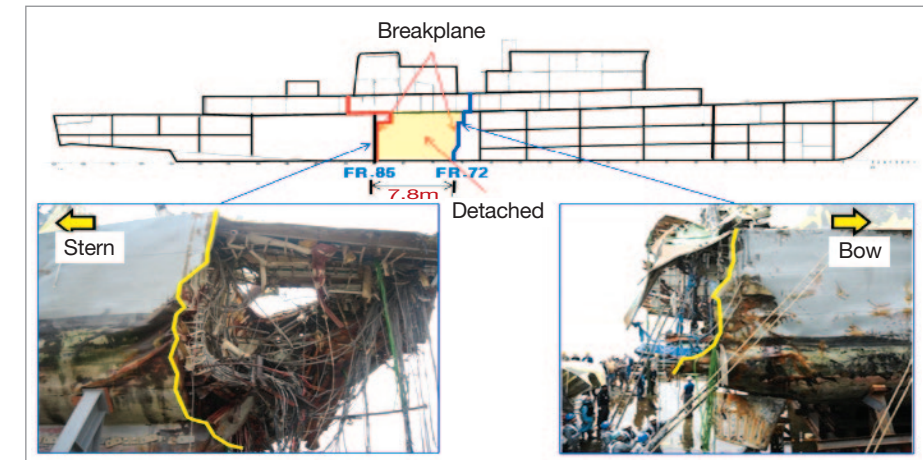
These signs indicate that the explosion force traveled diagonally from the portside bottom towards the upper parts of the starboard side. When the ship's maneuvering direction is taken into account, the fact that the gas turbine room was detached confirms that the point of explosion was at the gas turbine room on portside of the bow's hull bottom.

### 3) Form of the Hull Deformation

A precise deformation analysis was performed by 3 experts from the Defense Agency for Technology and Quality. The starboard side fracture was cut along Frame 72 and Frame 85 with a detachment of 7.8m as seen in <Figure III-1-3> and <Figure III-1-4>. The bow CVK deformation began in Frame 55 and moved upward towards Frame 72 for 1,367mm, and the stern CVK deformation began in Frame 100 and moved upwards towards Frame 85 for 510mm.

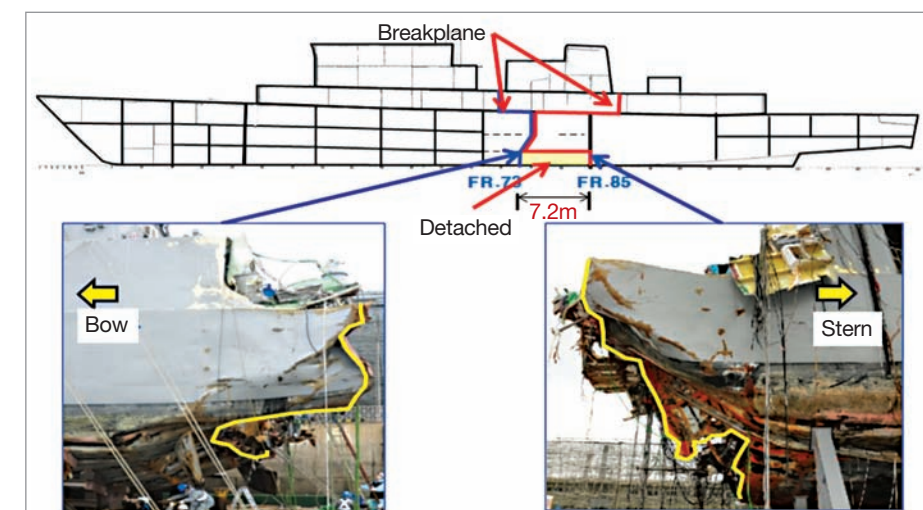


<Figure III-1-3> Starboard breakplane & CVK deformation



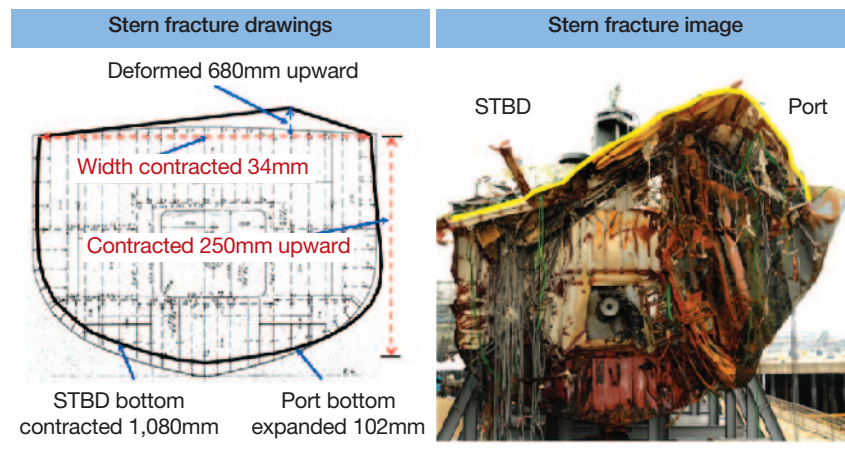
<Figure III-1-4> Starboard fracture

As seen in <Figure III-1-5>, the portside was fractured from Frame 73 on, and the detached portion is about 7.2m long on the bottom. For the stern, the inside of the ship was bent upwards between Frame 85 and Frame 73(7.2m), and the bow was bent upwards from Frame 70 and 73(1.8m) on the inside of the hull. This enabled the JIG to rule out internal explosion, fatigue fracture, and grounding. It was assessed that the shock wave, generated by a strong non-contact underwater explosion initiating from the bottom portside, was delivered to the internal structures on the starboard side, and the hull was inflicted with serious damage as a result.



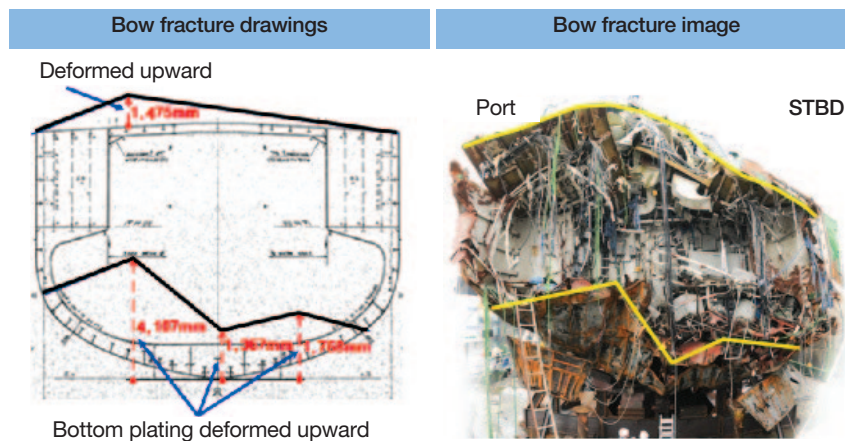
<Figure III-1-5> Portside fracture

The stern fractured surface on Frame 85, as shown in <Figure III-1-6>, shows that the center line of the ship contracted 250mm, that the portside bottom expanded 102mm along the width, and that the starboard bottom was compressed 1,080mm. The width of the Main Deck was compressed 34mm, and the hull was deformed 680mm upward from the point 3,600mm port from the center line.



<Figure III-1-6> Stern breakplane deformation

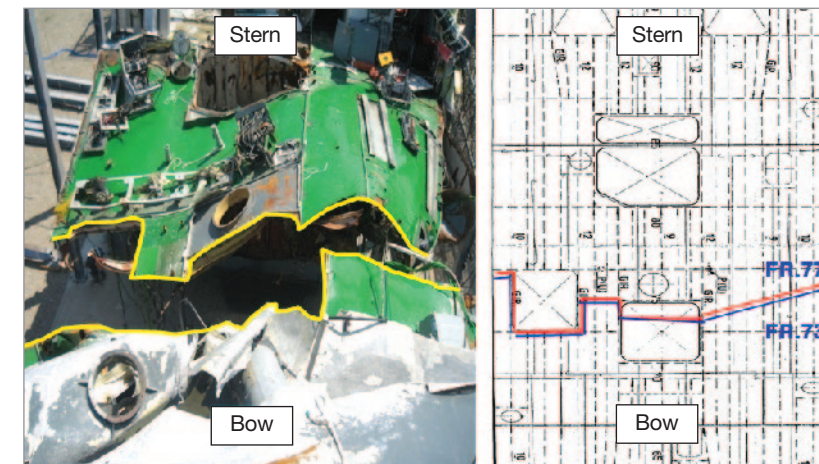
From the baseline, the bow fractured surface, as seen in <Figure III-1-7>, shows that the bottom was lifted upward at a maximum of 4,107mm at the point of 2,400mm to the portside. The CVK was deformed upward by 1,367mm, and the starboard bottom was bent upward by 1,758mm at the point of 1,800mm away from the baseline. The main deck was



<Figure III-1-7> Bow fractured surface deformation

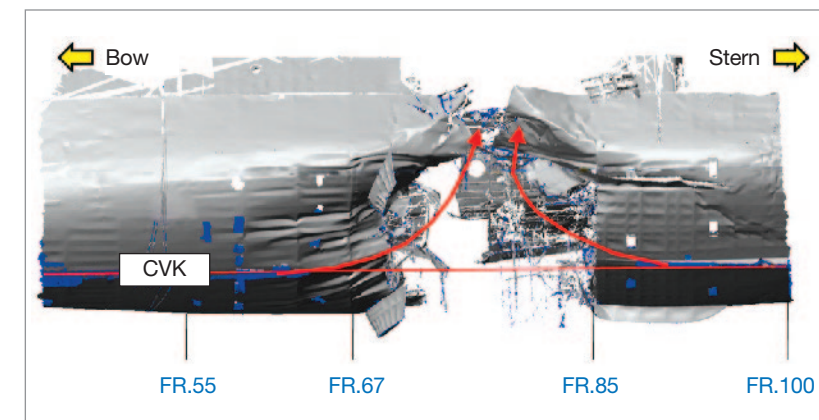
lifted 1,475mm from the baseline at the point 2,400mm to portside.

For the main deck, as seen in <Figure III-1-8>, the breakplane is located along Frames 73~77. The fracture occurred by the concentration of stress of an external force impacting on the round end of the deck opening, and the port side is more severely deformed upwards compared to the starboard side.



<Figure III-1-8> Main deck deformation

The precision analysis on the deformation of the hull, as seen in <Figure III-1-9>, supports the assessment that a non contact underwater explosion occurred below the portside gas turbine room, and the shock force generated migrated to the internal structures on the starboard side to cause the deformation.



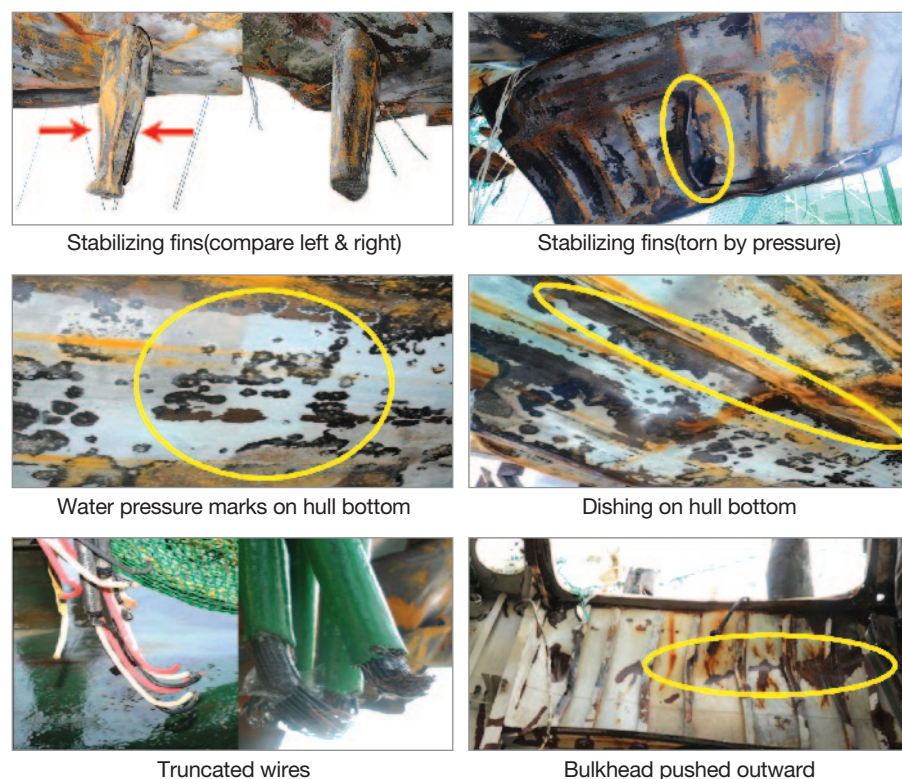
<Figure III-1-9> Fractured surface of portside bottom

## 4) Trace Analysis

Trace analysis examined minute traces of the pushes, pressures, cuts, and scratches on the hull and determined the types of external forces, such as an explosion or a shock, and assessed the origin of the force.

As <Figure III-1-10> shows, the portside stabilizing fins were crushed on the bottom portside, and the fin on the starboardside was torn with pressure marks. The bow breakplane's keel on the starboard side hull bottom had marks caused by a strong water pressure and bubble dishing marks on the bow breakplane region, where paint had been scratched off by a strong water pressure. The wires at the breakplane were truncated with a strong force without traces of melting by heat, and the gas turbine room's rear bulkhead stiffeners were pushed toward the upper starboard side, and traces of ripping were also observed.

Such pressure, water pressure, dishing, truncation, cutting, pushing, and ripping traces



<Figure III-1-10> Trace analysis

were assessed to have been caused by a shockwave and bubble effect from an underwater explosion.

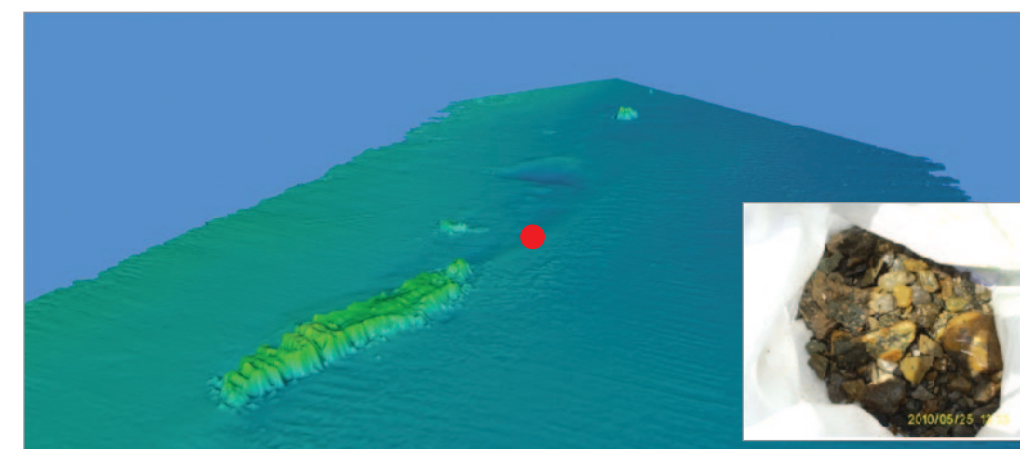
## 5) Sub-Conclusion

The overall study of shape and trace analysis indicates that bubble effect and shockwave caused by an underwater explosion were the external force exerted on the hull. The explosion originated from the point below the bow part gas turbine room on the portside bottom, and the explosion force traveled from the portside bottom diagonally toward the starboard side and caused the bow and stern to separate.

## 2. Evidence Analysis

### 1) Evidence Collection

Evidence was classified into gathered items from the sea area, collected items from the bow and the stern, and gathered items from the seabed. First of all, 12 warships including ROKS Jeju, ROKS Yeosu, ROKS Yangyang, ROKS Pyeongtaek, ROKS Jinhae, ROKS Chunghaejin, ROKS Sunginbong, ROKS Ongjin, ROKS Gimpo, ROKS



<Figure III-2-1> Soil with explosive substance near the explosion point and the collected location

Goryung, ROKS Dokdo, and USS Salvor, 5 coast guard boats which participated in the initial rescue operation for survivors, Daechung Island base, Baekryong Island base, Sochung Island R/S, and the 6th Brigade were committed in collecting items from the sea area. The JIG organized shore searching groups and thoroughly searched the seashore using RIBs. A total of 431 items was collected through the collection operation, and 29 items were selected and examined including soil collected from the origin of detonation, metal pieces that were suspected to be fragments, and materials that may have adhered some explosive components.

The evidence collection included the 10 items of clothes gathered from the severely wounded victims and lookouts, which were analyzed in prior to evidences from the hulls. As for the collected evidence from the hulls, an on-scene examination was conducted for urgently collected items, when the stern, bow, and stack were salvaged. Then items required to go through explosive components and metal component detection analysis were collected and analyzed more precisely on the overall hull when the hull was transported to the 2nd Fleet Command in Pyeongtaek.



〈Figure III-2-2〉 Collection activities on the barge when the hull was salvaged

During the stern salvage, from 1430 to 2330 hours on April 15, collection activities using gauze were focused on the breakplane. 11 items such as fibers and insulation material dispersed on the breakplane, and 2kg of mud from the diesel engine room were collected. After moving to the 2nd Fleet Command in Pyeongtaek on April 18, the first precise examination was conducted between 0800~1700 hours. A careful observation was ex-

cuted on the breakplane, along with O-1 deck, and the crews' mess hall(the areas near the breakplane). Asbestos, and fiber were collected from the breakplane, and metal fragments squeezed in fissures or mud were also extracted. 25 bags of mud were also collected from the diesel engine room and crews' mess hall floors(total of 147 items collected). Second precise examination was conducted on April 21 between 0800~1800 hours. During the process, new metal fragments and additional 60 items of evidence were discovered. The team used gauze to wipe the entire breakplane to collect evidence.



〈Figure III-2-3〉 Evidence collection at the stern

On April 24, when the bow was being salvaged, an on-scene analysis aboard the barge was conducted from 1220~1620 hours. Metal fragments were collected from the bow breakplane starboard side, and gauze was used to wipe and collect foreign substances on the damaged and fractured regions of the hull and stabilizing fins. 46 items such as fibers and heat insulations dispersed on the bow breakplane were collected, including 6 glass fibers and sponges underneath the stack damage area.



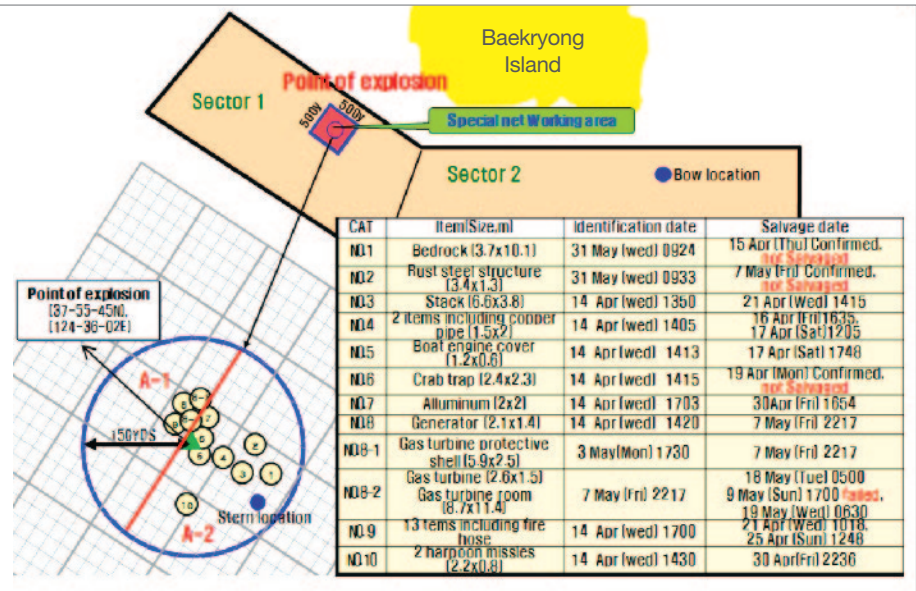
〈Figure III-2-4〉 Evidence collection at the bow

On April 26, after moving the bow and stack to the 2nd Fleet Command in Pyeongtaek, detailed analysis on the bow and stack area was conducted from 0800~1600 hours and metal fragments dispersed around the bow breakplane curvatures were collected. Through wiping with gauze, 33 items including asbestos and sponges on the breakplane, fibers tangled around the central pipelines, asbestos and fibers from the lower stack, and soot samples from the stack interior were also collected. From May 1 to 8, detailed analysis was conducted four times on the stack, and 19 additional items such as white powder from the internal and external surfaces of the stack, sponge, and fiber were collected. Thus, a total of 316 items were collected from the salvaged hull.



〈Figure III-2-5〉 Evidence collection at the stack

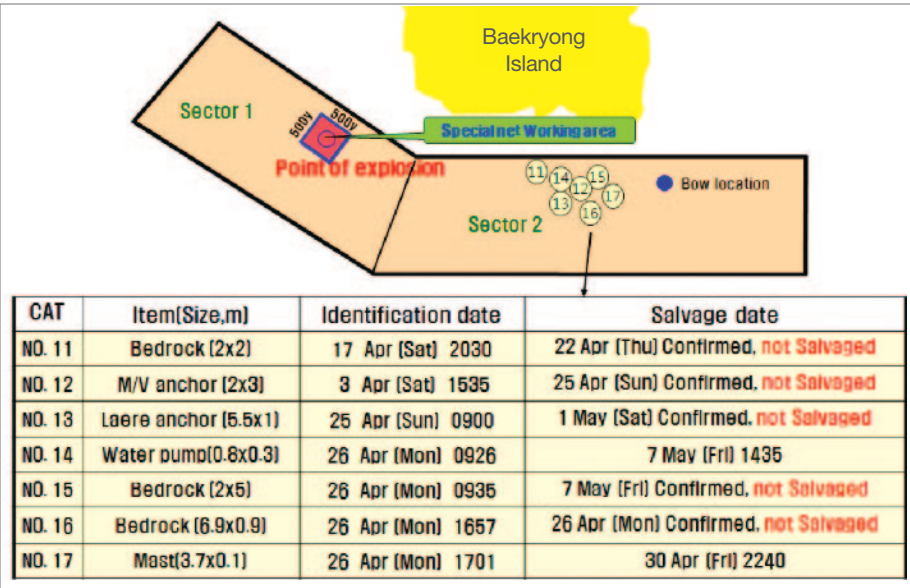
The JIG sought multiple measures in regard to the collection of items from the seabed, committing 8 ships from ROK<sup>1)</sup> including a mine searching ship, and a rescue ship; the US committed the USS Salvor; and Korea Ocean Research & Development Institute(KORDI) ships Jangmok and Yuhdo were employed for the search operations. 106 divers and the robot Haemirae were also committed in the search operations, but currents of 3~5 kts on average, the water depth of 47m, and the underwater visibility of 30cm made the operation very difficult. Until April 3, the focus was on rescue activities, and until April 24, salvaging the stern and the bow was on main concentration. Therefore, the evidence from the seabed, such as hull debris from the detonation, was actually collected after April 25.



〈Figure III-2-6〉 Sector 1 hull identification and salvaging status

The search operation was divided into sector 1 which included the origin of detonation, and sector 2 that included the sinking point of the bow as shown in 〈Figure III-2-6〉, and 〈Figure III-2-7〉. An extended search(ROKS Gimpo, ROKS Goryung, and ROKS Ongjin) was conducted on the outer ring of sector 1 and 2. As for detailed searching in sector 1, ROKS Yangyang and Ship Haemirae were utilized from April 14 to 16, and they identified items and collected some light items from waters surrounding the origin of det-

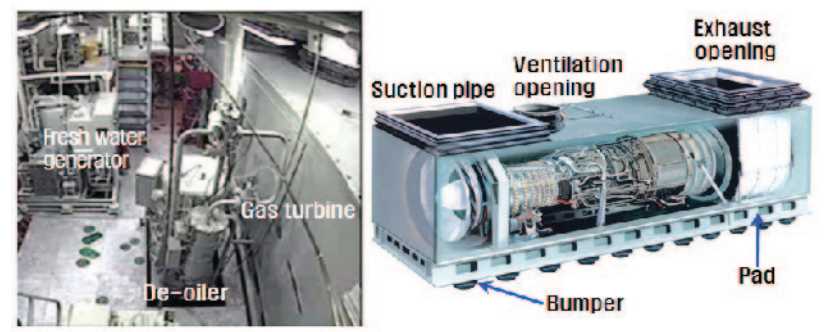
1) ROKS Goryung, Gimpo, Ongjin, Gwangyang, Sunginbong, Pyeongtaek, Chunghaejin, and Yangyang.



〈Figure III-2-7〉 Sector 2 hull identification and salvaging status

onation(1NM × 1NM). Through detailed searching in sector 2, ROKS Goryung identified items between April 25 and 26, and KORDI investigation ships(Ship Jangmok and Ship Yuhdo<sup>2)</sup>) were committed in order to conduct more precise investigation and search operations between April 17 and 20.

Although aforementioned search operation identified the locations of various items, the bad weather, strong currents, and limited underwater vision caused difficulties for the collection operations. However, when permitting, the JIG continuously conducted search



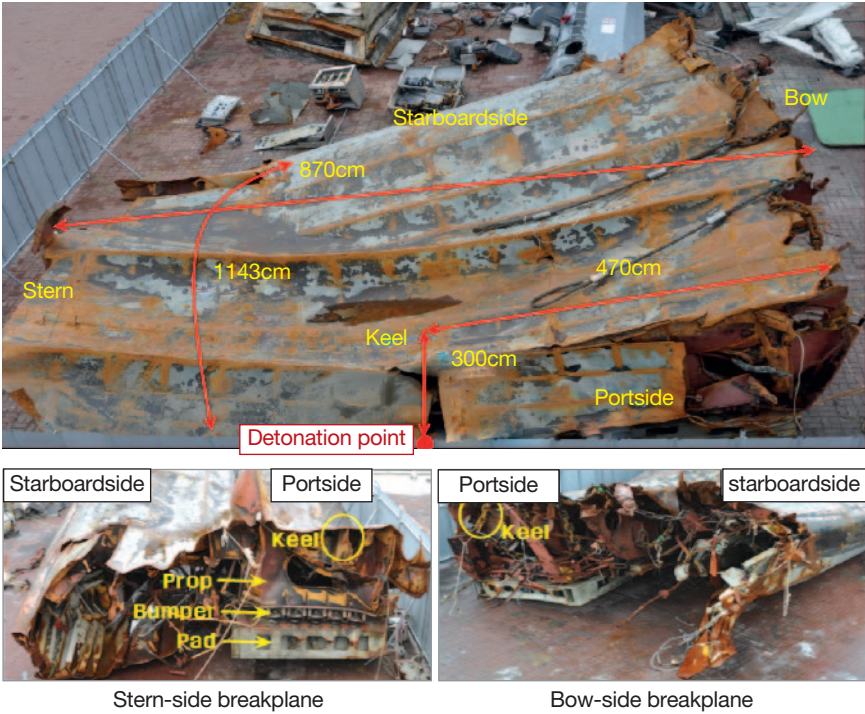
〈Figure III-2-8〉 The gas turbine room layout and gas turbine configuration

2) ROKS Jangmok and Yuhdo are equipped with side scan sonars that can identify items which are larger than 1m.

operations and salvaged the gas turbine protective shell, the generator armature, and the motor on May 7. On May 8, between 0930 and 1400 hours, the JIG collected 14 materials including fibers, and metal fragments from the salvaged items. Moreover, the JIG attempted to salvage what seemed to be the hull of the gas turbine room, but the ground condition of the area consisting of bedrocks, bad weather, and its heavy weight halted our attempt.

At last, on May 9, Navy UDT divers identified that the unknown material was in fact the actual gas turbine room. ROKS Gwangyang attempted to salvage it, but failed because the 5-inch(12.7cm) rope was severed on the water surface. Considering the limited capabilities<sup>3)</sup> of a 60-ton crane of the ROK Navy and the harsh underwater conditions of the area, the JIG decided to use a commercial crane and signed a contract with Yoosung Development. On May 17, a civilian company-owned crane arrived on scene, prepared to salvage the item, and succeeded in salvaging the item around 0630 hours on May 19.

The salvaged gas turbine room was 8.7m in length and 11m in width on the hull bottom and on the starboard side, and weighed about 30tons as shown in <Figure III-2-9>.

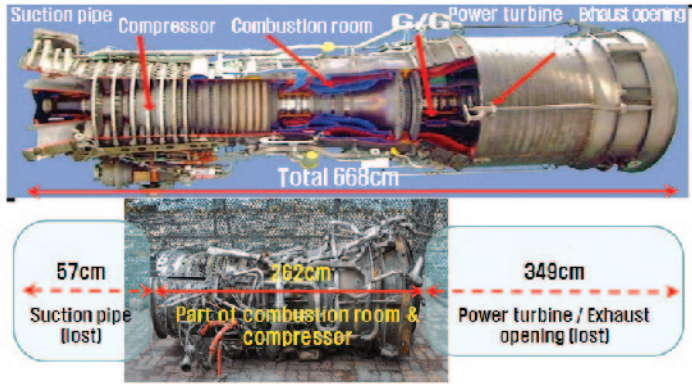


<Figure III-2-9> Salvaged bottom shell portion of gas turbine room

3) Maximum water depth of 20m, salvage height 25m.

The point about 3m away from the gas turbine room’s portside hull bottom, which was expected to be the location of detonation, was damaged. The gas turbine pad, bumper, and props that were formed with a strong steel-frame structure were not severed, but the fore and aft regions of the pad which are relatively vulnerable were severed. 3 pieces of gauze were used to wipe the hull bottom and the breakplane, and 2 metal pieces were collected from the gas turbine room.

Also, as for the turbo engine(gas turbine) which was salvaged on May 18, the suction pipe(57cm) and the power turbine/exhaust opening(349cm) were missing from the 668cm long body that is consisted of the suction pipe, compressor, combustion room, power turbine, and exhaust opening. The combustion room and the part of the compressor(262cm) were intact. Considering that this equipment is covered by the protective shell, the JIG assessed that metal fragments or explosive components are unlikely to be detected, so the JIG confirmed the deformation of shape without conducting an extra collection search.



<Figure III-2-10> Salvaged gas turbine

As for the evidences collected from the seabed using a special net, the JIG explained operation purpose and methods to the ROK Navy HQ, Navy Operations Command, Navy Search and Rescue Group, and ROK Marine 6th Brigade, and coordinated with them in terms of operation command and control, preparation and teaching collection and separation workforce, providing RIBs for transporting collected items, preparing working places on the Baekryong Island, and detailed matters that had to be prepared.

At the same time, the investigation result of underwater configuration by KORDI and the estimation result of an object’s traveling distance by an explosion by ADD were pro-

vided to the on-scene collection team. The collection operation for items on the seabed was started on May 10, and 21 items including the torpedo propulsion motor device were collected after over 10 days of the operations.

Category	Total	Examined	Not examined
Total	797	357	440
Gathered items from the sea area	431	29	402
Collected items	345	307	38
Gathered items from the seabed	21	21	0

〈Table III-2-1〉 Evidence status

As mentioned above, 29 items gathered from the sea area, 307 collected items, and 21 items gathered from the seabed, totaling 357 items overall, were examined.

The collected evidence was prioritized, considering the location that they were collected and the characteristics of the collected items, and then examined by KCIC scientific investigation lab and the NISI. Both physical and chemical analyses were conducted on 118 items. On the basis of the results the JIG organized an evidence assessment committee conducting 3 discussions to select the evidences for the investigation.

CAT	TOT	Fibers	Metals	Plastics	Asbestos	Soil	Gauze	Other
TOT	357	33	67	31	34	42	96	54
Metals	164	7	67	11	3	25	35	16
Explosives	311	33	41	25	31	31	96	54

〈Table III-2-2〉 Examination status

\* The total is a figure that excludes the overlapping items.

Also, the CCTV hard disk that could be used to verify the situation during the incident was primarily gathered and restored during the bow salvaging operation. Recovery process of the collected hard disks included hard disk separation, hard disk washing(of fuel and mud), providing electricity, hard disk operation, and data recovery. Data recovery in the hard disk took 8 days to complete, and on May 2, images from 6 CCTV locations out of 11 locations were successfully recovered, and the JIG was able to verify the images from right before the incident.

The evidence collection activities utilized every possible mean including the JIG, Navy search/rescue group, and civilian resources, and overcame difficult conditions of the scene, weather, and water. The collection, recovery, and examination status by each of the stern and bow salvaging and search/rescue operation stages is shown in 〈Table III-2-3〉.

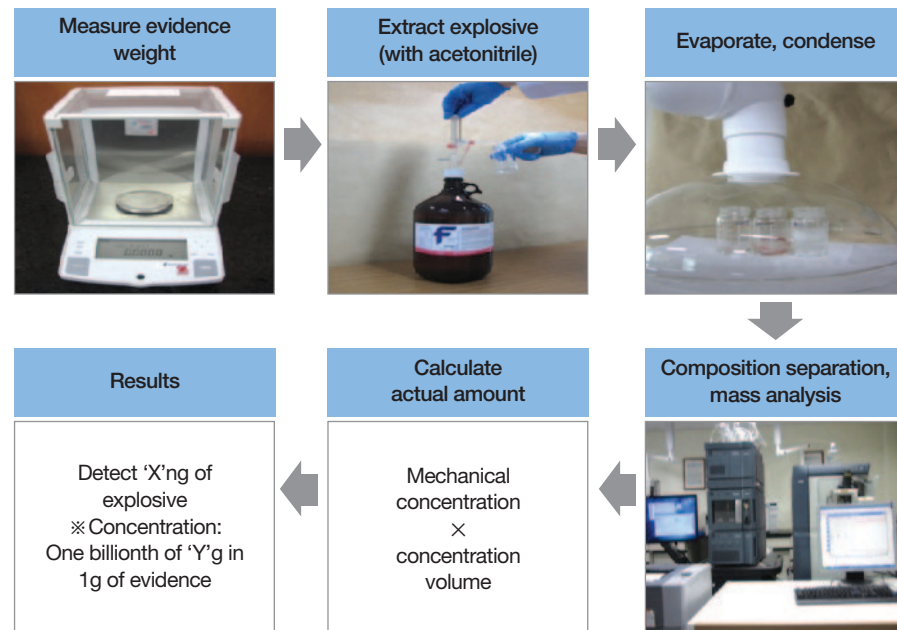
CAT	Contents
Stage 1 Stern salvage (Apr 15)	<ul style="list-style-type: none"> <li>Collected survivors' clothing, items on the sea, items on the stern(626 items), request for examination(219 items)</li> <li>Prepared to collect evidence on the seabed(approved by the Minister of National Defense) <ul style="list-style-type: none"> <li>Discussion with ROKAF Safety Director and company representatives: Apr 17</li> <li>ROK Navy HQs coordination meeting: Apr 19</li> <li>Making special nets(Apr 26), arrived on scene(Apr 30)</li> </ul> </li> </ul>
Stage 2 Bow salvage (Apr 24)	<ul style="list-style-type: none"> <li>Collected from the bow region and the stack, request for examination(98 items)</li> <li>Collected CCTV: Apr 24(Sat) 1100 hours, ward room</li> <li>Prepared to gather and collect underwater evidence</li> <li>* Committed collection team to Baekryong Is.(13 personnel) on May 1</li> </ul>
Stage 3 Propulsion motor device /gas turbine salvage (May 15~24)	<ul style="list-style-type: none"> <li>May 7, salvaged the generator and gas turbine room's protective shell</li> <li>May 15, collected propulsion motor device</li> <li>* Daepyeong Corp.(Daepyeong No. 11 and 12)</li> <li>May 18~19, salvaged gas turbine and gas turbine room</li> <li>* Yoosung Development(Ship Yoosung)</li> <li>Collected underwater evidence such as gas turbine's protective shell and the torpedo propulsion motor system(73 items), requested for examination(40 items)</li> </ul>

〈Table III-2-3〉 Status of the evidence collection, recovery, and examination by stages

## 2) Chemical Analysis

Chemical analysis was focused on detecting explosive substances, and the KCIC scientific investigation lab used the High Performance Liquid Chromatograph(Acuity model of Waters Inc.) and the Mass Spectrometer(Q-TOF Premier model of Waters Inc.) method to carry out analyses of 311 items.

### (1) Analysis Procedure

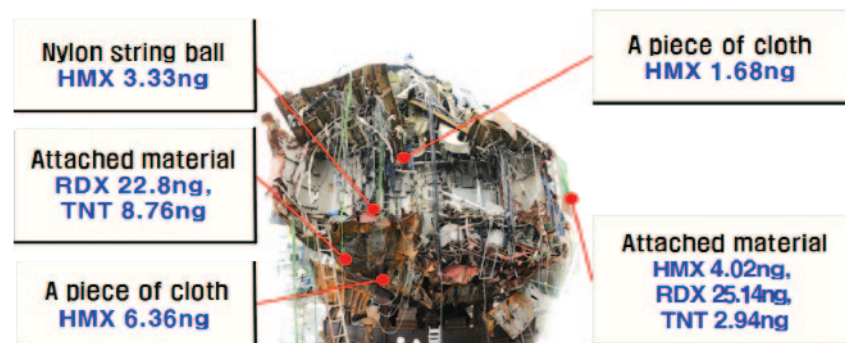


〈Table III-2-4〉 Explosive composition analysis procedure

### (2) Analysis Results

The explosive substances were detected on the bow breakplane, stack, gas turbine room, and oceanic and seabed evidence. In total, 527.91ng of HMX(28 items), 70.59ng of RDX(6 items), and 11.7ng of TNT(2 items) were detected.

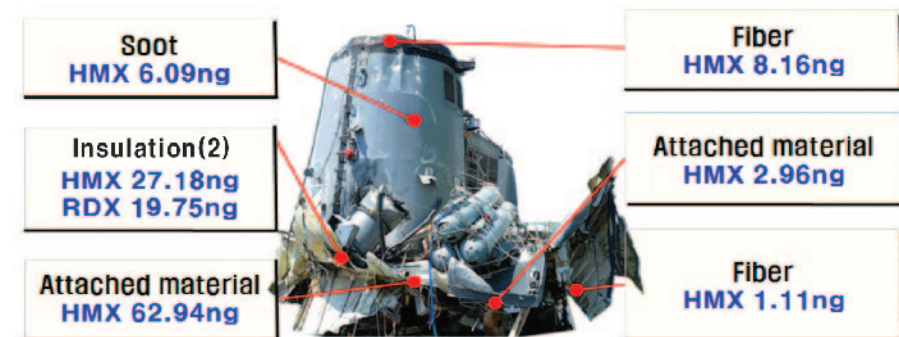
First, HMX was detected on the bow breakplane on items such as the nylon string ball from the 1st platform, attached materials on the shell of the draft line, and cloth near the piper and keel, and the JIG detected RDX, and TNT as well on the attached materials on



〈Figure III-2-11〉 Detected explosives in bow area

the shell of the draft line and stabilizer. In total, 15.39ng of HMX, 47.94ng of RDX, and 11.7ng of TNT were detected on 8 items.

On the stack that was detached due to the explosion pressure, HMX was detected on the internal soot, upper fibers, attached material underneath, attached material inside the pipe, crew galley's overhead bottom fiber, and the lower insulation. RDX was detected on the lower insulation(2 items). In total, 108.44ng of HMX and 19.75 of RDX were detected on 8 different items.



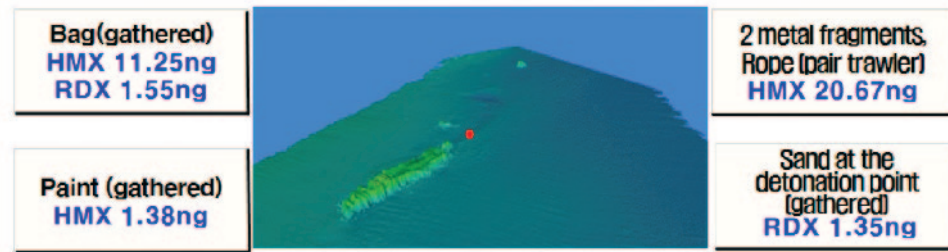
〈Figure III-2-12〉 Detected explosives in stack area

From the gas turbine room, which was damaged and lost from the explosion pressure directly impacting it, a total of 370.78ng of HMX was detected in 13 locations including the inner asbestos portside(2 items), plastic fragments at the protection compartment's ceiling(2 items), metal fragments within the protection compartment, metal fragment on the entrance shell, extracted gauze on the portside entrance shell(3 items), extracted gauze on the breakplane(2 items), and soils/fibers from inside the generator(2 items).



〈Figure III-2-13〉 Detected explosives in gas turbine room

The evidence collection operation of the seabed was conducted with bull trawlers during the search and rescue operation. Amongst the collected items, HMX was detected from the bag, rope, metal(2 items), and paint fragments, and RDX was detected from the bag, and sand around the incident site. In total, 33.3ng of HMX and 2.92ng of RDX were detected from 7 locations.



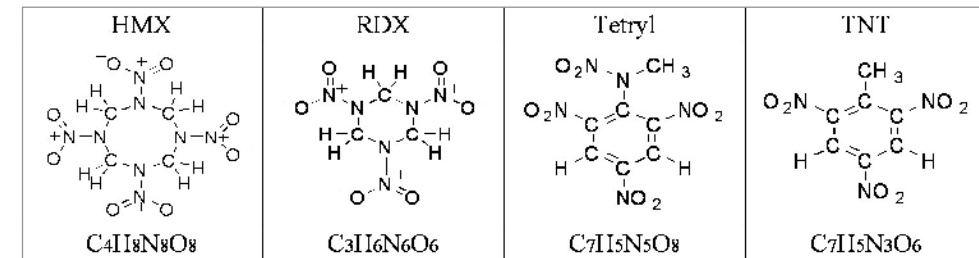
〈Figure III-2-14〉 Detected explosives from seabed evidences

After a comprehensive analysis on these discoveries, the team was able to confirm that explosives were detected in locations near the explosion area (bow portside, stack, gas turbine room, and seabed area). Additionally, the adhered materials were detected on the adhesive materials (insulation, fiber, and asbestos) and the explosive charge used in the incident consisted of HMX, RDX, and TNT.

After checking the manufacturing methods of the explosives, it was possible to confirm that pure RDX is manufactured through the Woolwich method for RDX production, but 5~10% of HMX can be generated if Bachmann method is used. In production of HMX, pure HMX is manufactured only through the Bachmann method.

Based on these facts, the JIG checked the type of explosives, and as a result, the JIG found that HMX (High melting point explosive, explosion speed of 9,100m/sec) is a colorless molecular crystal powder that has a high density and melting point and that since it is the most high-efficient explosive, it is used in precision weapon systems. RDX (Research Department explosive, explosion speed of 8,700m/sec) is a colorless crystal powder, which has comparatively high density and explosion speed, and since it has a stable sensitivity, it is commonly used in weapon systems. Tetryl (Tetranitromethylaniline, explosion speed of 7,850m/sec) has greater explosion power than TNT, and it is used as a substitute for TNT. It is widely used in mines and grenades. Lastly, TNT (Trinitrotoluene, explosion speed of

6,900m/sec) is widely used as a military explosive. It is chemically stable, so it is used in various propellants and explosives.



〈Table III-2-5〉 Molecular structure of the explosives

In order to determine whether the detected explosives were from ROK weapon systems, the JIG verified the records of firing exercises around Baekryong Island. As a result, the JIG was able to confirm that infantry battalions conducted integrated island defense firing exercises using 6 types of ammunitions in the year 2009, and 1,558 shells in total were fired. The artillery battalion's sea fires consisted of three types in 2009, which included a total of 636 shells fired. The firing of cannons consisted of three types with 712 shells and 257 shells in 2009 and 2010 respectively. But the majority of explosives used by the 6th Brigade and the infantry/artillery firearms contained RDX. Friendly torpedoes, sea mines, or ship-to-ship (Harpoon) missiles were not tested in the West Sea. It was also confirmed that the majority of ship gun ammunitions contain RDX.

CAT	Model	Charge	Major components
ROK	Torpedo A	DXC-04	Ammonium perchlorate, RDX, Al
	Torpedo B	DXC-05	HMX
	Mine A	H-6	RDX, TNT, Al
	Mine B	DXC-03	Ammonium perchlorate, RDX, Al
	76mm	Comp-A3	RDX
	40mm	Comp-A4	RDX
	Missile A	Destex	TNT, Al
	Missile B	DXC - 10	HMX, NTO, Al, Binder
Soviet SAET-60M (torpedo)			RDX, TNT ※ Bonn International Center for Conversion. 2005

〈Table III-2-6〉 Explosive components of major marine weapons

Explosive experts' opinions indicate that when a high explosive warhead is fired in the ocean and arrives at the sea surface, it explodes from the shock, and when high explosives explode on the sea surface most of the explosive components are transformed into explosive ash and explosive gases in order to generate the explosion. These are then lost in the water. The minute amount of unexploded explosive residue can be left in the water or on the seabed, but taking the currents and other factors into consideration, this is highly unlikely. On the basis of these factors, the JIG concluded that the detected explosives were not from friendly fire.

CAT	Ammunition type	Explosive components
1	High explosive A	RDX, TNT, WAX
2	High explosive B	RDX, TNT, WAX
3	High explosive C	TNT
4	Self-blasting bomb A	RDX, WAX
5	Tank gun high explosive	RDX, TNT, WAX
6	Coast gun high explosive	RDX, TNT, WAX
7	High explosive D	TNT
8	High explosive E	TNT
9	Hail bomb	RDX, WAX
10	High explosive F	RDX, TNT, WAX
11	High explosive G	TNT
12	76mm	RDX, WAX
13	40mm	RDX, WAX
14	Depth charge	RDX, TNT, AL, WAX

〈Table III-2-7〉 Explosive component by friendly ammunition types

The analysis attempted to determine the origin of the explosives using chemical fingerprint testing<sup>4)</sup>, and NISI conducted an isotope analysis of detected explosive residues from the collected items and explosive samples from the US, France, Canada, and ROK. However, the limitations arose in determining the specific origin of the explosives.

4) A testing method in order to determine the origin by looking at unique chemical fingerprint which is varied by the substance's raw material and manufacturing environment.

### 3) Physical Analysis

Even before the bow and the stern were salvaged, the physical analysis focused its efforts on securing North Korean torpedo samples, which were to be used for a comparison. Samples of a North Korean test torpedo were discovered by a civilian diver around Pohang on March 12, 2003. These had been stored in the Jinhae branch of ADD for research purposes, and the JIG was able to secure 3 pieces of a North Korean test torpedo for comparison.

In order to analyze the hull material of ROKS Cheonan, the JIG obtained standard metal and material parts of the hull from ADD; analyzed these components and their ratios; and also confirmed the component ratio of the gas turbine room by making several requests (these information are treated as corporate secret) to Samsung Tech-Win that manufactures and delivers military ship parts for detail information on the materials used for the gas turbine.

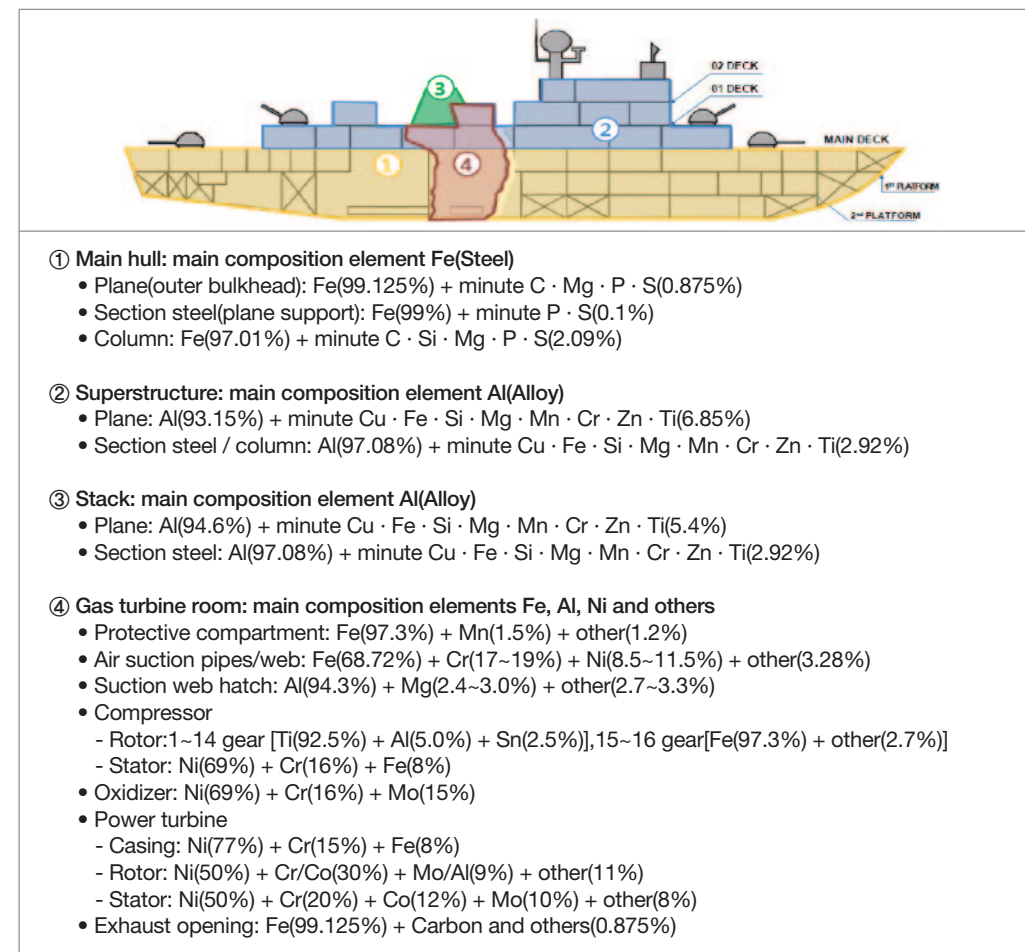
The aluminum fragments found on ROKS Cheonan's hull were small in size, between 1mm and 7mm. Furthermore, since they were mixed with mud and located in a gap on the breakplane, it was difficult to identify them with the naked eyes. After salvaging the stern, the bow, and the stack, the JIG concentrated on collecting microscopic items, and were able to collect a total of 164 metal pieces. KCIC scientific investigation lab conducted physical analyses on the collected items and the comparison samples by using SEM (Scanning Electron Microscope; Phillips Co. model XL30)/EDX method, and through a process of elimination by comparing these metallic fragments with materials found in North Korean test torpedo and in ROKS Cheonan, identified 6 pieces of aluminum and aluminum alloy fragments which were assessed to be parts used in a torpedo<sup>5)</sup>.

5) According to experts' opinions, the hull is not directly damaged or penetrated by a torpedo in case of an underwater explosion. Also, the torpedo external shell is made of Al alloys, causing it to become microscopic fragments or melt in the water when it explodes, so they may be swept away by the tides and is difficult to discover.

### (1) Composition of the Comparison Samples

The composition of ROKS Cheonan is as seen on <Figure III-2-15>; the main material of the main hull is steel, and the main material of the superstructure and the stack is aluminum. The main equipments such as the compressor, combustion, and the power turbine are composed of different materials such as aluminum alloys, or heat-resistant nickel alloys.

In case of a lightweight North Korean test torpedo, all of its components are made of aluminum alloy. The main body consists of 97.28% Al and 2.72% Mg; the propellers consist of 96.22% Al and 3.78% Mg; and the fixed-propellers consist of 95.88% Al and 4.12% Mg



<Figure III-2-15> ROKS Cheonan hull composition

CAT	Body (Al 97.28%, Mg 2.72%)	Propeller (Al 96.22%, Mg 3.78%)	Stationary fin (Al 95.88%, Mg 4.12%)
North Korea torpedo			

<Figure III-2-16> Composition of North Korean light weight torpedo samples

### (2) Composition of the Collected Items

Location	Gap on wall of food table in the galley	Fwd starboard side of crews' mess hall	Near bilge keel of the stern portside
Item			
Comp.	Al 96.08%, Mg 3.92%	Al 100%	Al 100%

Location	Central region of the stern starboard	In the mud from crews' mess hall	External wall of crews' mess hall
Item			
Comp.	Al 96.07%, Mg 3.93%	Al 100%	Al powder(contains Mg)

<Figure III-2-17> Composition of evidences

The JIG analyzed and compared 6 identified items with the samples from ROKS Cheonan's hull and the North Korean test torpedo, but the JIG was only able to conclude that each of the metal pieces is not identical to one another. Although every possible analysis method was employed such as the multi-element analysis by NISI and the precise composition examination through KAIST, the information concerning the types of metal used in torpedoes and their composition is classified in every nation, and therefore, there were fundamental limitations to the analysis. Especially, experts' opinion was that it

would be difficult to find fragments since they would have been broken down into minute pieces in case of an underwater explosion.

### (3) Analysis Result

A precise analysis was conducted on the 3 samples of a North Korean test torpedo (body, rudder, and propeller), 6 samples from ROKS Cheonan (stack shell plating, stack interior stiffener, stern interior, and outer bulkhead of the mess hall), and 6 main collected items, but the JIG was not able to identify any metal fragment that was actually used in the torpedo, which sank ROKS Cheonan.

### 4) Sub-Conclusion

From examining 219 items out of the 626 collected items, including items from the stern, survivors' clothing, and gathered items from the sea area, the JIG detected 12.63ng of HMX from 2 locations and 2.9 ng of RDX from 2 locations, and also identified 6 pieces of aluminum and aluminum alloys during the first stage when salvaging the stern (until April 15).

123.83ng of HMX from 10 locations, 67.69ng of RDX from 4 locations, and 11.7ng of TNT from 2 locations were detected from the 98 collected items from the bow region and the stack during the second stage, when salvaging the bow (until April 24).

391.45ng of HMX was detected from 16 different locations when the JIG analyzed 40 collected items from the generator, gas turbine room, and torpedo propulsion motor device during the third stage when salvaging the propulsion device and the gas turbine (until May 19).

In conclusion, ROKS Cheonan was hit and sunk by an underwater weapon carrying mixed explosive composed of HMX (527.91ng in 28 items), RDX (70.59ng in 6 items), and TNT (11.7ng in 2 items).

## 3. Testimony Analysis

Before collecting testimonies from the 58 survivors, the JIG first acquired the Military Capital Hospital director's approval and consulted respective surgeons in order to ensure that the individuals were stable enough to give out testimonies. 50 survivors including

the Commanding Officer issued their testimonies one day after the incident, on March 27, in the Military Capital Hospital. 8 severely injured personnel and those who had participated in the rescue activities were not included. On the next day, the JIG collected testimony concerning the location of the incident, measures that were taken following the incident, and crew members' behavior. On March 31, because the initial testimonies were assessed to be incomplete, the JIG asked for additional testimonies from those personnel whose testimonies were needed to be double checked and from those that the JIG did not inquire initially. On April 1, the JIG collected detailed testimonies from crew members regarding their actions right before and after the incident.

Along with these testimonies, the JIG also acquired the Commanding Officer's reports, phone logs with the Squadron Commander, and records of the communications of the officer's with the radar base soldier on duty.

Testimonies of the 2 sentry soldiers were collected. They witnessed the sinking of ROKS Cheonan at the guardpost in Baekryong Island. The JIG inquired 2 statements from each sentry soldier about the incident on March 28(1), April 2(2), and April 4(1). On May 2, the JIG conducted the polygraph tests on these individuals to conclude that their testimonies were truthful, and therefore the JIG accepted these testimonies as evidence.

### 1) Situation during the Incident

The Commanding Officer (CDR) and 26 of the other survivors said they heard the sound of an explosion, "Gwang! Gwa-ang," followed by a power outage. Then their bodies were lifted up 30cm~1m in the air before falling towards the starboard side of the ship. 41 survivors said that they smelled oil, and that there were no witnesses of flames, fire or a water column, nor did any injury result from these factors. There were 50 patients with bruises, fractures and sprain.

In particular, the chief radar officer said that an initial 'koong', then 'gwang' explosion sound was followed by a blackout. An ammunition serviceman said that he heard a 'gwang', when the ship tilted to the starboard side and the 'gw~ang,' and it seemed as if the stern was being ripped off the hull. Such testimonies indicate that an underwater explosion caused the initial explosion sound, then the pressure broke out, causing shock and the secondary explosion sound, and this is consistent with the UNDEX bubble effect.

## Major points of testimonies

- While I was checking KNTDS, operations and the daily schedule, I heard an explosion sound, then was lifted 30~40cm in the air and fell towards the starboard side. I was later rescued by my subordinates (Commanding Officer)
- While working on administrative duties at the XO's stateroom, I heard a 'gwang' sound, was lifted up in the air, and then fell as the power went out. When I opened the door and escaped to the deck, there was no stern, and the mast fell to the starboard side and was being rocked (XO)
- While on bridge duty, a 'gwang' sound occurred and the ship was tilted 80~90 degrees to the starboard side. I did not see any light, flashes, flames, water pillars, or smoke (duty officer)
- While I was working at the chief mechanic's office, I lost consciousness due to the explosion and shock. I stepped on the washstand and doorstep to escape and conducted rescue operations (chief mechanic)
- At the bow R/S, I was having a conversation with fellow service members when I heard a 'koong' sound and the lights went out. I also smelled fuel. I could not make an assessment on the cause of the incident (chief gunner)
- While I was on watch officer duty, I heard a 'koong' sound, after which I was lifted a little in the air, but did not smell any explosive or other substances (communications officer)
- I heard a 'gwang' sound while sleeping in the operations officer stateroom, and I opened the outer hatch and escaped to request rescue to the 2nd Fleet's situation cell (combat information officer)
- While studying for the non-commissioned officers' ability test at my berthing cabin, a 'koong' sound was followed by a power outage. Although there was no smell of explosives, I thought that the incident had occurred because of some external force (chief steerer, MCPO)
- While sleeping in my berthing, a 'gwang' sound was followed by the smell of seawater and fuel, but I had no idea what the cause was (internal machinery chief)
- I was sleeping in the berthing, and at the time, I did not hear any explosion sound. But I did feel the bed caving in, and I smelled fuel, but not explosives. I believed the cause of the incident was an attack from either a North Korean submarine or semi-submersibles (Chief electrician)
- While sleeping in the 2nd floor of the CPO berthing, I heard a 'gwang' sound, and my head banged against the 3rd floor bed. Then I fell to the ground. I didn't smell explosives, but I did smell fuel. I determine it to be due to an external explosion (chief deck officer)

- While on communications stateroom safety watch duty, a 'gwang' sound was followed by 30~40cm of lifting into the air, and then I fell toward the starboard side. When I came up to the port, the place was flooded with water, and therefore I felt water splashing under my feet while moving. I did not smell explosives, but did smell fuel (communications chief)
- While sleeping in the berthing, a 'gwang' sound pulled me to a corner of the room, and I heard tools falling. Nothing special, other than the smell of fuel (internal combustion engine chief)
- While working on my PC at the ammo admin room, I heard a 'gwang' sound followed by power outage when my body and the objects around me floated in the air then fell (Chief firearms officer)
- An initial 'koong' sound was followed by a secondary 'gwang' 2~5 seconds later, when the power went out and oil was splashed onto my face (Chief sonar officer)
- While sleeping in the CPO berthing, I did not hear shock sounds but anyway I fell from the third floor bed, and when I regained my consciousness the seawater was coming in and I smelled fuel (chief maintenance officer)
- While resting at the sailing crew berthing, a loud sound was followed by the tilting of the ship, and my fellow crews said we must escape because there was flooding, and I smelled fuel (deck officer)
- I was sleeping in the sailing crew berthing and smelled fuel after a 'koong' sound (steering petty officer)
- While asleep on the gunnery crew berthing two-story bed, I heard a 'gwang' sound, then my body was flung toward the starboard side bulkhead, hitting my arm and my legs, falling to the ground (control petty officer)
- While sleeping at the gunnery crew berthing, I heard an explosion sound, and I did not smell explosives, but did smell fuel, and the bridge had tilted about 90 degrees, but I could not verify the bow parts (ammunition petty officer)
- While on duty at the combat information center, I heard a shock sound, then was flung toward the starboard side bulkhead, along with other objects sliding down toward it (sonar radar officer)
- While on duty as the assistant watch officer, a 'gwang' sound was followed by the ship tilting 90 degrees, and I escaped to commence rescue of the crew members (deck officer)
- While sleeping at operation crew berthing, I banged against the right bulkhead and fell off to the floor (communications officer)
- I could not hear a shock or explosion because I was asleep in the gunnery crew berthing, but I heard the portside cabinets falling to the floor, and I could not see lights/flames/water pillars but I think that a torpedo accident had occurred (radar petty officer)

- While playing a cellphone game at the operations berthing one-story bed at the starboard side, a 'gwang' sound was followed by a severe shaking, and then the ship started to tilt toward the starboard side (Comms. officer)
- While on safety watch officer duty at the combat information center, I heard a loud sound and the ship tilted to one side, and I was pressed under piles of computers and other equipment, and sustained fractures at the head, waist, and legs (electrical warfare petty officer)
- While doing night-shift at the sonar room, I didn't detect any special signal or sound, but a sudden 'gwang' sound was followed by power outage, and I thought that the ship had abruptly collided with something. When I came out to the outer deck the portion from the stack on was fallen off, and I thought that a war had broken out (sonar petty officer)
- While sleeping at the operations berthing, a 'koong' sound was heard once, when my body floated up by 5~10cm, but there was no smell of flame or explosive at the time (sonar petty officer)
- While working night shift at the sailing portion, I was flung forward after a 'kwa-gwa-gwang' sound, but I could not smell any explosive or fuel (steerer)
- I was working night shift, and rescued by other crew members since I lost my consciousness at the time of incident. I don't think this was caused by some internal factors but an external force exerted a shock (fire control petty officer)
- While resting at the front gunnery berthing, a 'gwang' sound was followed by lifting in the air when the ship tilted 90 degrees and the objects in the room slid toward the same side (radar petty officer)
- While listening to music at the gunnery crew berthing, a one-time explosion sound was followed by power outage, and the ship tilted, making tools fall to the ground. Later on I saw that the stern wasn't there. I think the cause is a torpedo or a sea mine (firearms petty officer)
- While on safety watch duty, I was sprung toward the right after a 'gwang' sound. I smelled fuel and I think the incident's cause is a torpedo attack (radar petty officer)
- While sleeping at the operation crew berthing, a shock was followed by the ship tilting, and the cabinets fell to the ground, and when I came up to the deck I smelled a lot of fuel (radar petty officer)
- While reading at the gunnery crew berthing, I heard a one-time 'gwang' sound, and my body was lifted then the ship tilted. The stern was invisible from the portside (tracking petty officer)
- While sleeping at the operation crew berthing, a one-time 'gwang' sound was followed by power outage, when the bed tilted to the right. When I regained consciousness, I sensed the heavy smell of fuel (radar petty officer)

- While reading a book at the sailing crew berthing, I was lifted about 50cm~1m in the air and lost consciousness. After recovering my consciousness, I moved to the bow with 2 other crew members (gearing petty officer)
- While resting at the elec/maintenance room, I was lifted about 50cm with a 'gwang' sound. Then the ship was tilted to the starboard side and no flame was observed (electricity petty officer)
- Wearing winter workwear and 2 layers of coldproof wear, I was on sentry at the starboard side bridge wing, and the weather was so cold that I only watched the bow as I worked. The ship tilted to the starboard side with a 'gwang' sound, and I moved to where the life belts were on the port side through the bridge because water flooded in up to my thighs. This was followed by severe shaking at the bow bottom, but did not smell explosives (deck petty officer)
- While sleeping at the operation crew berthing, I heard a sound of mixed explosion and shock, and afterwards the ship tilted to the right, and I was sprung toward the portside section, where I was stuck. I did not witness any water pillar or flash of bright light, but did smell lots of fuel, and I assess it to have been due to a sea-mine or a torpedo or another type of external shock (radar petty officer)
- When listening to music at the deck administration room, a 'gwang' sound was followed by floating up in the air, and my body suddenly tilted to the left. I didn't smell explosives, but definitely smelled fuel (deck petty officer)
- While on the engine messenger duty, I heard a 'gwang' sound when my body was lifted 50cm in the air, when the ship tilted and the power went out (steerer)
- While sleeping at the operation crew berthing, I floated in the air a little then fell, when I heard the bed breaking and water flowed in (radar petty officer)
- While sleeping at the operation crew berthing, a 'gwang' sound was followed by the ship tilting to one side, and I floated in the air from the 3rd floor bed then fell, and when I escaped to the deck to see the surroundings, the ship was invisible, having been cut in half including the stack (communications petty officer)
- While conducting duty as the steerer, I heard a loud sound at the stern's portside, and then the bow was lifted up for the body to float upward, and the ship tilted toward the starboard side 90 degrees. I could not make out whether the loud sound was a shock sound or an explosion sound, but I heard the hull being ripped apart, and the smell of fuel came up from the stern (deck crew)
- While preparing to wash at the sailing crew berthing, a 'gwang' sound followed by a feeling of being hit by something, and a lot of weight was felt. At the same time the ship rocked side ways, tilting finally toward the starboard side. Right after the incident, I heard seawater flooding and smelled fuel (deck crew)

- While preparing to take a shower at the berthing, a 'kwang' sound, then I floated up in the air, falling toward the right. I couldn't see because the lights were out, and there were no flames or smoke, but I did smell fuel (galley crew)
- After hearing a clang of steel banging against each other, the ship tilted, and when I came outside the deck, I smelled a little bit of fuel. Coming outside, 1/3 of the deck bridge had been submerged (communications crew)
- While resting beside the stairs of the sailing crew berthing, I heard a 'koong' sound followed by lifting 30cm in the air then fell, when I escaped to the portside, and when I got there I smelled oil and the stern was invisible (deck crew)
- While on R/D duty at the combat information center, a 'kwang' explosion sound was followed by a 50cm jump in the air when the power went out, and when I opened my eyes 2~3 seconds later, the ship had tilted completely toward the starboard side, I did not smell any flame or explosives but did smell oil (radar crew)
- I heard a 'kwang' sound then the ship tilted when I heard another 'kwa~ang' sound as if the stern had been torn off, then the power went out and the ship tilted completely 90 degrees to the starboard side. I smelled a lot of fuel (firearms crew)
- While preparing to wash at the operations crew berthing, I heard an extremely loud explosion sound, and I could not smell explosives, but did smell fuel at the hull bottom parts. When I escaped the stern was invisible (steering crew)
- While stooling at the head, a 'koong' sound was followed by the ship tilting 90 degrees toward the starboard side, so I fell to the point beside the door of the deck administration room, and I did smell serious fuel (galley crew)
- While I was sleeping, I heard a 'gwang' sound when the ship started to sink, and when I escaped to the outer deck, the stern was invisible. I smelled none other but the fuel (electronics crew)
- While on duty at the portside bridge wing wearing winter workwear and coldproof clothing, a sudden 'gwang' sound was followed by 1m floating in the air then I fell onto the floor, but by that time I could not smell explosives neither could I see a water column or a fire (deck crew)
- While taking a shower at the head, I heard a big, short noise, then the noise of objects falling to the ground (medical crew)
- While taking the washed laundry to the drying machines, I heard some sort of a sound between a 'bang' and a 'koong', the sounds of steel bashing against each other, and also felt the ship floating in the air. I smelled burning fuel from the stack, but other than that I didn't notice any flash, flame, or smoke (ventilation crew)
- While washing at the head, I heard a 'gwang', but I could not tell whether the sound was coming from the inside or the outside (firearms crew)

## 2) Cause of Explosion

Considering the fact that the area that they were patrolling was close to the NLL, and because the ship broke apart so suddenly in a midst of normal operations, several survivors(11) thought that the ship had been sunk by a torpedo.

### Major points of testimonies

- After the accident occurred, as I came out to the portside deck, the stern was severed and could not be seen, and based on the loudness of the explosion, and the wireless communication report that ROKS Sokcho was opening fire, I assessed that this must have been an enemy torpedo attack(Commanding Officer)
- There was no smell of explosives, and considering the ship's separation in half, I would expect this incident was caused by either torpedo or mine explosion.(Executive Officer)
- Based on the nature of the patrolling area and hull structure I predicted that this was an attack from the North(combat information officer)
- My job is radar detection, so I'm sensitive to external shock sounds, and I thought initially that we were hit by a merchant ship, but looking at the area after escaping to the bow, I thought then that we were hit by a torpedo(radar chief)
- After rescuing the crew, having come to the outer deck, I saw that the stern was missing from the stack location, so I thought that a war had broken out, and also thought that something that could cause this kind of shock was a torpedo(radar officer)
- We were on the same route we'd always gone, and there was nothing special for hours, but we were suddenly sunk, so I think that a torpedo is more likely than a sea mine(steerer)
- I think it's a torpedo or a sea mine; if an explosion occurred within the ship, I would have been flown toward the bow or stern but I clearly flew toward the starboard side(ammo officer)
- I felt that we were hit by something and it was an external shock, so I think it's either a sea mine or a torpedo, but not rocks(radar officer)
- I think it's a North Korean torpedo attack or a sea mine explosion, a torpedo attack to the portside caused the ship to tilt to the starboard side and the explosion sank it(deck crew)
- The explosion was so loud that I can still recall it and I also fell and got hit by things and all the while I thought we were hit by a torpedo(steerer)
- The cause of the incident is, I think, a light torpedo from a North Korean sub hitting the portside stern, causing the ship to crack in half and the heavy stern to sink(deck crew)

### 3) Communication Details

The JIG confirmed that some survivors during the early stages of incident used imprecise diction such as ‘aground’ and ‘shipwreck’ when reporting because they had no mind to judge the situation accurately, the JIG also confirmed the communication records between commanding officer and the Squadron Commander determining the cause of this incident to be a torpedo, and between the communications officer and the radar base including the assessment that this incident is from a torpedo attack.

#### Main contents

- Chief gunner ↔ Chief of the situation room, 2nd FLT: 2128, Mar 26
  - Chief gunner: This is Cheonan. We’ve sunk. We run aground
  - Chief of the situation room: You’ve ran aground?
  - Chief gunner: The ship tilted to the starboard side and we need rescue.
  - ※ Chief gunner later stated that the urgency of the situation led him to use the word “ran aground” to receive expeditious rescue.
- Combat Information Officer ↔ Duty Officer, 2nd FLT: 2130, Mar 26
  - Combat Information Officer: ROKS Cheonan is in distress near Baekryong Island. Please instruct emergency departure of Daechung 235 sub-squadron.
  - Duty Officer: What is your status? (The communication ended due to poor signal)
  - ※ Duty Officer misunderstood the word distress with grounding, then reported and promulgated accordingly.
- CPO ↔ Radar base (wireless): 2151~2152, Mar 26
  - Radar base: Report cause of sinking
  - CPO : We think it’s a torpedo, torpedo, torpedo, we think it’s a torpedo, over
  - Radar base: Are you sure that it’s a torpedo?
  - CPO: We think we’ve been hit by a torpedo
  - Radar base: We are sending RIBs to rescue crew
  - CPO: End of contact, over
- Commanding Officer (CDR) ↔ Squadron Commander: 2232~2242, Mar 26
  - Commanding Officer: I think we’ve been hit by something.
  - Squadron Commander: What do you think it is?
  - Commanding Officer: I think it’s a torpedo, and I can’t see the stern at all.
  - Squadron Commander: The stern? Where from the stern?

- Commanding Officer: I can’t see the stack, please send us some motorboat or RIBs right away.
- Squadron Commander: Any survivor?
- Commanding Officer: There are 58 survivors, many of them are bleeding, and 2 are severely injured and can’t stand up.

### 4) Sentries

Two sentries(from the Marine 6th Brigade), who were on guard 2.5km away from the location of the incident, testified that they heard a ‘gwang’ sound around 2123<sup>6)</sup> hours and saw a white flash of light(20~30m wide, 100m high).<sup>7)</sup>

#### Main points of testimonies

- While on guard, a ‘gwang’ sound(much louder than the sound of gunfire, loud enough to astonish) was heard and a bright flash of light from 4~5km away spread through the region then disappeared (PO3)
- While on guard, I heard a ‘koong’ sound, then when I looked 4km out towards the sea at a 270° direction a bright flash of light(20~30m wide, 100m high) was seen for 2~3 seconds (PO3)

### 5) Sub-conclusion

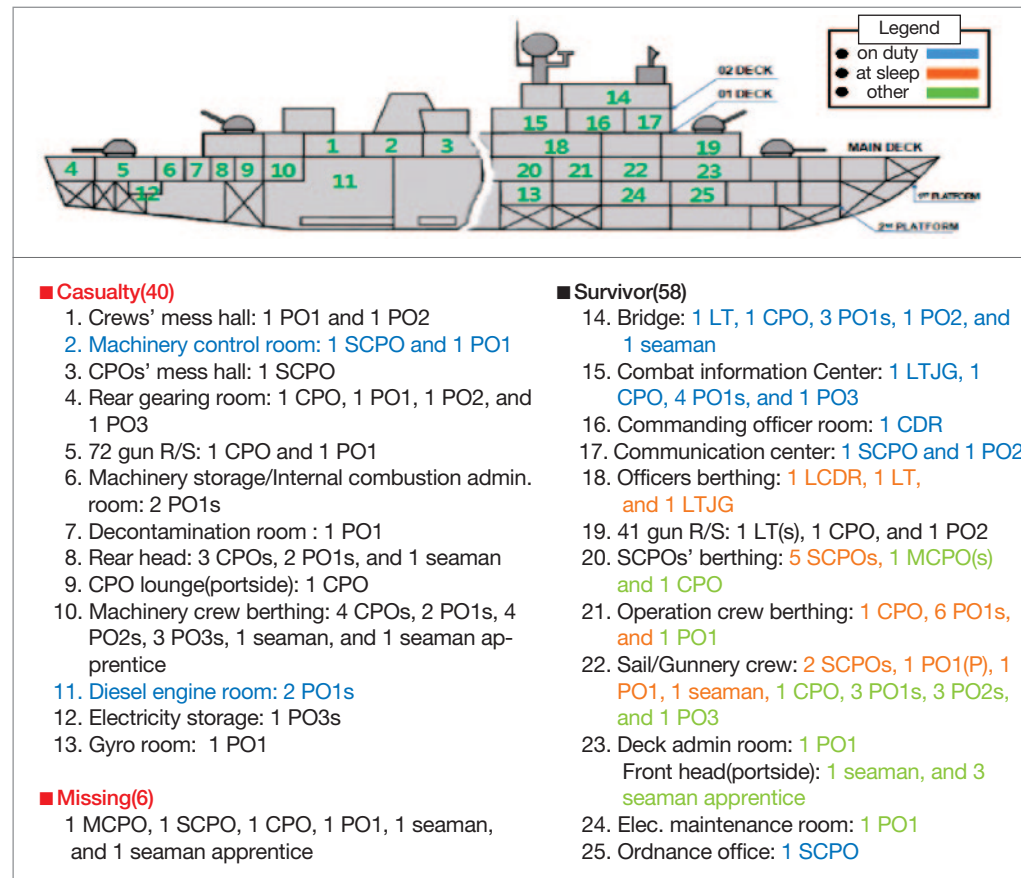
Results of the survivors’ and sentries’ testimony analysis revealed the following: many crew members had floated into the air before falling; two crew members heard the explosion sound twice; no one saw flames, fire or water columns, and no one suffered burn wounds; some personnel suffered from fractures and bruises; many of the survivors be-

6) The sentry said that he checked his watch right after hearing the shock. He witnessed the light flash when it was 2123 hours, but did not verify it up to seconds. After checking with the company records, it says a ‘thunder’ was heard on 26 Mar. at 2123 hrs at the guard post.

7) Weather condition during the incident occurred: 40% sea fog, 78% moonlight, visible range within 500m.

lieved that a torpedo caused the incident; furthermore, sentries testified they heard the noise and witnessed the flash of light. Considering all the observations above, these are consistent with the UNDEX bubble effect phenomenon.

#### 4. Results of Postmortem and Surviving Patient Examinations



〈Figure III-4-1〉 Location of crew members in ROKS Cheonan at the time of the incident

All of the 58 survivors were hospitalized for any possible stress from the psychological shock by the incident as well as for physical injuries. Patients with light injuries such as hypothermia, bruises, and sprain got out of the hospital after 10~12 days of treatment. 6

CAT	TOT	Hypothermia	Laceration and bruise	Concussion	Sprain	Cord rupture/teeth fracture
Light injuries	50	4	11	2	29	4

CAT	TOT	Neck bone, lumber vertebra fractures	Rib fractures	Thigh fracture	Clavicle fracture	Ankle fracture
Severe injuries	8	3	2	1	1	1

〈Table III-4-1〉 Patients status

patients among the 8 severely injured with rib fractures left the hospital after 1~2 months of treatment. But one patient with acute stress and two patients with fractures of the lumbar vertebra, and thigh received treatment for over 2 months before leaving the hospital.

According to Dr. Shin from KAIST(who had studied the conditions of survivors of a torpedo attack), and the UK Investigation Team(which had previous experience with under water explosion), bubble effects may result in fractures, laceration, and bruises to the crew members because of the shock and the pressure wave. This observation could be utilized in proving that the phenomena were caused by bubble effects.

The postmortem analysis was conducted on the 40 bodies recovered during the search and rescue and the bow/stern salvaging process, in order to verify the existence of fragments, scorch marks, and direct causes of death. The JIG carried out medical examinations, visual analysis, X-ray filming, and other precise analyses.

#### 1) Bodies Discovered during the Search and Rescue Activities(2)

Regarding the SCPO's body discovered during the search and rescue process on April 3rd, a postmortem examination was conducted on April 4 from 1000 to 1040. It was found that the SCPO's face and upper/lower jawbones, as well as the right arm's upper part, were fractured and that the right upper arm and its muscles were torn. There were several stab and torn wounds in the left facial region and the neck.

During the stern search and salvage process, the body of the SCPO was found near the machine control room's breakplane. A postmortem examination was conducted from 1953

to 2130 hours on April 7. SCPO's elbow was fractured, with several lacerations or scratch marks on the skin, but the body had not been hit by fragments or been punctured.

### 1) Bodies Found at the Stern(36)

For the 36 bodies collected during the internal search of the stern after salvaging operations had been complete, a postmortem analysis and X-ray assessments were performed from 1800 hours on April 15 to 0300 hours on April 16. Comparatively slight external wounds such as laceration, subcutaneous bleeding, bruises, and fractures were identified, and 5 bodies including 1 PO2, 3 PO1s and 1 seaman were discovered without any external wound.

Lacerations were found on the facial and occiput region. Subcutaneous bleeding, excoriation, and bruises were found on the overall body including the face, arms, legs, abdominal, ankles, and waist. The lumbar vertebra, temporal, and metatarsal bones were fractured. It must be noted that major damages on a body went from the right shoulder region, to the right upper arm, then to the right waist, and then to the right knee. Another body's major damages started from the left cephalic region, then moved down to the left shoulder, and then to the left arm. The single direction of wounds indicates that the hull was tilted to one side by an external force, and that the wounds occurred as the crew members fell to one side and hit the interior structures of the hull.

Overall, laceration, fractures, and bruises were found on the bodies, but no fragments or scorch marks were found. These external wounds did not seem to be the main cause of death. While the exact cause of death can be determined through autopsy, it was not conducted considering the opinions of the families of the deceased. The JIG assessed that the crew members were drowned rather than killed by external wounds. Based on the degree of decomposition, it was assessed that all of them had died around a similar time frame. The damage status is as follows.

CAT	Laceration	Excoriation	Subcutaneous bleeding	Bruise	Fracture	Cutting wound	Other
PAX	15	15	14	10	7	3	1 teeth loss, 1 skin rupture, and 1 dislocation

<Table III-4-2> Results of postmortem examination and X-ray on 36 bodies

### 3) One Body Collected from the Stack

An SSU<sup>8)</sup> member, while conducting underwater operations in order to hoist the stack which was fallen off from the stern, discovered a PO1 wearing BDUs in the stack at 2120 hours on April 22. The postmortem analysis of the PO1 was conducted on April 23, between 0930~1013 hours. As a result, lacerations on the PO1's left forehead and contusions on the right knee were discovered.

### 4) One Body Found at the Bow Gyro Room

During the initial drainage process, a PO1's body was found in the gyro room underneath the operation crews' berthing and in front of the gas turbine room during the initial drainage process. His body went through a postmortem analysis between 1703 and 1747 hours on April 24, and the JIG discovered fractures on the shinbones, crushed hyoid bone, and lacerations on the skin, soft tissue and left scalp area.

### 5) Sub-conclusion

Combined analysis of postmortem and surviving patients examination results indicates that burns, fragment injuries, or punctures did not occur, and that most bodies had light injuries such as fractures or lacerations. The conditions of injured crews included fractures, lacerations, and bruises. When it comes to the deceased members, it was assessed that injury unlikely caused the death, and the circumstances pointed to drowning as the most probable cause. When these bodies were found, they were wearing exercise clothing, workwear, or underwear, and they were located in berthing, lounges or heads. This indicates that they had died during off duty hours.

The observations on the bodies of the surviving patients identified injuries of fracture, laceration, and bruises, that are assessed to have resulted from falling to either right or left side and bumping against the hull structure. These are consistent with the phenomena of bubble effect.

8) SSU(Ship Salvage Unit): A special unit that carries out various tasks such as rescue missions on the sea, and removal of natural/artificial obstacles on harbors and watercourses.

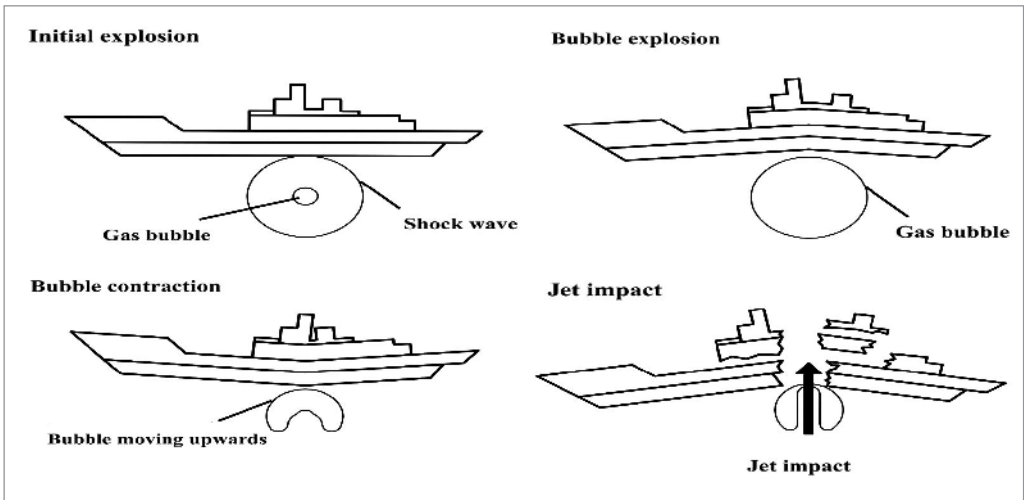
## 5. Explosion Type Analysis

The investigation on the cause of the sinking revealed that the hull of ROKS Cheonan was split by a strong non-contact underwater explosion. The propulsion device(the conclusive evidence) recovered from the seabed indicated that the underwater explosion was caused by a torpedo. Based on these results, this section focuses on estimating the performance of the torpedo(charge size) and the point(depth and location) of the explosion. The US and UK team estimated the charge weight and location with their own expert methods in support of the objective, and in basis of the US and the UK estimation, the ROK team carried out a simulation analysis.

### 1) Physical Aspects of Underwater Explosion

To facilitate the understanding on the cause of the sinking of ROKS Cheonan, the devastating effects of a bubble formed by an underwater explosion(below the hull) are shown in <Figure III-5-1>.

As an explosive charge is detonated below the hull, a shockwave is generated and impacts the hull after propagating in water at a very high speed. Although the peak pressure of the shockwave is very high initially, it gets attenuated very rapidly as the shockwave

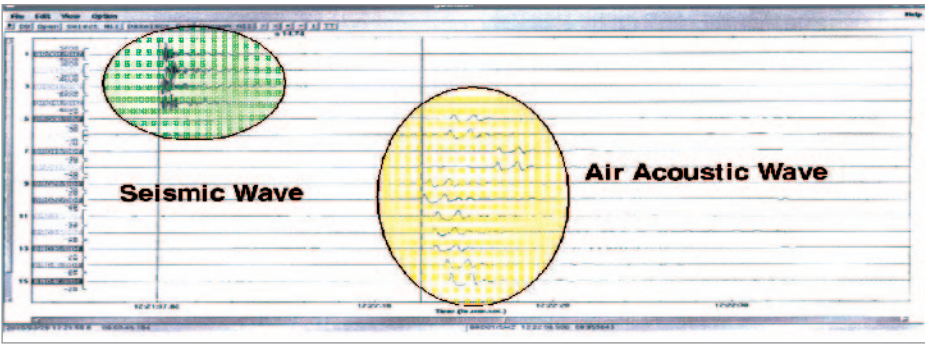


<Figure III-5-1> The progress of physical effects by bubble formed below the hull

propagates in water. Moreover, since the shockwave travels outward in a spherical form, the actual impact on the hull is not severe. For these reasons, the damage inflicted by the shockwave is known to be not significant, causing only mild damages and malfunctions to on-board power supply and communication systems. After the shockwave release, the bubble is formed slowly, with lower pressure inside compared to the shockwave. As the bubble expands, the hull is deformed into a reverse V-shape under the force acting upward. After reaching the maximum expansion, the bubble begins to contract, pulling the hull downward to produce a V-shape deformation. As the contraction continues, the bubble collapses and a high speed water jet is formed at the lower part of the bubble. As the water jet becomes larger, it inflicts a heavy impact on the hull, and eventually severs the ship. Since the water jet impact is much more destructive than the other shockwave, most countries employ a non-contact underwater explosion weapon system that maximizes the bubble effect. More details on the underwater explosion is included in Appendix II.

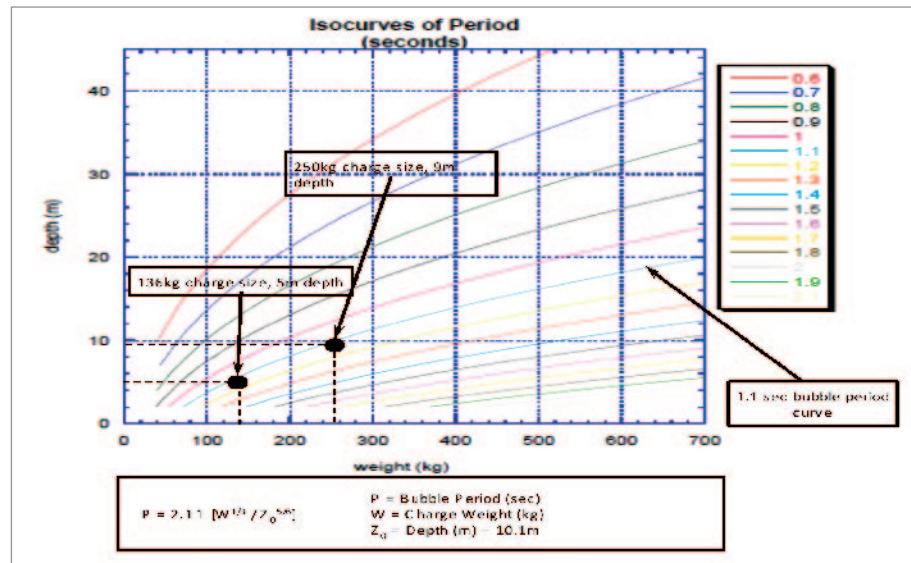
### 2) Explosion Type Analysis(Charge Size and Explosion Location) by the US Team

In order to verify the charge size and explosion location of the torpedo that severed ROKS Cheonan, the US team analyzed the seismic and acoustic waves detected from the seismic research center at the time of explosion as illustrated in <Figure III-5-2>. 1.5 magnitude of seismic wave was identified at 4 seismic detecting stations located on Baekryong Island, and acoustic wave containing 2 acoustic pulses with 1.1 second interval was detected at 11 acoustic detecting stations. When an explosive detonates un-



<Figure III-5-2> Detection results of seismic and air acoustic wave on the incident day

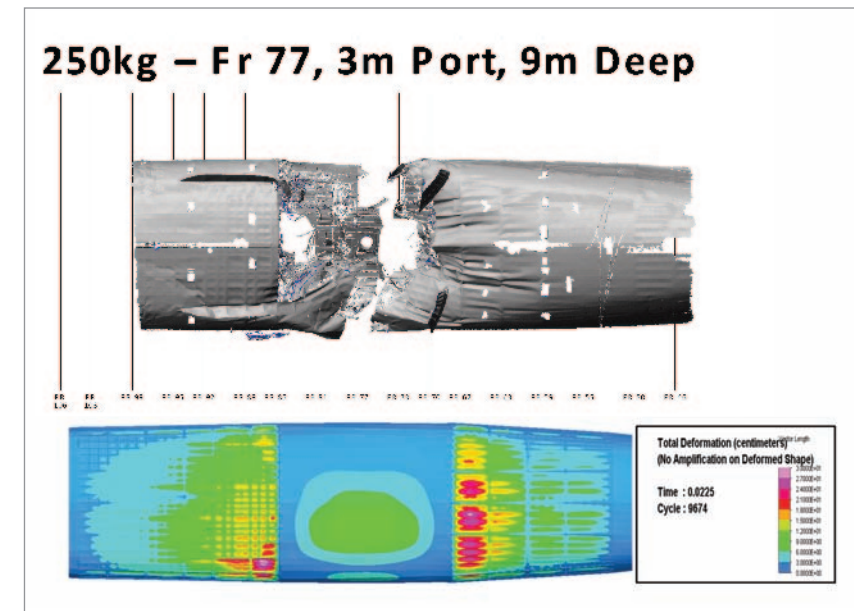
derwater, 2 acoustic pulse are generated; 1 initiated at the time of explosion, and the other produced upon the expansion of the bubble; the 1.1 second of interval represents the bubble period created by an underwater explosion. Based on the measured data, the charge weight and explosion depth are analyzed applying Willis formula, and the result is shown in <Figure III-5-3>.



<Figure III-5-3> Charge size and depth of explosion according to bubble periods

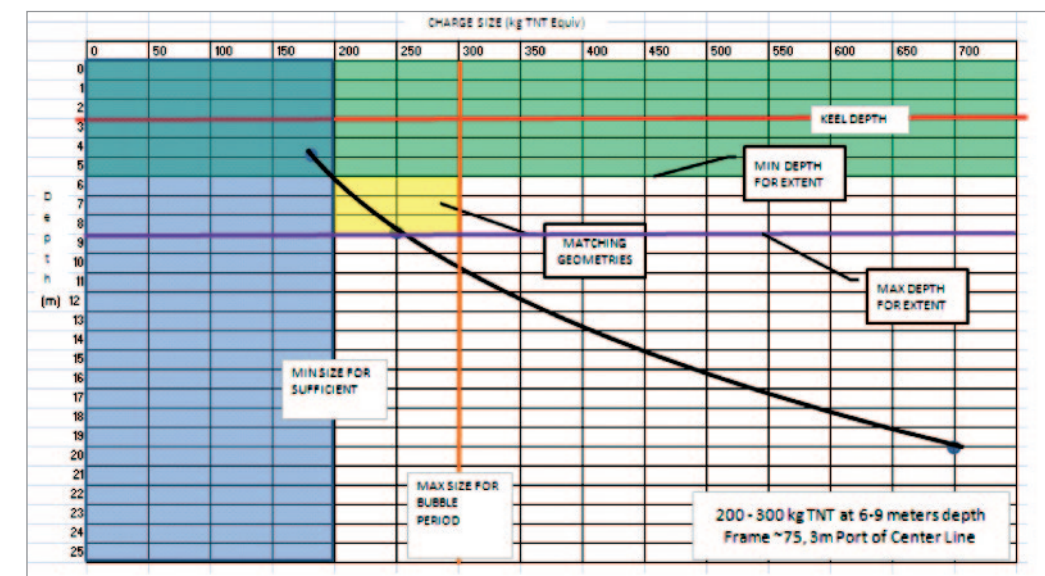
As a result of visual inspection carried out on the breakplane and hull bottom after the recovery of the hull, dishing was identified along with the damages and bending of the hull due to bubble effect. In order to analyze this phenomenon, an assessment on a possible charge size and depth sufficient to sever the hull was made by constructing a hull whipping computation model<sup>9)</sup> for the shock resistance of the hull against the whipping effect. After comparing the actual measurements of the dishing on the hull bottom and the estimated numbers according to the deformation finite element analysis<sup>10)</sup>, it was concluded that TNT 250kg detonated below the gas turbine room in depth of 6~9m, 3m port from the centerline(See <Figure III-5-4>).

9) Hull whipping computation model: A simulation model used to calculate the hull strength that can endure external shock.  
 10) Finite element analysis: A method of analyzing an object through a mathematical model made by dividing the object into a finite number of elements.



<Figure III-5-4> Explosion type similar to dishing of ROKS Cheonan hull bottom

<Figure III-5-5> depicts an analysis result considering depth, charge size, and internal shock model to produce bubble period 1.1 second, combined with the finite element analysis result on hull deformation.



<Figure III-5-5> Result of examination on explosion type of ROKS Cheonan

The depth shown in <Figure III-5-5> is estimated to be 6~9m considering the longitudinal distribution of dishing depicted in <Figure III-5-4>, and through the internal shock and bubble period analysis results, the charge size is assessed as TNT 200~300kg.

### 3) Explosion Type Analysis(Charge Size and Explosion Location) by ROK

Taking the analysis results of the US and the UK team as a reference, the ROK team analyzed the actual damage pattern of hull, utilizing a simulation technique on the hull. During the process, the torpedo propulsion motor(conclusive evidence) was recovered and used as an additional evidence, and the explosion location of the US team analysis was reconfirmed through an analysis on the fractured surface of the hull.

#### (1) Analysis on the Direction and Location of the Explosion(Analysis on Break-plane)

In order to confirm the direction and location of the explosion, the breakplane of the hull was observed, and based on those observations, the point of action and direction were analyzed.

As shown in <Figure III-5-6>, samples of approximately 15cm x 15cm size were collected from three locations at the breakplane of the stern. All the collected samples were identified to be shear and brittle fractures, and revealed no signs of ductile<sup>11)</sup> or fatigue fracture. Sample #2 shows shear fracture patterns, sample #3 displays a typical brittle fracture, and sample #1 presents a mixture of the two fractures. Also it was confirmed that the patterns showed only shear fracture between sample locations #1 and #2 and only brittle fracture between sample locations #1 and #3.

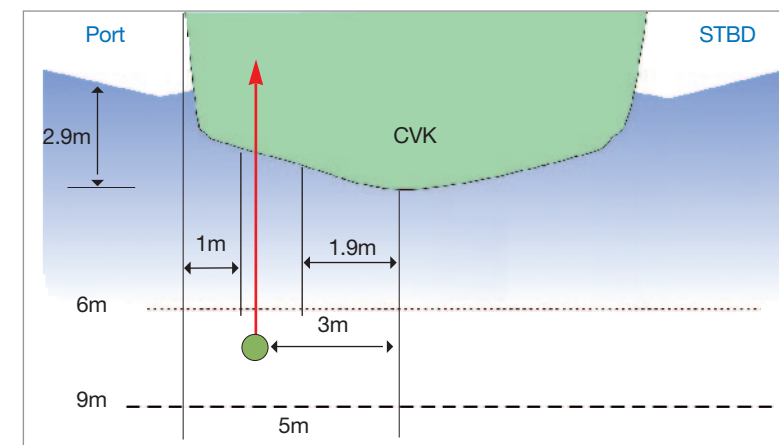
The detailed analysis on the breakplane of ROKS Cheonan(See Appendix III) revealed that an upward plastic deformation occurred in large curvature shape due to a strong explosion originating from the portside bottom, then a strong external force caused shear fracture. The origin of the fracture is estimated at 1.9m to the port from CVK. Thus, given that the hull is 5m in width on the port side, it could be estimated that an explosion took place between 1.9~5m to the port from CVK. The possible location of the explosion on the

<sup>11)</sup> Ductile fracture: As strength exceeding elasticity is exerted, an object gets over-stretched and fractured.

hull bottom was estimated to be 3m, which is the center of 1.9~4m from CVK(See <Figure III-5-7>).



<Figure III-5-6> Sample collection locations at fractured surface



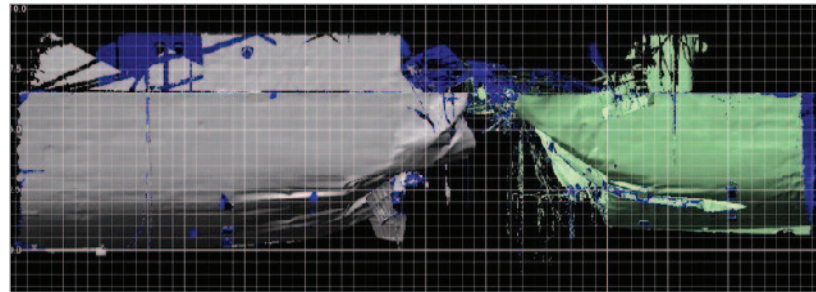
<Figure III-5-7> Possible range of explosion

#### (2) Simulation Analysis on Explosion Type

Based on the location and direction of explosion derived from the aforementioned analysis on the breakplane, a simulation analysis was conducted in order to estimate the explosion type(charge size and depth) similar to the explosion that occurred in ROKS Cheonan incident.

Regarding the scope of the simulation analysis, a simplified model(partial modeling

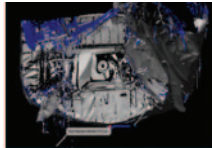
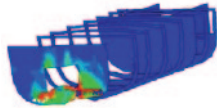
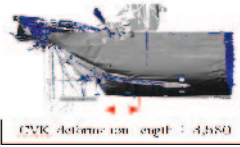
of the ship on the region of main damage, including hull, CVK, rib and bulkheads) was used to derive a result within a limited period of time. The simulation conditions with different charge size and location were set to recreate the damage similar to which is seen on ROKS Cheonan.



〈Figure III-5-8〉 Damage from the explosion seen on ROKS Cheonan

Three criteria were selected for a comparison of numerical analysis results with the actual damage presented in ROKS Cheonan, and the explosion types that satisfied all three as probable explosion types were nominated. 〈Figure III-5-9〉 shows the result of the comparison.

The simulation analysis on the charge weight of TNT 250kg resulted in depth of 6m as a possible explosion type. For TNT 300kg, the possible explosion type was at the depth

Criteria	Actual deformation	Simulation
Extent of hull bottom damage		
Deformation/ fracture at the stern breakplane bulkhead		
CVK deformation length from stern breakplane bulkhead		

〈Figure III-5-9〉 Three comparison criteria

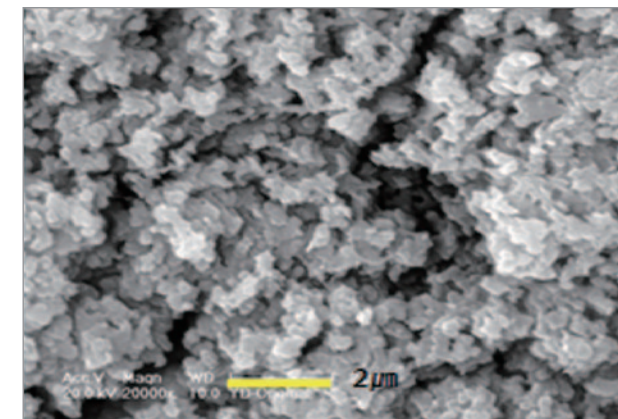
of 7m, and for TNT 360kg, the depth of 7m ~ 9m was selected as the possible explosion types to cause similar split pattern as ROKS Cheonan. More details regarding the simulation analysis are included in Appendix IV.

#### 4) Analysis of Adhered Materials

Significant amount of the adhered white powder was found on the fractured surface. Also, white adhered material similar to the ones discovered at the fractured surfaces was collected on the propulsion motor. These adhered materials were on the surface of aluminum materials as well as on that of non-aluminum materials.

As a result of analyzing through SEM images, EDS, and XRD, the adhered materials found in ROKS Cheonan and propulsion section of torpedo were found to contain the same elements and they were porous agglomerates of fine particles of sub-micrometer size, and mainly consisted of amorphous oxides of aluminum( $Al_2O_3$ ) and moisture with a small portion of carbon, sulfur or sulfur compound, sand, and salt.

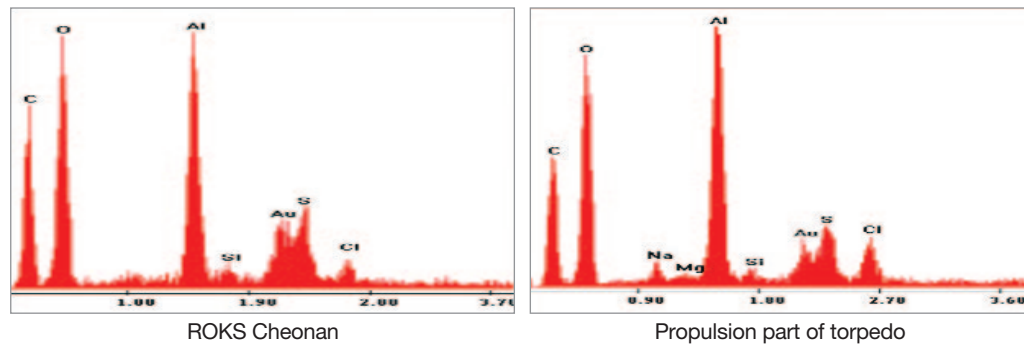
The substances adhered on the ROKS Cheonan hull and torpedo propulsion motor



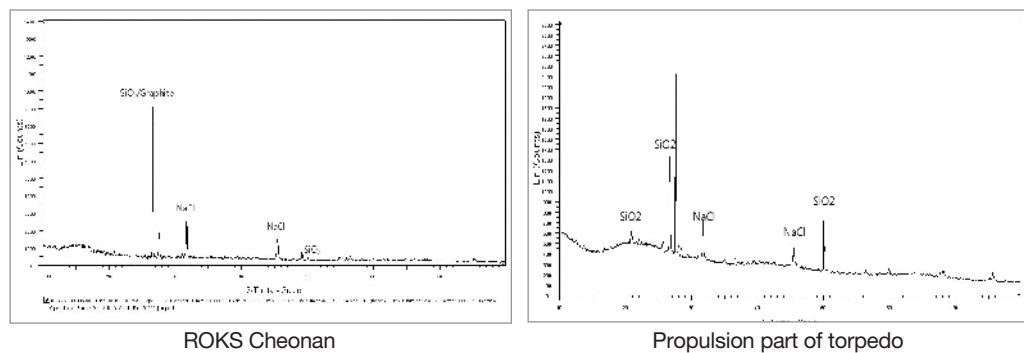
〈Figure III-5-10〉 SEM image of adhered materials

have been confirmed as the identical materials, consisted mainly of amorphous aluminum oxide. This led to the assessment that the adhered materials are the explosive residue from the underwater explosive charge containing aluminum.

The experiment result of the underwater explosion testing with small water tank, and the detailed analysis result on the adhered materials are included in Appendix II and V.



〈Figure III-5-11〉 EDS analysis result of adhered materials



〈Figure III-5-12〉 XRD analysis result of adhered materials

## 5) Sub-conclusion

The performance of the weapon system used in the ROKS Cheonan incident was analyzed through the results of US team analysis including detailed examinations on the acoustic and seismic signals, hull dishing, and internal shock by whipping, combined with the results of the ROK analysis such as inspections on the fractured surface(breakplane), and simulation analysis.

The result of the US team analysis showed that the possible explosion type (which can incur a similar damage as seen in ROKS Cheonan), is an explosion of TNT 200~300kg at a point of 3m to the port from the central bottom of gas turbine room, and at a depth of 6~9m.

Analysis result of ROK assessed that the explosion occurred at 3m port from the central bottom of the gas turbine room. As a result of simulations, the explosion type led ROKS Cheonan to sink was estimated to range in 250~360kg of TNT equivalent charge at a depth

of 6~9m, and the explosive was defined as an aluminized underwater explosive according to the analysis on the adhered material.

In conclusion, when the analysis on explosion type was taken into consideration along with the examination on the recovered conclusive evidence, it can be analyzed that ROKS Cheonan was sunk due to bubble effect caused by a torpedo, loaded with 250kg explosive, detonating in a non-contact manner, at a depth of 6~9m, and at a point of 3m to the port from the center of the gas turbine room.

## 6. Analysis on Shock Response to Underwater Explosion

At the initial stage of investigation, the whipping response of the hull girder of ROKS Cheonan from an underwater explosion gas bubble pulse was conducted for identifying possible cause of the incident with no explosion type(charge sizes, standoffs, etc.) defined. This analysis was based on the 1-dimensional beam analogy method to swiftly analyze forms of explosion that can cause the type of destruction inflicted on the ROKS Cheonan. Later on, damage patterns of the hull structure were analyzed in detail on the probable explosion condition provided by the Explosive Analysis Team. Comparative analysis, between the estimated damage patterns and the actual damage patterns observed in the ROKS Cheonan, was performed to evaluate the validity of the given explosion condition. A 3D analysis on close-in proximity underwater explosion was established by the detailed modeling on the structure.

### 1) Underwater Explosion and Shock Response Method

#### (1) General Shock Response Analysis Method

As for design of a naval ship, an underwater explosion is considered the most serious threat in combat survivability. However, in order to withstand a close-in underwater explosion severe enough to cause the separation such as the one inflicted on ROKS Cheonan, the design would become unrealistic for a ship to carry its structure and equipments. Therefore, a non-contact underwater explosion from a relatively long distance is assumed in design standard for underwater explosion condition.

For a long distance non-contact underwater explosion, the shockwave and the bubble can be considered as separate entities. When considering shockwave from a long distance, the designs of the internal equipments are primarily taken into account, and not overall structure, because the overall structure of the ship is strong enough to withstand it. Generally, the specific analysis code, developed by doubly asymptotic approximation<sup>12)</sup>, is employed for the analysis of the shock response effect on the ship(including the ship structure and its equipments).

The effects of the bubble expansion and contraction are related with the main strength of the hull(longitudinal strength), and since the lengthwise profile overwhelms the widthwise profile in the ship structure, the hull can be considered as the ‘beam’. The abrupt hogging<sup>13)</sup> and sagging<sup>14)</sup> of the hull girder under the effect of bubble expansion and contraction is defined as whipping, and the calculation for the whipping is referred as whipping analysis in ship design. The software employed to analyze the effect of the bubble pulse on the hull without the effects from the shock wave is called a whipping analysis code.

It is worth a note that the long distance non-contact underwater explosion is not reflected in the ship design as the phenomenon such as water jet, generated by the bubble collapse upon bubble’s contact with the hull, cannot occur in that condition.

**(2) Shock Analysis Method For ROKS Cheonan**

Normally, for a standoff underwater explosion, the shockwave and bubble effect are explained separately in designing a ship. For a close-in underwater explosion, the hogging and sagging caused by the bubble and the subsequent bubble effect(generated by the asymmetric contraction of the bubble through contact with the hull during the expansion) all occur almost simultaneously and interrelatedly, so they cannot be considered separately. The explosion that led to the sinking of ROKS Cheonan was assessed as a close-in underwater explosion, and the JIG had to consider all of these factors listed above; therefore, the JIG conducted a two-step analysis. First, since the ship’s loss of longitudinal strength contributed greatly to the fracture of the ship, a 1-dimensional whipping analysis based on the beam analogy method<sup>15)</sup>

•••••  
 12) Doubly asymptotic approximation: A kinetics technique that analyzes the interaction and phenomenon of water and ship structure in case of an underwater explosion.  
 13) Hogging: The bending phenomenon of a hull in which the center of the ship is lifted compared to the stern and bow.  
 14) Sagging: The bending phenomenon of a hull in which the center of the ship sags compared to the stern and bow.  
 15) Beam analogy method: A method used to calculate the sudden bending of the hull(caused by an underwater explosion) by considering the hull as a beam.

was conducted. This was done in the early stage of the investigation to swiftly analyze what kind of explosion could have caused a destruction found in ROKS Cheonan.

A 3D analysis using hydrocode considered the hull, water, air, explosive charge, and explosive effects to include the majority of impacts produced by a close-in underwater explosion. The hydrocode refers to an appropriate analysis code category for fluid-structure coupling, rapid deformation and destruction analysis. For the 3D analysis, the detailed finite element modeling of the ship was prepared from the early phase of the investigation; the actual analysis began after the probable explosion types were selected. It was assessed that the major process causing the separation of the hull could be derived from the analysis since it would allow the consideration in combined effects of the shockwave, and the expansion and the contraction of the bubble. The water jet causes the damage to the ship through the complex effects of the high speed water ejection and the dispersion of water; even though it is limited by current numerical analysis technology to encompass all the effects, it was believed that indirect effects such as the event sequence of the incident could be evaluated through the 3D analysis.

**2) Whipping Response Analysis of Hull Girder**

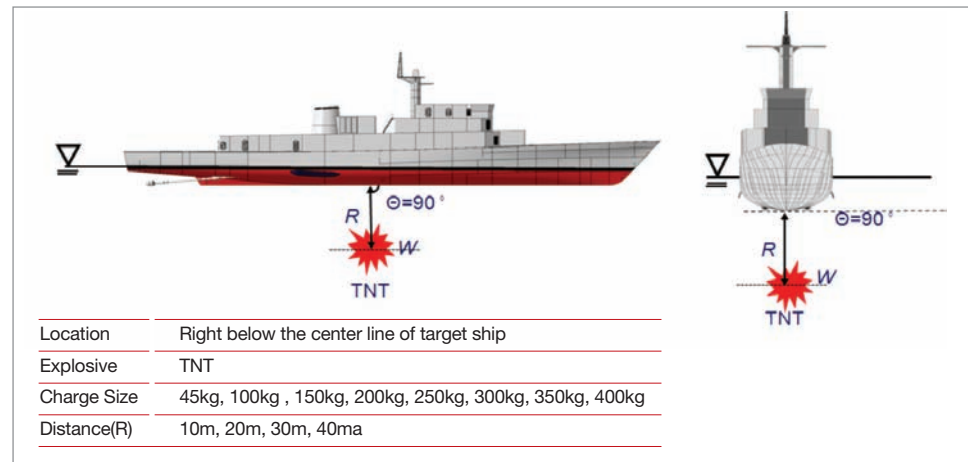
Through the whipping response analysis, the longitudinal strength of the hull girder of ROKS Cheonan against the repeated bubble expansion and contraction caused by an underwater explosion was investigated from the perspective of ultimate strength. <Table III-6-1> summarizes main specifications of ROKS Cheonan.

Items	Specs
Length overall	88.32m
Length between perpendiculars	83.47m
Width	10.0m
Depth	6.2m
Mean draft at full load	2.88m
Displacement at full load	1,223tons

<Table III-6-1> Main specifications of ROKS Cheonan

## (1) Underwater Explosion Conditions for Whipping Response Analysis

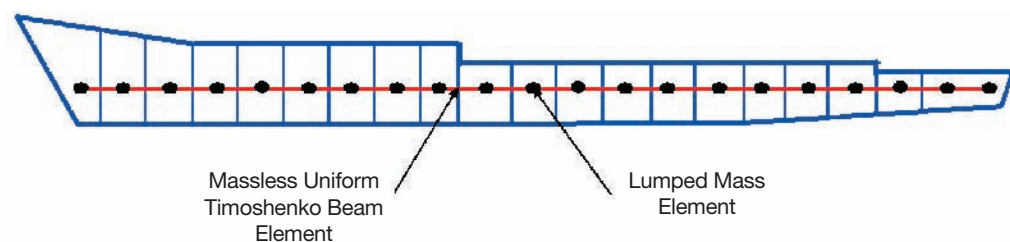
〈Figure III-6-1〉 shows underwater explosion conditions for the whipping response analysis. As shown in the figure, hypothetical situations under which charge weights of 45kg, 100kg, 150kg, 200kg, 250kg, 300kg, 350kg, and 400kg of TNT-equivalent explode right below the center line of target ship at standoff distance of 10m, 20m, 30m, and 40m were applied.



〈Figure III-6-1〉 Underwater explosion conditions for whipping analysis

## (2) Analysis Methods & Assumptions

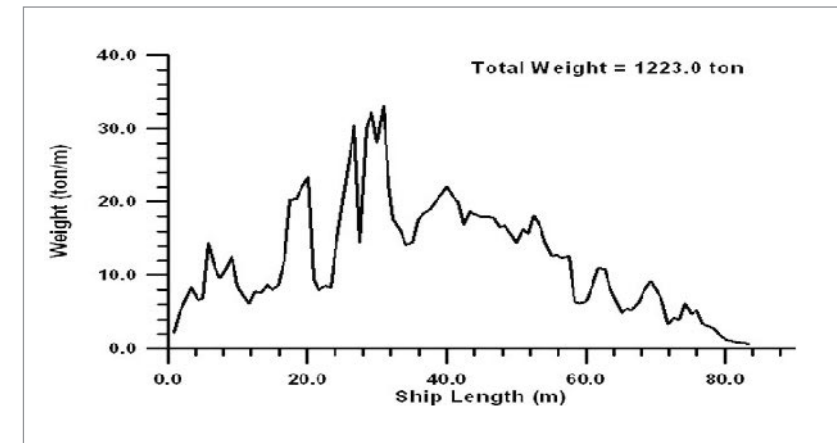
For the analysis, the JIG considered the hull as a Timoshenko beam (a simple beam theory incorporated with shear deformation and rotational inertia effect) and rendered it as a finite element model with 25 nodes<sup>16)</sup> and 24 equilateral uniform beam elements as shown in 〈Figure III-6-2〉. The JIG treated the weight of ROKS Cheonan (including added water



〈Figure III-6-2〉 Beam whipping analysis model

<sup>16)</sup> Node: The point that connects between elements of the structure in analysis model.

weight) as concentrated at the nodes and assumed that the beams connecting these nodes had zero mass. The full load condition was assumed for ship loading, and 〈Figure III-6-3〉 depicts the weight distribution in the longitudinal direction.



〈Figure III-6-3〉 Weight distribution along the ship in fully-loaded condition

The 2nd section moment, effective shear coefficient, modified bending rigidity coefficient for each modes of oscillation, 2D added water weight, and modified 3D added water weight coefficient of the Timoshenko beam element were calculated using the vibration analysis program VIBHUL<sup>17)</sup> developed by the Korea Institute of Machinery and Materials (KIMM).

For the whipping response analysis, the program UNDEX\_WHIP, developed by the KIMM based on the Hicks' bubble behavior analysis theory and the mode superposition method, was used. To calculate the whipping response by the mode superposition method, the JIG only considered the first 5 wetted vertical vibratory modes. The reasons are that the vibration analysis based on the beam analogy method illustrates relatively accurate results only for the first 5~6 modes and that the whipping response of the hull girder is governed by these lower vertical vibratory modes. The damping<sup>18)</sup> effects were neglected.

Also, the JIG only considered the impact of 1st bubble pulse for calculation of hy-

<sup>17)</sup> VIBHUL: The program developed by KISTI for analyzing the vibration of the hull when designing, constructing, and commissioning a ship.

<sup>18)</sup> Damping: The material returning to the original(normal) state from phenomenon of the bending, vibration, etc.

drodynamic impact on hull, because the Hicks' bubble behavior analysis theory only shows a relatively accurate result on the 1st cycle of the bubble. For calculation of the hydrodynamic impacts due to the bubble behavior, the JIG considered the free surface effect and the vertical migration of the bubble.

Before the whipping, ROKS Cheonan is assumed to have been afloat in calm with draft of 2.88m, the average when in full load. After the start of the whipping motion, the change in draft was neglected.

Considering the 1st bubble pulsation period calculated on each underwater explosion condition, the whipping response of the hull girder was calculated in two seconds, because it was assessed that two seconds worth of analysis is enough to reveal the property of the whipping response of ROKS Cheonan hull.

In order to investigate the longitudinal strength stability of the hull girder against the underwater explosion bubble pulse from the perspective of the ultimate strength, the calculated whipping bending moment and the ultimate bending moment were compared. The ultimate bending moment was calculated with the program ULSAN, which was developed by Ulsan University based on the Smith theory.

**(3) Analysis Result**

**① Wetted Vertical Vibration Analysis Result**

The analysis results of the wetted vertical vibrations on the load conditions of ROKS Cheonan are listed in <Table III-6-2>. As shown in the table, the minimum difference in natural vibration of the hull girder is 2.32Hz, and its mode shape is 2 node.

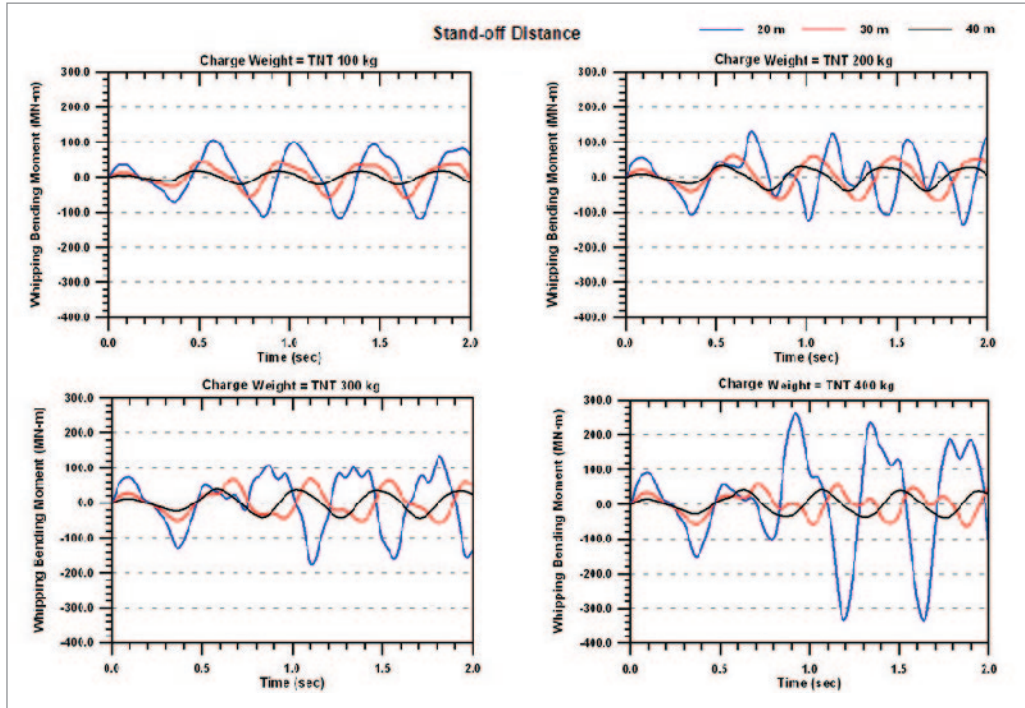
#	Vibration mode	Calculated(Hz)
		Full load condition
1	2-node vibration form	2.32
2	3-node vibration form	4.74
3	4-node vibration form	7.71
4	5-node vibration form	10.41
5	6-node vibration form	13.40

<Table III-6-2> Natural frequency analysis in a fully-loaded condition

**② Calculation Result on Whipping Bending Moment**

Of the considered underwater explosion conditions, the JIG excluded that of standoff distance at 10m from the whipping analysis. The reason for that is, in order for the Hicks' bubble theory to hold true, the explosion depth has to be at least 2.5 times deeper than the maximum width at the waterline. Since ROKS Cheonan's max width at the waterline is 10m, in order to get a valid whipping analysis, the explosion depth must be at least 25m(standoff distance of 22.12m); therefore, in principle, it needs to exclude standoff distance of 20m also, but since it is close enough to the limit line and the conditions were assessed to be valuable for us to conduct the analysis, the analysis was conducted in that condition.

In <Figure III-6-4>, the calculated whipping bending moments from the center of ROKS Cheonan over time was plotted for charge weight of 100kg, 200kg, 300kg and 400kg. As shown in the figure, the whipping response of the hull girder is mostly governed by the first vertical vibratory mode, and if the charge weight is the same, one can see that the shorter the standoff distance, the larger the whipping bending moment. Especially, if

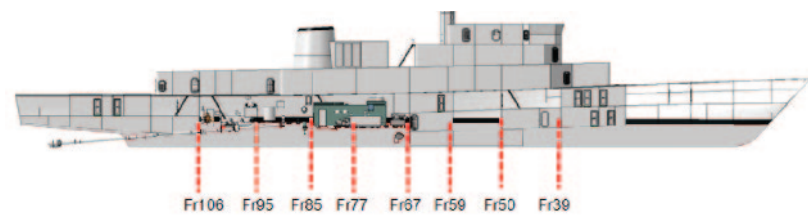


<Figure III-6-4> Calculated whipping bending moments for different charge weights and standoff distances

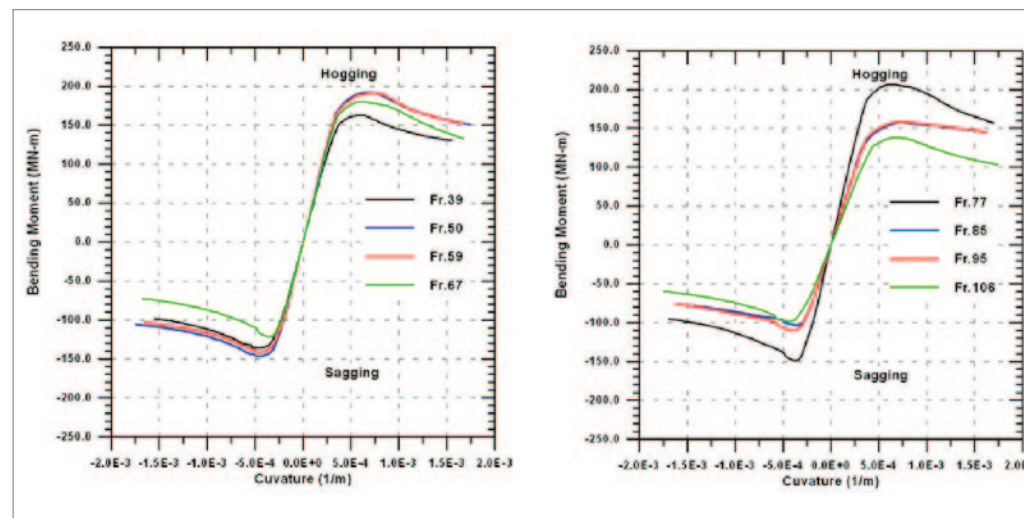
the charge weight is 400kg and 20m away, the whipping bending moment is a lot bigger than when the standoff distance is 30m or 40m away.

### ③ Ultimate Bending Moment Calculation Result

As shown in <Figure III-6-5>, ULSAN was used to calculate the ultimate bending moments on the 8 frames<sup>19)</sup>. In <Figure III-6-6>, the JIG calculated curvature-bending moment for each section, and the resulting ultimate bending moments are summarized in <Table III-6-3>. As shown in the figures and the table, ROKS Cheonan was more vulnerable to the sagging than the hogging.



<Figure III-6-5> Frame locations calculated in ultimate bending moment



<Figure III-6-6> Curvature-bending moments for each frame

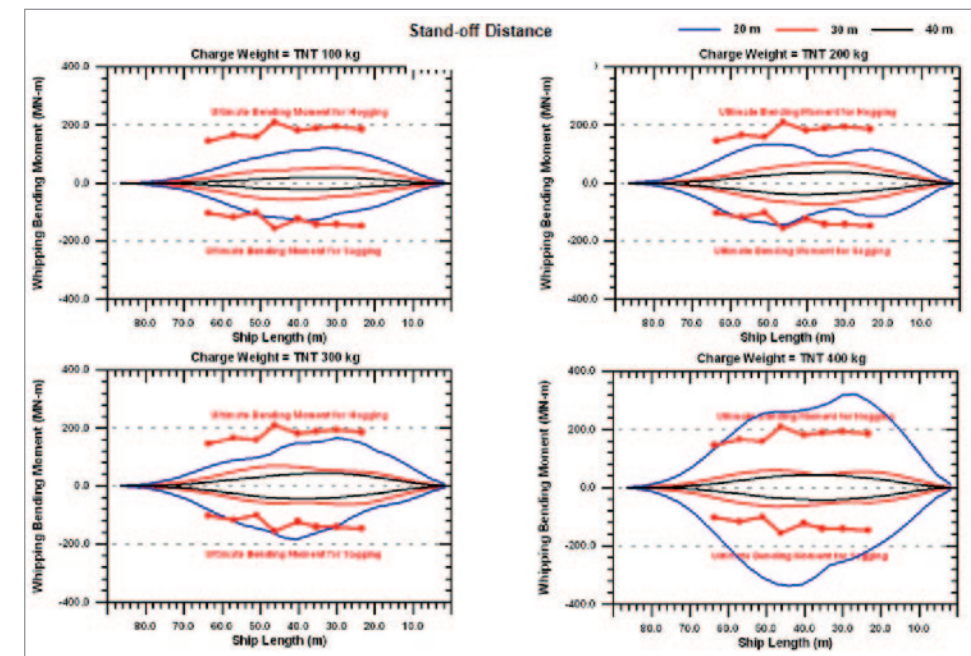
19) The concentrated area for this analysis was between Frame 67 and Frame 85 because of the lost gas turbine room and other adjacent compartments.

Frame location	Ultimate bending moment:( 10 <sup>6</sup> N-m)	
	Hogging	Sagging
Frame 39	185.7	147.4
Frame 50	194.4	141.3
Frame 59	188.5	141.0
Frame 67	182.0	122.7
Frame 77	210.7	156.0
Frame 85	159.3	100.4
Frame 95	165.8	116.2
Frame 106	144.9	103.2

<Table III-6-3> Ultimate bending moments for each frame

### ④ Results for Longitudinal Strength Stability Review

In order to examine the longitudinal strength stability of the hull girder, the JIG compared the maximum whipping bending moment with the ultimate bending moment for charge weights of 100kg, 200kg, 300kg, and 400kg, and the result is shown in <Figure III-6-7>. As shown in the figure, for TNT charges of 100kg, 200kg, and 300kg, hogging, for



<Figure III-6-7> Comparison of whipping bending moments and ultimate bending moments for various charges

up to 20m, is sufficiently stable in perspective of the ultimate strength, but for sagging, TNT charge of 100kg at standoff distance of 20m can cause damage to the longitudinal members which contribute to the longitudinal strength of ROKS Cheonan hull girder.

#### (4) Sub-conclusion

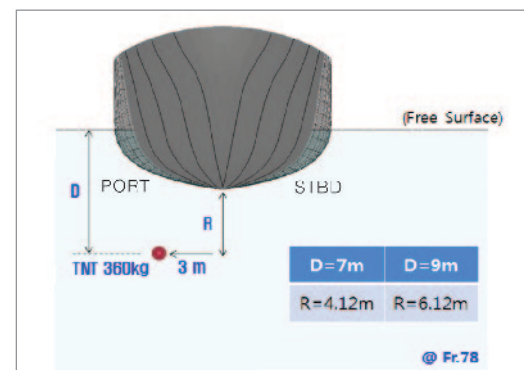
Through the whipping response analysis on ROKS Cheonan hull experiencing the bubble pulsation from the repetitive expansion and contraction due to underwater explosion based on the 1-dimensional beam analogy method, a TNT charge of above 100kg, if exploded under the center of ROKS Cheonan and at a standoff distance of 20m, is assessed to be able to cause a massive whipping bending moment bigger than the ultimate bending moment in some frames of ROKS Cheonan. This can cause a severe damage to longitudinal members which contribute to the longitudinal strength of the hull girder.

### 3) Close-in Underwater Explosion Shock Analysis

With 2 close-in underwater explosion conditions provided by the Explosive Analysis Team, the JIG conducted a 3D simulation of the fluid-structure interaction of the hull. After comparing the calculated damage and the actual damage of ROKS Cheonan, the JIG tried to deduce how ROKS Cheonan was sunk.

#### (1) Conditions of Underwater Explosion

Conditions of a close-in underwater explosion are shown in <Figure III-6-8>. As shown in the figure, the conditions included TNT charge of 360kg at a depth of 7~9m<sup>20)</sup> near frame 78(2 frames(1.2m) away from frame 76 that is located at the longitudinal center of detached gas tur-



<Figure III-6-8> Conditions for a close-in underwater explosion analysis

<sup>20)</sup> The simulation for close-in underwater explosion analysis was conducted under the condition of TNT 360kg charge size detonating at depth of 7 and 9m, (these were the conditions for generating the most similar deformation pattern) and TNT 360kg is included in the explosion range for high performance explosive of 250kg.

bine room), and the explosion point was 3m on the portside from the centerline.

#### (2) Analysis Method & Assumptions

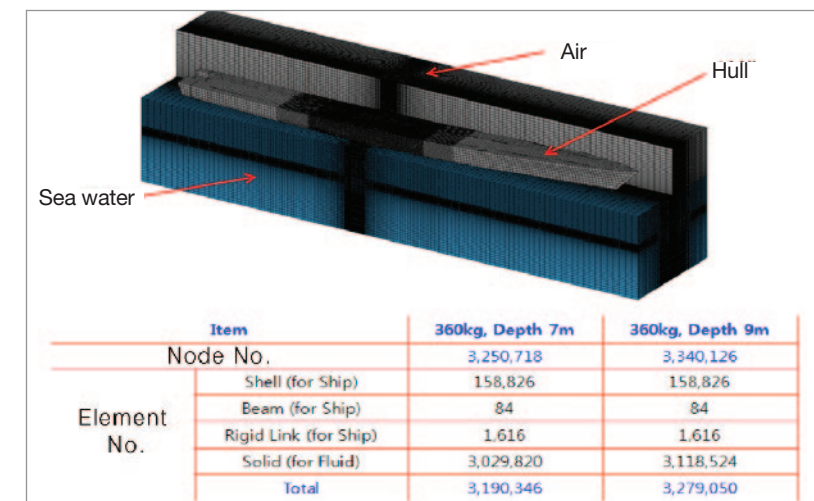
Before the underwater explosion, the assumption was that ROKS Cheonan was at full load and floating over calm water with mean draft. Since structural response was considered, which happens at a very short time period, damping effect was ignored.

For the analysis, the JIG used LS-DYNA Version 971<sup>21)</sup>, a commercial program.

In order to consider the fluid-structure interaction, the JIG included explosives, sea water, ship interior, and the air above the free surface as factors in modeling, and utilizing the Multi-Material Arbitrary Lagrangian Eulerian fluid-structure coupling analysis technique. The JIG assumed the form of the explosion to be a sphere.

#### (3) Analysis Model

All finite element and other relevant information are shown in <Figure III-6-9>. Since comprehensive finite element model includes over 3 million nodes and elements as listed in the table of <Figure III-6-9>, 16 Xeon E5430 2.66GHz CPUs were used to conduct the calculation. The following describes models for the ship structure, charge, and fluids (seawater and air).

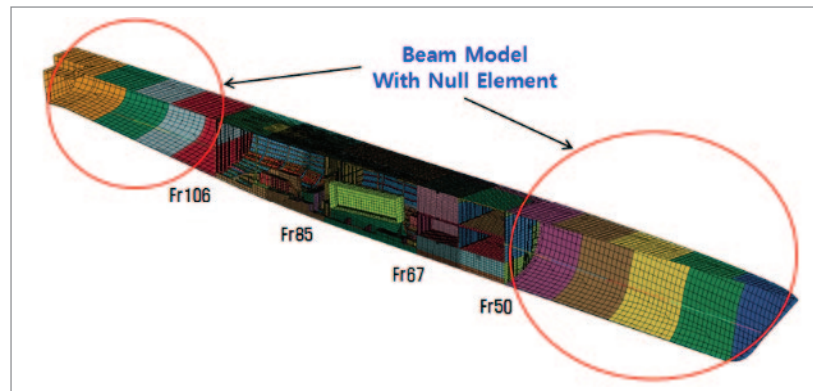


<Figure III-6-9> Comprehensive finite element analysis model

<sup>21)</sup> The program used to describe and analyze the phenomenon that occurs in a short period of time. It is usually used for testing ground vehicle mobilization.

### ① Analysis Model for Hull

The analysis model on the hull is shown in <Figure III-6-10>. The main objective of this analysis is to simulate the damage to the gas turbine room and to identify the cause of gas turbine detachment. Therefore, the JIG made a detailed model for the gas turbine room and the adjacent compartments(Frame 50 ~ Frame 106), and the remaining parts were modeled in equivalent Timoshenko beam elements. The JIG used a Rigid Link element<sup>22)</sup> between null elements<sup>23)</sup> without mass, rigidity, and other beam elements in order to maintain the original form. Also, for the ship structure modeling, the JIG only considered up until the main deck which contributes to the longitudinal strength. The openings such as soft patch at the upper main deck of gas turbine room have been excluded and replaced with the plate of equivalent rigidity.

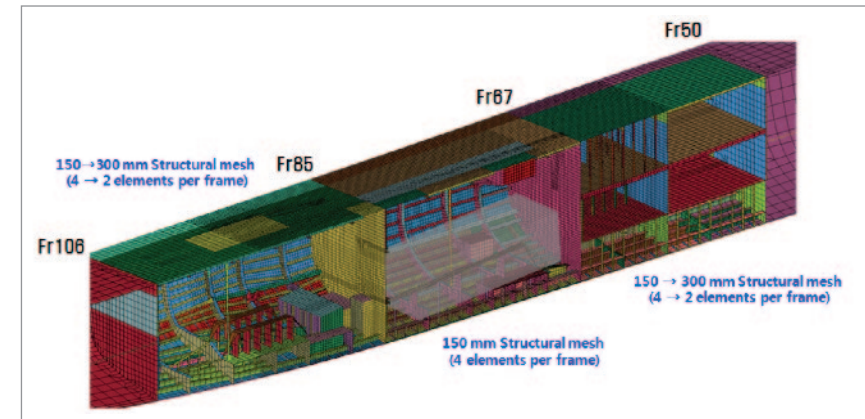


<Figure III-6-10> Finite element analysis on the hull

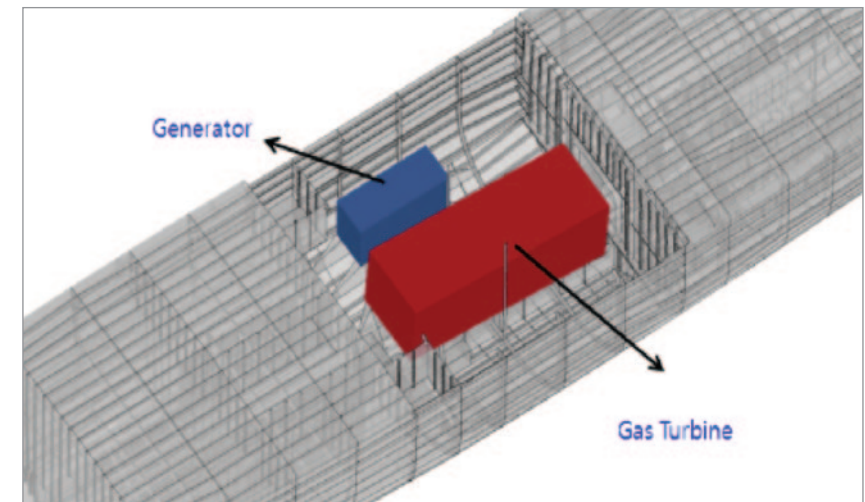
<Figure III-6-11> shows the detailed modeling in the center of the ship structure between Frame 50 and Frame 106, the main area of interest for the analysis. As shown in the figure, for the gas turbine room, four elements were modelled for each frame(=600mm), and 2 elements between frames for the adjacent compartments that are further away from the gas turbine room. In order to include damages to the stiffeners along with other shell members, the JIG modelled all the stiffeners as a shell element. Also, the gas turbine, the generator, the diesel engine, and the reduction gear struts were modelled. As shown in

22) Rigid link element: An element that links the null element and the load element for deformation analysis in case of an impact.

23) Null element: An element in a ship design that does not have mass or rigidity, which is used to maintain the shape of the hull.



<Figure III-6-11> Detailed modeling through Frame 50 to Frame 106



<Figure III-6-12> Modeling for gas turbine and generator

<Figure III-6-12>, the gas turbine and the generator were modelled almost to the exact specification with 3D rigid blocks.

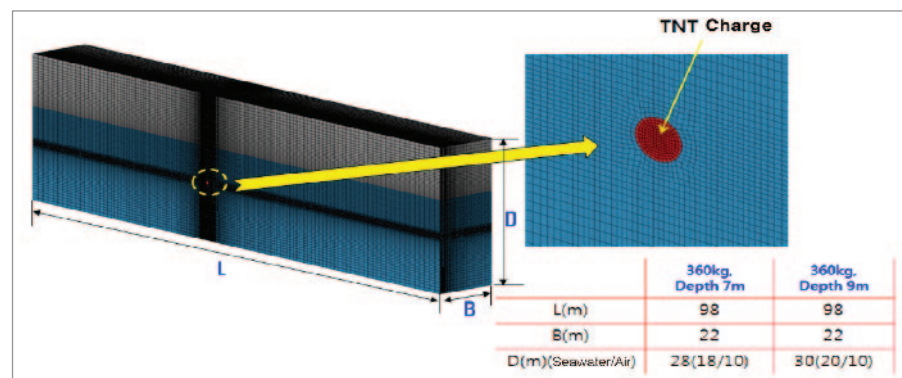
For the analysis of the damage, the materials of the shell were modelled to be carbon material, in order to consider the strain rate effect(possible to be included in Cowper-Symonds model) that corresponds to 'Piecewise Linear Plasticity Material Model, LS-DYNA Material No. 24.

### ② Analysis Model for Charge, Seawater, and Air

The model for charge, seawater and air is shown in <Figure III-6-13>. The explosive

charge was modeled as Euler<sup>24)</sup> element that has Jones-Wilkins-Lee(JWL)'s equation of state(EOS), while seawater and air were modeled as Euler element subject to polynomial and Gruneisen EOS. The height and width of box-shaped fluid model were set to encompass maximum size bubble in the model(that is, considering the maximum radius of the bubble in given underwater explosion conditions).

As seen in <Figure III-6-13>, the height of fluid area would be 28m(seawater 18m, air 10m) at explosion depth of 7m, and 30m(seawater 20m, air 10m) at depth of 9m. The width of fluid area was set as 22m in both explosion depths. The length of the fluid area was modeled 98m, sufficient to cover the longitudinal length of ROKS Cheonan.



<Figure III-6-13> Modeling for charge, seawater, and air

#### (4) Analysis Result and Discussion

Regarding the 1st bubble pulse period of the considered two close underwater explosion conditions, that each explosive of 360kg TNT equivalent explodes at depths of 7m and 9m, an analysis was going to be executed for 2 seconds on both of the conditions.

However, as shown in <Figure III-6-14>, an analysis on the condition that an explosive of 360kg TNT equivalent explodes at a depth of 9m revealed that the projected damage level is minimal compared to that of ROKS Cheonan, and hence, an analysis carried out until 0.9 second for this condition.

The side view observation of the hull response and bubble behavior according to the explosion of an explosive of 360kg TNT equivalent at a depth of 9m is depicted in <Fig-

.....  
24) A formula made by a mathematician, Leonhard Euler, that is used to find out the movement of a fluid that does not have any viscosity.

ure III-6-15> along with representative time periods. As shown in <Figure III-6-15>, since it is a close underwater explosion, the weight generated by the shockwave and bubble behavior is condensed and acts specifically upon the gas turbine room and the compartments in adjacent. Also, the occurrence of hogging and sagging of the hull as a result of the expansion and contraction of the bubble can be clearly observed.

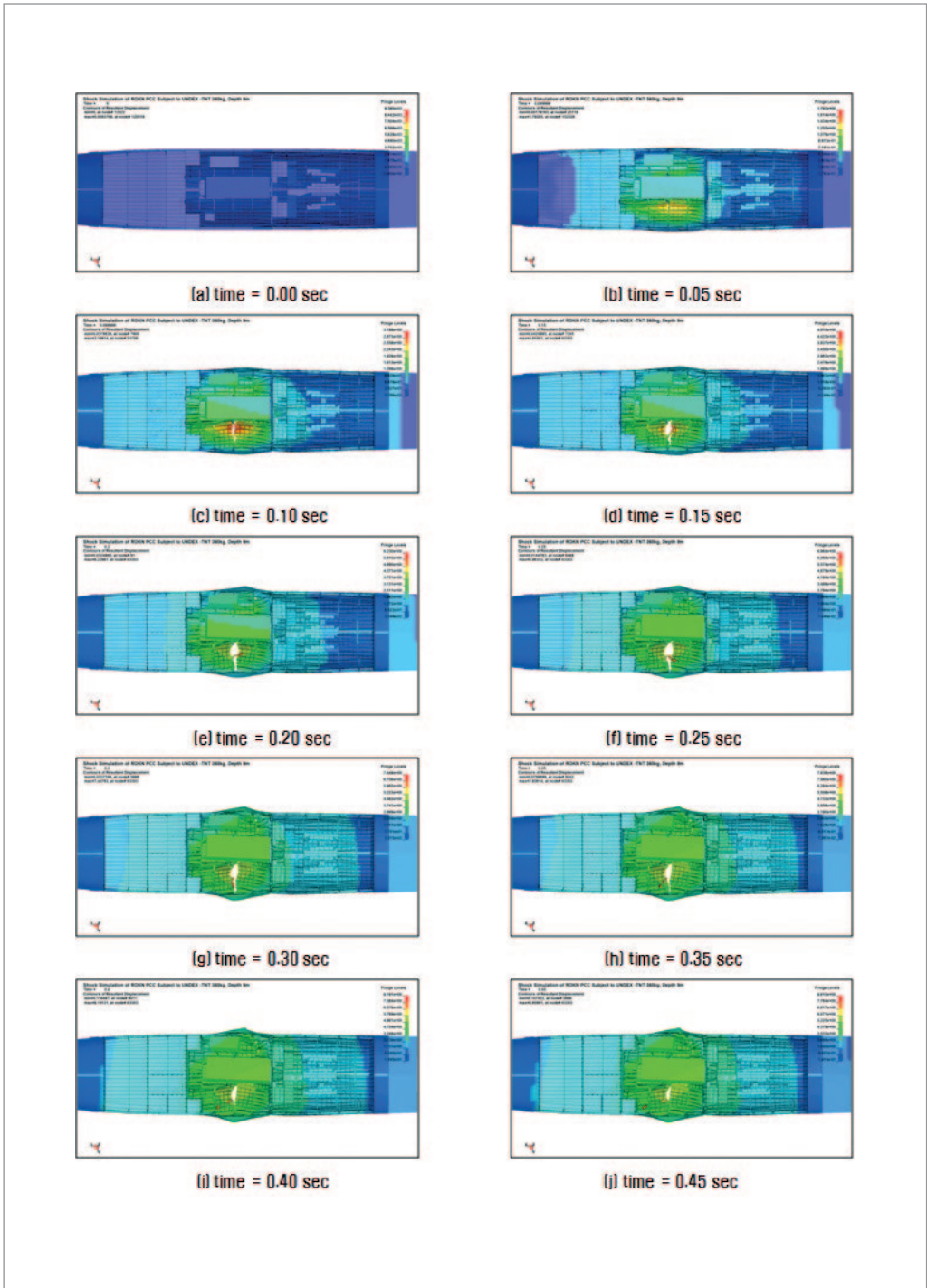
Based on the analysis result of an explosion of 360kg TNT equivalent at a depth of 7m, separation and loss of gas turbine room and the sequence of events leading to the sinking can be explained in detail.

In <Figure III-6-16> and <Figure III-6-22>, the analysis results of an explosion of 360kg TNT equivalent at a depth of 7m seen from different angles and divided according to critical time periods are illustrated.

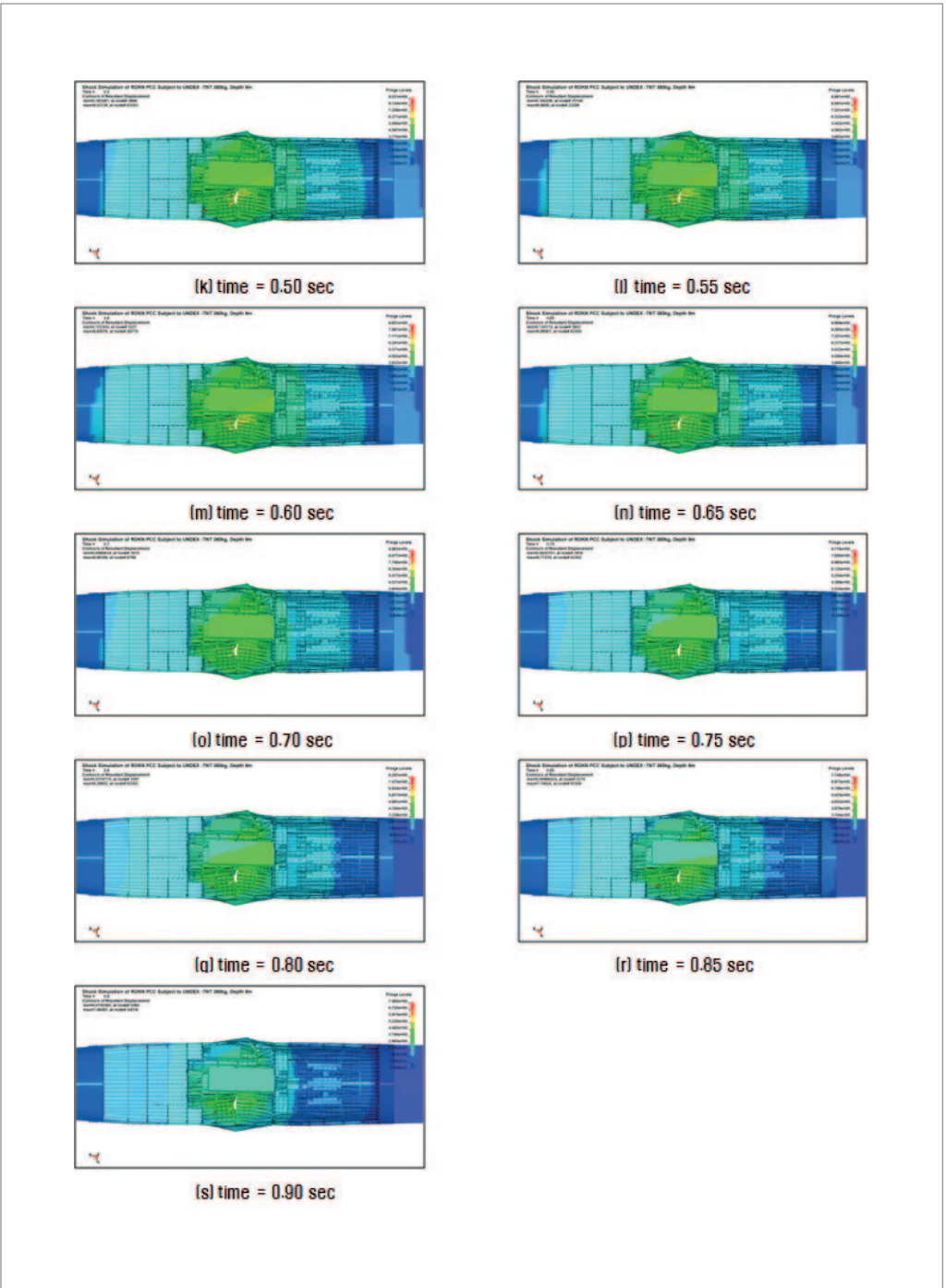
As shown in <Figure III-6-16> and <Figure III-6-17>, an energy created by shockwave and bubble pulsation is concentrated toward the gas turbine room and its adjacent compartment, as well as sagging and hogging, especially on hull, through repetition of bubble expansion and contraction.

Through <Figure III-6-18> ~ <Figure III-6-22>, the JIG was able to infer clear damage sequence of how ROKS Cheonan's gas turbine room was detached. First, as the shockwave contacted the ship, a "Punching Shear" effect was created(diagonal fracture in the direction of thickness due to sudden pressure acting perpendicular to the plates) tearing the weakest member on the portside bottom shell plates of the gas turbine room, after a series of bubble expansion, contraction, and re-expansion(bubble process) deforming the hull severely upward, downward, and then again, upward; this causes the tearing fracture of the hull to grow. The gas turbine at the center of the gas turbine room and the generator at the starboard side, along with their foundations, are sharply inclined to the starboard direction due to the shockwave and series of bubble process. The members and bottom shells near the foundations towards stern are severely deformed and torn apart as a result. However, members on the foundation towards the respective bottom plates have undergone less severe deformation with sufficient level of strength maintained.

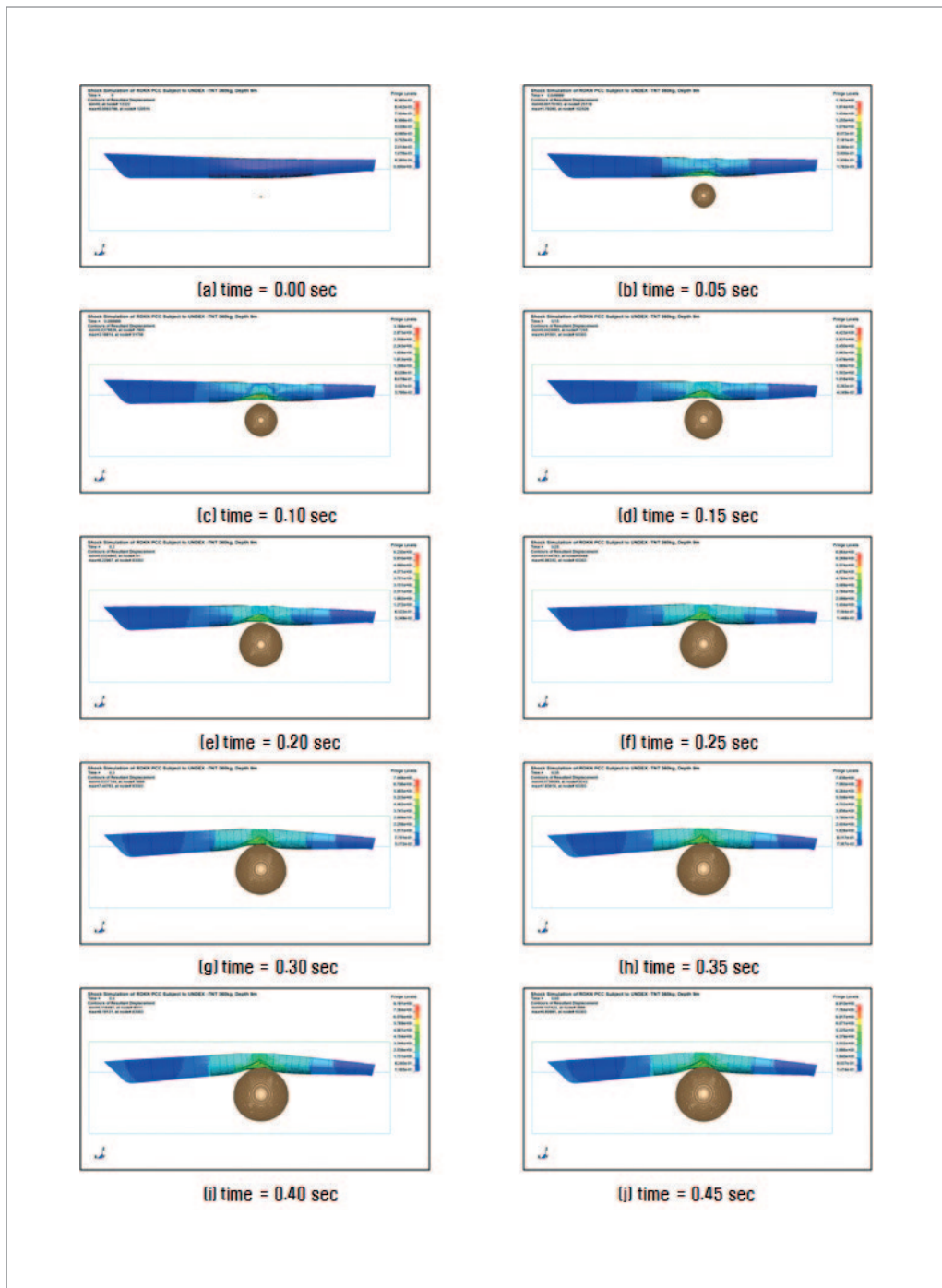
Additionally, although a mass deformation is observed on the starboard shell plates, no destructive damages are found. This enabled us to infer the possibility of gas turbine and generator foundation, shell plates supporting them, as well as starboard shell plates being detached without separation.



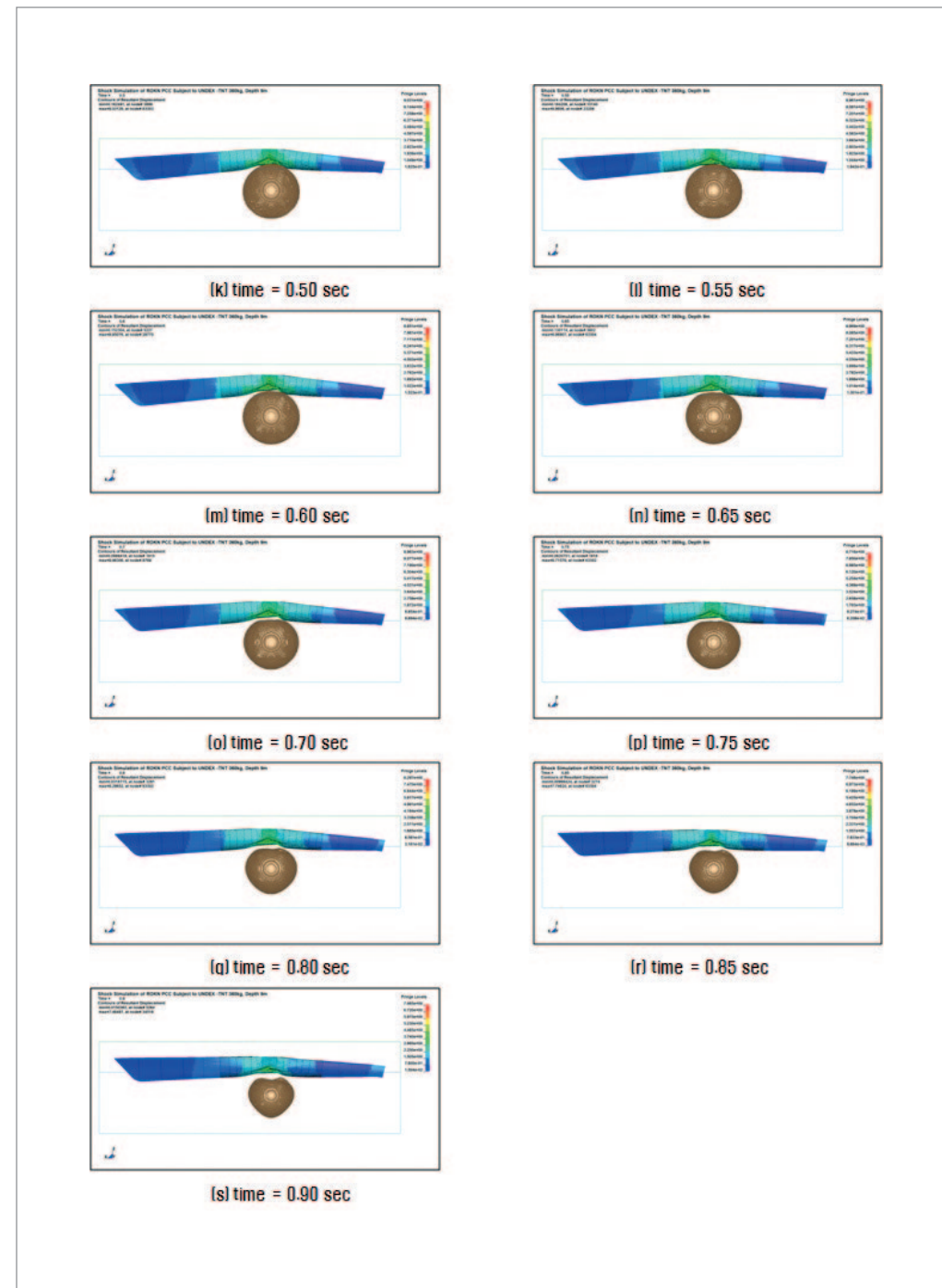
<Figure III-6-14> Analysis result(TNT 360kg at 9m depth): damage in gas turbine room



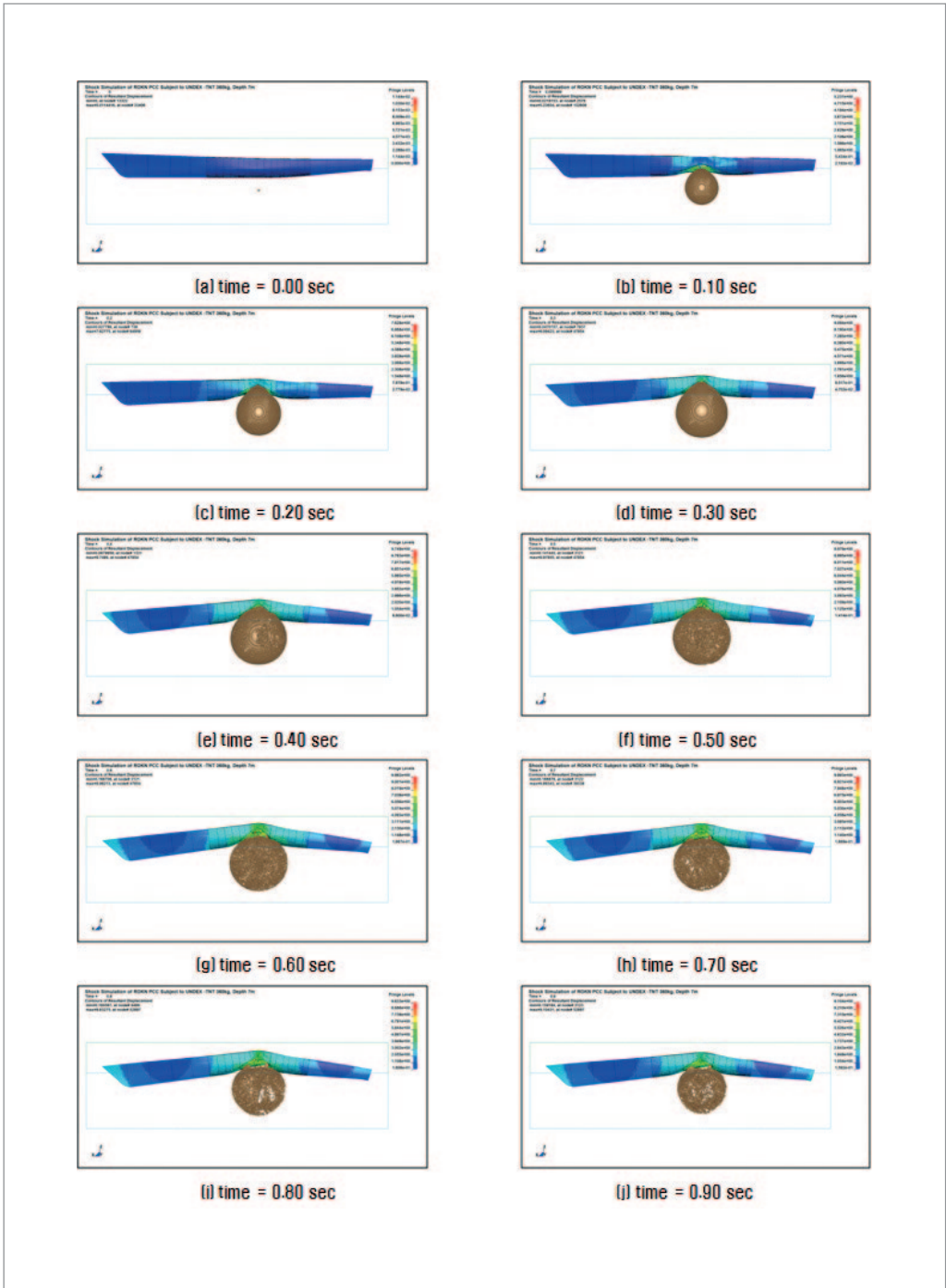
<Figure III-6-14> Analysis result(TNT 360kg at 9m depth): damage in gas turbine room (continued)



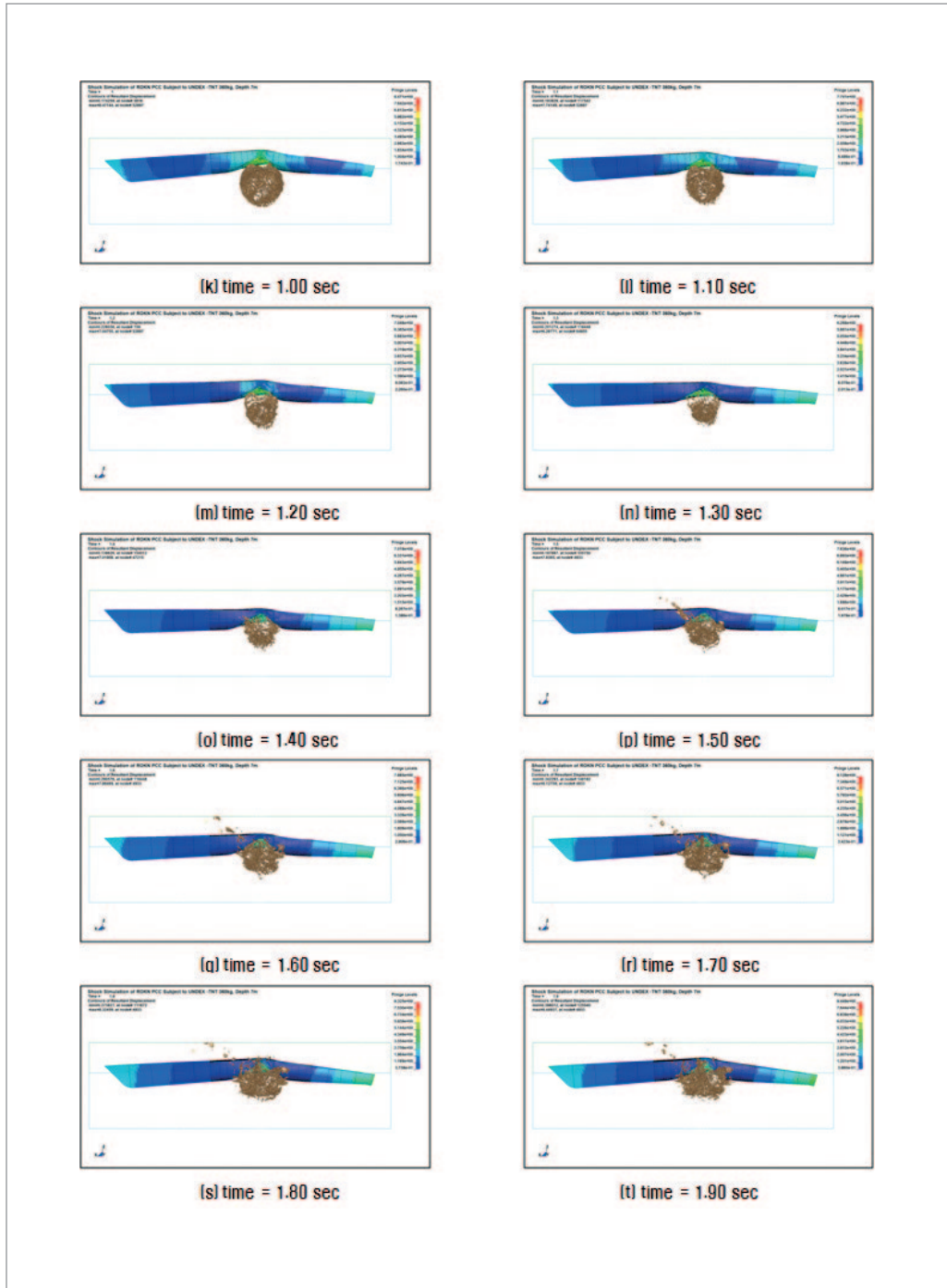
<Figure III-6-15> Side view of analysis result(TNT 360kg at 9m depth) on bubble migration and shock response



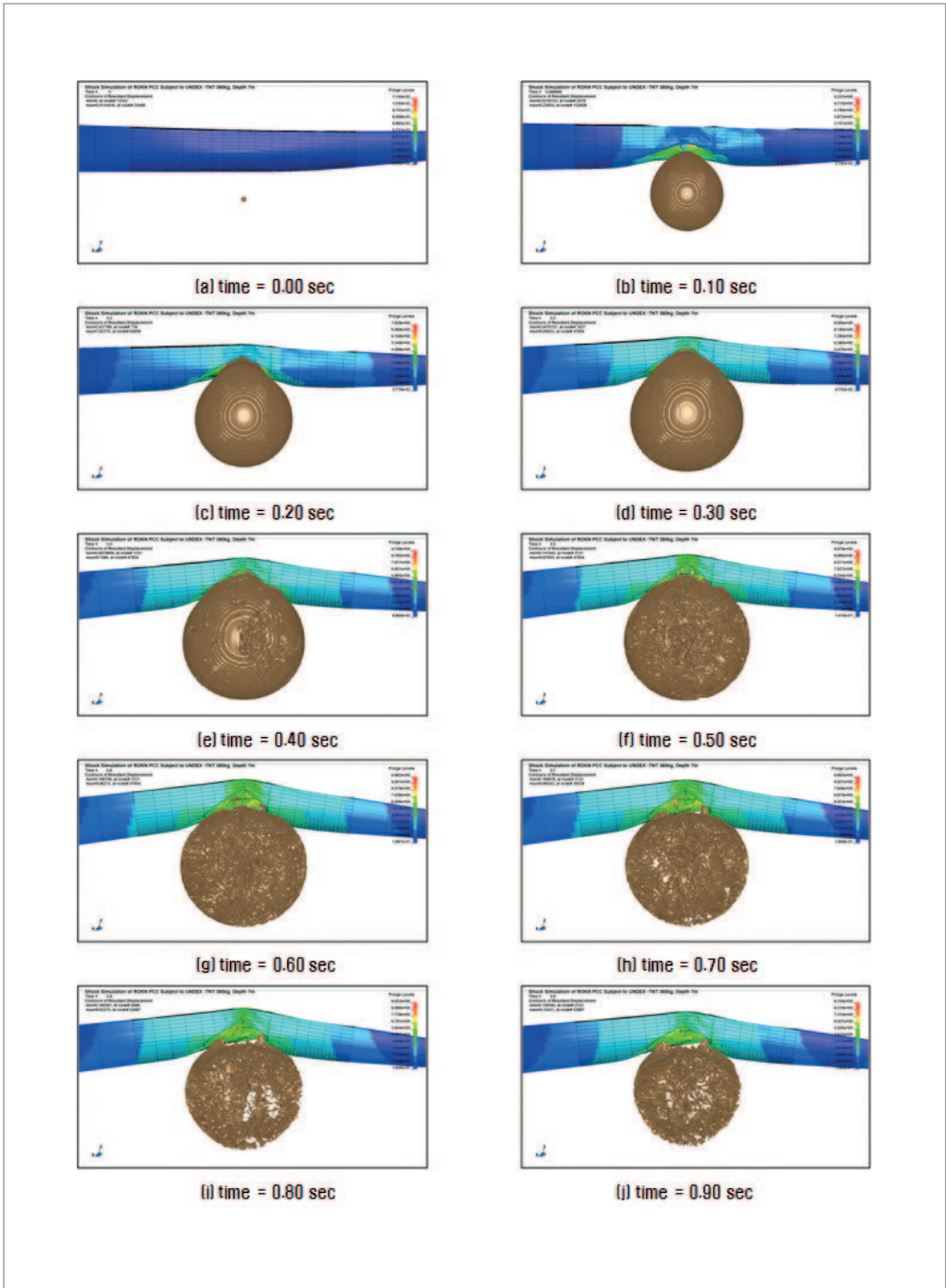
<Figure III-6-15> Side view of analysis result(TNT 360kg at 9m depth) on bubble migration and shock response (continued)



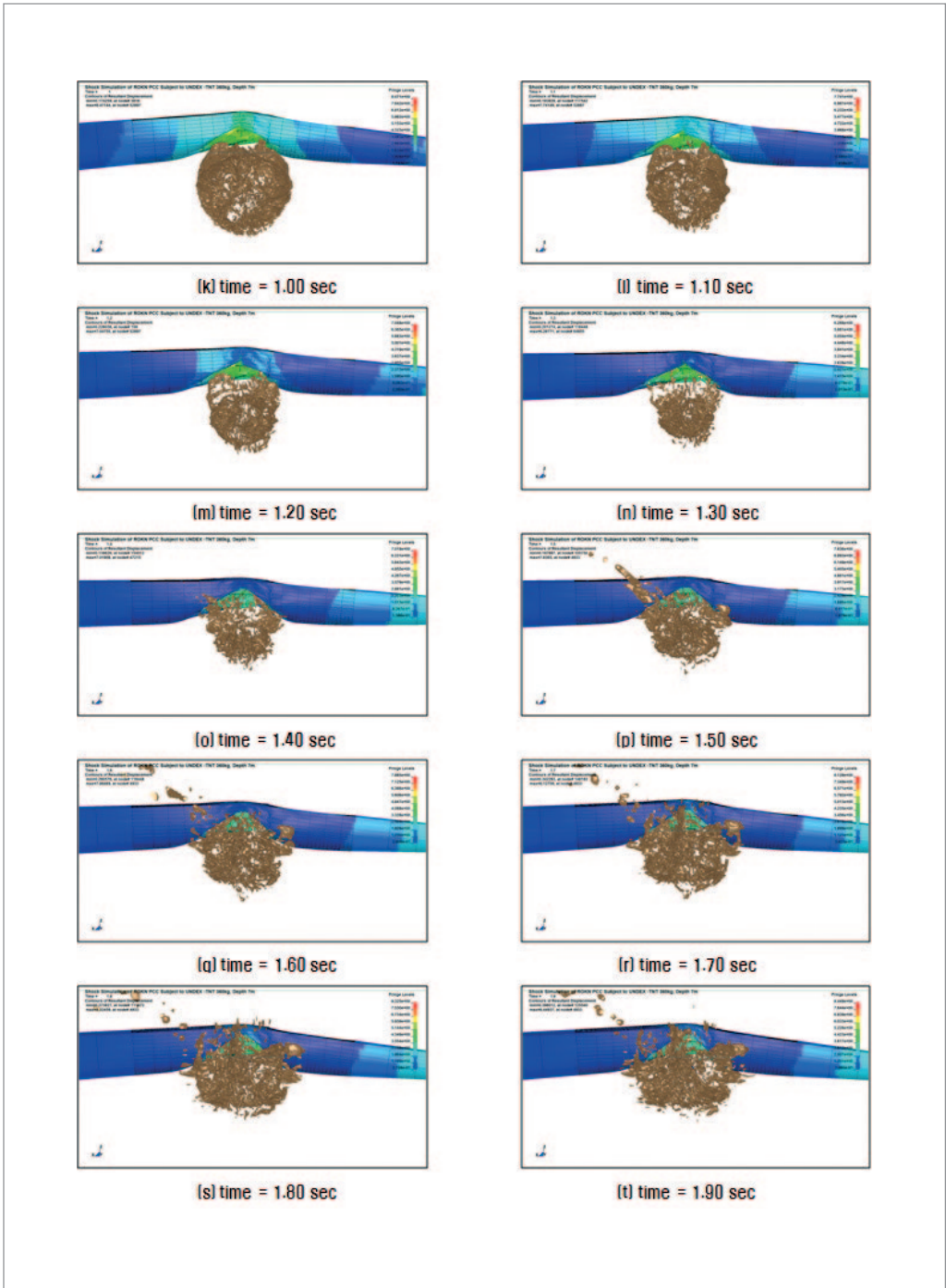
<Figure III-6-16> Side view of analysis result(TNT 360kg at 7m depth)



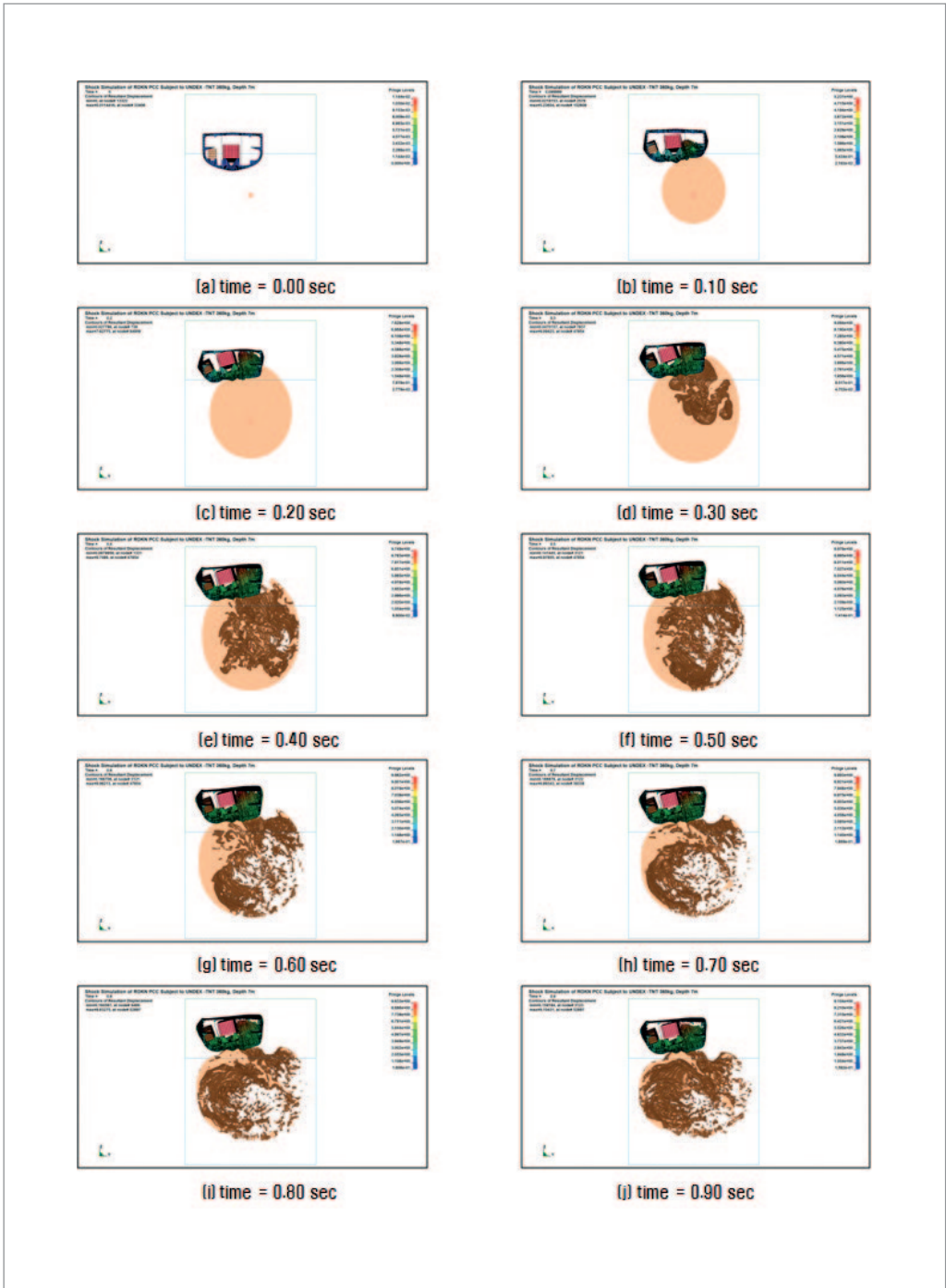
<Figure III-6-16> Side view of analysis result(TNT 360kg at 7m depth) (continued)



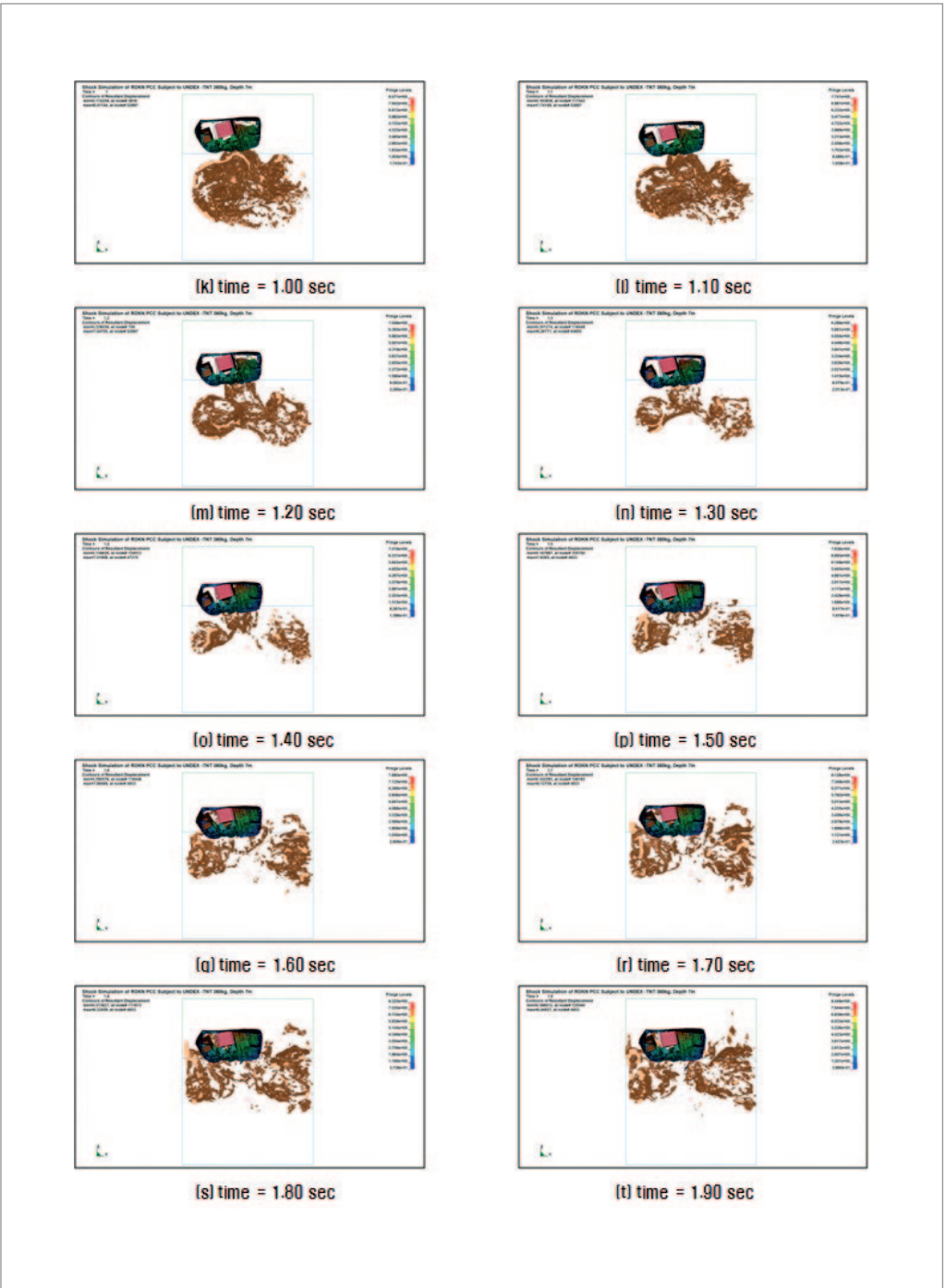
<Figure III-6-17> Side view(closed-in) of analysis result(TNT 360kg at 7m depth)



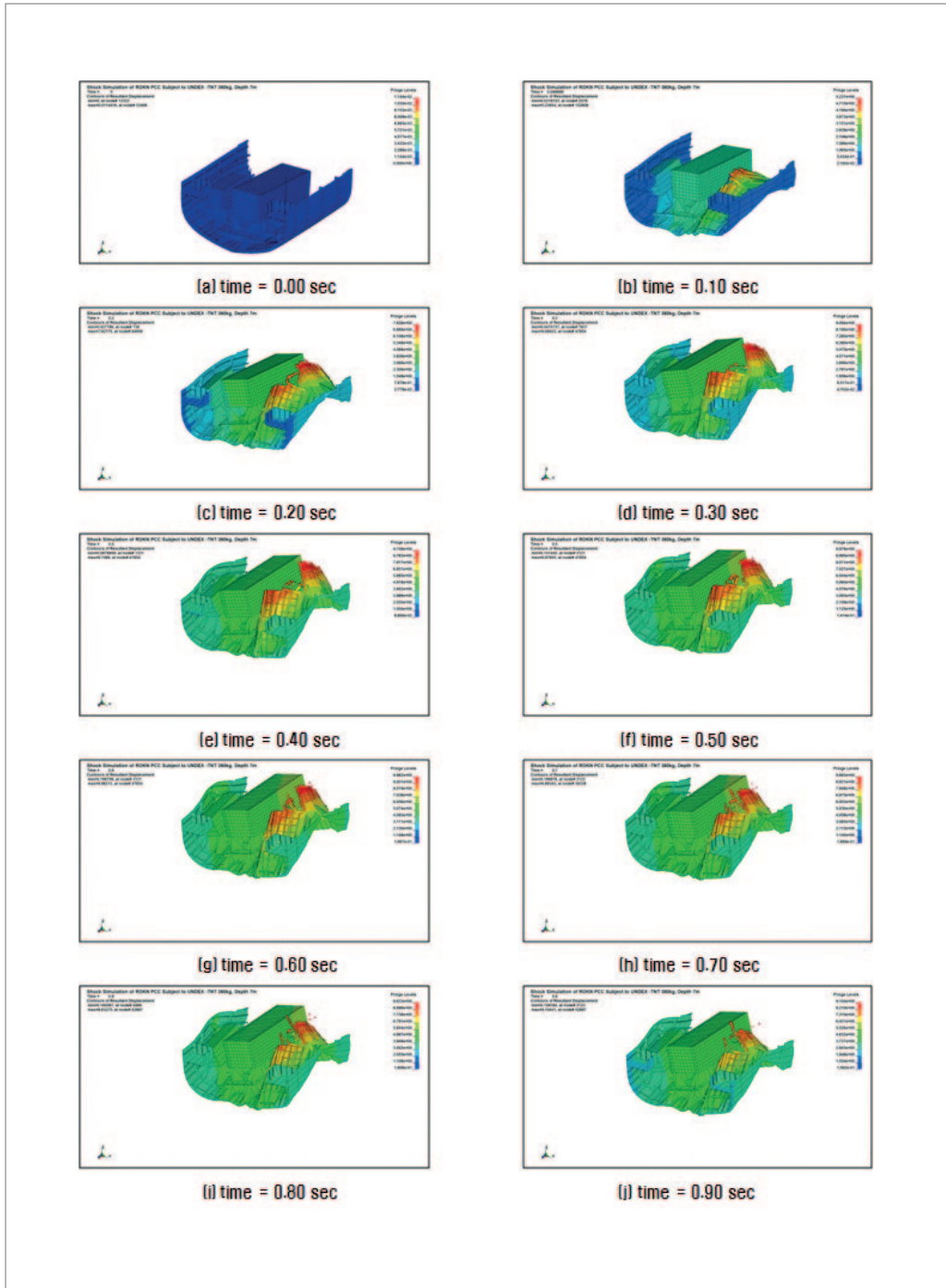
<Figure III-6-17> Side view(closed-in) of analysis result(TNT 360kg at 7m depth) (continued)



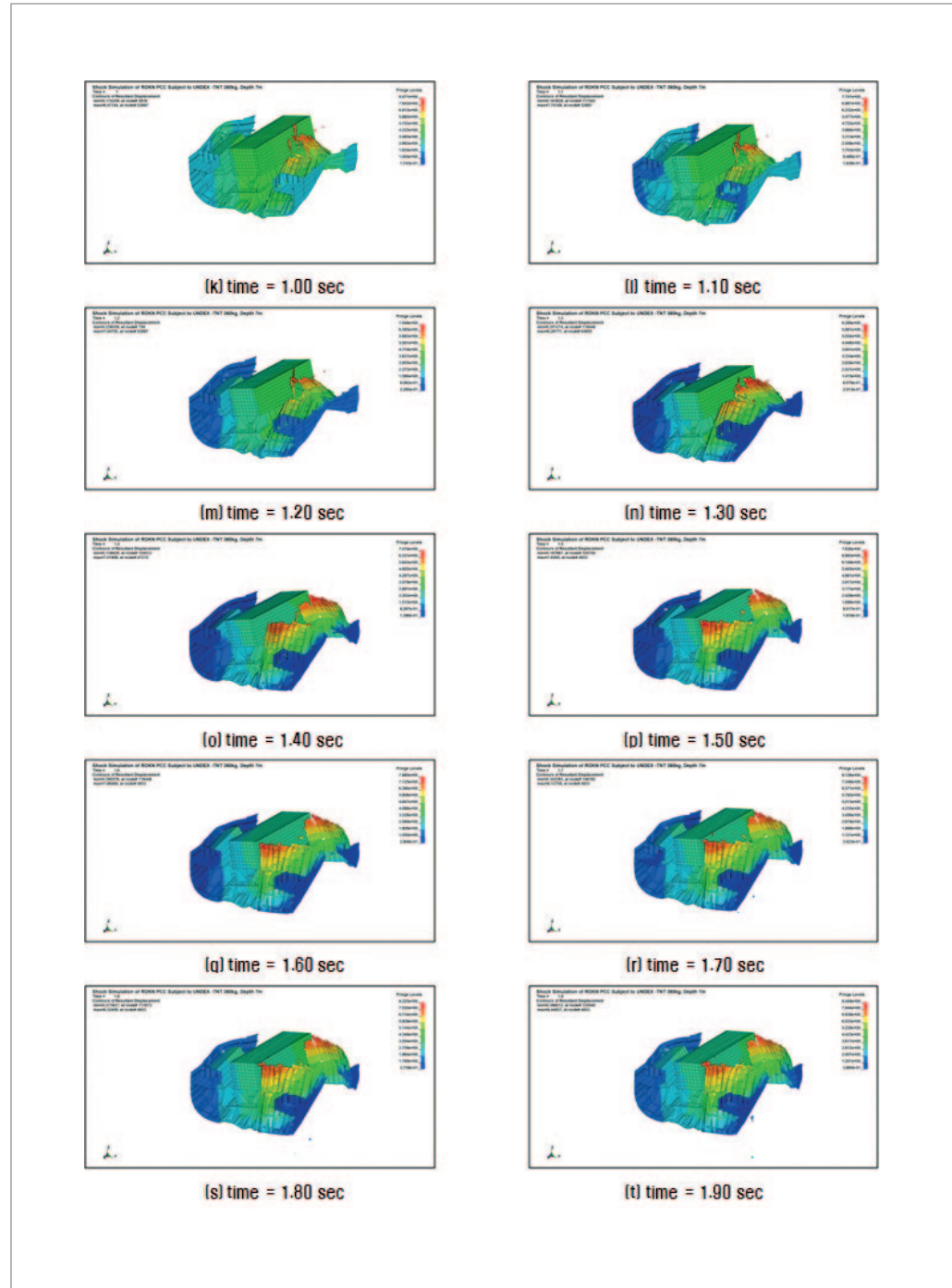
<Figure III-6-18> Section view of analysis result(TNT 360kg at 7m depth)



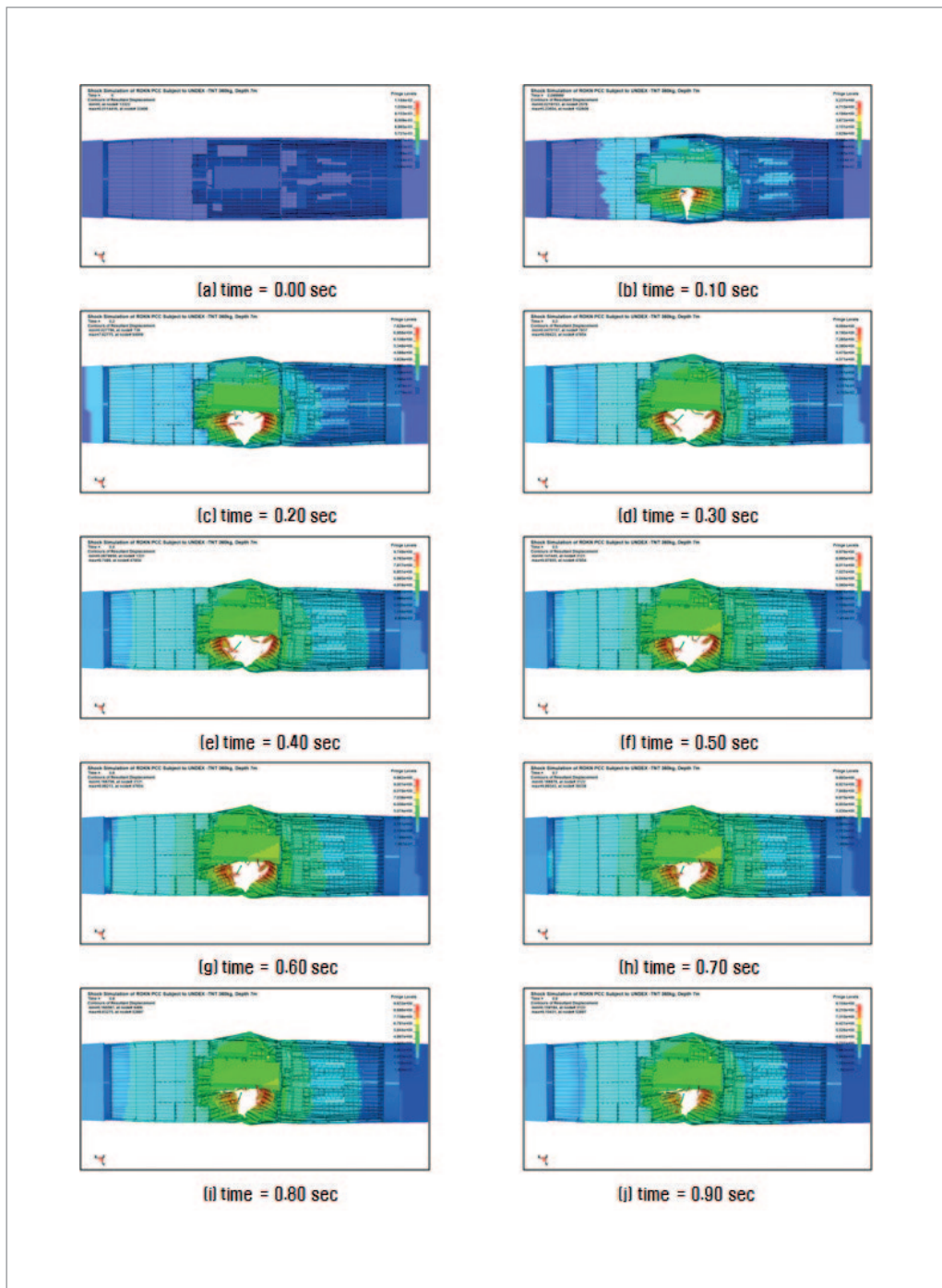
<Figure III-6-18> Section view of analysis result(TNT 360kg at 7m depth) (continued)



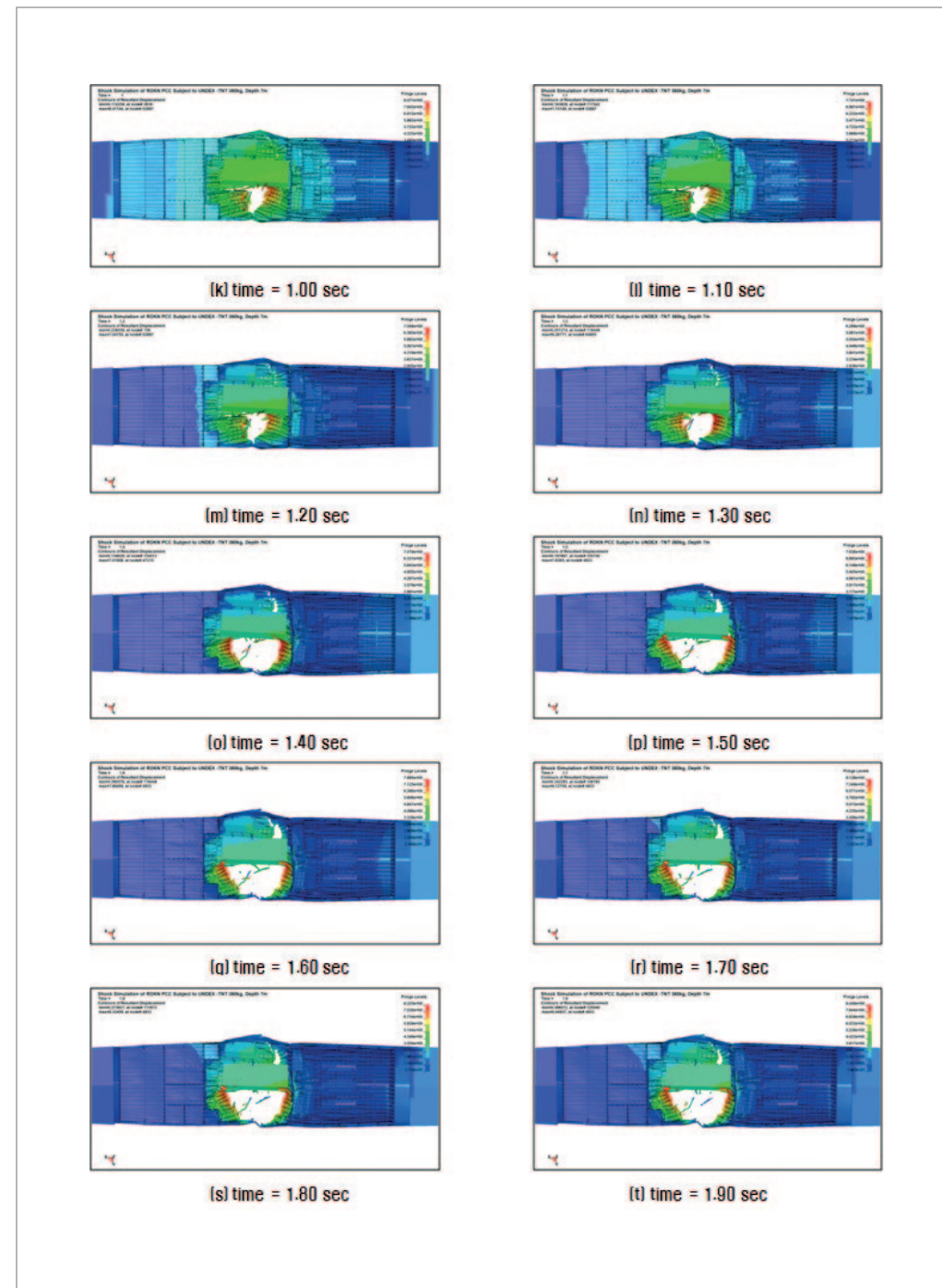
<Figure III-6-19> Internal view of analysis result(TNT 360kg at 7m depth)



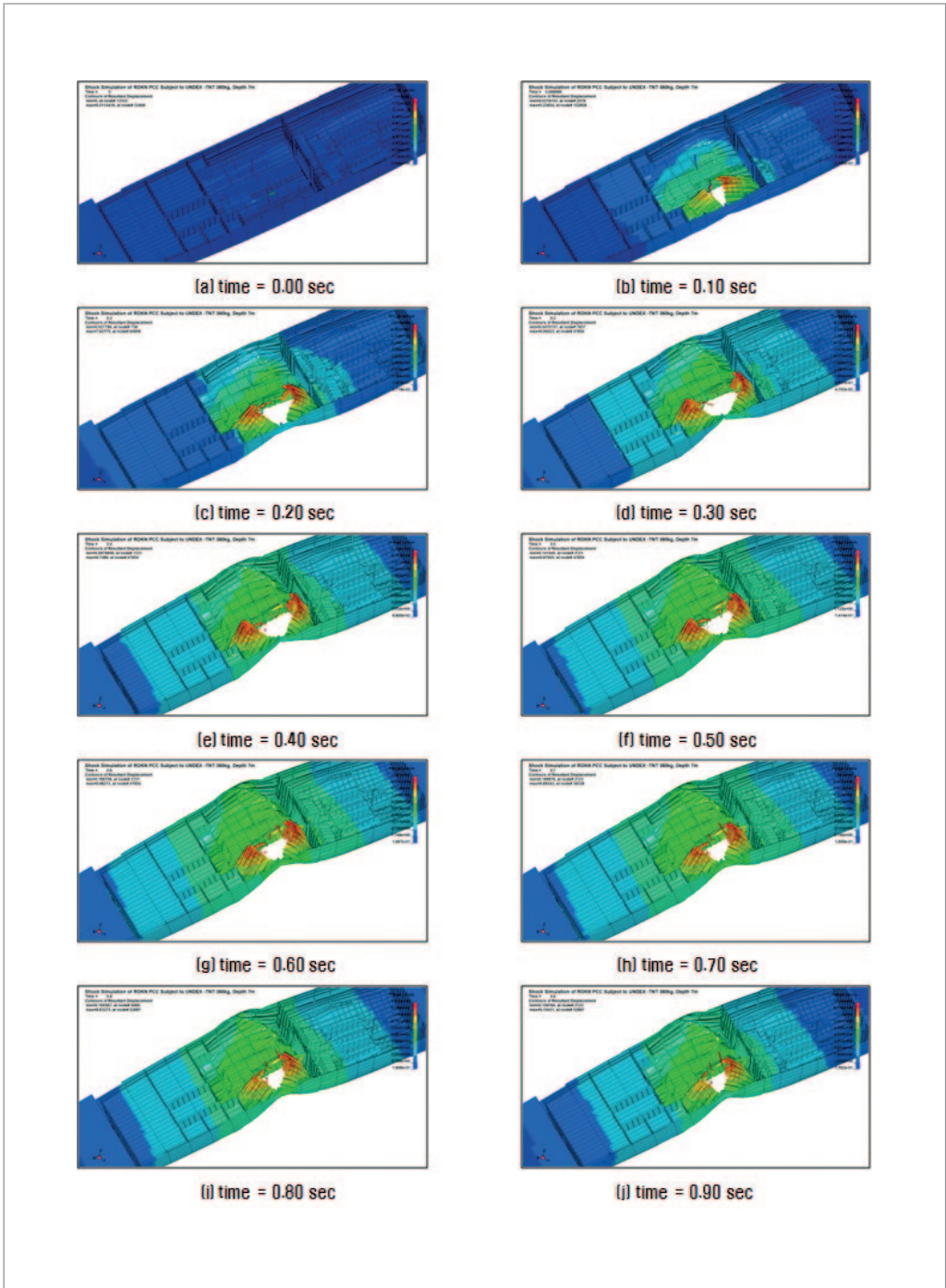
<Figure III-6-19> Internal view of analysis result(TNT 360kg at 7m depth) (continued)



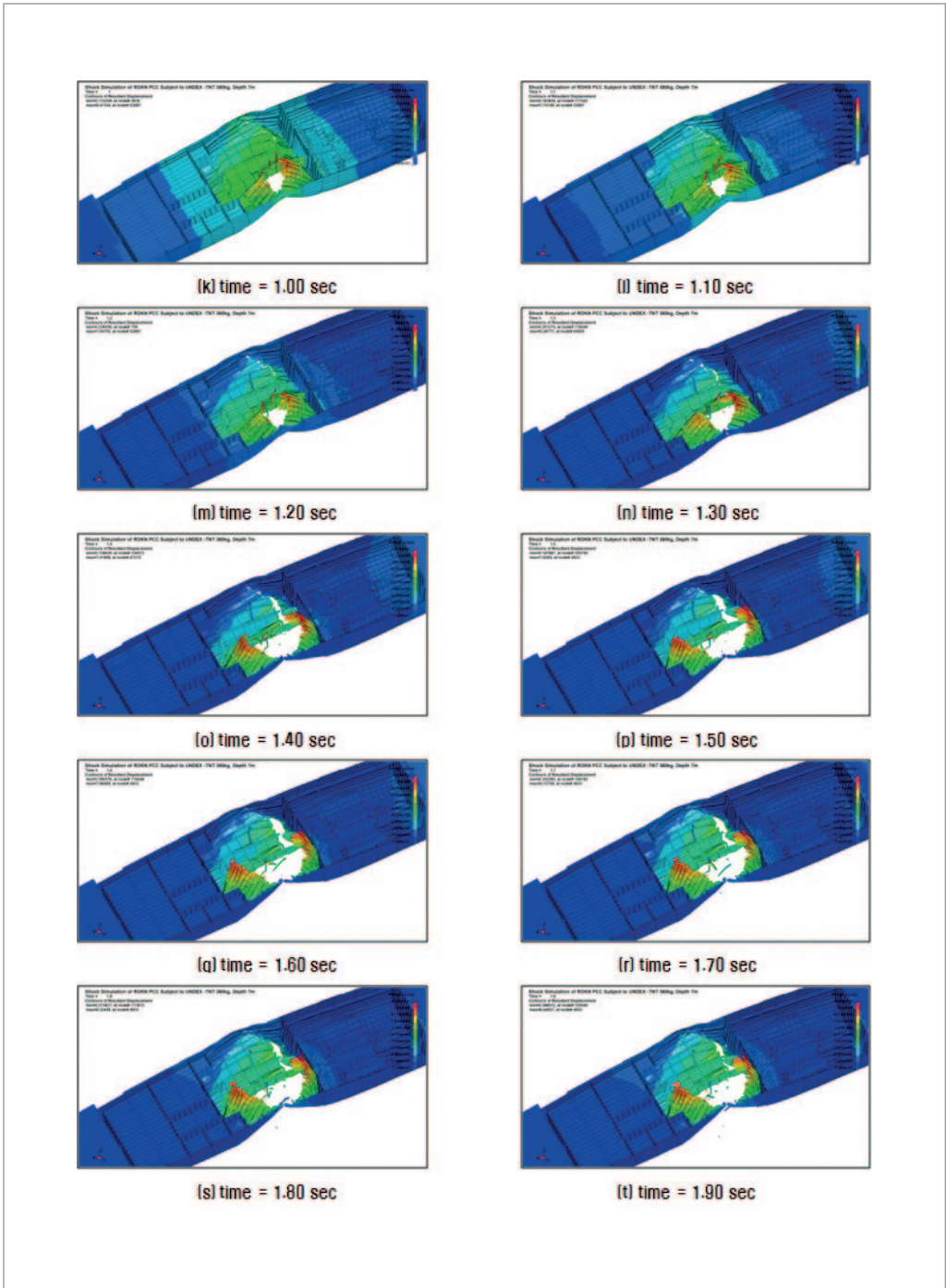
<Figure III-6-20> Internal top view of analysis result(TNT 360kg at 7m depth)



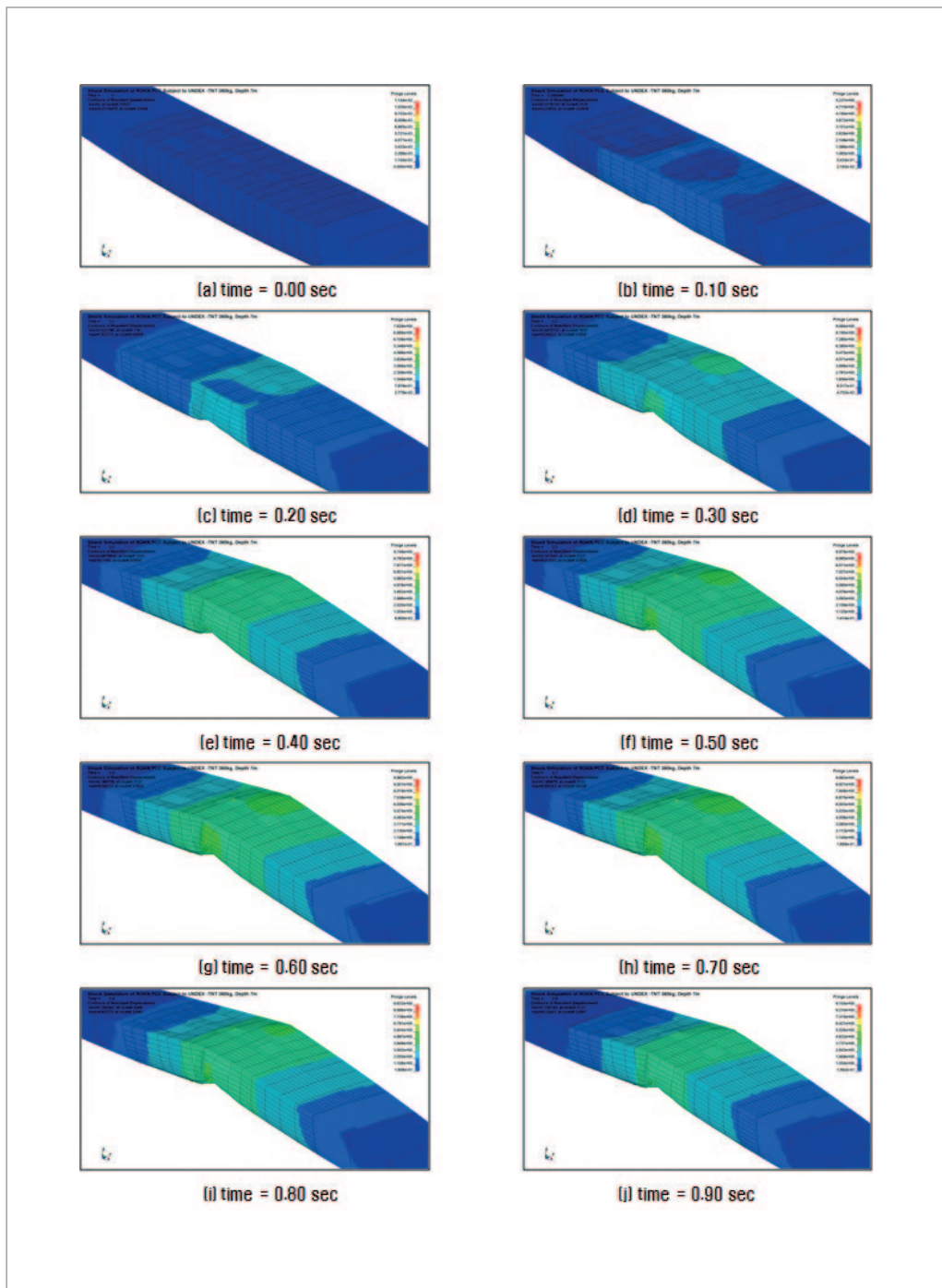
<Figure III-6-20> Internal top view of analysis result(TNT 360kg at 7m depth) (continued)



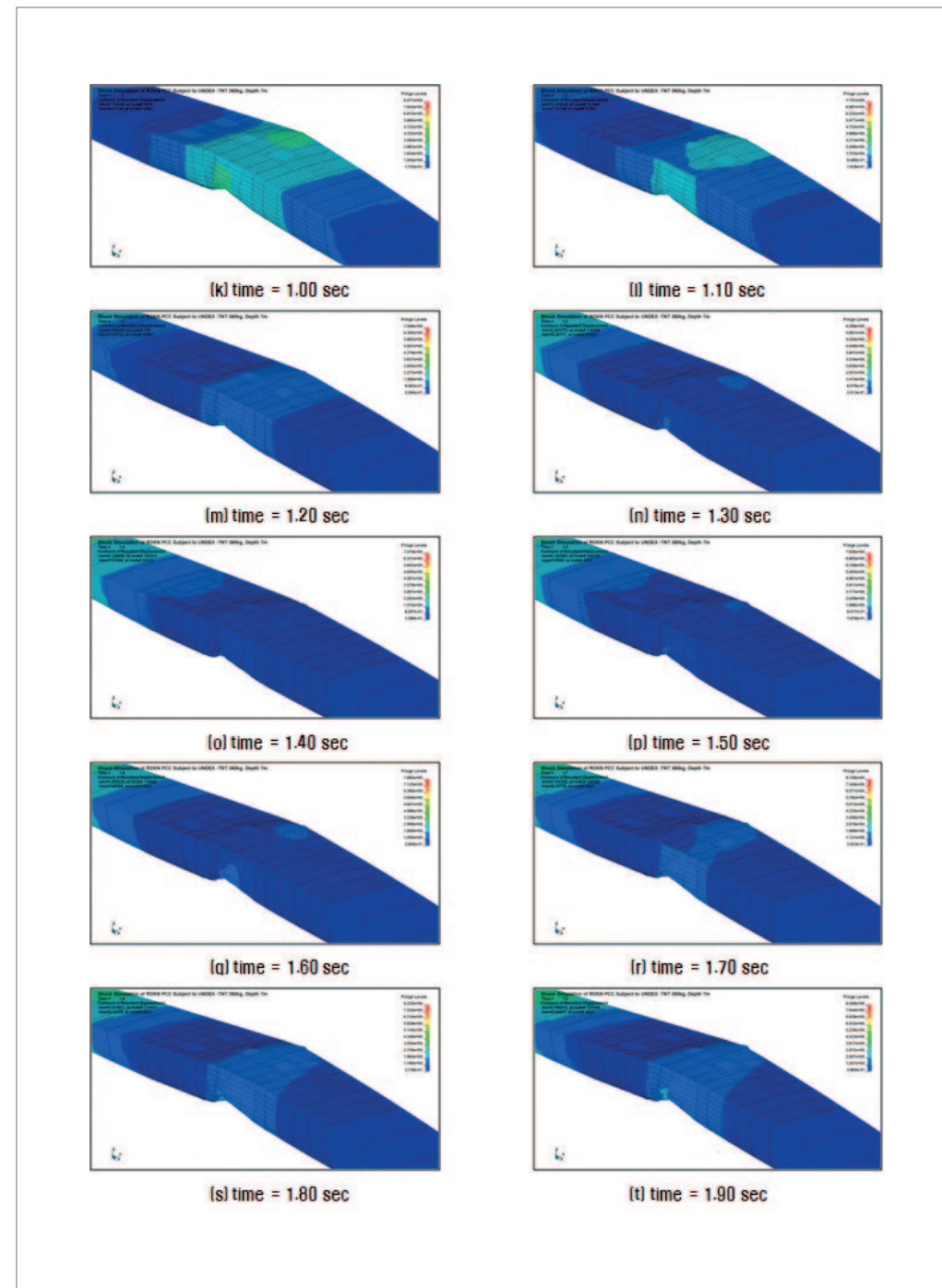
<Figure III-6-21> Internal-side view of analysis result(TNT 360kg at 7m depth)



<Figure III-6-21> Internal-side view of analysis result(TNT 360kg at 7m depth) (continued)

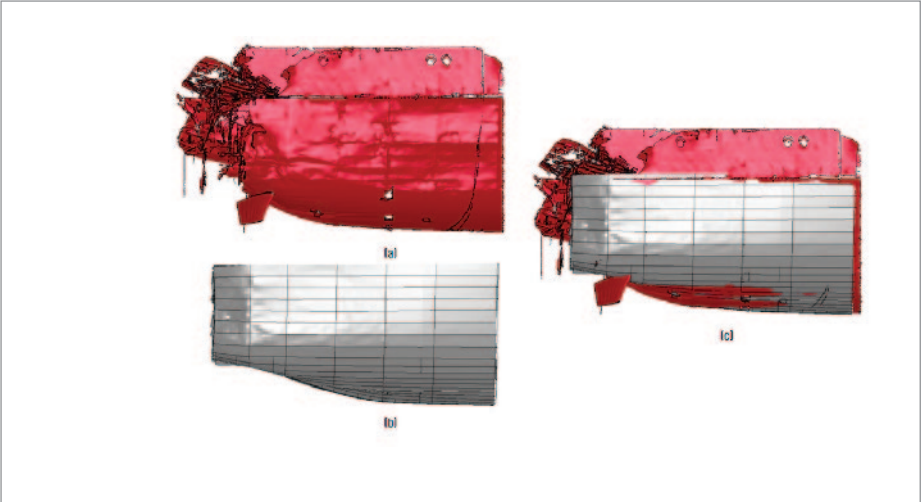


<Figure III-6-22> Deck view of analysis result(TNT 360kg at 7m depth)

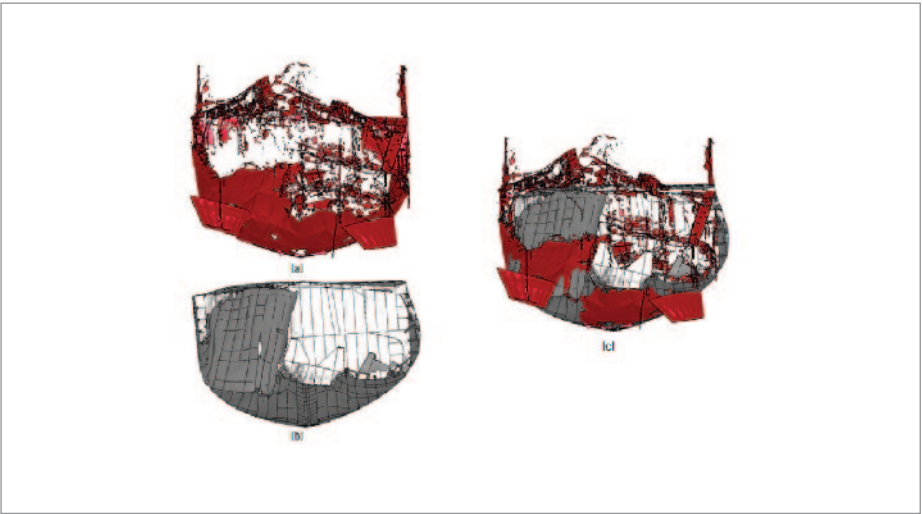


<Figure III-6-22> Deck view of analysis result(TNT 360kg at 7m depth) (continued)

〈Figure III-6-23〉 ~ 〈Figure III-6-28〉 illustrate the comparison between modelled damage result and the damages actually measured from 3D laser scanning image of ROKS Cheonan. Sub-caption (a) indicates the actual damage, (b) indicates the estimated damage results by the model, and (c) is the overlap of (a) and (b). As seen in these sub-captions, the modelled damage and the actual damages appear fairly similar.



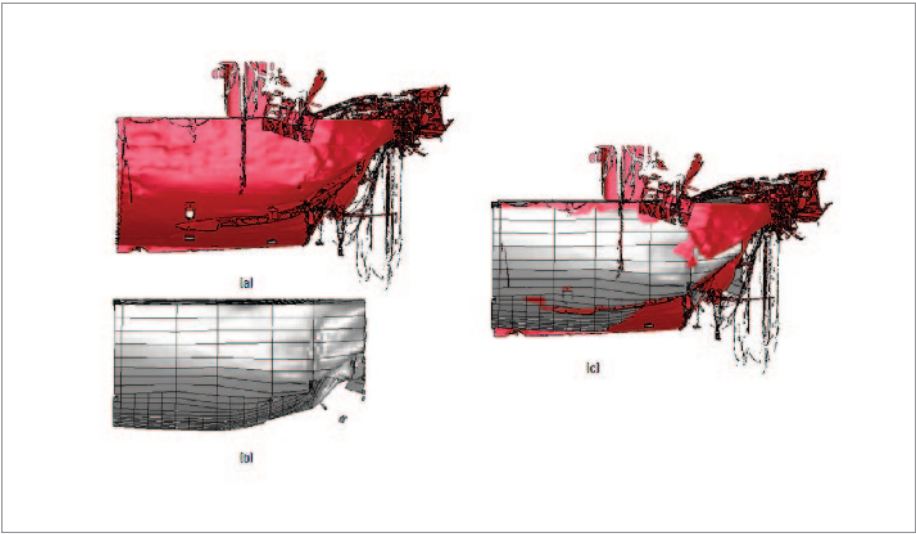
〈Figure III-6-23〉 Comparison between modelled damage and actual damage of ROKS Cheonan (side view of bow)



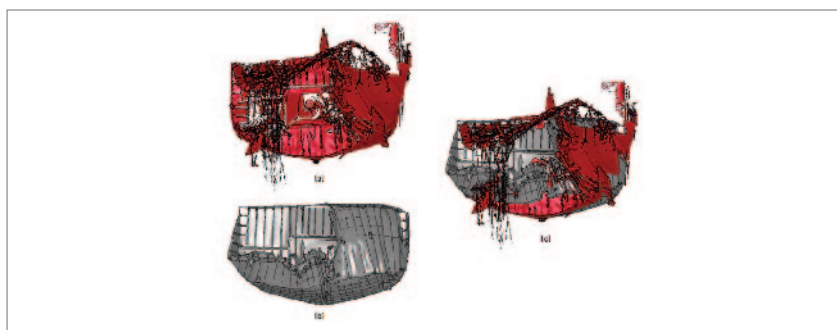
〈Figure III-6-24〉 Comparison between modelled damage and actual damage of ROKS Cheonan (front view of bow)



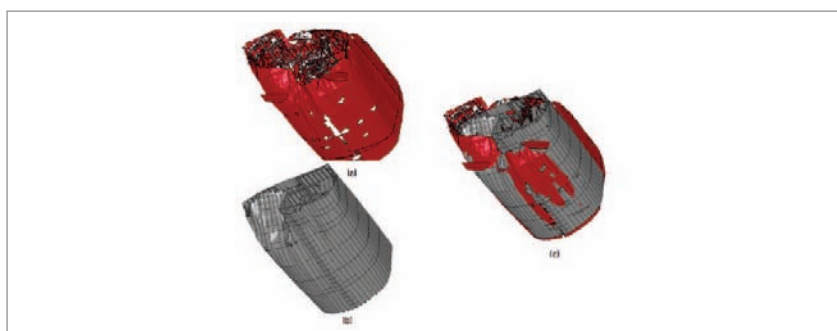
〈Figure III-6-25〉 Comparison between modelled damage and actual damage of ROKS Cheonan (bottom view of bow)



〈Figure III-6-26〉 Comparison between modelled damage and actual damage of ROKS Cheonan (side view of stern)



〈Figure III-6-27〉 Comparison between modelled damage and actual damage of ROKS Cheonan (front view of stern)



〈Figure III-6-28〉 Comparison between modelled damage and actual damage of ROKS Cheonan (bottom view of stern)

### (5) Sub-conclusion

The JIG received 2 explosion conditions from the Explosive Type Analysis Team, of TNT 360kg charge size in 7m and 9m depths. The JIG confirmed fairly similar damage results between modelled damage and actual damage of ROKS Cheonan from TNT 360kg charge size and 7m depth by conducting 3D finite element analysis incorporating the interrelation between the structure and the fluid.

Also, the JIG was able to obtain scientifically credible inference on the process of the gas turbine room split and detachments of the structures leading to ROKS Cheonan's sinking through the analysis result of TNT 360kg explosion at 7m depth. That is, the initial shock wave reached the hull and created the fracture called "punching shear", tearing out the most vulnerable areas of portside bottom shell plates in the gas turbine room. This became more severe due to the series of bubble process(expansion, contraction, and re-expansion of the bubble); the estimated damage results on the portside were very similar to

the actual damages from a 3D laser scanning. Additionally, the detachments of gas turbine foundation, generator foundation, bottom shell plates, and starboard shell plates as a whole(without separation) were consistent with the damage patterns from the analysis.

## 7. Analysis on Sea Area of the Incident

### 1) Overview

A precise investigation on the underwater terrain and the tidal current at the site of the sinking in the vicinity of Baekryong Island was conducted in order to find how they can possibly affect the cause of the incident and North Korean infiltration assets such as submarine or midget submarine.

### 2) Situation at the Time of the Incident

The ROKS Cheonan sank at 2122, March 26, in 2.5km Southwest of Baekryong Island(37°55'45"N – 124°36'02"E), at 47m in water depth. At the time, sea weather<sup>25)</sup> was: southwest 2wind 20kts, wave height 2.5m, tidal current<sup>26)</sup> 161°–2.89kts, visibility 2.5NM, flood tide<sup>27)</sup> at 0225(2.3m) / 1515(2.7m), and ebb tide at 0843(0.7m)/2147(0.8m).

### 3) Investigation Focus

#### (1) Underwater Terrain in vicinity of Baekryong Island

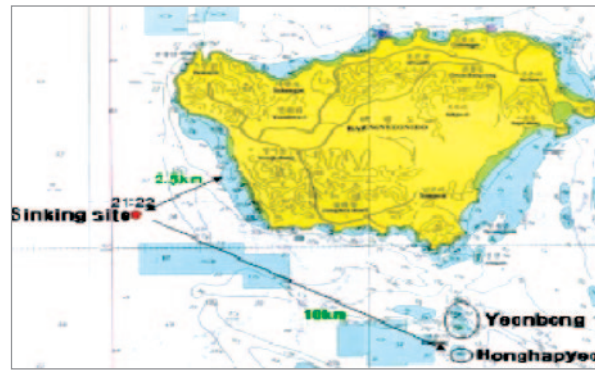
The investigation was conducted to identify existence of underwater obstacles, focusing on the maneuvering route(patrol area at the time of the incident) of ROKS Cheonan. Conducted in a joint manner with advisory committee members<sup>28)</sup> from National Oceanographic Research Institute(Ministry of Land, Transportation and Maritime Affairs) and

25) At 1625 on March 26, 2010, Hwangcheon class 5(wave height of 2.6-3.0m and wind speed of 26-30kts) was declared in the waters near Baekryong Island.  
 26) Tidal current is a horizontal movement of seawater generated by ebb and flood tide.  
 27) Tide is a gradual movement of seawater in vertical direction.  
 28) NORI Maritime Branch chief and a researcher from KORDI participated as advisory members.

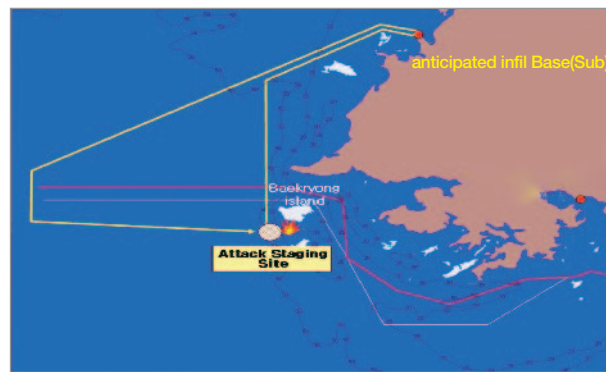
Korea Ocean Research and Development Institute(Ministry of Education, Science and Technology), the investigations and verifications were systematic and scientific.

## (2) Tidal Current in the vicinity of Baekryong Island

The investigations and analyses were carried out in order to find out how the tidal movement and currents in the vicinity of Baekryong Island affected maneuvering of ROKS Cheonan during the time of incident and how tidal currents between Baekryong Island and anticipated North Korea infiltration bases affect maneuvers of North Korean infiltration assets such as submarine or midget submarine. The investigations and analyses also attempted to reveal how tidal currents affect employments of arms such as torpedo launch and mine installation by North Korean submarine or midget submarine.



〈Figure III-7-1〉 The sinking site of ROKS Cheonan



〈Figure III-7-2〉 Anticipated infiltration routes of North Korean submarine or midget submarine

## 4) Analysis on Underwater Terrain in the vicinity of Baekryong Island

### (1) Investigation Method

First, the JIG obtained every available chart to confirm any underwater obstacle. Then, the JIG committed Navy Search and Rescue Group ships(March 28 ~ April 17) and Korea Ocean Research and Development Institute's research vessels(April 4 ~ May 8) to conduct search operations. Furthermore, the JIG checked with Baekryong Island local mem-

bers of fishery group, government ships and fishers whether there was any underwater obstacle missing on the charts.

### (2) Investigation Result

#### ① Verification of all Available Charts for Waters around Baekryong Island

Through coordination with National Oceanographic Research Institute(NORI)<sup>29)</sup>, the JIG acquired 6 relevant charts including the underwater terrain chart shown in 〈Table III-7-1〉. Comparison on the water depth and underwater obstacles(reef, unknown sunken vessel, and fishery) was made using the charts. The result was that there were no underwater obstacles in the actual maneuvering route of ROKS Cheonan.

CAT	Chart no.	Scale	Published by	Purpose
Chart	① No.360	1:30,000	NORI('05)	Military(maritime police)/merchant/fishery
	② No.360	1:30,000	NORI('08)	NORI research project
	③ No.315	1:75,000	NORI('04)	Military(maritime police)/merchant/fishery
	④ No.323	1:250,000	NORI('06)	Military(maritime police)/merchant/fishery
Underwater terrain chart	⑤ No.4534	1:200,000	NORI('90)	Military
Marine zone chart	⑥ No.101	1:2,000,000	NFFC(NORI)	Fishery

〈Table III-7-1〉 All available charts for waters near Baekryong Island<sup>30), 31)</sup>

Maritime branch chief at the NORI, while serving also as an advisor to the Joint Investigation Group, stated that all obstacles such as fishing ground that could affect the safety of ships on maneuvering have been depicted on charts upon identification, although no pre-planned research on the waters such as measuring water depth has been conducted since 1992 due to the sensitive nature of the area in the vicinity of Baekryong Island. He confirmed that there were no underwater obstacles on any chart that could have affected the maneuvering of ROKS Cheonan(maneuvering course of ROKS Cheonan in the patrol area)<sup>32)</sup>.

29) NORI is responsible for the publication of domestic marine charts.

30) The charts ①, ③ and ④ published by the NORI are used commonly by the civilian & military. The chart ② is the latest chart kept within the NORI only.

31) The chart ⑤ also published by the NORI is used only in military and the Marine zone chart ⑥ published by National Federation of Fisheries Cooperatives does not include information about water depth and reef.

32) On March 30, 2010, the NORI officially announced that there was no reef in the vicinity of the sinking site of ROKS Cheonan.

### ② Search Operation by Navy Search and Rescue Group in the Sinking Site

From March 28 until April 17, 4 minesweeping ships (ROKS Yangyang, Ongjin, Gimpo, and Goryong) conducted search with Side Scan Sonar<sup>33)</sup>, focusing on ROKS Cheonan's patrol area. Except for the unknown sunken vessel (75 × 15 × 10m), 18 contacts found were minor objects consisting mostly of crab fishing net, iron object, and bedrock as shown in <Table III-7-2>, confirming that there were no underwater obstacles in ROKS Cheonan's maneuvering route.

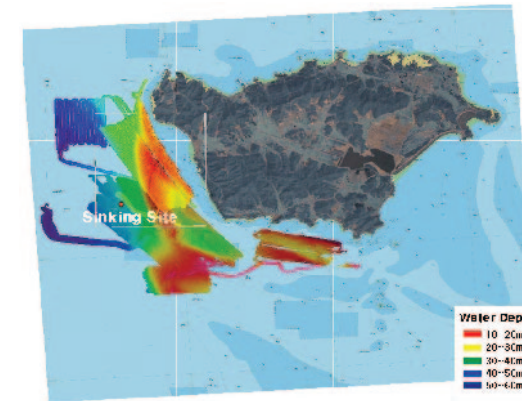
CAT	ID time	Location of object	Size(m)	Depth(m)	Found
1	2231 Mar 28	37° 55' 40"N, 124° 36' 06"E	33×10	47	Stern
2	1427 Mar 29	37° 55' 48"N, 124° 36' 00"E	75×15×10	42	Unknown sunken vessel
3	1550 Mar 30	37° 55' 22"N, 124° 34' 03"E	-	50	Bedrock
4	0924 Mar 31	37° 55' 41"N, 124° 36' 06"E	3.7×10.1	44	Bedrock
5	0933 Mar 31	37° 55' 42"N, 124° 36' 06"E	3.4×1.3	44	Metal object
6	1315 Apr 2	37° 54' 12"N, 124° 37' 57"E	2×3	18	Concrete structure
7	1345 Apr 2	37° 54' 52"N, 124° 37' 07"E	2×2	25	Concrete structure
8	1435 Apr 2	37° 54' 45"N, 124° 37' 12"E	2×2	27	Concrete structure
9	1515 Apr 2	37° 54' 46"N, 124° 37' 52"E	-	34	Bedrock
10	1858 Apr 2	37° 55' 42"N, 124° 36' 22"E	-	17	Bedrock
11	1350 Apr 14	37° 55' 41"N, 124° 36' 05"E	6.6×3.8	42	Stack
12	1405 Apr 14	37° 55' 42"N, 124° 36' 04"E	1.5×2	44	Copper pipe
13	1413 Apr 14	37° 55' 42"N, 124° 36' 03"E	1.2×0.6	43	Boat engine cover
14	1415 Apr 14	37° 55' 43"N, 124° 36' 03"E	2.4×2.3	44	Crab fishing net
15	1420 Apr 14	37° 55' 44"N, 124° 36' 03"E	2.1×0.7	43	ROKS Cheonan generator
16	1430 Apr 14	37° 55' 41"N, 124° 36' 03"E	2.2×0.8	42	ROKS Cheonan harpoon
17	1700 Apr 14	37° 55' 43"N, 124° 36' 02"E	5×0.1	43	External pipe
18	1703 Apr 14	37° 55' 43"N, 124° 36' 03"E	1.8×0.5	43	Triangular Aluminum particle
19	2030 Apr 17	37° 55' 10"N, 124° 37' 37"E	2×2×1.1	31	Bedrock

<Table III-7-2> Objects found in the sinking site by Navy Search and Rescue Group

33) Side Scan Sonar: It obtains sea bottom terrain informations by detecting the irregularity using sonar with supersonic transmitter.

### ③ Search Operation by KORDI Vessels in the Sinking Site

From April 4 to May 8, 2 research vessels (Yiuhdo and Jangmok) were committed for search operation with Multi-Beam Echo Sounder<sup>34)</sup> and Side Scan Sonar, focusing on the sinking location of the stern of ROKS Cheonan and following the maneuvering route of ROKS Cheonan. The operation found 1 unknown sunken vessel (75 × 15 × 10m) and only 11 small objects ranging from 0.4 to 4m in size (See <Table III-7-3>). The operation con-

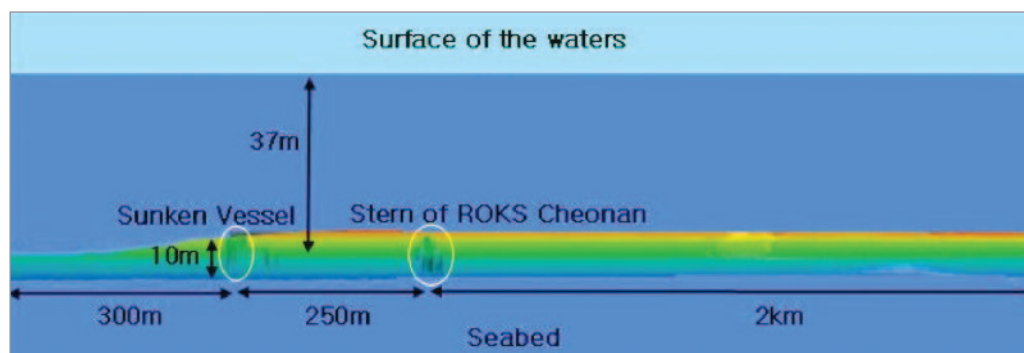


<Figure III-7-3> Area of underwater terrain search operation at the sinking site by the KORDI

CAT	ID time	Location of object	Size(m)	Depth(m)
1	0214 Apr 18	37° 55' 40"N, 124° 36' 03"E	1.7×0.6	47
2	0214 Apr 18	37° 55' 41"N, 124° 36' 04"E	0.8×0.6	46
3	0214 Apr 18	37° 55' 40"N, 124° 36' 04"E	0.7×1.1	46
4	0214 Apr 18	37° 55' 40"N, 124° 36' 04"E	4.0×0.7	47
5	0214 Apr 18	37° 55' 38"N, 124° 36' 03"E	0.6×1.6	47
6	0218 Apr 18	37° 55' 32"N, 124° 36' 13"E	0.7×1.2	46
7	0239 Apr 18	37° 55' 36"N, 124° 36' 08"E	0.5×0.4	47
8	0240 Apr 18	37° 55' 39"N, 124° 36' 05"E	0.4×0.7	46
9	0240 Apr 18	37° 55' 40"N, 124° 36' 05"E	2.5×0.5	46
10	0241 Apr 18	37° 55' 40"N, 124° 36' 03"E	2.5×0.5	47
11	0243 Apr 18	37° 55' 44"N, 124° 36' 02"E	1.3×0.5	48

<Table III-7-3> Objects found in the sinking site by the KORDI

34) Multi-Beam Echo Sounder: a depth finder that emits multi-beam echo sound and receives returning sound to measure the depth and the underwater terrain simultaneously. It can measure transverse cross section of the seabed and depict contour lines and terrain in color graphic.



〈Figure III-7-4〉 Result of underwater terrain search in the sinking site

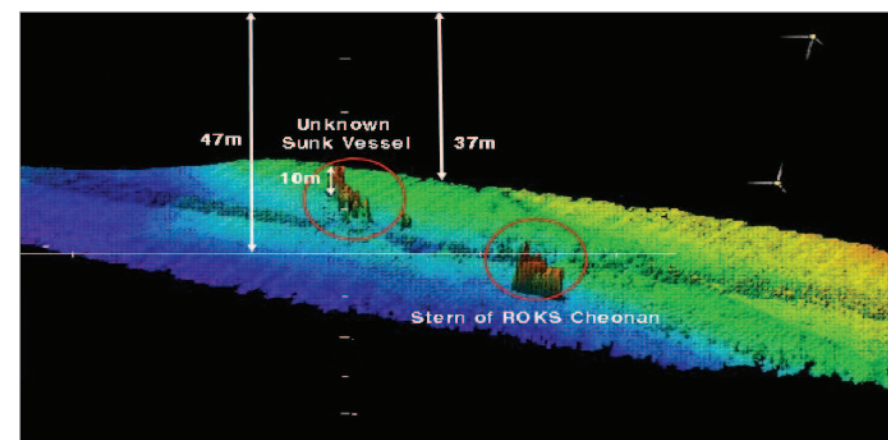
cluded that there were no underwater obstacles in ROKS Cheonan's maneuvering route.

The unknown sunken vessel found in the sinking site is not depicted on the charts. The type of the vessel and the time of its sinking were unknown, and Navy Search and Rescue Group divers conducted investigation on the vessel several times. Acoustic image from Side Scan Sonar found that the vessel had the shape of a merchant vessel (steering gear room in the stern and multiple columns in the middle deck), and many rivetings of the metal structure recovered from near the unknown sunken vessel support the high likelihood that it was a merchant vessel which sunk scores of years ago.



〈Figure III-7-5〉 Metal structure found near unknown sunken vessel

Given the water depth of the location of the unknown sunken vessel (47m), the height of the unknown sunken vessel (10m), and the draft of ROKS Cheonan (2.88m), it was confirmed that the unknown sunken vessel would not have impacted the safety of ROKS Cheo-

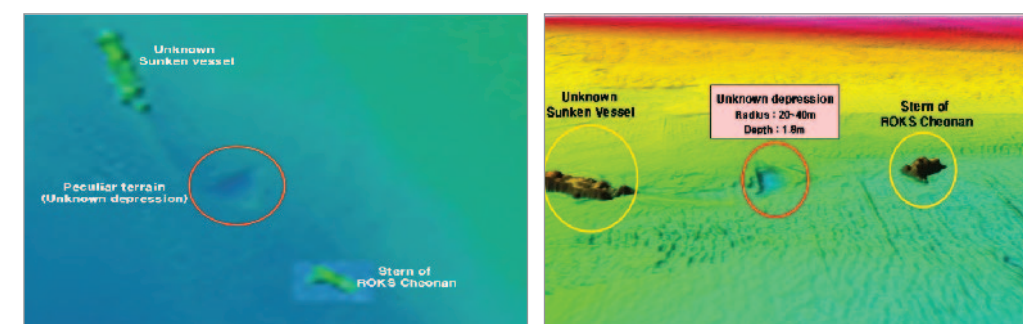


〈Figure III-7-6〉 Underwater terrain around the unknown sunken vessel

nan's maneuvering.

KORDI Research vessels found an unknown depression (20~40m in radius and 1.8m in depth) at the seabed between the unknown sunken vessel and the stern of ROKS Cheonan. In order to verify the cause on the formation of this depression, a month long accumulation and erosion process on the seabed was observed through 3D Multi-Beam Echo Sounder. This combined with the further on-site search conducted by the divers resulted in a confirmation that the seabed geography consisted of hard mud and gravels.

After having a discussion with these results of investigation, experts<sup>35)</sup> concluded that the depression was created not artificially but by alteration of current flow due to the unknown sunken vessel and that it had no relevance to ROKS Cheonan incident.



〈Figure III-7-7〉 Depression at the seabed near the incident site

<sup>35)</sup> The civilian chairman of the JIG, a professor from KAIST, researchers from ADD, a researcher from KORDI, and an advisor from National Assembly Recommended Investigation Committee participated in the discussion among the experts on the unknown depression.

④ Consulting Local Personnel on the possible Underwater Obstacles in vicinity of the sinking site

The JIG visited relevant members of fishery group, government vessels, and fishers in Baekryong Island and checked whether there exist underwater obstacles in the vicinity of the sinking site but are not depicted on charts. Regarding the unknown sunken vessel, a fisher in Baekryong Island stated that he heard from his father that the vessel sunk sometime during Japanese colonial rule. Regarding the reef, Honghapyeo, reported by the Korean Broadcasting System(KBS) on March 30, 2010, is 10km southeast of the sinking site as shown in <Figure III-7-8>, and no unknown obstacles were found.



<Figure III-7-8> Reef(Honghapyeo) near Baekryong Island shown on a chart

(3) Sub-conclusion

Ships of Navy Search and Rescue Group and of KORDI identified 30 objects underwater in total in the vicinity of ROKS Cheonan's sinking site. Most of the objects were confirmed to be debris of ROKS Cheonan, bedrock, and abandoned fishing net which could not have affected the sinking of ROKS Cheonan. All findings relevant to the maneuvering route of ROKS Cheonan such as the KORDI's research on underwater terrain, investigation on obstacles including the unknown sunken vessel and artificial reef, and NORI's confirmation on chart measurement data ultimately verified that there were no factors that could have affected the sinking of ROKS Cheonan.

5) Analysis on the Tidal Currents Near Baekryong Island

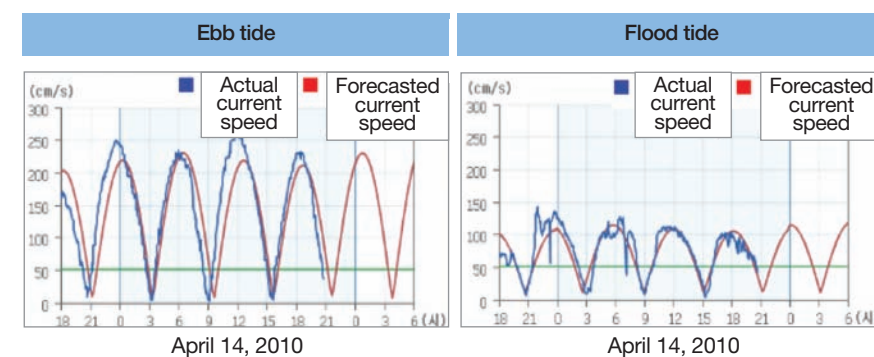
(1) Investigation Method

Analysis on the tidal currents near Baekryong Island utilized 「Military Operational Tidal Movement and Tidal Currents Forecasting System」<sup>36)</sup> jointly developed by ROKN Maritime Tactical Intelligence Group and NORI. NORI verified the forecasting system with actual measurement data from 2 meteorological observation buoys installed in the sinking site to support the search and rescue operation since the sinking of ROKS Cheonan.

The comparison between 「Military operational tidal movement and tidal current forecasting system」 and the actual current speed measurement of data of buoys confirmed that the first one serves as a credible numeric model.



<Figure III-7-9> Locations of observation buoys of the NORI near Baekryong Island



<Figure III-7-10> Comparison between 「Military Operational tidal movement and tidal current forecasting system」 and the actual current speed measurement data of buoys

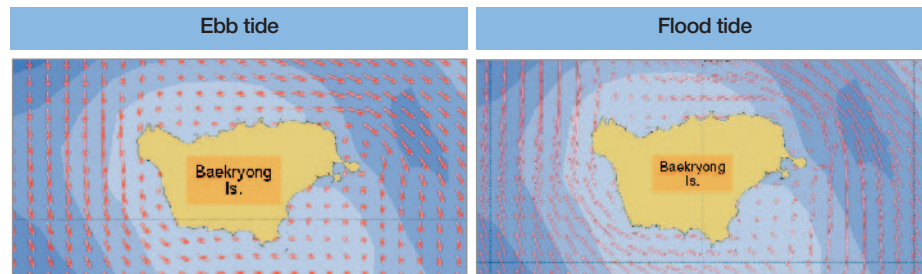
36) 「Military Operational tidal movement and tidal currents forecasting system」 is digital forecasting program that exactly forecasts flood and ebb tide and current. It was developed in and has been operating since 2008. It forecasts speed of the current, time of flood and ebb tide by date.

## (2) Investigation Result

### ① Analysis on the Tidal Movement and Currents Near Baekryong Island

#### ⓐ Characteristics

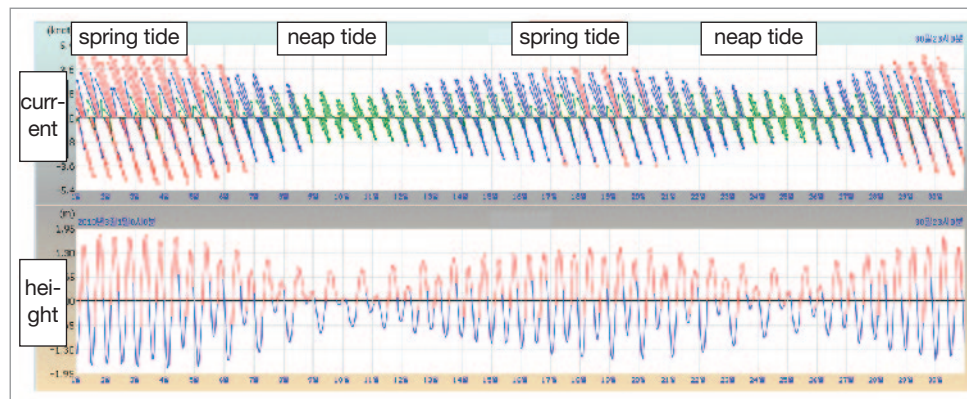
Tidal movement occurs twice a day(ebb and flood tide)<sup>37)</sup>. Generally the tidal current is parallel to the coastline. The flood tide moves to the north, whereas the ebb tide moves to the south. The highest current speed is 5.3kts(the lowest current speed is 0.3kts). The time difference between the ebb and flood tide is 6 hours.



〈Figure III-7-11〉 Tidal current at ebb and flood tide near Baekryong Island

#### ⓑ Tidal Movement and Current in March

Normally, the speed of current in March is between 0.3 ~ 5.3kts and is low at neap tide<sup>38)</sup> and is fast at spring tide<sup>39)</sup>. Tidal difference<sup>40)</sup> at neap tide is 0.3m and spring tide is 3.6m.

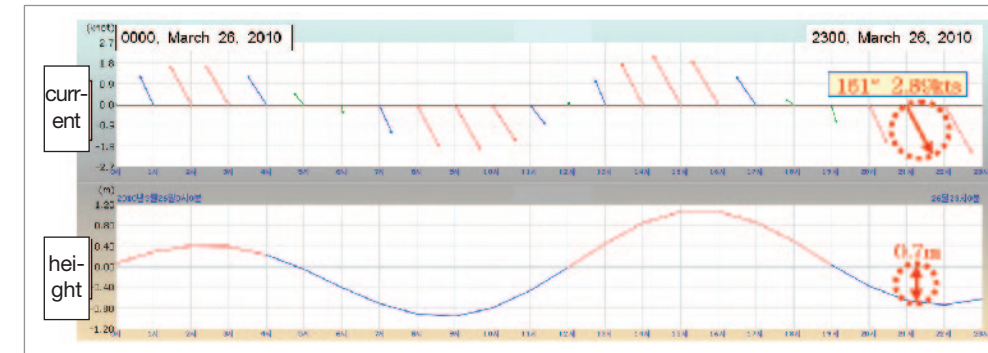


〈Figure III-7-12〉 Tidal current and height in March  
(↖: direction and speed of tidal current, 〰: height of flood and ebb tide)

37) Flood tide is when sea water rises to its highest, and ebb tide is when sea water falls to its lowest level.  
38) Neap tide is when the tidal difference is at its minimum.  
39) Spring tide is when the tidal difference is at its maximum.  
40) Tidal difference is the difference of height between flood tide and ebb tide.

### ⓒ Tidal Current(Direction and Speed) and Movement on the Incident Day(March 26)

Simulation result for the incident day calculated that the direction and speed of the tidal current were 161°-2.89kts and that the height of current was 0.7m(the lowest current is 0.8m) at the time of the incident(2122).

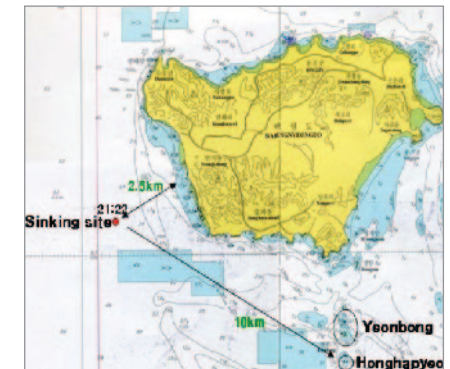


〈Figure III-7-13〉 Tidal current and height on the incident date(March 26)

### ② Effects of the Tidal Current on Maneuvering in ROKS Cheonan's Patrol Area

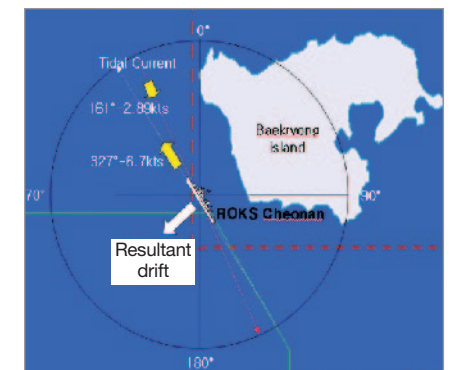
#### ⓐ Conditions

At the time of the incident(2122 March 26), the wind was blowing from southwest at 20kts, the wave height was 2.5m, the visibility was 2.5NM, and the course and speed of ROKS Cheonan was 327°- 6.7 kts.

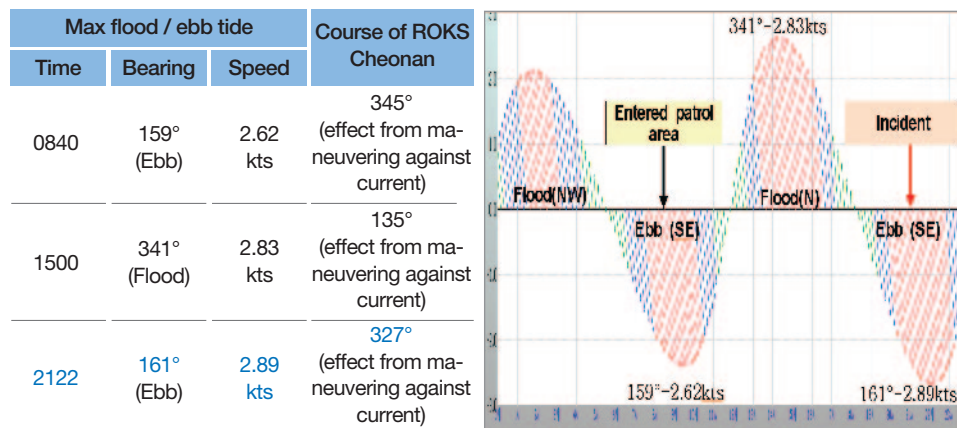


#### ⓑ Simulation Result

At ebb tide(161° - 2.89kts), strong current can push maneuvering ship towards the open sea by some extent. But it was assessed that the maneuvering of ROKS Cheonan experienced no limitation because the speed of ROKS Cheonan(6.7kts) was greater than the speed of the tidal current.



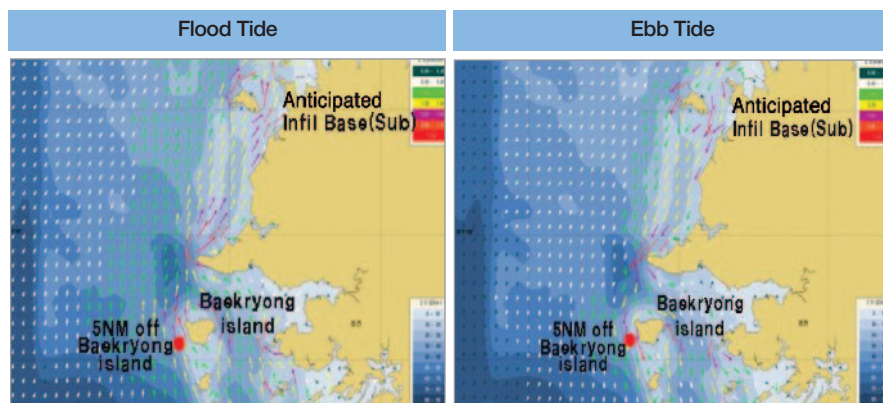
〈Figure III-7-14〉 Maneuvering course of ROKS Cheonan on the incident day(March 26)



〈Figure III-7-15〉 Direction and speed of current on the incident day(March 26)

### ③ Analysis on the Tidal Current between Anticipated North Korea Infiltration Base of North Korean submarine or midget submarine and Baekryong Island

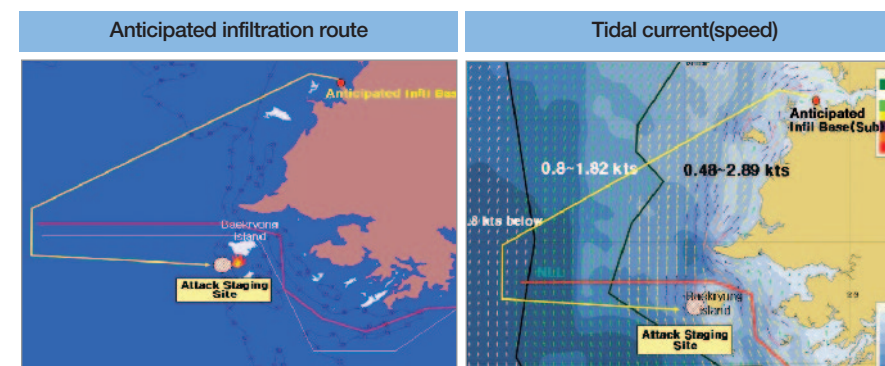
In the region, the tidal current near the coast is fast(0.48~2.89kts) but becomes gradually slower(below 0.83kts) towards the open sea. Attack position, assessed to be 5NM west of Baekryong Island, has currents at 0.22~4.66kts. Therefore, it is assessed that infiltrating and escaping of submarine or midget submarine through the open sea that has less effects of the tidal current rather than along the coastline is advantageous.



〈Figure III-7-16〉 Result of simulation on the tidal current from March 23 until 2120 March 26 between the anticipated infiltration base and Baekryong Island

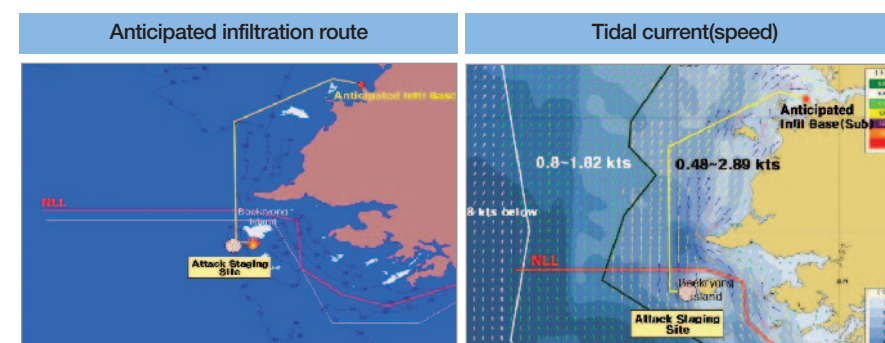
### ④ Effects of the Tidal Current on Maneuvering of North Korean submarine or midget submarine

① Infiltration through the open sea(anticipated North Korea infiltration base → turning point in the open sea → attack staging site near Baekryong Island) would receive relatively less effect from the tidal current because the speed of current near the coastline is 0.48~2.89kts whereas the speed in the open sea is 0.23~1.82kts with average speed of 1.2kts. Given the total infiltration distance(○○○ NM) and infiltration duration(○○ hours), modifying the speed of infiltration according to necessary mode of maneuver(snorkel<sup>41</sup>, submerged) will allow the vessel to overcome the effect of the current.



〈Figure III-7-17〉 Anticipated infiltration route and current speed when submarine or midget submarine from the anticipated North Korea infiltration base infiltrates through the open sea

### ② Infiltration using the shortest route(anticipated North Korea infiltration base →



〈Figure III-7-18〉 Anticipated infiltration route and current speed when submarine or midget submarine from the anticipated North Korea infiltration base infiltrates through the shortest route

41) Snorkel is a mode of submarine or midget submarine maneuvering only exposing snorkel induction mast above the surface in order to charge electric battery.

NLL → attack staging site near Baekryong Island) would receive more effects of current(speed of current 0.48~2.89kts/average speed of current 2.4kts) than when infiltrating through the open sea. Given the total infiltration distance(○ ○ NM) and infiltration duration(○ hours), covert underwater infiltration would be limited due to strong current occurring in opposite direction every 6 hour.

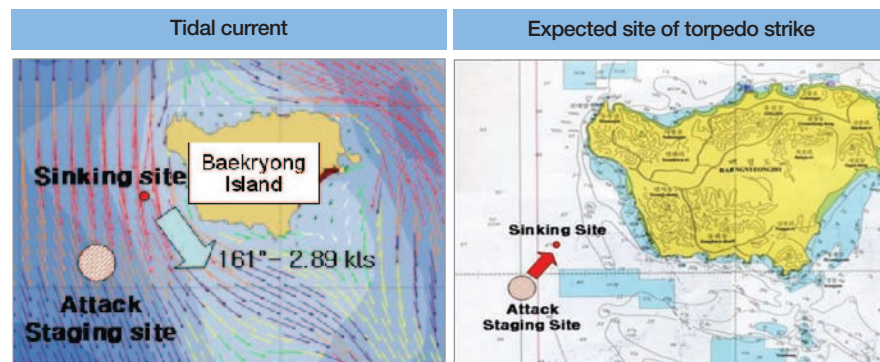
⑤ Effects of tidal current on the employment of North Korean submarine or midget submarine armaments

㉑ Assumptions

North Korean infiltration submarine or midge submarine has weapons to strike ROKS Cheonan at the sinking site, 2.5 km southwest of Baekryong Island.

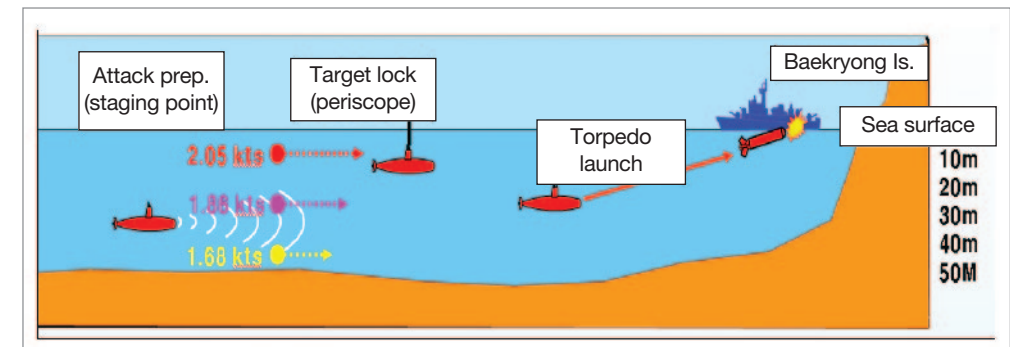
㉒ Effects of Tidal Current on Torpedo Launch

If a North Korean submarine or midget submarine is going to fire a torpedo, in order to conduct a TMA<sup>42)</sup>, it needs a speed of at least 6kts, and at least 5kts for the torpedo to stay on course. In order to minimize the effect of current, the torpedo would need to be fired from deeper than the surface of the sea. However, considering the speed of torpedoes(at least 30kts) and guiding method(acoustic), the current would not have a significant effect on the torpedo.



〈Figure III-7-19〉 Current at time of incident & expected attack staging site

42) TMA(Target Motion Analysis): An analysis of a target's movement(distance, speed) by a submarine for a torpedo launch.

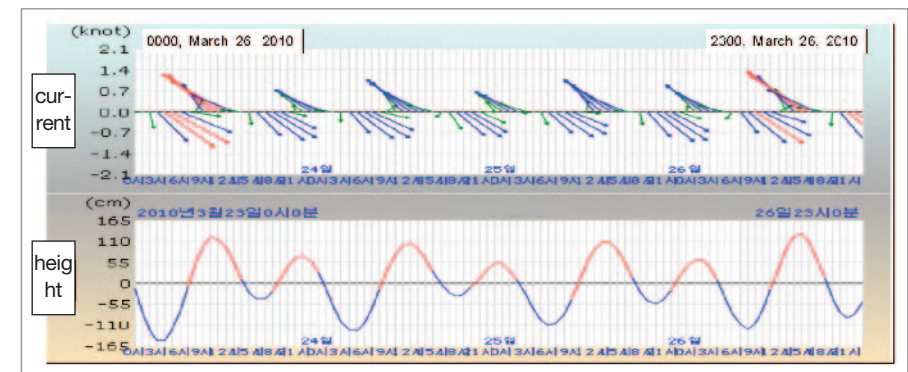


〈Figure III-7-20〉 Current speed at various depths near Baekryong Island and tactics for torpedo employment by North Korean submarine

㉓ Effects of Tidal Current on Mine Laying

In order to lay a mine precisely, a North Korean submarine or midget submarine has to choose the time when the current has the least effect in mine laying, so it is most likely to select slack tide time or favorable tide to lay the mine. Considering the expected arrival date of the submarine or midget submarine(before March 26) in the vicinity of Baekryong Island and the current direction and speed at the time of the incident(approx. 2122)<sup>43)</sup>, the expected course of

	March 23	March 24	March 25	March 26
Current direction & speed (Time)	220°-0.10kts (0100)	222°-0.10kts (0220)	217°-0.12kts (0400)	260°-0.14kts (0520)
	225°-0.11kts (1400)	231°-0.17kts (1530)	219°-0.18kts (1700)	253°-0.19kts (1800)



〈Figure III-7-21〉 Current direction & speed at slack tide during March 23~26

43) The current at the time of the incident on March 26 was 161°-2.89kts.

mine laying would be 161°~ 253°. However, in case of mine laying, it would have to maneuver at low speed of about 3kts, so the current would have severely affected the laying.

### (3) Sub-conclusion

The current near Baekryong Island is considerably strong(max 5.3kts); however at the time of the sinking incident(2122 March 26), the current through detailed simulation was 161°- 2.89kts(charter current 142°- 2kts). Although how much the current affects the maneuver of ROKS Cheonan and North Korean submarine or midget submarine may vary depending on different waters, it is believed that North Korean submarine or midget submarine would have overcome the effect the current might have had by altering its speed or mode of maneuvering(snorkel/submerged). Also, if the North Korean submarine or midget submarine used a torpedo, considering the speed(at least 30kts) and guiding method(acoustic), current would not have a significant effect on the torpedo. Employment of sea mines must have been executed operating in a low speed for its precise emplacement, and therefore it would have been heavily affected by currents.

## 8. Propulsion Motor System of Torpedo

The scientific investigation team actively looked for a critical evidence in the early stages of the incident. The Navy search/rescue group played a central role in collecting underwater evidences. Also, 8 ships including a mine searching vessel and rescue boats were committed from the ROK side, the US used USS Salvor, and the KORDI committed Ship Jangmok and Ship Yuhdo in support of collecting underwater evidences. Also, 106 divers(73 from SSU and 33 from EOD) and the robot Haemirae participated in the searching operations. However, Baekryong Island, the incident site, is surrounded by frequent fogs causing limited visibility of 100y~1NM(91m ~ 1.828m), high current of 3~5kts on average, and water 40~50 meters deep. These environmental conditions made the operation more difficult.

Accordingly, not only civilian and military personnel, but also foreign experts were involved in numerous discussions for identifying the effective method for collecting evidences. As a result, the employments of special magnets for collecting magnetic fragments and remains, and dredging ship that conducts indraft and separates muds and sands on the seabed with water pump were suggested along with the application of fishing boats with nets.

However, special magnet was unable to collect non-magnetic fragments and remains, and employment of dredging ship was restricted due to the shallow water depth in the incident area as well as its preparatory period of more than 30 days. The fishing boat with nets could only be utilized in regions with only mud and sand of smooth surface. Therefore, all three options were not expected to make any significant finding.

While searching for other effective and practical collecting methods, the team became aware of a previous case where the ROK Air Force used a special net to collect the remains of a wrecked plane, and hosted a meeting for discussing the method of collecting the remains on April 17 with 3 personnel including the ROKAF Safety Office inspector, CEO of Daepyong Corp., and primary contractor at that time.

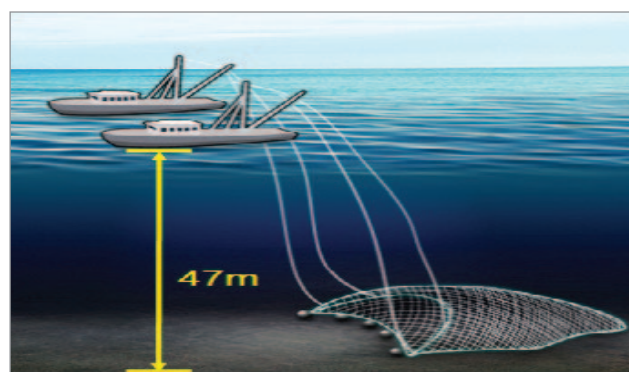
At this meeting, the ROKAF inspector notified that the ROKAF utilized the special net made by Daepyong Corp., and successfully collected in three weeks most of the remains of a F-15 fighter jet that had sunk on June 7, 2006 in East Sea, 372 meters deep, and those of a F-16 sunk on July 20, 2007 in West Sea, 45 meters deep. Therefore, the JIG saw that the special net can be a viable option in collecting the evidence and conducted a thorough review on the subject. As the co-chairmen of the JIG received the approval of the Minister of National Defense on April 18, the JIG began the underwater evidence collection operation using the special net.

### 1) Time sequence

On April 19, representatives from JIG and ROK Navy HQ met with CEO of Daepyong Corp. at ROKN HQ, and signed a contract(Navy construction contract-1327). The operation period was decided to be from April 27 until May 24. The initial operation was to be carried out with 500 × 500yds net with additional contract as required, and all operating personnel were to go under appropriate security measures.

Daepyong Corp. initiated the manufacturing of the special net on April 21 and finished on April 26, one day ahead of schedule. After loading the special net on the ship, the ship departed Busan Port on April 27. Upon arrival in Daechung Island on the dawn of April 30, preparations were made by understanding the underwater terrain and currents near the operation site.

With evidence collection team(13) from JIG deployed on May 1 by a CH-47, the



〈Figure III-8-1〉 Conceptual diagram of the special net and bull trawler

stones weighing over 300kg, 70kg of gravel, 30kg of shellfish, 4 sandbags were collected as results of two test runs of the special net twice outside the core area on May 3. However the geography of seabed consisted of more gravels and bedrocks than anticipated, causing severe damaging to the special net. Therefore, on May 4, the JIG entered Pyeongtaek port where the net was rewoven and strengthened with 14mm wires, and two reserve sets of the net were picked up. The team departed Pyeongtaek port on the 6th and arrived at Baekryong Island site on the 7th.

The ROK Joint Chiefs of Staff directed to “utilize the special net after salvaging massive objects such as the gas turbine in the operational area” thus putting off the usage of the net; however, on May 9, the 5-inch rope of the sea crane used by ROKS Gwangyang broke while salvaging the object later identified as the gas turbine. The ROK Navy proposed to the ROK JCS to contract a civilian company<sup>44)</sup> for another sea crane. These circumstances(including preparation and transportation period) delayed the process as the company was planned to arrive at the site on May 17; thus, SAR Group proposed to JCS to start special net operations earlier than planned. After approval of this proposal, the collection operation using the special net began at 1800 on May 10.

The multinational investigation personnel(USA 4, Sweden 1, England 2) visited the seabed evidence collection site, where a special net was applied on the operation, during 1300~1800 on May 14. After conducting an inspection on the site boarding a helicopter, they moved to segregated collection area of Battalion(ROKMC), the place where all the collected materials from the seabed were categorized and evidences were selected. Later,

44) Yusung Underwater Development, which salvaged the stern side and whose ship Yusung can salvage up to 150t

they embarked RIB at Jangchon pier and transferred to the bull trawlers to observe the evidence collection site. Through those above, the multinational investigation personnel could verify the procedure and method of seabed evidence collection which utilized a special net.

## 2) Procedures for Collection and Gathering

Concerning the specifications of the special net, the dimensions were 60m × 25m × 15m, the size of the mesh was 5mm by 5mm<sup>45)</sup>, and the weight was 5 tons. Objects, sand, and mud larger than 1mm could be collected with the net. The net was operated by two 135-ton ships(Daepyong 11 and 12) and 500 × 500yds operational area was set up centering on the point of explosion and was divided into 25 blocks(20 × 20yds). Daily areas of operation were set up accordingly to make sure no area was missed. In particular, it was assessed that it would be difficult to locate the special net under strong current using the fish detectors on the ships, and thus a minesweeper was used to support the operation.

Concerning the procedures for the collection of the objects and gathering the evidences, two ships cast the net under the sea while moving in the speed of 2~4kts, then after collecting the objects on the seabed the net was pulled, after which JIG Collection Team, UDT control personnel, and the crew of Daepyong 11 and 12 conducted a preliminary classification

Date	# of Operations (AM/PM)	Collected Objects	Gathered Evidences
May 10(Mon)	0 / 3	Rocks, etc.	2, including soil under seat cover
May 11(Tue)	3 / 2	7, including guidance deception device	7, including aluminum pieces
May 12(Wed)	3 / 4	1 x iron structure	4, including asbestos pieces
May 13(Thu)	3 / 5	24, including cook stove	1 x metal piece from stokehold floor
May 14(Fri)	3 / 3	17, including laminated blueprint	2, including metal piece from stokehold dashboard
May 15(Sat)	1 / 4	35, including PC	7, including torpedo propulsion device
May 16(Sun)	5 / 0	14, including pipe switch	
May 19(Wed)	4 / 0	3, including military binoculars	

〈Table III-8-1〉 Recovery and collection status applying special net

45) The special net was manufactured in a sack shape. Not the overall net mesh was composed with 5mm density but only the end part; in underwater, the density is reduced to 1mm due to tensile force created after casting.

on the deck. Then the objects were transported to a port(Jangchonri Port) via RIB and in turn to the collection site set up at Battalion, Marine Corps 6th Brigade via vehicle(military vehicle 5/4t) stationed in Baekryong Island. At the collection site, the objects were classified in further detail using hands and metal(mine) detector, after which JIG Collection Team gathered objects that were considered as evidence<sup>46)</sup>.

### 3) Collection of Torpedo Propulsion Device

Despite the risks involved due to weather conditions such as wave height above 2m, wind speed above 20kts, and limitations on visibility, the operation was conducted at X-axis 8, 10, and 11 from incident site in range of 3 to 8 times a day from May 10, in order to secure successful outcome.

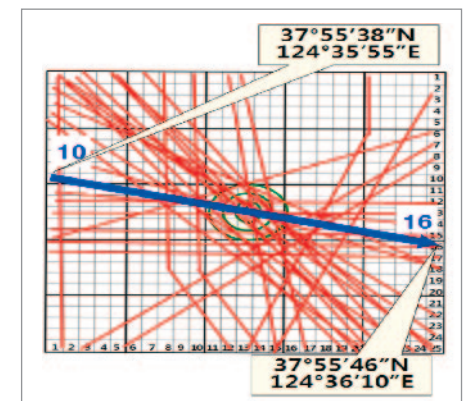
Date	Weather condition	Operation	Operation
4.30(Fri)	Wave height 1.5m, visibility 3NM	Arrival	Coord. discussion(1400)
5. 1(Sat)	Wave height 1.5m, visibility 3NM	X	On-site visit, preparation
5. 2(Sun)	Wave height 2m, visibility 3NM	O	Experimental employment(2)
5. 3(Mon)	Wave height 2m, wind 25kts, visibility 3NM	O	Experimental employment(net damage)
5. 4(Tue)	Wave height 1.5m, visibility 100y	X	Return to Pyeongtaek for net repair
5. 5(Wed)	Wave height 2m, wind 30kts,visibility 50y	X	Net repair
5. 6(Thu)	Wave height 3m,wind 30kts,visibility 1NM	X	Additional net loading, depart(1800)
5. 7(Fri)	Wave height 2m,wind 30kts,visibility 3NM	X	Returned to Baekryong Island(0800)
5. 8(Sat)	Wave height 1.5m, visibility 5NM	X	Standby for gas turbine recovery
5. 9(Sun)	Wave height 1m, visibility 7NM	X	Failed to recover gas turbine
5.10(Mon)	Wave height 1.5m, visibility 3NM	O(3)	Ops. began(JCS instruction)
5.11(Tue)	Wave height 1.5m, visibility 5NM	O(5)	
5.12(Wed)	Wave height 1.5m, visibility 3NM	O(7)	
5.13(Thu)	Wave height 1.5m, visibility 4NM	O(8)	
5.14(Fri)	Wave height 1.5m, visibility 5NM	O(6)	
5.15(Sat)	Wave height 1m, visibility 5NM	O(5)	Propulsion device recovered
5.16(Sun)	Wave height 1m, visibility 5NM	O(5)	

46) For large objects that cannot be transported via RIB, a Navy ship was used to transport directly to 2nd Fleet Command.

Date	Weather condition	Operation	Operation
5.17(Mon)	Wave height 1m, visibility 5NM	X	Standby for gas turbine recovery
5.18(Tue)	Wave height 1.5m, visibility 1NM	X	Adverse weathe
5.19(Wed)	Wave height 1.5m, visibility 100y	O(4)	
5.20(Thu)	Wave height 1~1.5m, visibility 3NM	Departure	
<b>Total</b>	<b>3 test runs in 2 days, 43 operations in 8 days</b>		

〈Table III-8-2〉 Recovery Operation status applying special net

The seabed evidence collection team boarded the bull trawler which was embarked near the Jangchon pier in Baekryong Island around 0750 hours on May 15<sup>47)</sup>, left the pier and started the operation from the Y-axis block 10 as seen in 〈Figure III-8-2〉. From that, the ship maneuvered to the block 16 and started the 30th round of the operation, which ended around 0923 hours, and started salvaging the collected objects using the Daepyong No. 11.



〈Figure III-8-2〉 Propulsion device location

Around 0925 hours, a crew member of Daepyong No.11 told a JIG investigator (MSG<sup>48)</sup>) that “there is a strange object in the net”, and investigators and crew members confirmed that the object was a material with two propellers. The Navy search and salvage leader who came aboard at 0930, and the UDT Squadron Commander, CDR, were there to double check. With the measurements during on-site examination of the overall length of the propulsion device that included the propeller width, blade length, and other parts sizes, and after photographs of each part were taken by an investigator of the JIG at 0931, the recovery of the propulsion device was reported to the JIG HQ at 0936. Afterwards, a bulk of copper considered to be the motor was addi-

47) Daepyong 11, 17 crew: The Navy search and salvage leader, UDT Squadron Commander, Chief Steering Officer, 2 JIG investigators, captain and 11 crews

Daepyong 12, 15 crew: UDT(LCDR), steering(SCPO), JIG investigator(SCPO, CPO), Captain, and crew

48) MSG had previously witnessed a torpedo while visiting a military acquisition company(LIG Nexone) who, based on that memory, assessed the evidence to be a torpedo.

tionally recovered at 0938 which was assessed to be associated with the torpedo, and the JIG took photographs and conducted size measurements of the object. Search and Rescue Group Commander, and 5 personnel arrived at the scene at 0940 and verified the evidence.

The JIG Evidence Collection Team leader and 2 other members arrived at 0950, verified the evidences, and conducted a precise evidence collection on the site at 0955<sup>49)</sup>. At 1005, the JIG requested some blankets for packaging the evidence at ROKS Sunginbong, and used the blankets to do the initial packaging at 1015, the secondary packaging using vinyl tents, tying it up with rope, and at 1023 the JIG collection team leader and 2 others, and 4 people who packaged the evidence used RIBs to transport the evidence to Port Jangchon at Baekryong Island.

An Air Force helicopter at the 6th Brigade(ROKMC) helipad was used to transport them to Pyeongtaek; the helicopter arrived at the 2nd Fleet helipad at 1320. The evidences were moved to the JIG office at the 2nd Fleet, where security measures such as entrance/exit restrictions were taken into effect, after which the JIG Military chairman and the Scientific Investigation Team leader verified the evidence at 1400, and conducted precision analyses from 1500~1630.

During 0900~1000 May 17, four foreign investigation representatives(US Naval Captain Mark Thomas, Australia Naval Commander Powell, Sweden Agne Widholm, UK David Manley), torpedo experts from the Multinational Combined Intelligence TF, and ADD(Alexander Kathy and Dr. Lee respectively), Chief of the scientific investigation division, and Chief of general management team convened and had a joint discussion regarding the recovered torpedo propulsion device.

The recovery and evidence selection procedure of the torpedo propulsion device is shown in <Figure III-8-3>.



① Cast the special net

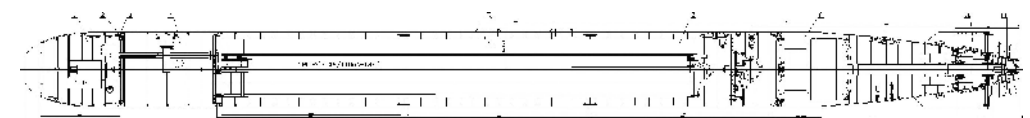
② Salvage collected objects



<Figure III-8-3> Recovery and collection of the evidence

#### 4) Analysis Results

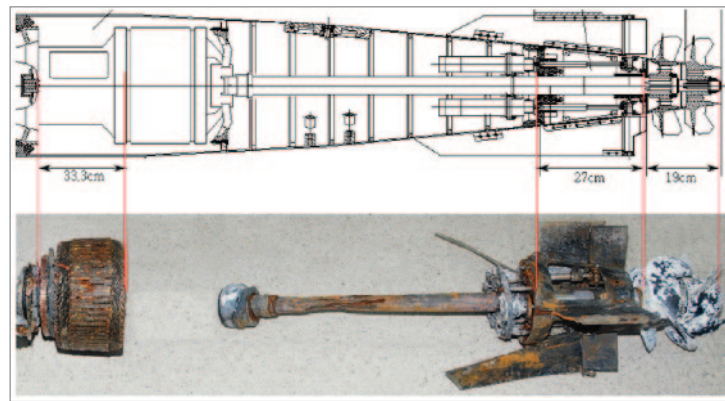
The conclusive evidence is a propulsion device of a torpedo and consists of steering device(71.1kg) and propulsion motor(81.85kg). The steering device is composed of the shaft, propeller, and aft section that contains 4 fins, each of which had stabilizer in the anterior and rudder in the posterior. To determine what model of torpedo this evidence belongs to, many models of torpedoes from different countries were analyzed. As a result it was confirmed that it resembles North Korean CHT-02D torpedo manufactured for exportation, and the JIG obtained the blueprint and conducted the analysis.



<Figure III-8-4> Blueprint of CHT-02D

49) CPO filmed the videos and photographs of the torpedo propulsion section, and the site vicinity, and re-did the measurements.

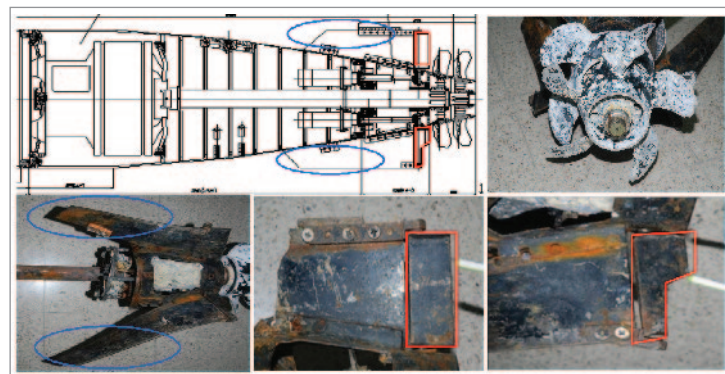
The JIG received the image of CHT-02D torpedo from Intelligence Analysis Team and obtained the length of each part after magnifying the image over 10 times in order to confirm the consistency with the evidence. Also, upon investigation of the inscriptions resembling Japanese character on the blueprint, the JIG concluded that it did not make any sense in Japanese and appeared in the process of reading and printing the North Korean computer font with ROK computers and printers. It was confirmed that the blueprint pre-printed by North Korea has Korean on it.



〈Figure III-8-5〉 Size comparison between the blueprint of CHT-02D and the evidence

As shown in 〈Figure III-8-5〉, the length from the propeller to the shaft is: 112cm, propeller: 19cm, the rear: 27cm, propulsion motor: 33.3cm, upper stabilizer: 33cm, and the lower stabilizer was 45cm. All of these coincided with the data from the blueprint.

For the shape of the evidence, the contra-rotating propeller has 5 blades, the slanted stabilizer, the rectangular upper rudder, and the P-shaped lower rudder, all of which were the same as the blueprint. The lower stabilizer contained 9 supporting holes while the lower



〈Figure III-8-6〉 Shape comparison between the blueprint of CHT-02D and the evidence

rudder had 2, which also coincided with the blueprint.

Also, as a result of conducting an analysis on the white adhered material from the propeller part, aluminum oxide, carbon (partially graphite), and aluminum powder were detected, which later turned out to be identical with the adhered material on ROKS Cheonan hull and stack.

Additionally, at 0925 on May 15, the scientific investigation team found the Korean marking (1번 or No. 1 in English) inside the end of the propulsion part. This was not initially found when examined aboard the recovery ship due to the lack of a precise examination. However, it was found when being observed after having been transported by a helicopter to 2nd ROK Fleet (Pyeongtaek), where the civilian-military JIG is located.

Also, it was acknowledged that the Korean marking '1번 (No. 1 in English)' found on the end of propulsion part is similar to that found on the inside of the head cap of a light weight torpedo collected off Pohang in 2003, which says '4호 (Unit 4 in English)'<sup>50)</sup> and the JIG considered conducting handwriting analysis. Even though it was limited by the difference in the markings themselves (they were made of different vowels and consonants), as the composition analysis of the ink of the marking was conducted, it was confirmed that the marking '1번' was written before the corrosion since salt was precipitated on the marking and corroded interior steel was found to be risen above the ink.



〈Figure III-8-7〉 The Korean inscriptions on torpedo propulsion motor and North Korean light torpedo

50) According to the "North Korean Dictionary of Korean", North Korea uses both '호(unit)' and '번(no.)'. According to statements made by North Korean defectors, North Korea uses '번(no.)' to indicate order, and '호(unit)' to distinguish different types of objects. In locations where order is necessary such as a distribution office or a bus stop, the '번' is used. For other objects, depending on their user, or type of object, such as 'Resort Unit 1' and 'Unit 15 Concentration Camp', and 'Unit 10', the '호(unit)' is used, and when two different types of missiles are being produced in a factory, the missiles are distinguished by using the letters 'Unit 1' or 'Unit 2'. Among the same type of missiles, the missiles are differentiated by using 'No.', for instance in 'No.1' or 'No.2'

No explosive was detected on the torpedo parts, and the propeller was made of an aluminum alloy (Aluminum 86%, Silicon 14%) while the fixed wings were made of iron(Fe).

In addition, samples were collected from the bow and stern breakplanes in order to analyze the degree of corrosion that had occurred both on the torpedo propulsion section and the hull of ROKS Cheonan. Seoul National University(Prof. Kwon Dong-il), Kangneung Wonju University(Prof. Choi Byung-hak), and the National Institute of Scientific Investigation(Dr. Kim Ui-su), conducted joint visual analysis of the evidence. They found that the torpedo propulsion section iron portions(rudder) and ROKS Cheonan hull metal fragments' degrees of corrosion were similar.

The '1번' markings had not evaporated or discolored despite exposure to high temperatures of over 150°C, but were left clear blue. To determine the reason for this, the JIG used a spectrometer to conduct precision analysis of the rear propulsion section where the marking was located, as a result of which it was found that a type of anti-corrosive paint was used upon the stainless steel(polyvinyl butyral)<sup>51)</sup>. This incident was a non-contact underwater explosion at 3°C water temperature, and the torpedo consisted of the target detection section(70cm), the warhead section(72cm), the battery section(4.125m), and the propulsion section(1.805m). Therefore, even if the explosion had occurred at the warhead section(72cm), the battery section which is 4.125m long would have provided a shock absorber. Also, The portion with the '1번' markings in the propulsion aft section was protected by a maintenance cover; it was filled up with seawater at the time of launch; and a gas bubble of 6m in diameter was created during the explosion of 250kg charge weight, pushing the propulsion section backwards 30~40m. Given these facts, the high heat would not have damaged the surface of the propulsion aft section and the ink(where the anti-corrosive paint had been applied), leaving the markings in its original state and clear condition.

Related to this matter, an expert in the field of thermodynamics from KAIST, professor Tae-ho Song, conducted a study on the changes of the temperature in case of an underwater explosion caused by a torpedo. His findings were that the flame of 3,000°C caused by the explosion cools down to normal temperature(28°C) within 0.1 second due to adiabatic expansion, and that although the flame may raise the disk temperature 2~3°C above the water temperature(3°C) in the process, heat transfer would not occur all the way to the

51) Polyvinyl butyral is a high-polymer substance, which is applied to prevent rusting on metals, glass, and ceramics, and is comprised of Al, Mg, Si, Ti, P, and Zn.

rear, and thus no significant change in temperature would have resulted in the area where the marking '1번'(No. 1 in English) is written. Also, professor Song suggested that even under harsher conditions, no part of the propulsion motor is heated above 20°C and thus the marking on the rear cannot receive heat damage. Through such results, professor Song explicated the scientific reason for the marking '1번'(No. 1 in English) to remain intact.

Comparison analysis between five marker ink samples made in China was conducted to determine the source of the '1번' ink. The ingredients for the paint was analyzed at the KIST Characteristic Analysis Center, where precise analysis of the ingredients was conducted; however, since many countries use the same type of ingredients to produce paint, the JIG was unable to identify the country in which it was produced.

### 5) Sub-conclusion

The facts that the evidence, the propulsion device of torpedo, matches in size and shape with the blueprint of North Korean CHT-02D torpedo with Korean alphabet('1번' : No.1) marked on it, and that the inventory inspection on ROKN underwater weapons resulted with no missing assets, indicate that the propulsion device of torpedo collected near the origin of explosion is the remains of CHT-02D torpedo manufactured in North Korea. This confirms the assessment that ROKS Cheonan was sunk by the explosion of a North Korean CHT-02D torpedo.



Diameter	21 inches(53.4cm)	Length	7.35m
Explosive	250kg	Weight	1,700kg±10kg
Cruising distance	10~15km	Homing method	Sonic track · manual

〈Figure III-8-8〉 CHT-02D Torpedo

Part IV

# *Conclusion*



ROKS Cheonan was sunk by a **North Korean** torpedo attack while conducting its normal mission in vicinity of Baekryong Island at 2122 hours on March 26, 2010. Immediately following the sinking of the ship, the ROK military conducted a surface, coastal and underwater search until April 3, and transitioned from a personnel recovery operation to a salvaging operation on April 4.

The salvage and transportation of the separated bow and stern section were completed on April 25. During the salvage of the ship, 40 bodies were recovered as well. Following the salvage of the ship, emphasis was placed on search operations and a detailed search was conducted focusing on the areas where the likelihood of collecting debris was assessed to be the highest. A detailed search of the seabed using special nets commenced on May 10 and parts of a torpedo propulsion section, including a propulsion motor and propellers, were recovered on May 15.

The analysis on the cause of the sinking initially left open every possibility and explored the possibilities of a non-explosion, internal explosion or external explosion for causing the sinking. However, a detailed investigation following the salvage of the ship eliminated the possibilities of a non-explosion and internal explosion, leading the JIG to assess that an external explosion, and more specifically an underwater explosion, was the most likely cause behind the sinking. The possibility of a non-contact torpedo generating an underwater explosion was assessed to have the highest likelihood and the possibility of a moored mine was not ruled out despite its low likelihood.

The basis of our assessment that a torpedo attack caused the sinking is as follows:

**First**, precise measurement and analysis of the damaged hull showed that a shock-wave and bubble effect caused significant upward bending of the Center Vertical Keel compared to its original state. The shell plating was steeply bent with parts of the ship fragmented. On the main deck, fractures occurred along the large openings used for the maintenance of equipment in the gas turbine room and the portside was deformed significantly in an upward direction. The bulkhead of the gas turbine room was significantly damaged and deformed. The upward bending of the bottom of the stern and bow proves that an underwater explosion occurred.

**Second**, a thorough investigation of the interior and exterior of the ship found evi-

dence of extreme pressure on the fin stabilizer(which prevents significant rolling of the ship); traces of high water pressure and bubble effect on the bottom of the hull; and wires cut with no traces of heat; and traces of spherical pressure on the gas turbine room. The above indicate that a strong shockwave and bubble effect caused the splitting and sinking of the ship.

**Third**, the JIG analyzed statements made by survivors that they heard a near simultaneous explosion once or twice and water was splashed on the face of the port lookout who fell from the impact. Furthermore, the statements were made by coastal sentries on Baekryong Island that they saw a 100-meter high pillar of white flash for 2~3 seconds. The analysis of these testimonies indicated that the aforementioned phenomena are consistent with the occurrence of a water plume resulting from a shockwave and bubble effect. Also, no traces of fragmentation or burn injury were found from our examination of the wounded survivors and the deceased service members, while fractures and lacerations were observed. These observations are consistent with phenomena resulting from a shockwave and bubble effect.

**Fourth**, the seismic and air acoustic wave analysis conducted by the Korea Institute of Geoscience and Mineral Resources(KIGAM) showed the following. A seismic wave of magnitude 1.5 was detected at 4 stations. Two air acoustic waves with a 1.1 second interval were detected at 11 stations. The seismic and air acoustic waves originated from an identical site of explosion. All these are consistent with the phenomena that arise from a shockwave and bubble effect produced by an underwater explosion.

**Fifth**, the 1st analysis result by US team, from the hull deformation showed that the possible explosion type is an explosion of TNT equivalent of 200~300kg charge size at a point of 3m to the port from the central bottom of the gas turbine room, and at a depth of 6~9m. 2nd analysis result on simulation, by the ROK, resulted in the identical location, with TNT equivalent 250~360kg charge size. The efforts on this was also supported by the UK Investigation Team.

**Sixth**, based on the analysis of tidal currents in the vicinity of Baekryong Island, the

JIG determined that although the currents would have had a minimal influence on the launch of a torpedo, they were strong enough to limit the emplacement of mines.

**Seventh**, analysis of the explosive residue found HMX from 28 locations including the stack and fractured surface; RDX from 6 locations including the stack and seabed; and traces of TNT from 2 locations including the fin stabilizer. Based on this analysis, the use of an explosive compound containing HMX, RDX, and TNT was confirmed.

**Lastly**, on May 15, 2010, the JIG recovered conclusive evidence that confirmed the use of a torpedo while conducting a detailed search in the vicinity of the incident location using special nets. The conclusive evidence was a torpedo propulsion motor system including propellers, a propulsion motor and steering section. The evidence is consistent in its size and design to the torpedo schematics included in an introductory brochure produced by **North Korea** for export purposes.

A composition analysis of the adhered materials from ROKS Cheonan showed that the materials are identical to that found on the rear section of the torpedo. The Korean marking ‘1번(No. 1 in English)’ inside the rear section of the propulsion system is also consistent with the marking of a **North Korea** test torpedo obtained in 2003. The above evidence confirm that the recovered torpedo parts were manufactured by **North Korea**.

In conclusion, taking the entirety of the analysis results of the CIV-MIL Joint Investigation Group and Multinational Combined Intelligence TF on the following factors into consideration – the torpedo propulsion system recovered from the incident location, deformation of the hull, statements by related personnel, medical examination of the deceased and wounded service members, seismic and infrasound waves, simulations of underwater explosions, tidal currents in vicinity of Baekryong Island, analysis of explosive components, recovered torpedo parts, and the identification of the perpetrator – the JIG and MCITF concluded the following:

**ROKS Cheonan was split and sunk due to shockwave and bubble effect generated by the underwater explosion of a torpedo. The detonation location was 3m to port from the center of the gas turbine room and at a depth of 6~9m. The weapon sys-**

**tem used was a CHT-02D torpedo with approximately 250kg of explosives manufactured and used by **North Korea**.**

# *Appendix*

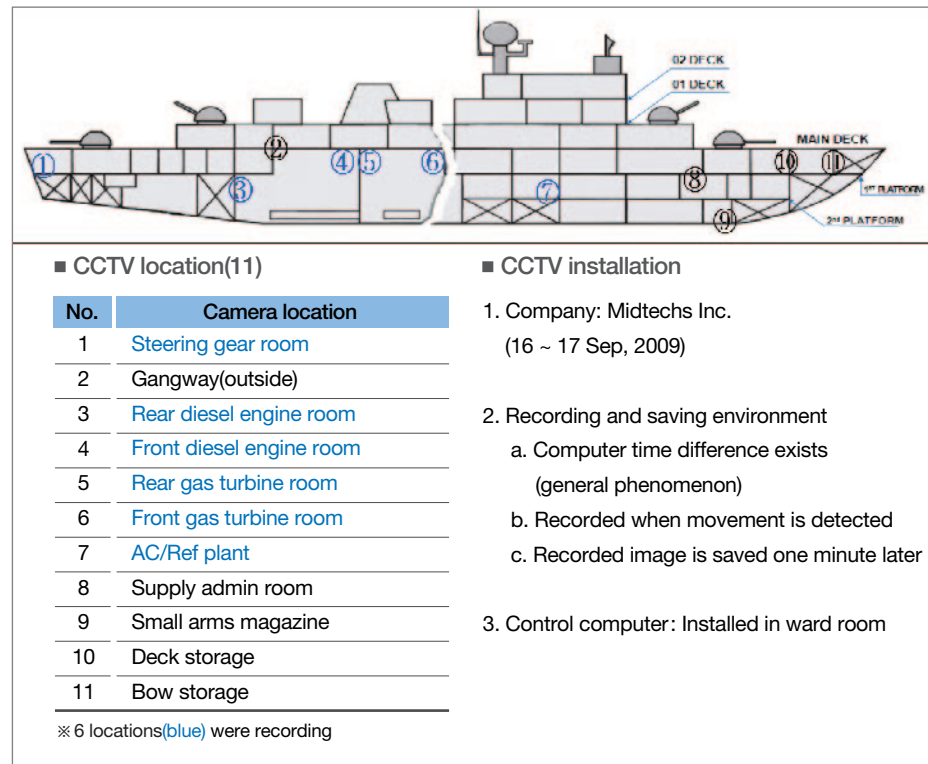
- I. CCTV Recovery and Analysis Result
- II. Underwater Explosion Phenomenon
- III. Analysis Result on Direction and Location of the Explosion
- IV. Analysis Result on Charge Size and Depth
- V. Analysis Result on Adhered Materials
- VI. Stability Analysis Result
- VII. Basic Hull Strength Analysis Result



## Appendix I. CCTV Recovery and Analysis Result

### 1. Overview

In order to facilitate the CCTV analysis, the JIG cooperated with the company that installed the CCTV, and identified locations of the control computers(the ward room), number of internal and external locations of the cameras, and CCTV characteristics. On April 24, during the salvage operation for the bow, the JIG quickly recovered the ones located at the gangway and the gas turbine room, since the prioritization was made upon the assessment that these footages with the records from 2100 on the incident day would assist the most in the efforts to determine the cause of the incident. The JIG also made appointments with a contractor(Myung Information Technology in Oh-chang) that would be responsible for the hard disk recovery process.



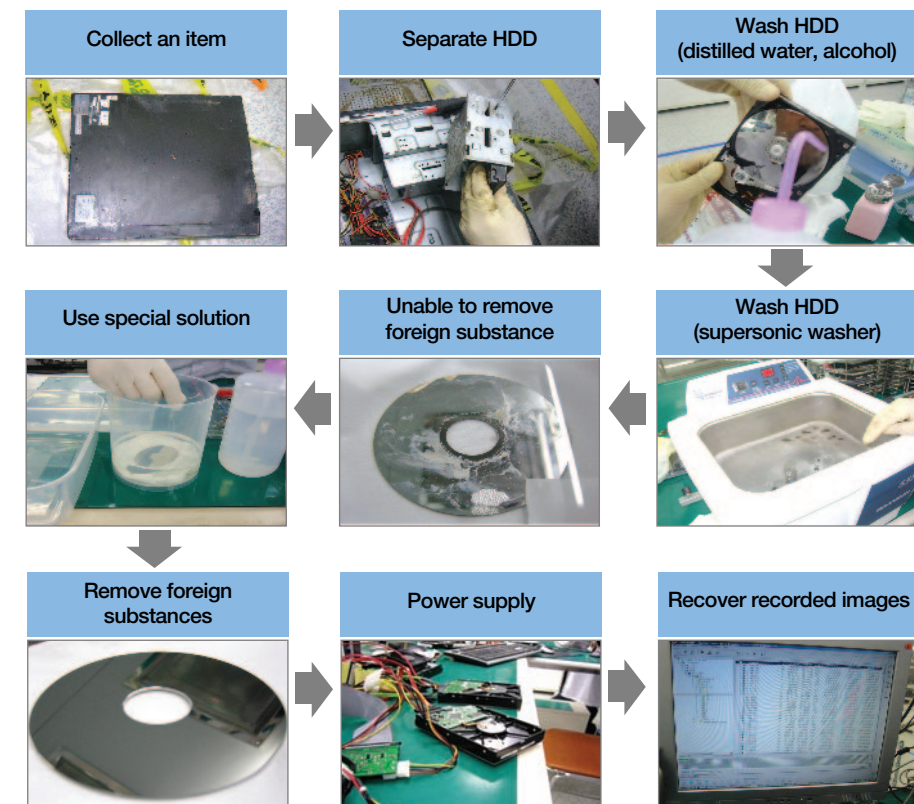
〈Figure Appendix I-1-1〉 ROKS Cheonan CCTV location

### 2. Procedure of CCTV Recovery Operation

The CCTV recovery operation was hampered due to oil, mud, and other foreign substances that were attached to the hard drive for over a month. Through the spraying of pure alcohol, distilled water and thinners along with ultrasound waves(these are the most effective means for success) for 6 days, the JIG made repeated attempts to remove these substances; however, the attached foreign substances could not be completely removed.

Therefore, a group of experts discussed whether to partially carve out the hard disk's surface, or to melt down the foreign substances as suggested by the JIG analysis team. They assessed that the latter course of action would have a better chance for success, and decided to take a careful approach on this matter.

The JIG requested for a composition analysis on the foreign substance to the KCIC scientific investigation lab. The foreign substance was composed of Al, and NaOH was identified.



〈Figure Appendix I-2-1〉 CCTV recovery process

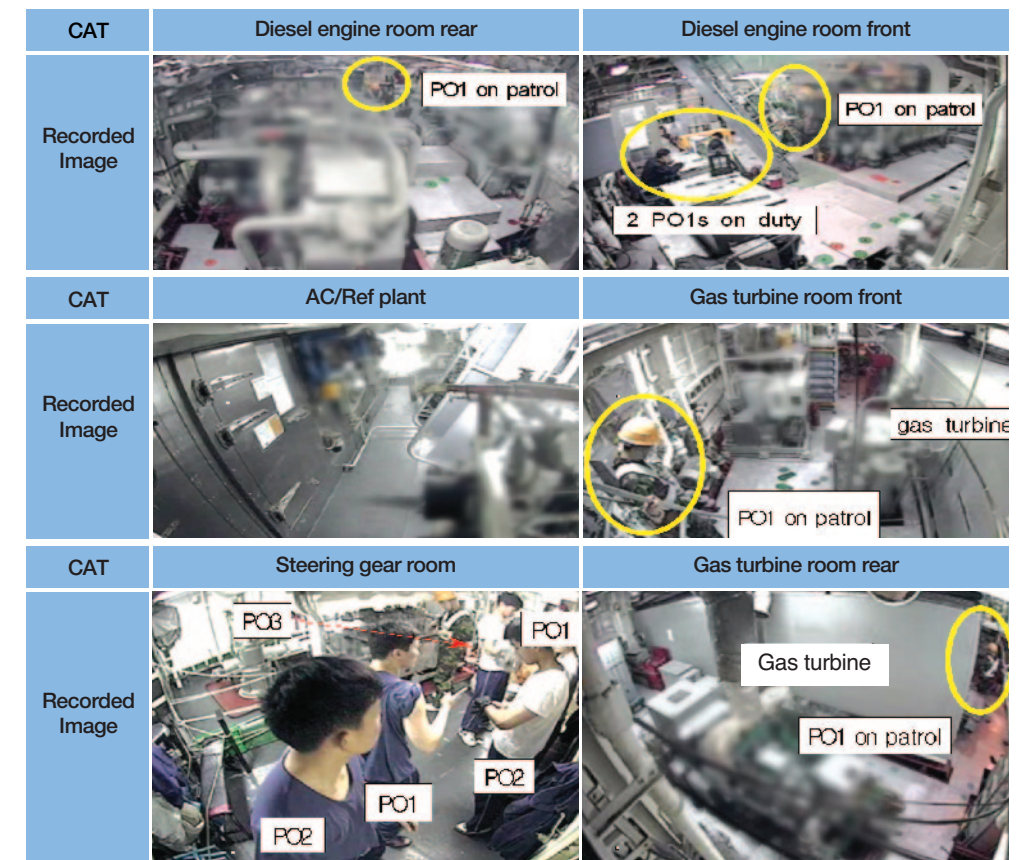
tified as the solution to remove the foreign substances. The melting process took 2 days, and the amount of NaOH solution was increased incrementally to prevent damage to the disk. After dozens of trials, the elimination of the foreign AI from the disk succeeded, and the operation was able to recover partial image of the 6 CCTVs saved in the hard disk, and the image from the other 5 CCTVs were not restored, because there were no movements within the covering area of these CCTVs.

### 3. Recovery Result

Because of the way the settings were set up for ROKS Cheonan's 11 CCTVs, the initially inserted recording time did not get updated, and this resulted in a time difference with the actual time of recording. The CCTV begins recording when movement is detected, and the images are saved 1 minute after the recording. After taking this setting into account as well as the statements from survivors, the analysis showed that the CCTV that recorded the latest time frame was the one that was located in the gas turbine room, and the JIG estimated it to have halted recording at 2121 hours(21:17:03 on the CCTV time).

No.	Installed locations	Contents of image	Time on screen		
			Start	Finish	Duration
1	Diesel engine room rear(stern)	Safety watch PO1 on patrol	21:12:23	21:13:06	43"
2	Diesel engine room front(stern)	① 2 PO1s on duty ② Safety watch PO1 on patrol	21:02:21	21:13:16	10' 55"
3	AC/Ref plant (bow)	Unable to verify movement due to file damage	21:02:40	21:15:50	13' 10"
4	Gas turbine room front(stern)	Safety watch PO1 on patrol	21:15:20	21:16:12	52"
5	Steering gear room (stern)	① 3(PO1, PO2, PO3) working out ② PO2, PO1 entering ③ Safety watch PO1 on patrol	21:02:20	21:17:01	14' 41"
6	Gas turbine room rear(stern)	Safety watch PO1 on patrol	21:02:20	21:17:03	14' 43"
TOT	6 locations	8 moving personnel	21:02:20	21:17:03	TOT: 55' 04"

〈Table Appendix I-3-1〉 CCTV recovered contents



〈Figure Appendix I-3-1〉 CCTV recorded footage

### 4. Analysis Result

From the recovery, the images of the gas turbine room and diesel engine room were confirmed, as well as those of the patrolling of a safety watch, and other crew members exercising in the steering gearing room. Based on the routine circumstances in the observed compartments, outfits and facial expressions of crew members, along with stable sailing status, it was concluded that ROKS Cheonan was on normal operations without any emergency situation such as grounding, until a sudden explosion fractured the hull and caused the sinking.

## Appendix II. Underwater Explosion Phenomenon

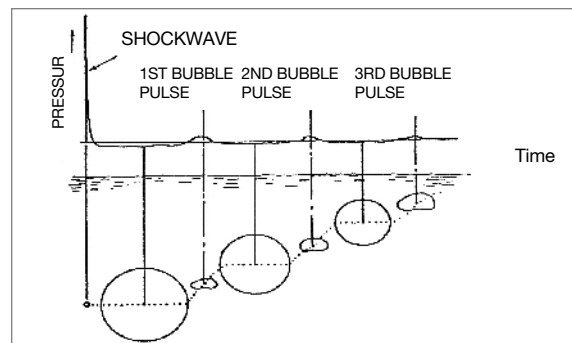
### 1. Physical Aspects of Underwater Explosion<sup>1)</sup>

When an explosive charge is detonated underwater, shockwave of extremely high pressure propagates into water, and spherical bubble of high-temperature(2,000~6,000K) and high-pressure(150~400kbar) detonation products are formed. <Figure Appendix II-1-1> shows the pressure of the shockwave and bubble pulses, and process of bubble oscillation, with respect to time. The shockwave generated by an underwater explosion commences to propagate into surrounding water spherically at a high velocity(~7km/s) initially, and soon it slows down to the level of the sound speed(~1.5km/s) as it moves away from the point of detonation. As the shockwave travels, the peak overpressure( $P_m$ ) decreases and the duration increases. Therefore, the shockwave pressure depends on the type of explosive, charge weight( $W$ ), distance( $R$ ), and time( $t$ ), as follows:

$$P(R, W; t) = P_m(R, W) \exp\left[-\frac{(t-t_0)}{\theta(R, W)}\right] \quad (1)$$

$$P_m(R, W) = K \left(\frac{W^{1/3}}{R}\right)^{\alpha}, \quad \theta(R, W) = W^{1/3} K' \left(\frac{W^{1/3}}{R}\right)^{\alpha'}$$

where  $K, \alpha, K', \alpha'$  are constants having values depending on the types of explosives.



<Figure Appendix II-1-1> Shockwave & bubble pressure-time graph

1) Michael M. Swisdak, "Explosion Effects and Properties : Part II - Explosion Effects in Water", NSWC/WOL TR 76-116, 1978.

As shown in <Figure Appendix II-1-1>, the bubble pulses after the shockwave indicate pressure generated when the gas bubble of detonation products contracts and starts to expand. This bubble process takes place slowly and under relatively low pressure compared to that of the shockwave. Due to high pressure and temperature at the initial stage, the gas bubble pushes water toward outside the spherical surface while expanding. Because of the inertia of the expanding water, the expansion stops after passing the point of pressure equilibrium(hydrostatic pressure at the point of detonation). The bubble at its peak of expansion retains a very low internal pressure of less than about 0.01 atm. Thus, the hydrostatic pressure in the vicinity of the bubble becomes higher than the pressure inside the bubble, and as a result the bubble is forced to contract. Similar to the expansion, the bubble continues to contract even beyond the pressure equilibrium, and the pressure inside the bubble reaches hundreds of atmospheric pressure, much higher than the hydrostatic pressure of the surrounding water. At this moment, the bubble starts to expand again, releasing a pulse of relatively high pressure. While repeating the expansion and contraction, the bubble oscillates. As the bubble pulsation is a very slow process compared with the shockwave propagation, the bubble movement is influenced by gravity, and thus, the bubble jumps toward the water surface when its volume is reduced to its minimum.

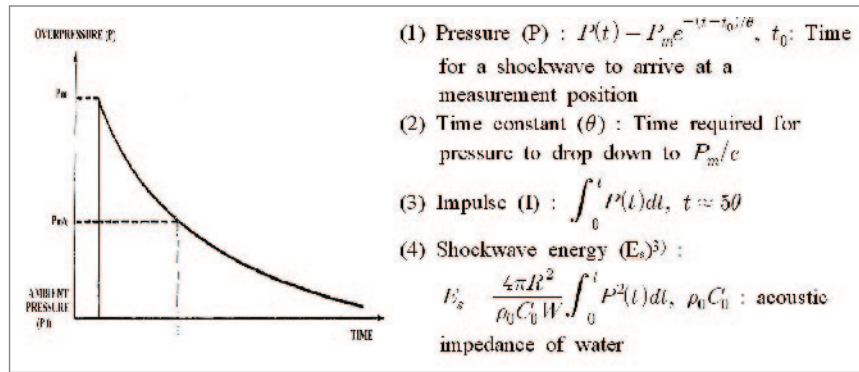
The energy of underwater explosion is partitioned into two parts, the generation and dissipation of the shockwave, and the expansion and contraction of the bubble, as listed in <Table Appendix II-1-1><sup>2)</sup>. That is, the shockwave energy is lost while radiating spherically and propagating in surrounding water, and the bubble energy is spent through interaction with the water, radiation, and bubble pulse. In case of a shallow-depth underwater explosion, it is known that most of the bubble energy is consumed during the first bubble period.

<Figure Appendix II-1-2> is a magnification of <Figure Appendix II-1-1> and shows important parameters for understanding propagation of an underwater shockwave.

Total energy liberated (100%)	Initial shockwave energy(53~54%)
	Energy in first bubble oscillation(46~47%)

<Table Appendix II-1-1> Energy partition of a bulk warhead fired underwater

2) Warren C. Strahle, "Conventional Weapons Underwater Explosions", AD-A201 814, December 1988.



〈Figure Appendix II-1-2〉 Shockwave parameters

Also, in order to compare UNDEX effects for explosive charges other than TNT, it is necessary to define the terminologies, as listed below:

(1) Equal weight ratio (D <sub>wd</sub> )	The ratio of the outputs of a particular parameter(peak overpressure, time constant, impulse, energy) for equal weights of two explosives at the same distance.	
(2) Equal volume ratio (D <sub>vd</sub> )	The ratio of the outputs of a particular parameter(peak overpressure, time constant, impulse, energy) for equal volumes of two explosives at the same distance.	
(3) Equivalent weight ratio (W <sub>wd</sub> )	The ratio of weights of two explosives required to produce the same magnitude of a particular parameter at the same distance.	
(4) Relative bubble energy (RBE)	Cube of the ratio of the first bubble period constants(K's):	$RBE = \left( \frac{K_{experimental}}{K_{reference}} \right)^3$
(5) Relative potential bubble energy(RPBE)	Cube of the ratio of the maximum bubble radius constants(J's):	$RPBE = \left( \frac{J_{experimental}}{J_{reference}} \right)^3$

### 1) Characteristics of an Underwater Shockwave

The parameters, P<sub>m</sub>, θ, I, E<sub>s</sub> which represent the characteristics of shockwave generated by an underwater explosion of a high explosive, depend on the weight(W) of the charge and the distance between the point of the explosion and the measurement location(R), as ex-

3) Robert H. Cole, "Underwater Explosions", Princeton University Press, 1948.

pressed in the following similitude relation<sup>4)</sup>:

$$\text{Shock Parameter} = K \left( \frac{W^{1/3}}{R} \right)^\alpha \quad (2)$$

Where constants determined by the type of the explosive charge, R is distance(m) from the explosive charge, and W indicates weight of the explosive charge(kg). 〈Table Appendix II-1-2〉 lists values of constants in the similitude relation, Equation(2), for various explosives. 〈Table Appendix II-1-3〉 summarizes the Equal Weight Ratios applicable to explosive charges over a weight of 20kg. 〈Figure Appendix II-1-3〉 shows peak overpressure(P<sub>m</sub>) of the shockwave from various charge weights of TNT with respect to dis-

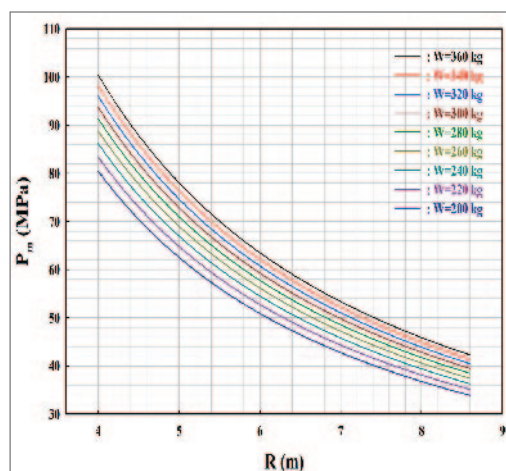
Explosive	Shock parameter		P <sub>m</sub>		θW <sup>1/3</sup>		1/W <sup>1/3</sup>		EW <sup>1/3</sup>		Range of validity (MPa)
	K	α	K	α	K	α	K	α			
TNT	52.4	1.13	0.084	-0.23	5.75	0.89	84.4	2.04	3.4-138		
PENTOLITE	56.5	1.14	0.084	-0.23	5.73	0.91	92.0	2.04	3.4-138		
H-6	59.2	1.19	0.088	-0.28	6.58	0.91	115.3	2.08	10.3-138		
HBX-1	56.7	1.15	0.083	-0.29	6.42	0.85	106.2	2.00	3.4-60		
HBX-1	56.1	1.37	0.088	-0.36	6.15	0.95	107.2	2.26	60-500		
HBX-3	50.3	1.14	0.091	-0.218	6.33	0.90	90.9	2.02	3.4-60		
HBX-3	54.3	1.18	0.091	-0.218	6.70	0.80	114.4	1.97	60-350		

〈Table Appendix II-1-2〉 Shockwave constants for various explosives

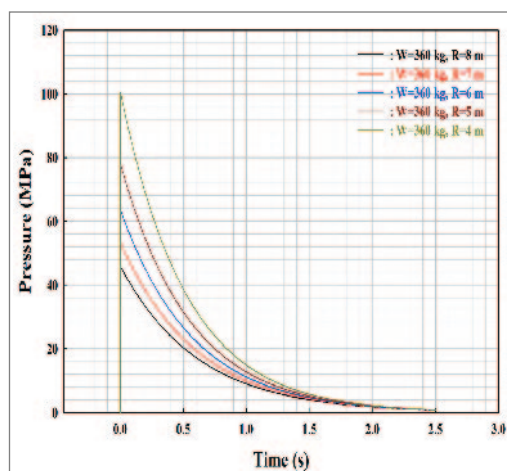
Explosive	Equal weight ratio				Equal weight ratio				(RBE) <sub>TNT</sub>	(RPBE) <sub>TNT</sub>
	D <sub>wd</sub> (relative to HBX-1)				D <sub>wd</sub> (relative to TNT)					
	P <sub>m</sub>	θ	I	E	P <sub>m</sub>	θ	I	E		
HBX-1	1.00	1.00	1.00	1.00	1.08	0.99	1.12	1.26	1.48	1.44
TNT	0.92	1.01	0.90	0.79	1.00	1.00	1.00	1.00	1.00	1.00
HBX-3	0.89	1.10	0.99	0.86	0.96	1.08	1.10	1.08	1.93	1.82
H-6	1.04	1.06	1.02	1.09	1.13	1.05	1.14	1.37	1.69	1.59
PENTOLITE	1.00	1.01	0.89	0.87	1.08	1.00	1.00	1.09	1.00	1.02

〈Table Appendix II-1-3〉 Conversion factors between shockwave and bubble

4) Similitude relation: The relation applied to calculate the shock wave factors such as pressure, time constant, shock amount, and shock energy.



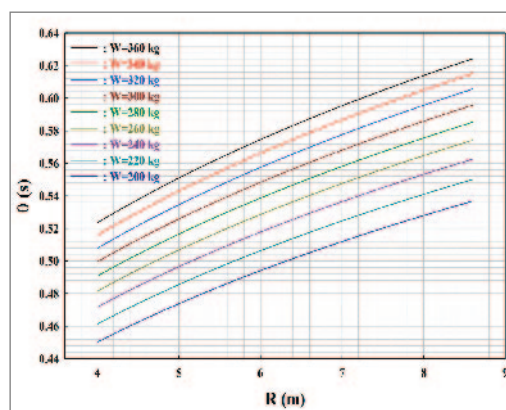
〈Figure Appendix II-1-3〉 Shockwave peak overpressure of various weights of TNT



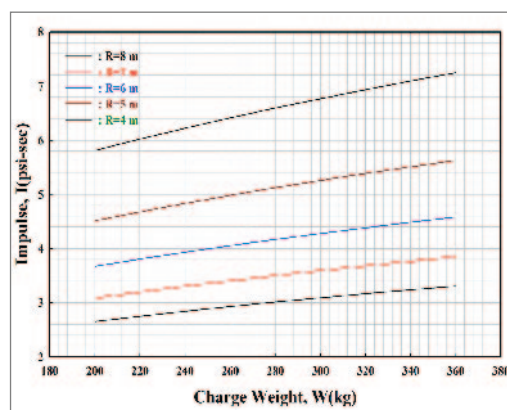
〈Figure Appendix II-1-4〉 Shockwave peak overpressure at several distances from underwater explosion of 250kg TNT

tance(R) from the explosive charge.

In addition, 〈Figure Appendix II-1-4〉 shows the changes in peak overpressure of the shockwave in time at several distances from an underwater explosion of TNT of 250kg. 〈Figure Appendix II-1-5〉 shows the time constant( $\theta$ ) which implies time required for P(t) to fall from Pm to Pm/e. P(t) and  $\theta$  are essential data in calculating the impulse ( $I = \int_0^{\infty} P(t) dt$ ). The shockwave impulse from a given charge weight of TNT(W) at distance(R) away from the charge can be obtained from 〈Figure Appendix II-1-6〉.



〈Figure Appendix II-1-5〉 Time constant( $\theta$ ) for different charge weights



〈Figure Appendix II-1-6〉 Shockwave impulse vs. TNT charge size

## 2) Characteristics of an Underwater Bubble

The characteristics of an underwater bubble are delineated in the 〈Figure Appendix II-1-1〉, and Willis P.M., based on his experiment, proposed that oscillation period(T) and maximum radius( $A_m$ ) of a bubble can be expressed as:

$$T = K \frac{W^{1/3}}{Z^{5/6}} \quad (3)$$

$$A_m = J \frac{W^{1/3}}{Z^{1/3}} \quad (4)$$

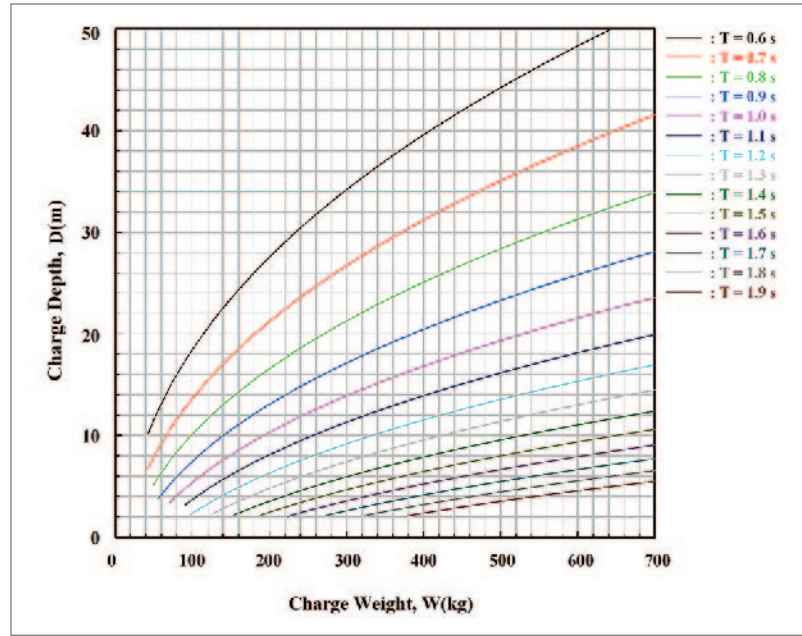
$$Z = 10.1 + D(m)$$

where, K and J are bubble constants determined by the types of explosives, and values obtained from experimental data for selected explosives are listed in 〈Table Appendix II-1-4〉.

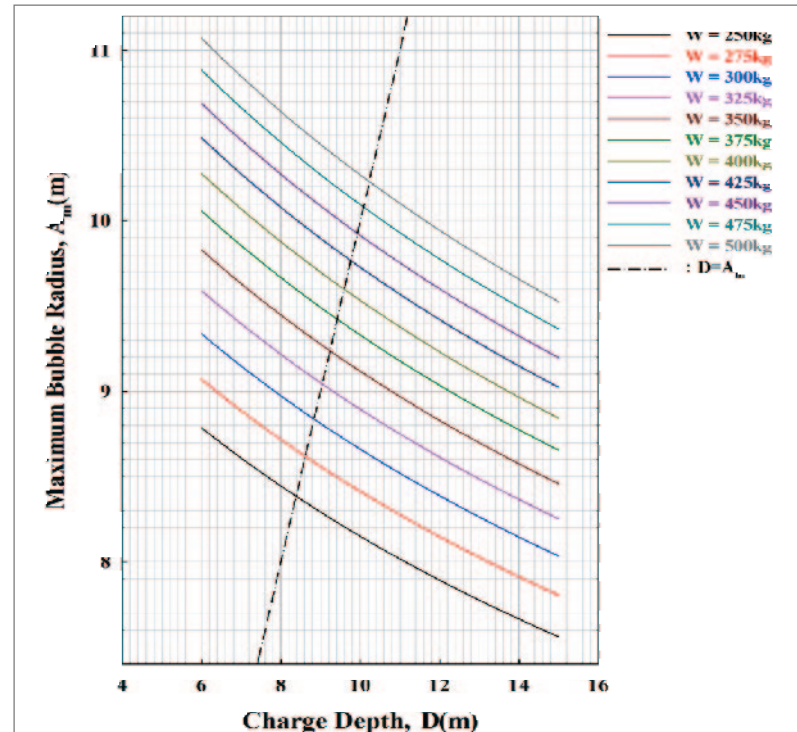
EXPLOSIVE	J	K
TNT	3.50	2.11
PENTOLITE	3.52	2.11
HBX-1	3.95	2.41
HBX-3	4.27	2.63
H-6	4.09	2.52

〈Table Appendix II-1-4〉 Bubble constants for selected explosives

〈Figure Appendix II-1-7〉 and 〈Figure Appendix II-1-8〉 show the bubble period(T) and maximum bubble radius( $A_m$ ) for a TNT charge as a function of the depth(D) of the explosive, respectively.



〈Figure Appendix II-1-7〉 Bubble period(T) of the bubble formed by TNT at different depths



〈Figure Appendix II-1-8〉 Maximum bubble radius(A<sub>m</sub>) of the bubble formed by TNT at different depths

### 3) Formation of Water Column and Water Jet generated from Underwater Explosion

Summarized below are the formulas for the maximum height of the water jet, and the maximum diameter of the water column and smoke plume generated from a relatively shallow underwater explosion of TNT at seabed. 〈Figure Appendix II-1-9〉 and 〈Figure Appendix II-1-10〉 are the plots of maximum jet height and maximum column diameter as a function of scaled charge depth.

$$H_{max}/W^{1/3} = 32.4(Y/W^{1/4})^{0.1}, \quad 0.0037 < Y/W^{1/4} < 0.74 \quad (5)$$

$$H_{max}/W^{1/3} = 21.7(Y/W^{1/4})^{-1.24}, \quad 0.74 < Y/W^{1/4} < 1.56$$

$$D_{max}/W^{1/3} = 3.71(Y/W^{1/4})^{0.166}, \quad 0.08 < Y/W^{1/4} < 0.88$$

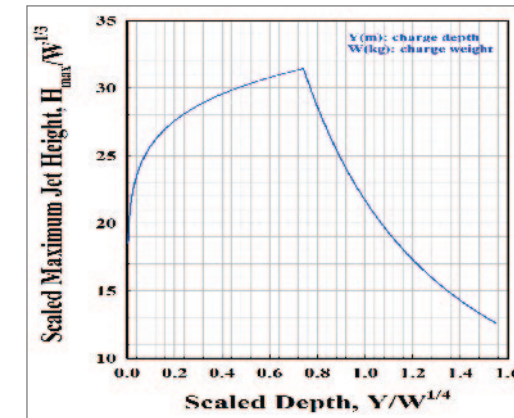
$$S_{max}/W^{1/3} = 9.00$$

$$H_{max}/W^{1/3} = \text{scaled maximum jet height (m/kg}^{1/3}\text{)}$$

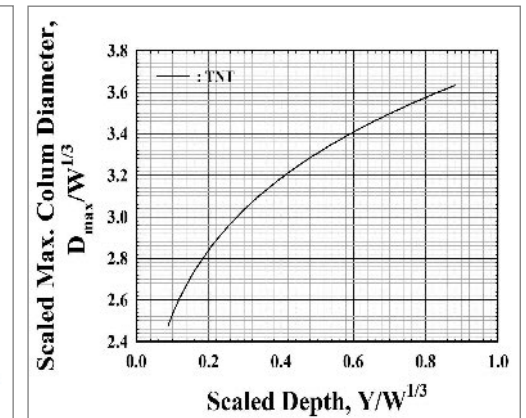
$$D_{max}/W^{1/3} = \text{scaled maximum column diameter (m/kg}^{1/3}\text{)}$$

$$S_{max}/W^{1/3} = \text{scaled maximum smoke crown diameter (m/kg}^{1/3}\text{)}$$

$$Y = \text{Charge Depth (m)}$$



〈Figure Appendix II-1-9〉 Maximum jet height vs. scaled depth for TNT



〈Figure Appendix II-1-10〉 Max. column diameter vs. Scaled depth

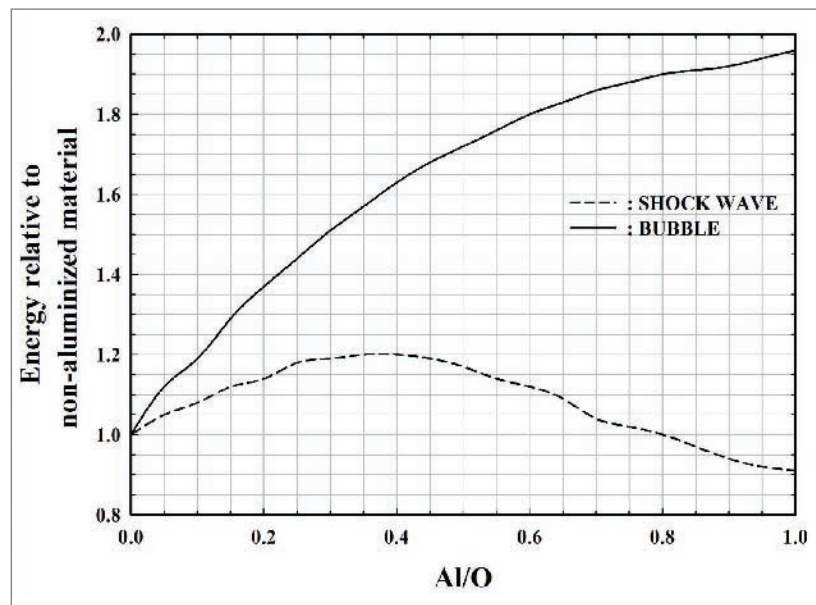
For example, by applying the graph on 〈Figure Appendix II-1-9〉, the maximum height of the water jet from an underwater explosion of a TNT charge of 250kg at a depth of 6m can be calculated in the following order:

- (1)  $W=250\text{kg}$ ,  $W^{1/4}=3.98$ ,  $W^{1/3}=6.30$
- (2)  $Y=6\text{m}$ ,  $Y/W^{1/4}=6/3.98=1.51$ ,  $Y/W^{1/3}=6/6.30=0.95$
- (3) In  $\langle$ Figure Appendix II-1-9 $\rangle$ ,  $H_{\text{max}}/W^{1/3}=13$  at  $Y/W^{1/5}=1.51$
- (4)  $H_{\text{max}}=13 \times W^{1/3}=13 \times 6.30= 82$  meters

The column diameter calculation as shown in  $\langle$ Figure Appendix II-1-10 $\rangle$  also uses the same method as above.

#### 4) Underwater Explosion Performance of Aluminized Explosives<sup>5)</sup>

Non-ideal explosives containing a large amount of aluminum show dramatically increased bubble energy as their content increases, as shown in  $\langle$ Figure Appendix II-1-11 $\rangle$ . It is usual to adjust the amount of aluminum in order to obtain the optimum ratio of the shockwave energy to the bubble energy according to their specific purposes. Most explosives for underwater weapon systems are aluminized explosives because bubble energy is more effective in destroying targets than shockwave energy.



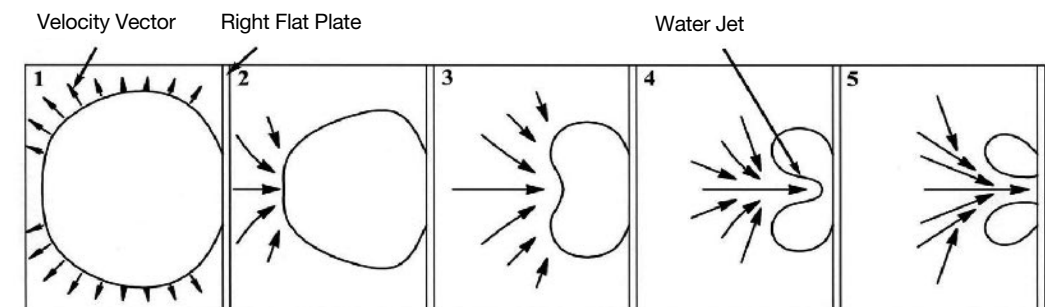
$\langle$ Figure Appendix II-1-11 $\rangle$  The effect of aluminum on underwater explosion properties

5) J. E. Shepherd, "Interface Effects in Underwater Explosions", AD-A201 814, December 1988.

When CHNO explosive containing aluminum is detonated underwater, it dissociates into elements such as C, H, N, O, Al almost instantly, and subsequently these elements undergo exothermic chemical reactions to form aluminum oxide( $\text{Al}_2\text{O}_3$ ),  $\text{H}_2\text{O}$ ,  $\text{H}_2$ ,  $\text{CO}$ ,  $\text{CO}_2$ , and C(graphite) in a few micro-seconds. These high-temperature, high-pressure gaseous products push water in the radial direction to form a gas bubble, which expands and contracts as time continues.

#### 2. Interaction between Rigid Wall and Gas Bubble<sup>6)</sup>

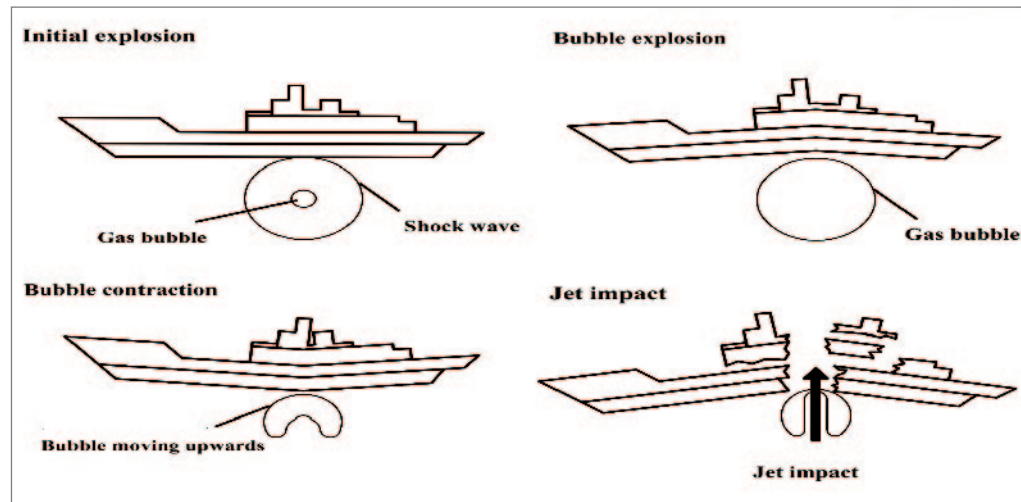
The descriptions on the gas bubble from underwater explosion hold only for deep underwater explosions where boundary conditions can be neglected. If there are free surface, seabed surface, or rigid wall located near the origin of explosion, the gas bubble behaves in a different manner. As shown in  $\langle$ Figure Appendix II-2-1 $\rangle$ , when a bubble contracts near a rigid wall, the speed of the water is the highest on the opposite side of the wall and slowed down as it is closer to the wall, since the wall hampers free flow of water near it. Therefore, the bubble collapses toward the wall due to attraction, which results in the water jet effect on the opposite side of the wall. As the water jet develops, it applies a strong jet impact on the wall. After the water jet, the remaining bubble is deformed into a toroidal shape and gradually vanished. The collapsing procedure is heavily influenced by the size and oscillation period of the bubble, standoff from wall, gravity, and relative curvature of the wall and bubble.



$\langle$ Figure Appendix II-2-1 $\rangle$  Bubble collapse and formation of water jet

6) Julius W. Enig, "Underwater Explosion Bubble Dynamics", AD-A201 814, December 1988.

To facilitate the understanding of the sinking of ROKS Cheonan, the devastating effects of a gas bubble formed by an underwater explosion below hull will be explained with <Figure Appendix II-2-2>.

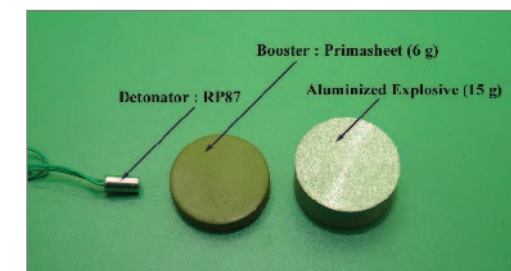


<Figure Appendix II-2-2> Physical effects of bubble formed below hull as time elapses

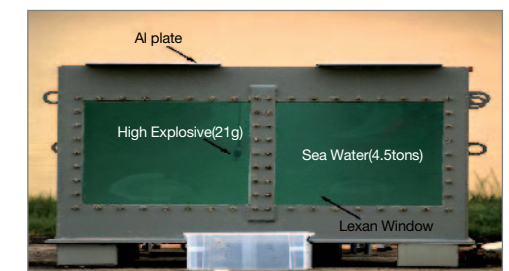
As an explosive charge is detonated below hull, shockwave is generated, and impacts the hull after propagating in water at a very high speed. Although the peak pressure of the shockwave is very high initially, it gets attenuated very rapidly as the shockwave propagates in water. Moreover, since the shockwave travels outward spherically, the actual impact on the hull is not severe. For these reasons, the damage inflicted by the shockwave is known to be insignificant, such as malfunctioning of on-board power and communication systems, and light damage of the body. After the shockwave passes, the bubble is formed slowly, and the pressure inside the bubble is relatively low compared to that of the shockwave. As the bubble expands, the hull is deformed into a reverse V-shape under the force exerting upward. Then, the bubble starts to contract, pulling the hull downward to produce a V-shape deformation. As the contraction continues, the bubble collapses and the high speed water jet starts to be formed in the lower part of the bubble. As the water jet gets larger, it produces a heavy impact on the hull, and eventually breaks the hull. Since the water jet impact is much more effective than the shockwave, most countries employ aluminized explosives for non-contact underwater weapon systems.

### 3. Small-scale UNDEX Experiments

In order to demonstrate the formation of a bubble and analyze the chemical components of the white substance adsorbed on the fractured surface and the stack of ROKS Cheonan, a small-scale underwater explosion experiment was conducted. A water tank (2m × 1.5m × 1.5m) was filled with 4.5 tons of water, and an aluminized explosive of 15g was detonated in the aquarium by using 6g of a booster and a RP87 detonator, as shown in <Figure Appendix II-3-1>.



<Figure Appendix II-3-1> Explosive train used in the experiment



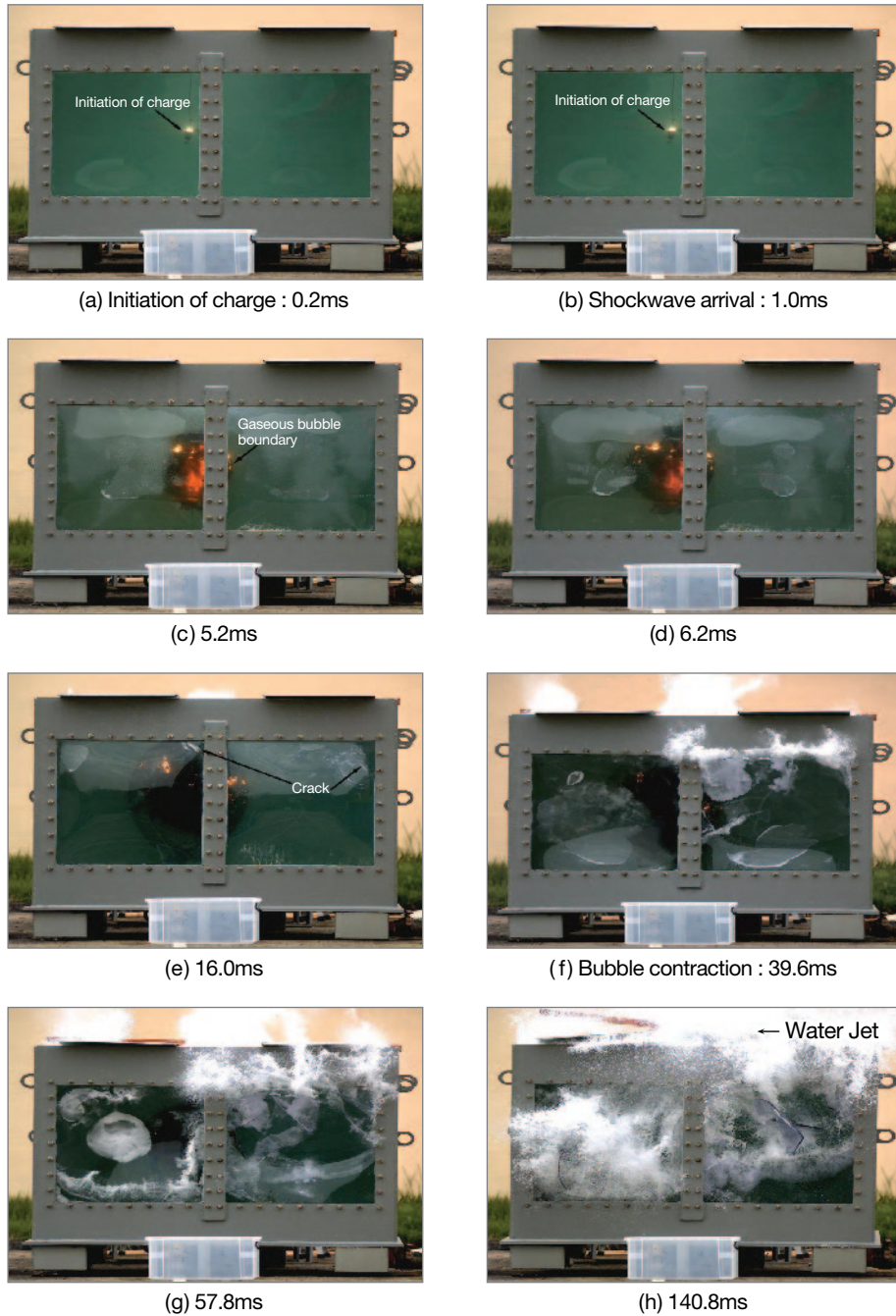
<Figure Appendix II-3-2> Small water tank used in the UNDEX test

To obtain the adsorbed materials, the team placed 2 layers of 4 aluminum plates on top of the tank, and fixed them with bolts to prevent the aluminum plates from being thrown by the water column. Also, 2 polycarbonate windows were installed for high-speed image as shown in <Figure Appendix II-3-2>. The writing speed of the high-speed camera was set 5,000fps(frames per second).

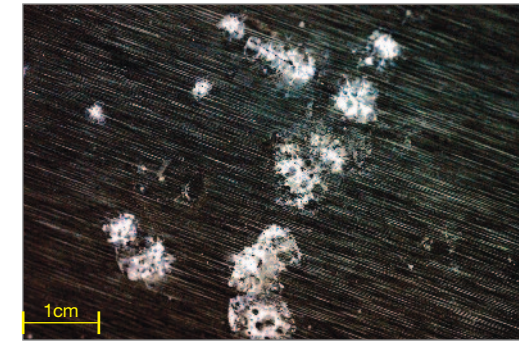
<Figure Appendix II-3-3> are pictures of the selected frames taken from the high-speed photograph record, showing the development of the bubbles formed by the underwater explosion. In <Figure Appendix II-3-3> (a), the charge produces strong flash at 0.2ms after initiation. In (b), the window becomes opaque by the impact of the shockwave to the window at 1ms. In(c) and (d), the heat is released inside the high-temperature and high-pressure bubble. The bubble expands and begins to apply pressure against the window. In (e), the window starts to break. The window continues to break until the bubble reaches its maximum radius. In (f), the bubble starts to contract. In (g), as the contraction continues, the left window experiences a strong attraction force towards the contracting bubble. In (h), the window breaks completely.

In this small-scale underwater explosion test, white substance adsorbed on the alu-

minimum plate was obtained as shown in <Figure Appendix II-3-4>. Through detailed analysis and comparison of the white substance, an important clue for the sinking of ROKS Cheonan was found.



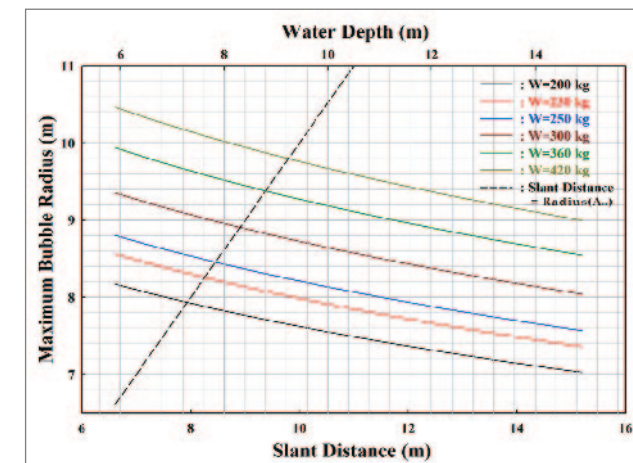
<Figure Appendix II-3-3> Images obtained through the experiment(5,000 frames/sec)



<Figure Appendix II-3-4> White substance obtained from the small-scale UNDEX experiment

#### 4. Conditions for the Maximum Bubble Effects

To determine the type of the weapon system, a depth of the explosion, the TNT equivalent weight of the explosive from surfaces of the salvaged hull, and theoretical and empirical formulas for an underwater explosion were applied. <Figure Appendix II-4-1> summarizes the most plausible explosion conditions chosen under the assumption that bubble jet caused the break. Since the bubble jet is formed only in the presence of a rigid wall near the origin of the explosion, the maximum effect occurs when the maximum bubble radius( $A_m$ ) and the slant distance between the keel and the origin are approximately the same. Hence the maximum bubble jet effect is obtained in the range of charge size(200~360kg TNT equivalent) and depth(6~9m) near the dashed line in <Figure Appendix II-4-1>.

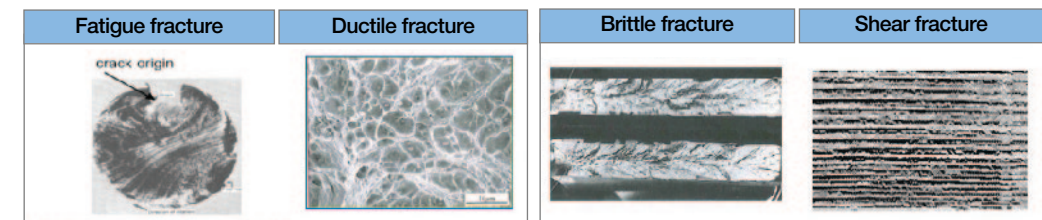


<Figure Appendix II-4-1> Maximum bubble radius vs. slant distance

For instance, when 250kg of TNT equivalent and 6m depth are applied to the equation (5), which is used for a calculation under the free sea surface environment, the projected value of the maximum height of the water jet is computed as approximately 82m.

### Appendix III. Analysis Result on Direction and Location of the Explosion

In order to analyze explosion effects with varying charge size, the direction of the explosion with respect to the ship needs to be determined first. For this end, the breakplane of the hull, the most assured evidence, was analyzed. The types of damage on the breakplane were visually investigated and analyzed. From this, it was determined whether the fracture includes fatigue, ductile, brittle or shear fracture. Based on this observation, the direction and location of the explosion were estimated.



〈Figure Appendix III-1〉 Types of fractures

Fatigue fracture stems from repeated stresses over a long period of time, and contains a beach mark from the crack origin. Ductile fracture occurs when the stress is applied relatively slowly, and is accompanied by a large plastic deformation. The cross section is relatively rough and contains many dimples. Brittle fracture occurs with a small plastic deformation when the stress is applied rapidly. The section is relatively smooth and contains chevron marks. Shear fracture results from high stress applied rapidly in shear direction, and it shows no chevron marks, dimples, or beach marks. In the shear fracture, fracture occurs in the direction of the stress.

## 1. On-site Investigation and Sample Collection

The first on-site investigation was conducted on April 30, and the breakplane of the stern hull bottom was observed. As shown in <Figure Appendix III-1-1>, samples of approximately 15cm × 15cm size were collected from three locations at the breakplane of the stern hull bottom. The second on-site investigation was conducted on May 4, to check the probable direction of fracture on the bottom of the stern hull, and to observe the breakplane on flank of the stern hull as well as on the bottom and flank of the bow hull. On May 10, the third on-site investigation was conducted in order to check the direction of fracture on the bottom and flank of the bow, and breakplane of main deck of the bow and stern was observed.

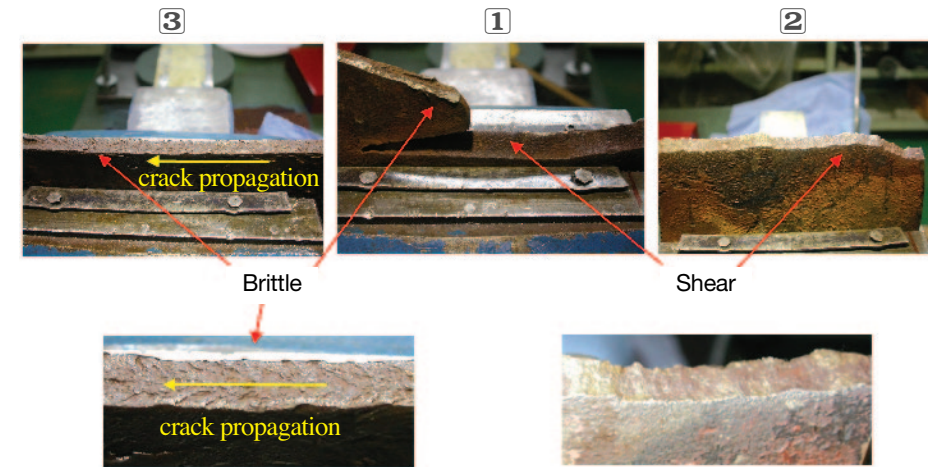


<Figure Appendix III-1-1> Sample collection locations at breakplane

## 2. Results for Breakplane Analysis

### 1) Estimation of Fracture Type

All the fractured surfaces of the samples, as shown in <Figure Appendix III-2-1>, were identified to be shear and brittle fractures with no signs of ductile or fatigue fracture. Sample #2 shows shear fracture patterns and sample #3 shows a typical brittle fracture, whereas sample #1 contains a mixture of the two.



<Figure Appendix III-2-1> Fracture surfaces of collected samples

### 2) Estimation of Fracture Direction

Additional visual observation was made on May 4, and it was confirmed that the pattern showed shear fracture between sample locations #1 and #2 and brittle fracture between sample locations #1 and #3 as shown on <Figure Appendix III-2-2>.

Therefore, it was estimated that one third of breakplane on the port side of the stern hull underwent shear fracture caused by instantaneous external force, and the rest of bottom part of the stern hull suffered brittle fracture caused by tensile force. And the origin of crack was estimated to be near sample location #1.



<Figure Appendix III-2-2> The pattern of fracture on the stern

As shown in <Figure Appendix III-2-3>, it was confirmed that in the fractured surface of the stern part, shear fracture(highlighted in red) occurred in the estimated region of direct impact, and that brittle fracture(highlighted in blue) occurred starting where shear fracture ends, towards the starboard side. In addition, all of the three fractures on the port side, which was rolled up into a U-shape, also showed shear fracture patterns.



<Figure Appendix III-2-3> Overall fracture pattern of the stern part

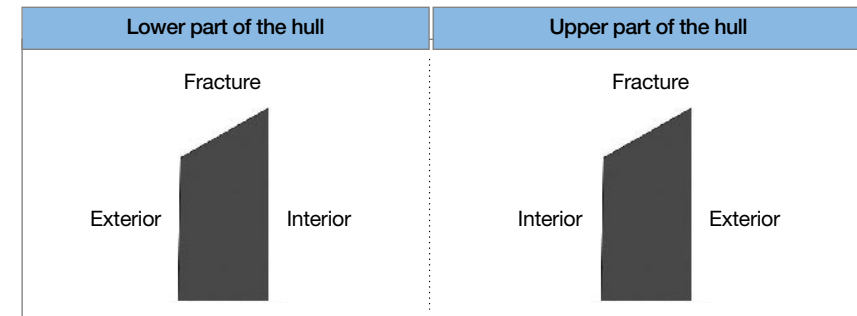
The JIG also conducted visual observation for the fractured surface of the bow section, and confirmed that the overall pattern is similar to that of the stern section. Both shear fracture and brittle fracture were observed partially near the estimated origin of impact on the port side, and it was assessed that this condition was due to the influence of internal structures on the fracture surface in a complicated manner.

### 3) Observation Results for Fracture Direction(Stern and Bow)

The brittle fracture patterns were observed in the vicinity of the keel for both the bow and stern part, and the shear fracture patterns were shown in all the rest. The estimated origin of the brittle fracture was the lower-left part of the port hull(near sample location #1). In the lower part of the port side and starboard side of both the bow and stern that show the shear fracture patterns, the overall cross section was slanted from the vertical direction and lifted higher towards the interior of the hull as shown in <Figure Appendix III-2-4>(the di-

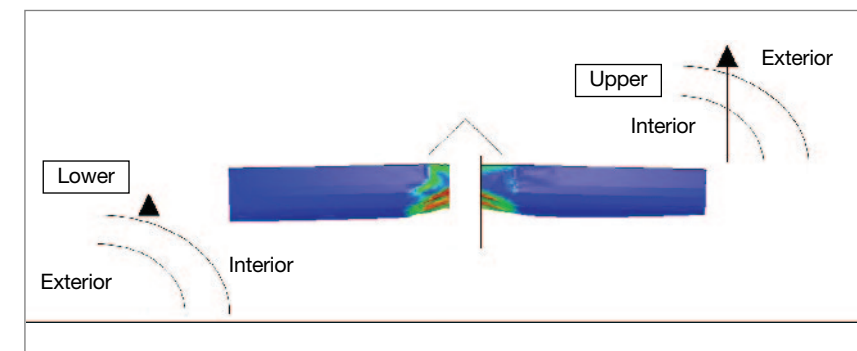
agram on the left) at every location.

For the port and starboard sides of the upper main deck of both the bow and stern, the overall section was also slanted; however, the direction was reversed and oriented higher towards the exterior of the hull as can be seen in <figure Appendix III-2-4>(the diagram on the right) at every location.



<Figure Appendix III-2-4> Shape of fracture on the hull

The situation that could have caused the aforementioned section shapes, as shown in <Figure Appendix III-2-5>, was estimated to happen when a large plastic deformation occurs first to curve the outer structure of the ship, followed by a shear fracture caused by a strong, uni-directional external force(presumably water jet).

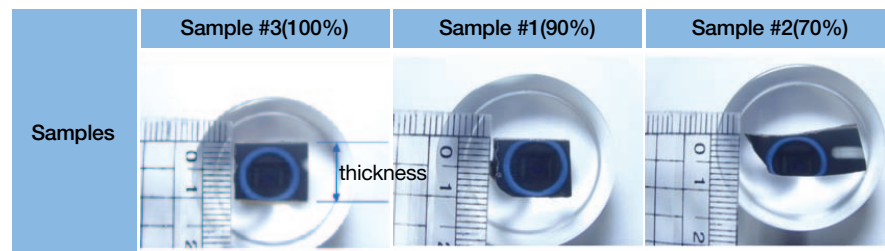


<Figure Appendix III-2-5> Analysis of cutting shape of upper and lower hull

### 3. Microstructure Analysis of Collected Samples

#### 1) Thickness Comparison of Collected Samples

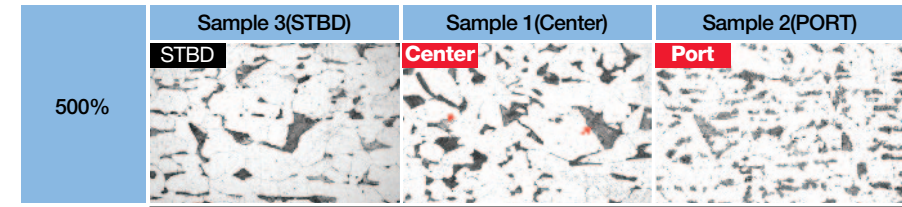
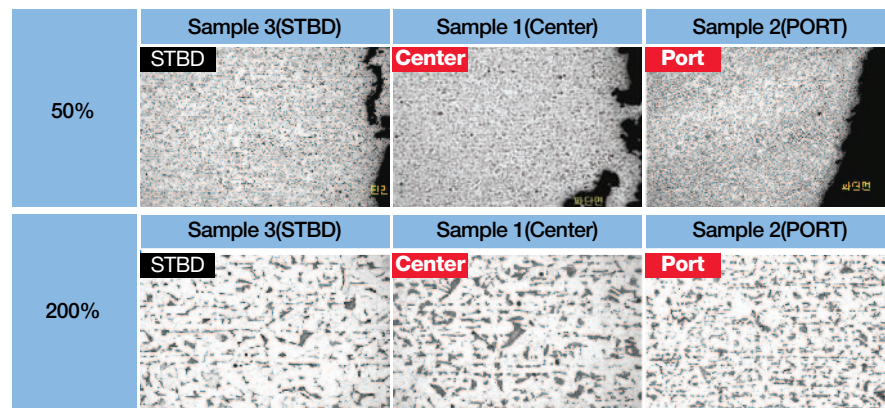
From the measurement of the thickness of collected samples, sample 2 which was estimated to be near the origin of explosion showed to be 30% less thick than sample 3 at starboard side, while sample 1 showed 10% less compared to sample 3, as shown in <Figure Appendix III-3-1> below.



<Figure Appendix III-3-1> Thickness measurement of collected samples

This confirmed the assessment mentioned earlier that a plastic deformation with substantially large curvature occurred at the port side bottom before fracture.

#### 2) Comparison of Microstructures



<Figure Appendix III-3-2> Microstructures of collected samples

The observations of the microstructures of each sample and the results are shown in the <Figure Appendix III-3-2>.

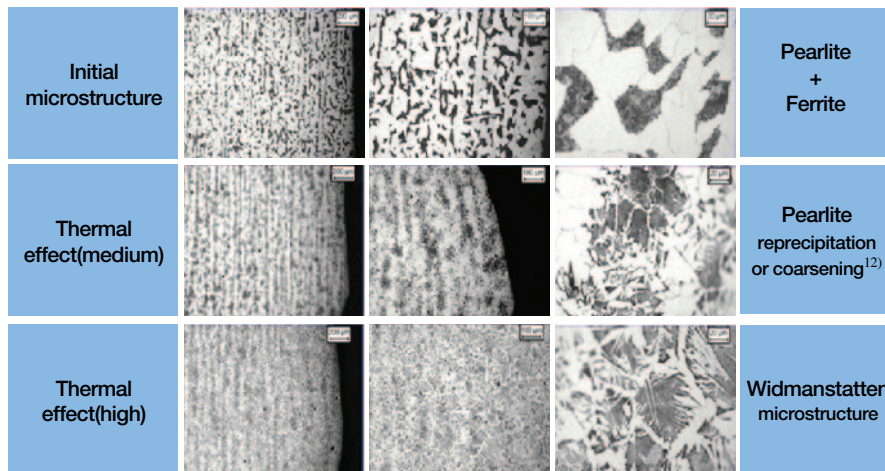
For the 50× magnified images, all the samples showed a rolling structure<sup>7)</sup> with horizontal stripes<sup>8)</sup>; however, sample 2 from portside showed denser stripes than the initial structure due to about 30% thickness reduction and longitudinal extension.

For the 200× magnified images, the sample 2 showed the stripes spaced closer and thinned out compared to sample 3 collected from starboard side, and showed typical pearlite + ferrite<sup>9)</sup> microstructure. The black parts were pearlite structure. If there were a heat deformation on the portside, as shown in <Figure Appendix III-3-3>, rolling stripe melting due to pearlite coarsening should be observed; however, since such phenomena were absent on the samples, it was confirmed that there had been no heat over 723℃. This can be a basis in proving the cause as a non-contact external explosion.

For the 500× magnified images, the sample 2 showed grain refinement<sup>10)</sup> due to relatively greater plastic deformation stemming from thickness reduction and longitudinal extension.

Micro hardness for samples 2 and 3 was Hv=163 and Hv=146 respectively, and it was assessed that the hardness of sample 2 would become higher due to the significant strain hardening<sup>11)</sup> of the sample on the portside.

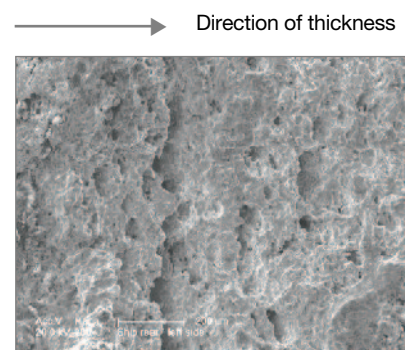
7) Rolling structure: Metallic formation with more thorough crystalline particles. This structure is produced by the pressure created from the metallic material being inserted between two spinning rollers.  
 8) Rolling stripe: The marks arranged in stratified fashion as a result of rolling process.  
 9) Pearlite and Ferrite: A microscopic structure from during the process of steel that has approximately 0.25% less carbon freezing after being melted in a high temperature.  
 10) Grain refinement: The size reduction of certain crystalline substances due to external pressure or heat.  
 11) Strain hardening: An increased hardness of a metal through a deformation or method of processing.



〈Figure Appendix III-3-3〉 Typical microstructure change due to heat influence(example)

### 3) Microstructure Analysis on the Fractured Surface of the Samples

As the microstructure of the sample 2 from portside was observed, numerous cavities grown perpendicular to thickness appeared as shown in 〈Figure Appendix III-3-4〉, which indicated a strong tensile force having been applied in the direction of thickness. This tensile force was caused to be from the tensile wave due to the interaction between shockwave in the direction of thickness and rarefaction wave<sup>13)</sup> on the opposite free surface side of the impact. Therefore, this was another basis that could prove the strong impact upon the portside bottom.



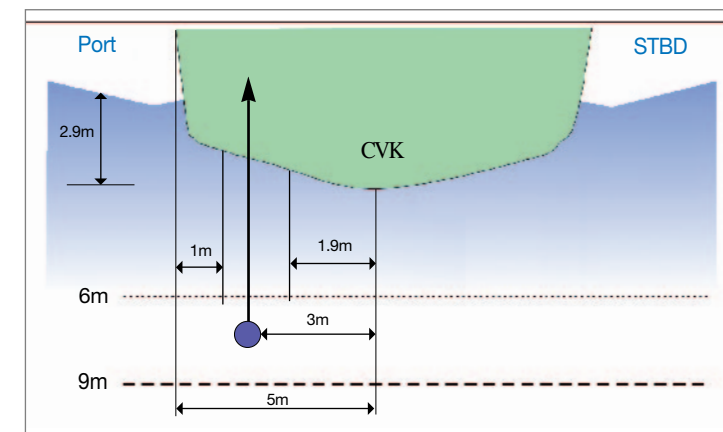
〈Figure Appendix III-3-4〉 A microstructure of fractured surface

12) Pearlite coarsening: Crystalline substances getting bigger than original size. Reprecipitation: Certain crystalline substances are recreated.

13) Rarefaction wave: A phenomenon in which shockwave is propagated to the opposite side after it encounters free surface and slows down during its progression.

### 4. Estimation on Location and Direction of the Explosion

The analysis on the breakplane of ROKS Cheonan revealed that an upward plastic deformation with large curvature due to a strong explosion from the portside bottom occurred(hogging), and then, a strong external force, presumably water jet, caused shear fracture which began at 1.9m left of the CVK. Thus, given that the hull is 5m in half breadth of the port, it could be estimated that an explosion might have occurred between 1.9~5m left of the CVK. The possible location for a torpedo strike could be estimated to be 3m, which is the center of 1.9~4m range left of the bottom CVK(See 〈Figure Appendix III-4-1〉).



〈Figure Appendix III-4-1〉 Possible range of torpedo explosion

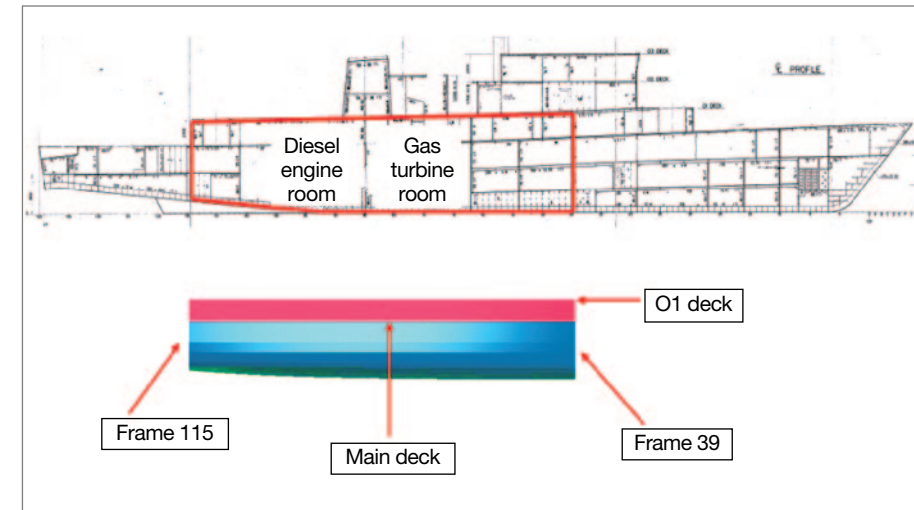
## Appendix IV. Analysis Result on Charge Size and Depth

Based on the location of explosion and the direction of external force derived from the earlier mentioned analysis of breakplane, simulations were conducted in order to estimate the charge size and depth similar to the explosion that occurred in the ROKS Cheonan incident. Explosion Analysis Team utilized a simplified model(localized area and simplified ship modeling) in order to derive the range of probable explosion types in a short period time. Based on this result, Ship Structure Management Team conducted a detailed analysis using full modeling of the entire ship. The result from the simplified model is presented here.

### 1. Numerical Model

Though the entire ROKS Cheonan should have been modeled in 3D for accurate results, a portion centered around the gas turbine room, which was lost, was covered in this simulation, and only the local damage of this portion was analyzed. This was because plausible explosion types had to be estimated within a short time, and simulations on the entire ROKS Cheonan for all possible loads(shockwave, bubble pressure, whipping effect, and water jet) were assigned to Ship Structural Management Team. Probable explosion types(charge sizes and locations) were derived from numerical simulations using this simplified model. Therefore, this analysis was expected not to include detailed whipping effects, with a 3D modeling confined to the region between Frame 35 and Frame 119 of ROKS Cheonan that included the gas turbine room and the diesel engine room as shown on <Figure Appendix IV-1-1>.

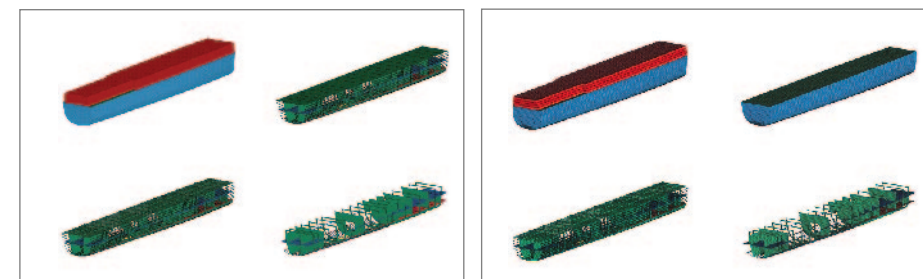
For the simulation, LS-DYNA™ code was used, a commercial code developed in the United States. Many government and civilian labs of ROK as well as the US, Japan, PRC, and EU countries use this code to analyze high pressure hydrodynamic phenomena such as explosions and collisions, and the credibility of this code is widely recognized. This code had also been used in Korean labs for design and performance prediction of various warheads.



<Figure Appendix IV-1-1> Simulation range for explosive analysis

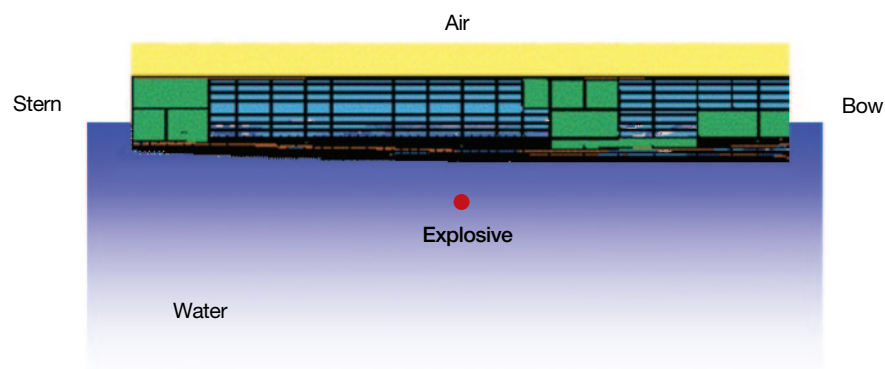
Prior to the simulation, a 3D geometrical modeling should be conducted first, which usually takes a lot of time and manpower. This is because the 3D modeling itself is a time-consuming process, and normally several modifications to the 3D model are needed due to errors and inaccurate results in calculations.

<Figure Appendix IV-1-2> shows a ship configuration(45.6m) modeled from Frame 39 to Frame 115 of ROKS Cheonan, and <Figure Appendix IV-1-3> shows the configurations with approximately 300 × 300mm meshes superimposed on the geometrical model to enable numerical simulations. I-DEASTM code, which is used widely, was used in the modeling process.



<Figure Appendix IV-1-2> Modeling shape

<Figure Appendix IV-1-3> Mesh shape



〈Figure Appendix IV-1-4〉 Initial analysis model

## 2. Conditions for Numerical Simulation

In order to derive probable explosion types that caused the ROKS Cheonan incident, simulation conditions were first determined based on simulation results of US Team, break-plane analysis, and analysis of probable hostile weapon systems.

Explosive charge weights of 45~500kg TNT equivalent and depths of 6~13m were selected considering a detection capability of weapon systems and assuming a non-contact explosion. Three meters to the portside from the center of the gas turbine room was selected as the widthwise location of the explosion from the results of the breakplane analysis. Frame 71, 2.4m to the bow from the center of the gas turbine room, and Frame 75, the center of the gas turbine room, were selected as lengthwise locations of the explosion. Frame 71 was selected because the bulkhead of the gas turbine room at the breakplane and CVK of bow part experienced deformation greater than that of the stern part. Frame 75 was selected in order to exclude explosion types with smaller explosive charge weights that inflict less deformation than the actual damage, by performing calculations at a location where the greatest deformation of the gas turbine room is produced. The simulation was conducted from Frame 75 to derive probable explosion types, and then additional simulation was carried out at Frame 71. A final range of explosion types was derived by comparing and analyzing the two results. 〈Table Appendix IV-2-1〉 shows selected conditions for the simulation.

Charge weight (kg, TNT equivalent)	Frame location	Depth of explosion(m)
45	75	6
200	75	6, 7, 8
250	75	6, 7, 8, 9, 12
300	71, 75	6, 7, 8, 9, 11
360	71, 75	6, 7, 8, 9, 11
420	71, 75	6, 9, 12
500	71, 75	10, 11, 12, 13

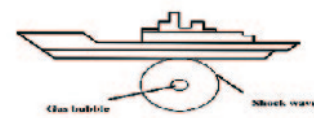
〈Table Appendix IV-2-1〉 Simulation conditions(3m to port)

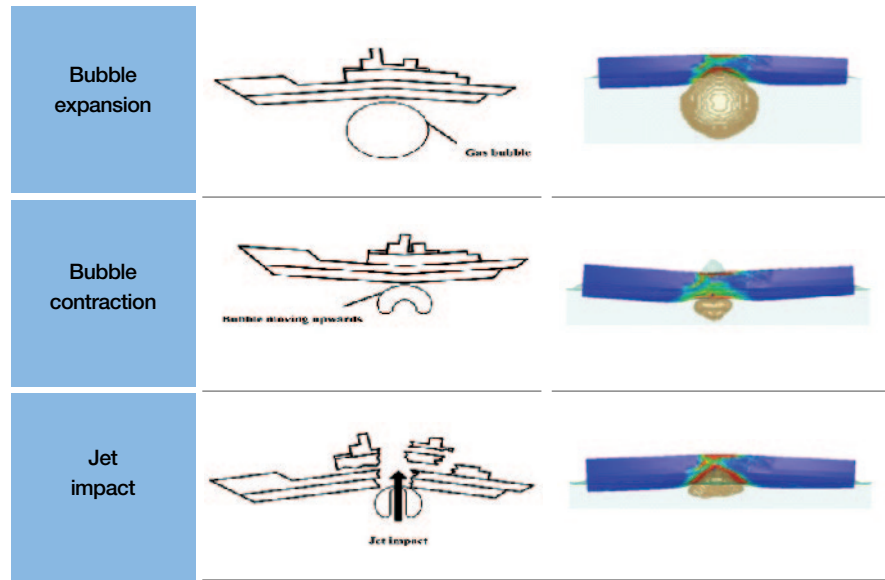
For validation of the simulation results, computation results of shockwave pressure on different distances from a point of underwater explosion were compared with results from well-known empirical equations before performing numerical simulations on each model. 〈Table Appendix IV-2-2〉 summarizes the results. As shown in the table, calculated values and empirical values were consistent, and they fell under 5% difference.

Charge size (kg, TNT)	Measured radius(m)	Empirical value(MPa)	Calculated value(MPa)	Error(%)
250	3	130.14	135.39	4.0
	6	50.25	52.97	5.4
	9	31.66	33.20	4.9

〈Table Appendix IV-2-2〉 Comparison of shockwave pressure

Secondly, the credibility of the results was ensured by comparing the bubble behavior appeared on the simulation with the actual behavior shown in 〈Figure Appendix II-1-1〉. 〈Figure Appendix IV-2-1〉 compares the two cases.

Bubble behavior	Actual	Simulation
Initial explosion		



〈Figure Appendix IV-2-1〉 Comparison of bubble behavior

### 3. Criteria for Selecting Probable Explosion Types

The team established three criteria and selected explosion types that satisfied all three as probable explosion types.

The explosion types were selected on the basis of the extent of hull bottom damage at the gas turbine room which is visible on both port and starboard sides, and the way two damaged parts engage with each other. This was because the entire gas turbine room of ROKS Cheonan was lost.

Since this simulation model did not include the entire ship as well as interior components, the calculated deformation would have been greater than the actual deformation. Therefore, the CVK deformation at the sides of the stern part, where many of the structures were arranged transversely, was selected as a criterion. On the actual bulkhead of the break-plane, the CVK deformation was smaller at the stern part than at the bow part. The deformation length(actual value: 3,580mm) was selected as a criterion of the CVK deformation. CVK deformation length was set to one shown in 〈Figure Appendix IV-3-1〉. From the simulation result of each case, the deformation length within 1~1.2 times of the actual de-

formation was selected to meet the criterion. This, as mentioned earlier, was because the simulation would have yielded a greater deformation than the actual value due to the simplified modeling.

Lastly, the shape of deformation/fracture at the stern breakplane bulkhead was included. 〈Figure Appendix IV-3-1〉 shows all three criteria.

Criteria	ROKS Cheonan	Simulation, example
① Extent of hull bottom damage		
② Deformation/fracture at the stern failure-section bulkhead		
③ CVK deformation length toward stern from failure-section		

〈Figure Appendix IV-3-1〉 Three comparison criteria

### 4. Simulation Result

Simulations for charge weight of 230kg TNT equivalent or below, at Frame 75, 3m to the port were conducted and compared with the actual damage observed on ROKS Cheonan. As a result, it was concluded that the explosion caused by charge weight of 230kg TNT equivalent and below was unlikely to have occurred. For the charge weight of 250kg TNT equivalent, the explosion type to partially match the actual damage was estimated to be at

a depth of 6m, and for 300kg of TNT equivalent, the possible explosion type was at a depth of 7m. The result of the simulation at Frames 71 and 75 at 3m to the portside from the center and with 360kg TNT equivalent, a depth of 7~9m was selected to be the possible explosion types.

Therefore, from numerical simulations of various conditions of different charge sizes and standoffs(6~13m), and by using 3m to portside as location range of explosion from the breakplane analysis, the explosion types showing similar damage pattern as the actual were derived as shown in <Table Appendix IV-4-1>.

Explosive wt.(TNT, kg)	Depth(m)
250	6
300	7
	7
360	8
	9

<Table Appendix IV-4-1> Summary of simulation results

## Appendix V. Analysis Result on Adhered Materials

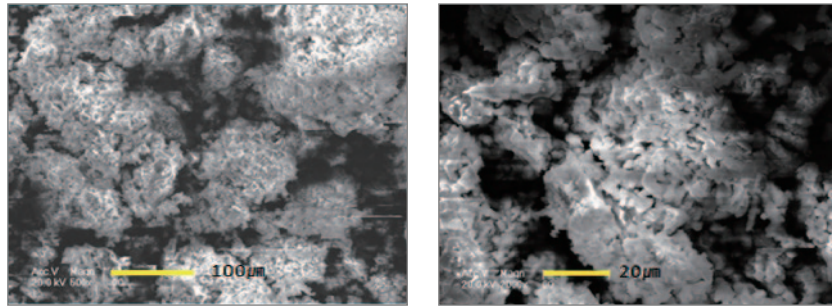
In order to analyze the explosion pattern, the explosive weight and location of explosion were estimated so far. In this section, a large amount of adhered material found on ROKS Cheonan was analyzed for confirming possible weapon system that might have caused such explosion.

When the stern of ROKS Cheonan arrived at 2nd Fleet(Pyeongtaek), the initial visual inspection was made on April 18. While observing the fracture on the stern, a large quantity of white powder was found adsorbed on crumbled aluminum panels of the upper deck on the portside. In addition, the same kind of material was observed around the fracture surface on the upper deck, as well as on the shell plating of the stern. Such adhered material was found not only on aluminum panels but also on power cables composed of non-aluminum material. A five-step analysis was performed on the adhered material: the first analysis was preliminary to understanding the characteristics of white powder found during the initial observation, and the second and third analyses were detailed examinations on the adhered material found on the stern and bow. The fourth analysis was conducted to investigate whether the adhered material from the recovered propulsion parts of the torpedo(conclusive evidence) was the same as the material adsorbed on the bow and stern. The final analysis was conducted with the explosion products from the small-scale underwater explosion experiment in order to verify that the adhered material found inside ROKS Cheonan was a product of aluminized underwater explosives.

### 1. First Analysis

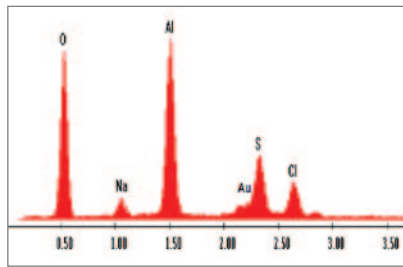
The apparatuses employed in the composition analysis were SEM(Scanning Electron Microscopy; Philips XL30), EDS(Energy Dispersive Spectrometer; Philips EDAX) and XRD(X-ray Diffraction; Bruker D8 Discover).

The SEM images of the adhered material are shown in <Figure Appendix V-1-1>. Fine particles were agglomerated as if melted.

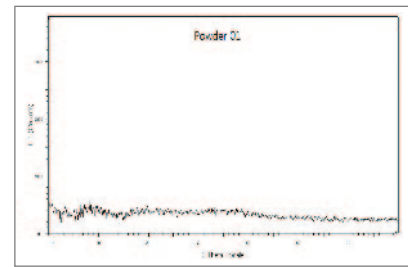


〈Figure Appendix V-1-1〉 SEM Images

For EDS analysis, electrons of an atom are ejected upon irradiation of an electron beam, and subsequently the hole is filled with other electrons from higher shells which accompany energy release. Since the released energy is different for each element, the elements composing of a material can be identified. As presented in 〈Figure Appendix V-1-2〉, the EDS results show that the adsorbed material consisted of oxygen, sodium, aluminum, sulfur, and chlorine (The Au(gold) peak was observed due to the gold plating on the sample necessary for the experiment). Based on the elemental composition, the adhered material was considered to be a mixture of oxides of aluminum ( $Al_xO_y$ ), salt (NaCl), and sulfur or sulfur compounds.



〈Figure Appendix V-1-2〉 EDS result



〈Figure Appendix V-1-3〉 X-ray diffraction result

In XRD analysis, X-rays scattered from different atoms within the crystal mutually interfere with each other. If the incident X-ray is monochromatic, the scattered beams for each type of atom interfere to give strong diffraction patterns in a certain direction. The diffraction peak<sup>14)</sup> depends on the distance between each lattice in the crystal, i.e. the size of

14) Diffraction peak: The display of the reinforcement interference of an x-ray. This display can be observed in certain angles when the x-ray is projected on the object and gets scattered by the object's crystal.

unit cell. Therefore, each crystal has its own X-ray diffraction peak, while amorphous material does not show one.

As shown in 〈Figure Appendix V-1-3〉, the adhered material did not show any noticeable X-ray diffraction peak, which means it contains mostly amorphous material, not crystalline ones. By combining the analysis results obtained from SEM, EDS, and XRD, the adhered material was agglomerates of fine particles, and mainly consisted of amorphous oxides of aluminum with a small portion of sulfur or sulfur compound along with salt.

Normally, the surface of pure aluminum undergoes oxidation in a very short time and becomes a thin layer (several nanometer) of amorphous aluminum oxide. Since this layer is quite dense and oxygen is unable to penetrate this layer, there ought to be no further oxidation inside this layer. However, when the aluminum is exposed to moisture, acids and bases for a long time, it forms white corrosion products. The major components of these white corrosion products are aluminum hydroxide ( $Al(OH)_3$ , bayerite) along with boehmite ( $AlO(OH)$ ) and  $Al_2O_3$ , all of which are known to be crystalline, rather than amorphous. On the contrary, the adhered white material found on the stern of ROKS Cheonan is white amorphous oxides of aluminum, which is assessed not to have experienced corrosion in a natural state.

## 2. Second Analysis (Material Adhered on the Stern)

Based on the first analysis results, samples were collected from five different locations on the stern on April 22, 2010 to perform more extensive analysis. Sample locations were near the center of the fracture plane, where a significant amount of the adhered powder was found, and included surfaces of different types of materials (aluminum and non-aluminum). The team also sampled from the 76mm naval gun barrel which was relatively far from the fracture plane.

Sample #	Location	Surface material
1	Aluminum angle bar in crew's mess kitchen	Aluminum alloy
2	Crew's mess kitchen wall (water fountain)	Aluminum alloy
3	Mesh cable of switch board in crew's mess kitchen	Non-Al alloy
4	Mesh cable above crew's mess kitchen	Non-Al alloy
5	76mm naval gun barrel	Iron

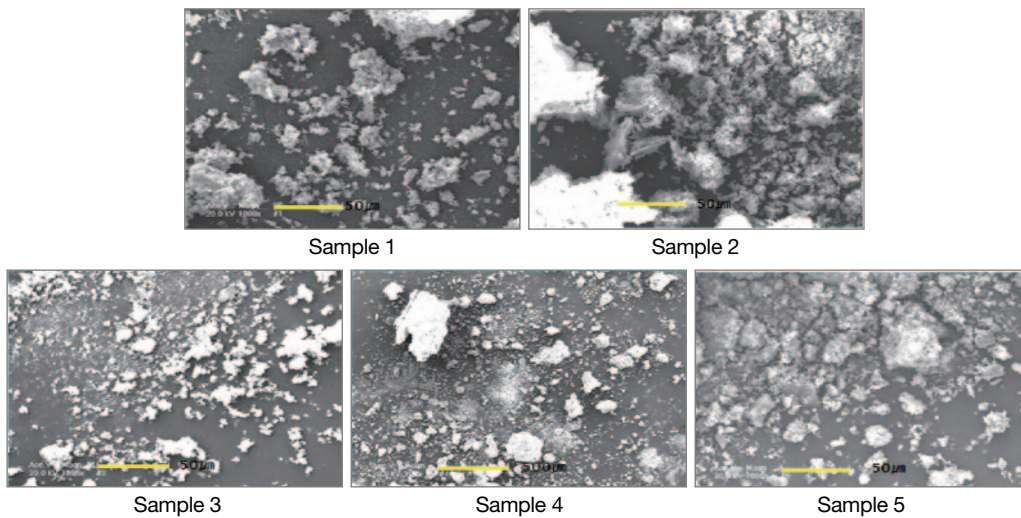
〈Table Appendix V-2-1〉 Sampling locations



〈Figure Appendix V-2-1〉 Sampling locations

Along with the instruments used in the first analysis, the second analysis utilized CHNS<sup>15</sup>-EA(CHNS - Elemental Analyzer, Thermo EA1112) and TGA(Thermal Gravity Analyzer, Mettler TA30).

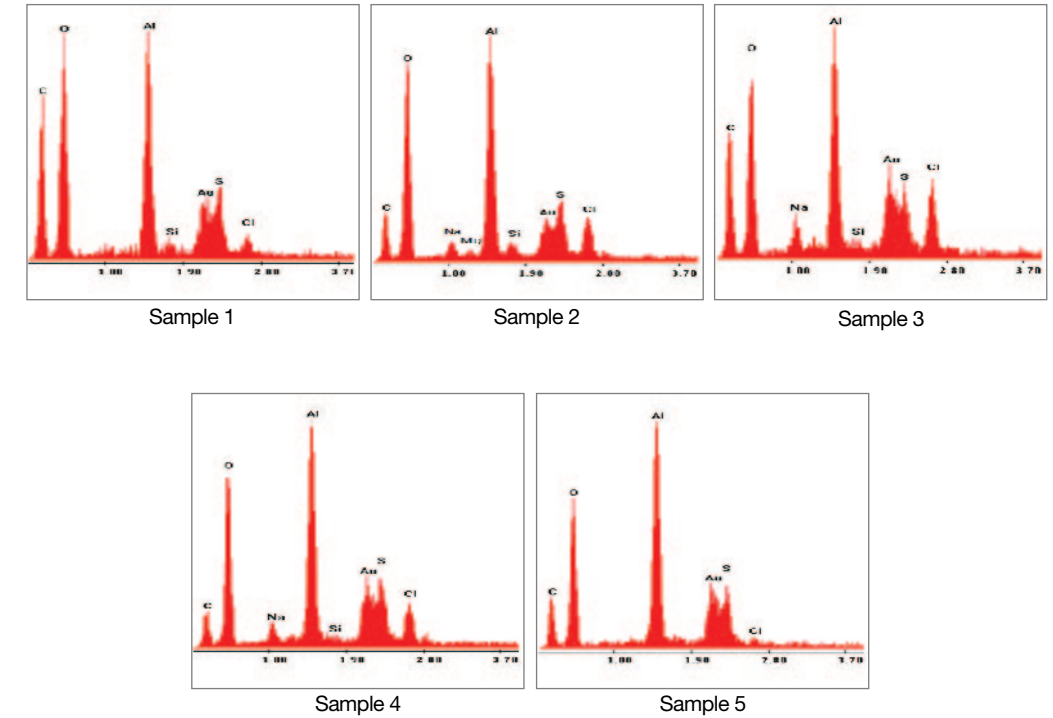
The SEM images of the collected samples showed agglomerates of fine particles, which were similar to those obtained in the first analysis(See 〈Figure Appendix V-2-2〉). In the EDS analysis, the detection range was increased to detect elements with low atomic weight, and consequently the carbon was detected.



〈Figure Appendix V-2-2〉 SEM images of the adhered material(stern)

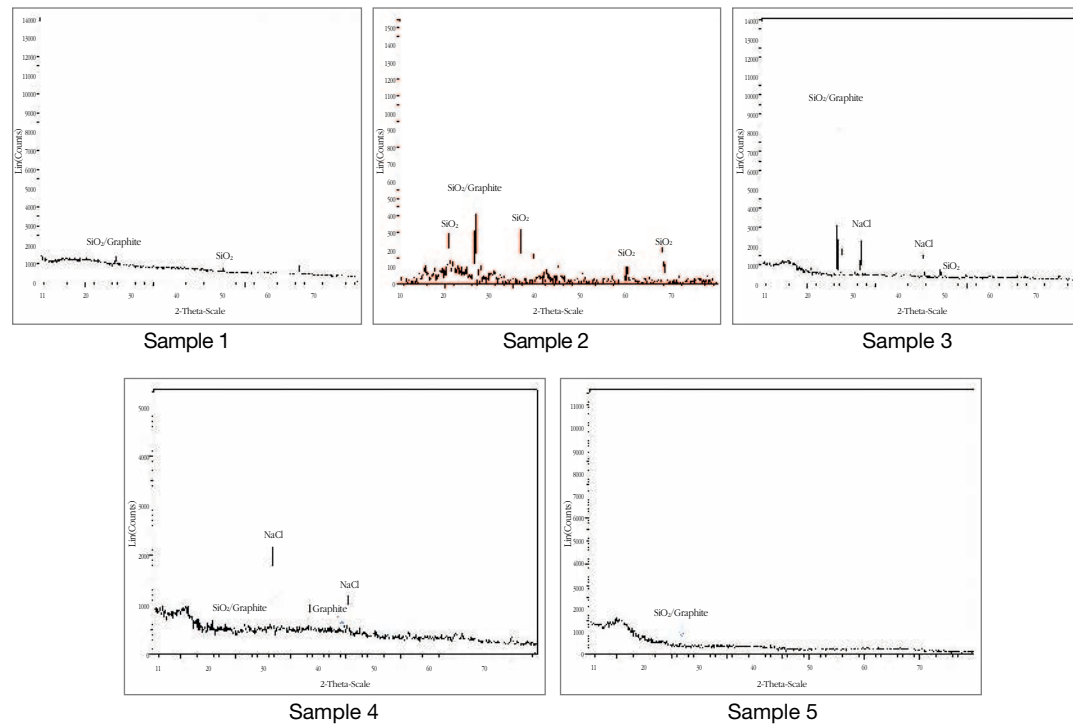
15) CHNS: Carbon Hydrogen Nitrogen Sulfur

As shown in 〈Figure Appendix V-2-3〉, all samples consisted of carbon, oxygen, sodium, magnesium, aluminum, silicon, sulfur, and chlorine. This result was similar to that of the first analysis. Considering the elemental composition, the adhered material consisted of oxides of aluminum( $Al_xO_y$ ), salts( $NaCl$ ,  $MgCl_2$ , etc.), and sulfur or sulfur compounds.



〈Figure Appendix V-2-3〉 EDS results of the adhered material(stern)

The XRD results showed silicon dioxide( $SiO_2$ ), graphite, and salt( $NaCl$ ) crystals from the adhered material. The overlap of the peaks of silicon dioxide and those of graphite made it difficult to distinguish one another, but a small peak at  $44.5^\circ$  diffraction angle clearly identified the presence of the graphite(See 〈Figure Appendix V-2-4〉 sample 4). The EDS results showed that the main component of the adhered material was oxides of aluminum, and the XRD results confirmed that the oxides of aluminum were amorphous.



〈Figure Appendix V-2-4〉 XRD results of the adhered material(stern)

CHNS elemental analysis(for analyzing the content of combustible elements in the adhered material) showed that nitrogen was absent, but carbon, hydrogen, and sulfur were present in amounts ranging from 0.64~3.00wt.%<sup>16)</sup>, 3.42~5.25wt.%, and 4.40~8.63wt.%, respectively(See 〈Table Appendix V-2-2〉). Combining this result with the EDS results, the adhered material was composed of solid-producing elements upon combustion such as aluminum, sodium, and silicon, and three gas-producing elements upon combustion, i.e. carbon, hydrogen, and sulfur. The hydrogen component appears to have come from the moisture.

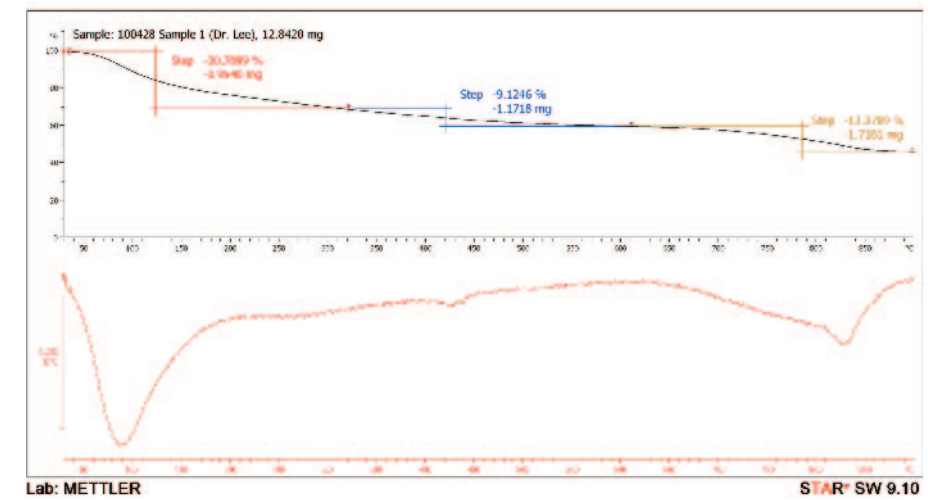
Sample name	Nitrogen(%)	Carbon(%)	Hydrogen(%)	Sulfur(%)
Sample 1	Below 0.01	0.64	4.45	5.21
Sample 2	Below 0.01	1.15	3.42	4.40
Sample 3	Below 0.01	3.00	4.56	4.87
Sample 4	Below 0.01	1.69	5.25	8.63

〈Table Appendix V-2-2〉 CHNS elemental analysis results

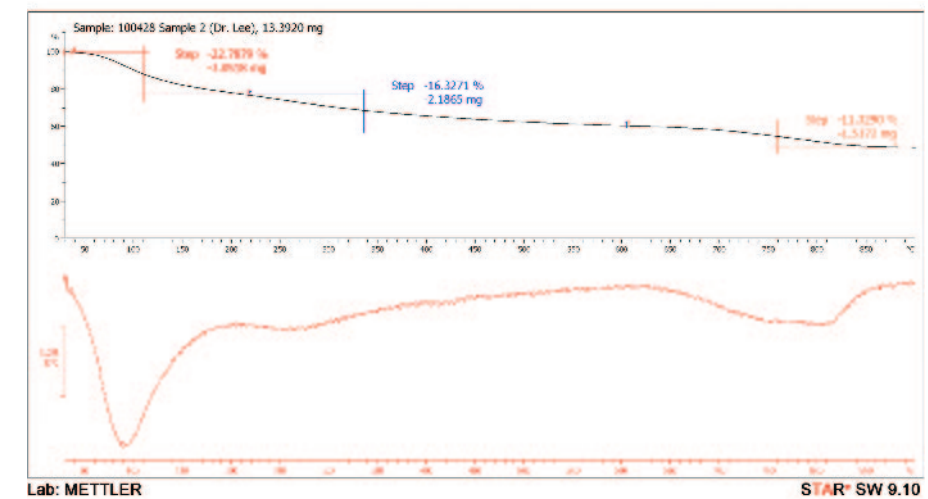
16) wt. % : weight %

The analysis of TGA pyrolysis for the adsorbed material was performed at temperature range of 30~900℃ and temperature increase rate of 10℃/min. The analysis on sample # 5 could not have been carried out due to shortage in the amount of the sample.

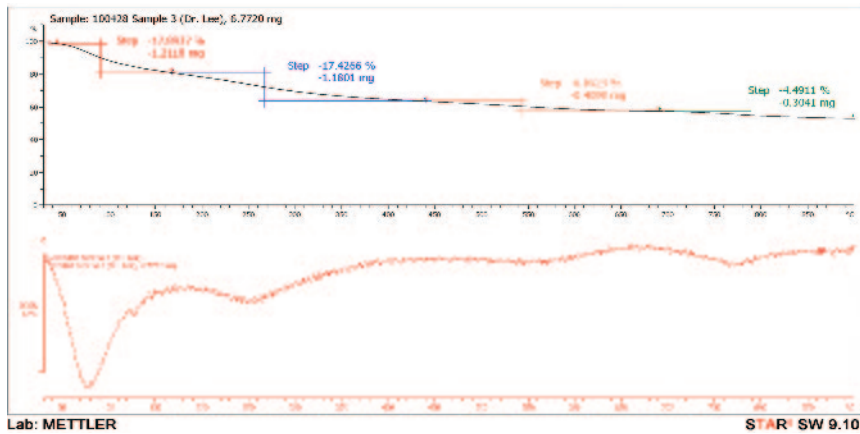
In a temperature range of 30 to 200℃, approximately 20% of the moisture evaporated. Additional 20% of the moisture evaporated slowly between 200℃ and 600℃. Above 600℃, carbon and sulfur components were oxidized and disappeared(See 〈Figure Appendix V-2-5〉). The detailed thermal analysis will be discussed later.



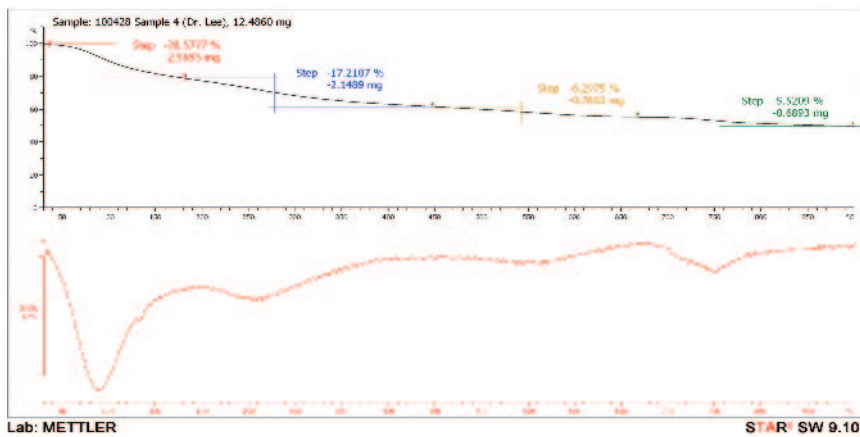
Sample 1



Sample 2



Sample 3



Sample 4

〈Figure Appendix V-2-5〉 TGA results of the adhered material(stern)

The analysis on the white adhered material of the stern showed that the adhered material was the agglomerates of fine particles, which was in good agreement with the assessment of the first analysis. It also showed that it consisted of mainly amorphous aluminum oxides with small amounts of sulfur or sulfur compounds along with salt and silicon dioxide. The composition was shown in 〈Table Appendix V-2-3〉. The water content was calculated using the hydrogen content obtained from CHNS-EA.

Component	Content(% weight)	Remarks
Al <sub>x</sub> O <sub>y</sub>	36.4 ~ 55.1	Contains small portion of silicon dioxide
Water	30.8 ~ 47.3	
Sulfur	4.4 ~ 8.6	
Carbon	0.6 ~ 3.0	Some portion of graphite
Salt	3.7 ~ 10.3	

〈Table Appendix V-2-3〉 Composition of the adhered material

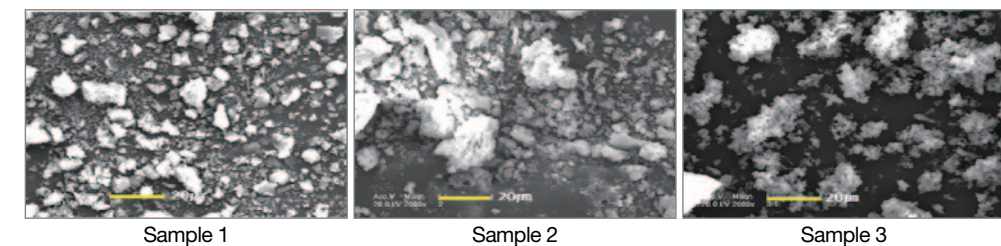
### 3. Third Analysis(Material Adhered on the Bow and Stack)

After visual identification of the bow on April 30, 2010, a similar adhered material was found; especially, an enormous amount of white powder was also observed on the inner and outer platings of the stack. To compare the composition of these white powders with the adhered material found on the stern, the JIG collected samples from two locations on the bow and one location on the stack as shown in 〈Table Appendix V-3-1〉.

Sample #	Collected Locations	Surface Material
1	76mm naval gun barrel	Iron
2	Portside entrance	Aluminum alloy
3	Stack	Aluminum alloy

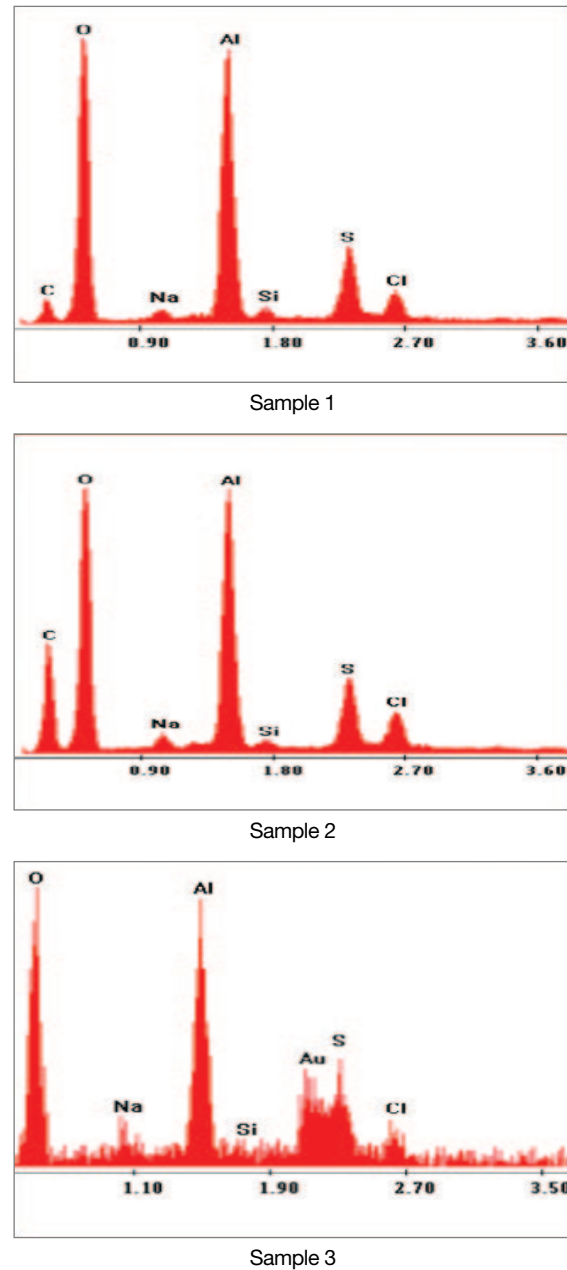
〈Table Appendix V-3-1〉 Sampling locations

The same equipments utilized in the first analysis were employed. The SEM images of this adhered material were similar to those of the stern(See 〈Figure Appendix V-3-1〉).



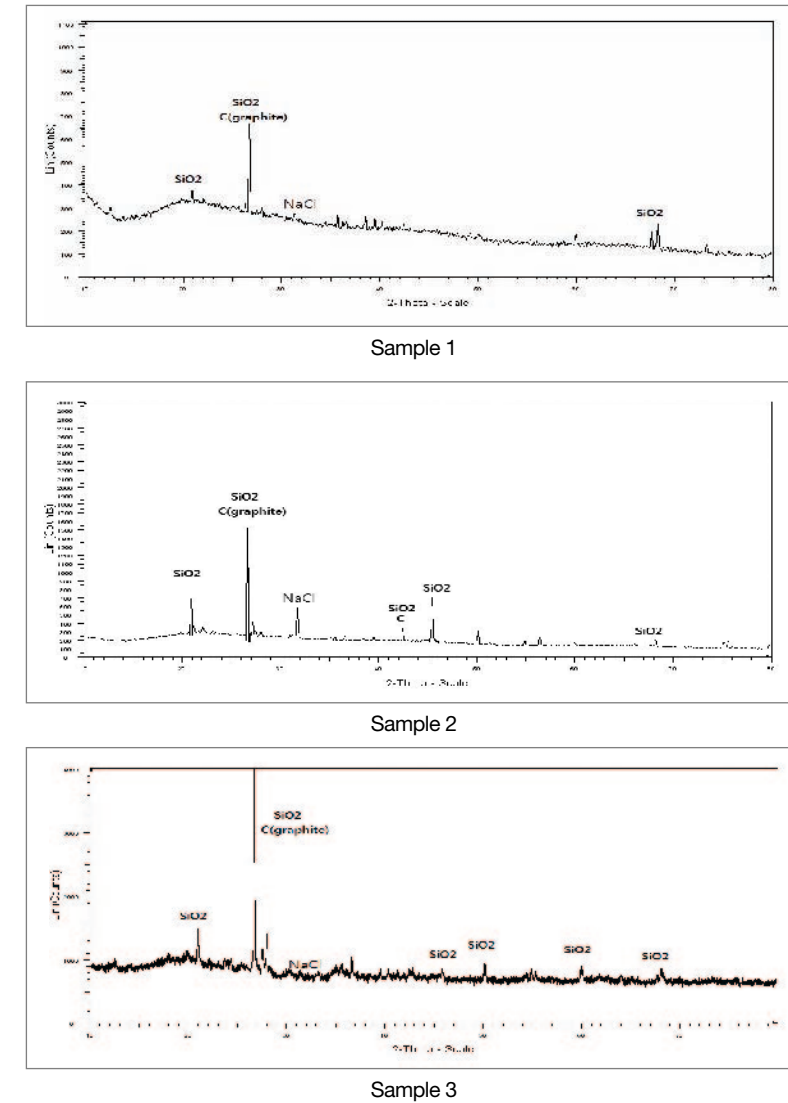
〈Figure Appendix V-3-1〉 SEM images of the adhered material(bow and stack)

As shown in <Figure Appendix V-3-2>, the EDS analysis results showed that the adhered material from both the bow and stack consisted of carbon, oxygen, sodium, magnesium, aluminum, silicon, sulfur, and chlorine. This result was similar to those of stern side samples.



<Figure Appendix V-3-2> EDS results of the adhered material(bow and stack)

The XRD results confirmed that silicon dioxide( $\text{SiO}_2$ ), graphite, and salt( $\text{NaCl}$ ) crystals were present from the adhered material and that the main component of the adhered material was oxides of aluminum. These results are in good agreement with those of stern sample(See <Figure Appendix V-3-3>).



<Figure Appendix V-3-3> XRD results of the adhered material(bow and stack)

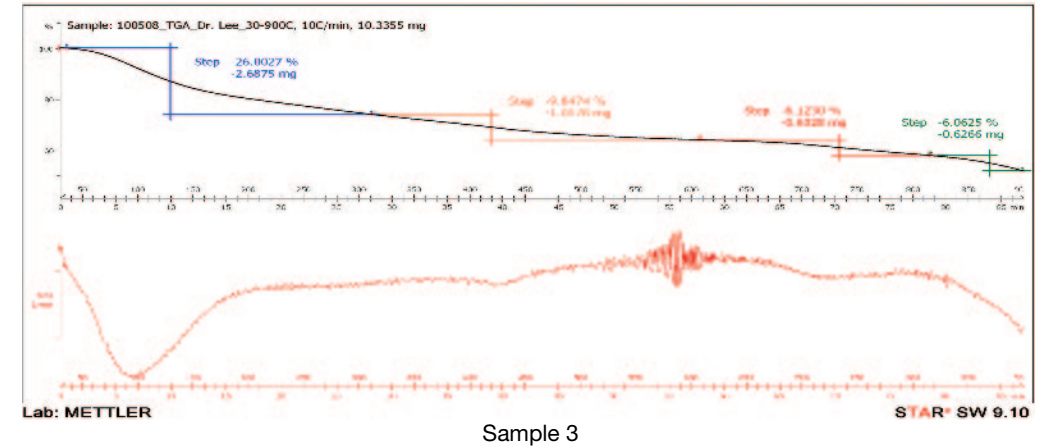
CHNS elemental analysis confirmed carbon, hydrogen, and sulfur to be 0.76~1.12wt.%, 3.62~3.93wt.%, and 2.43~3.58wt.%, respectively(See <Table Appendix V-3-2>), which was similar to those of the stern samples.

Sample name	Nitrogen(%)	Carbon(%)	Hydrogen(%)	Sulfur(%)
Sample 1	Below 0.01	0.76	3.93	3.50
Sample 2	Below 0.01	1.12	3.62	2.43
Sample 3	Below 0.01	0.84	3.63	3.58

〈Table Appendix V-3-2〉 CHNS elemental analysis results

The same conditions for the TGA pyrolysis of the adhered material were employed as those of stern samples; namely, the temperature range of 30~900℃ and the temperature increase at the rate of 10℃/min.

The pyrolysis results were similar to those results from the stern samples(See 〈Figure Appendix V-3-4〉).

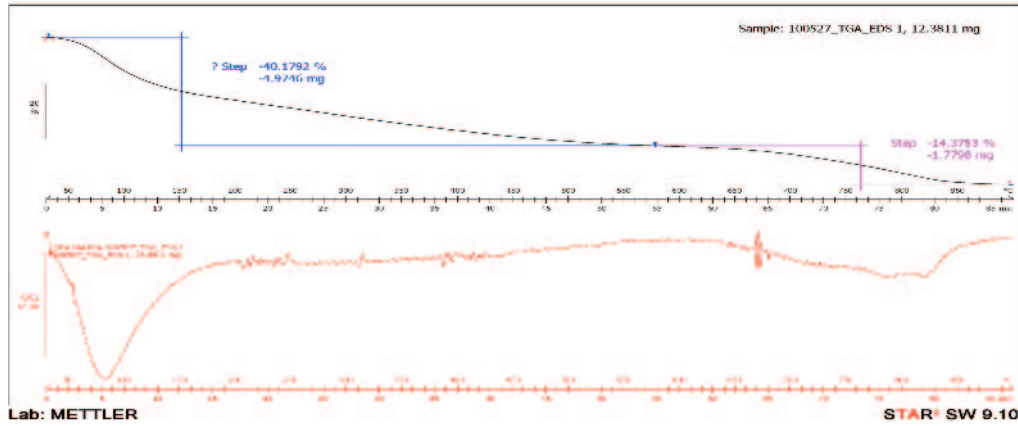


〈Figure Appendix V-3-4〉 TGA results of the adhered material(bow and stack)

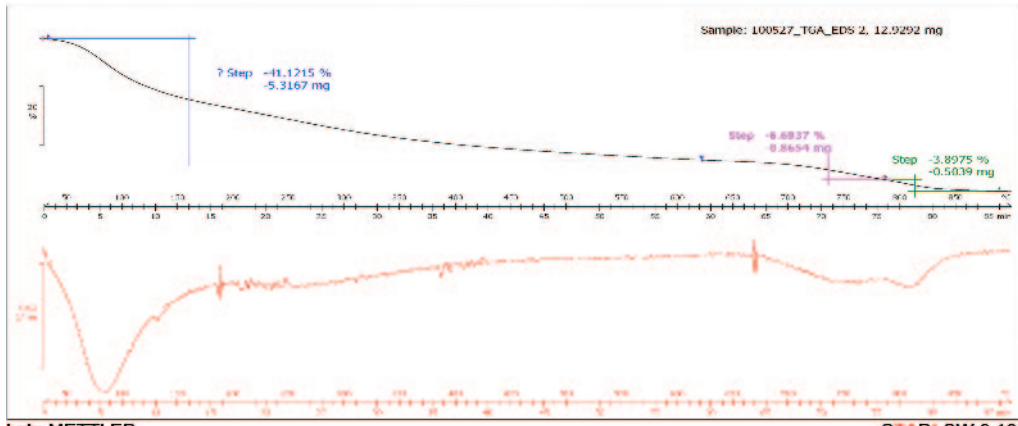
The analysis results of the white adhered material on the bow and stack were identical to those of the stern samples, and the adhered material consisted of mainly amorphous oxides of aluminum and small amounts of sulfur or sulfur compounds along with salt and silica. The composition was shown in 〈Table Appendix V-3-3〉.

Component	Content(% weight)	Remarks
Al <sub>x</sub> O <sub>y</sub>	53.5 ~ 54.6	Contains small portion of silicon dioxide
Water	32.6 ~ 35.4	
Sulfur	2.4 ~ 3.6	
Carbon	0.8 ~ 1.1	Some portion of graphite
Salt	6.9 ~9.3	

〈Table Appendix V-3-3〉 Composition of the adhered material(bow and stack)



Sample 1



Sample 2

#### 4. Fourth Analysis(Adhered Material on the Propulsion Section of the Torpedo)

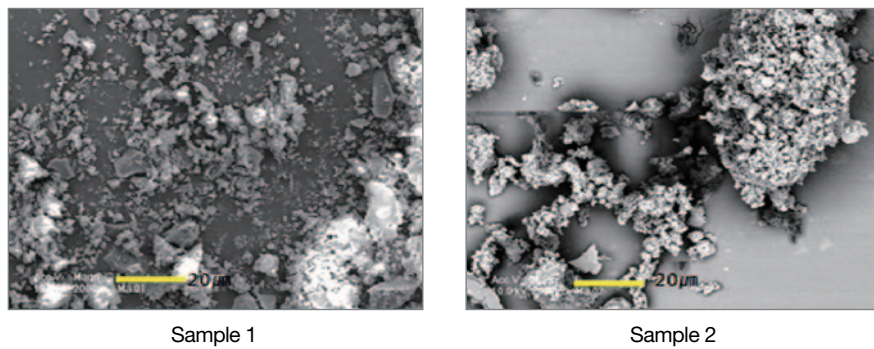
After visual examination of the propulsion motor system upon the salvage on May 15, white adhered material was found on the surface of propulsion section and inside the motor. Visually, it appeared to be the same material found in the fractured surfaces of ROKS Cheon-

nan. In order to investigate whether they were the same material as those found on ROKS Cheonan, the JIG collected samples from each part as shown in <Table Appendix V-4-1>.

Sample #	Location	Surface material
1	Salvaged torpedo propulsion section	Aluminum Alloy
2	Salvaged torpedo motor	Iron

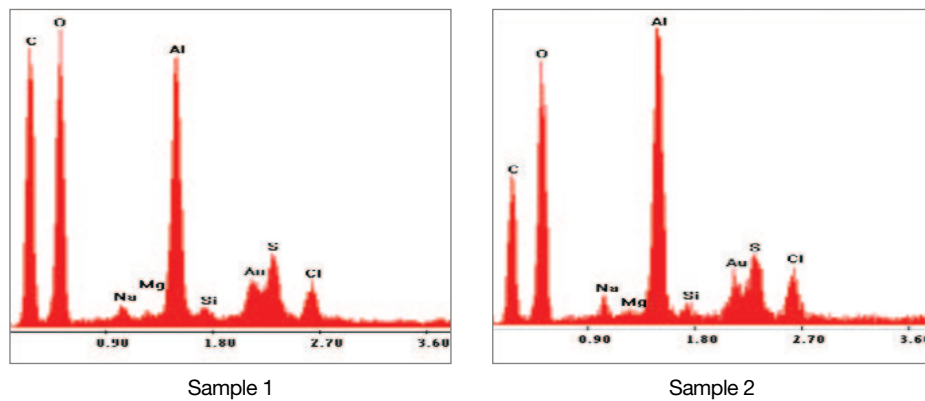
<Table Appendix V-4-1> Sampling locations

The analysis utilized the same apparatus used in the first and second analyses except elemental analysis, where the model EA1110 of CE Instruments was used. The SEM images of these two samples of the adhered materials were similar to those of hull samples.



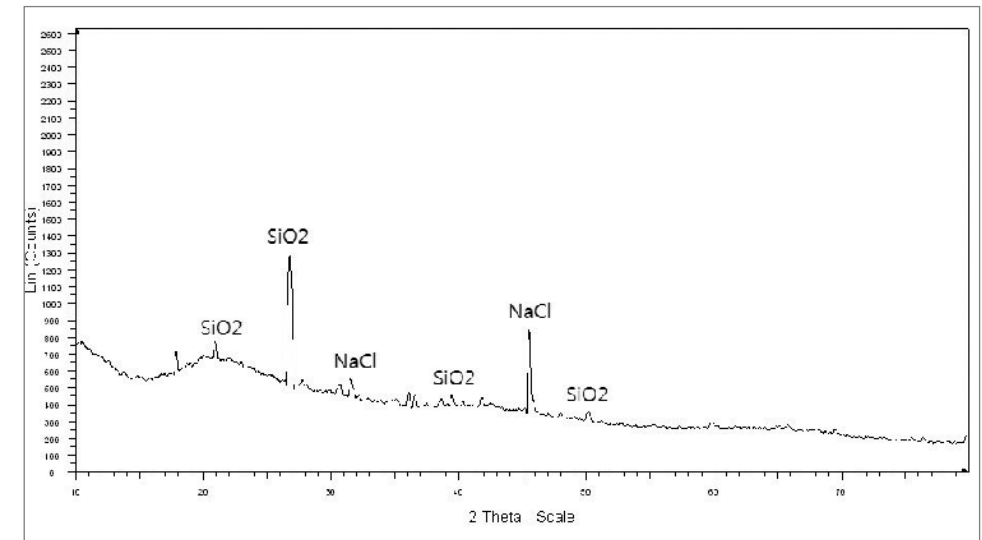
<Figure Appendix V-4-1> SEM images of the adhered material(propulsion section and motor)

As shown in <Figure Appendix V-4-2>, the EDS analysis results showed that the adhered material consisted of carbon, oxygen, sodium, magnesium, aluminum, silicon, sulfur, and chlorine. Those results were similar to those of hull samples.

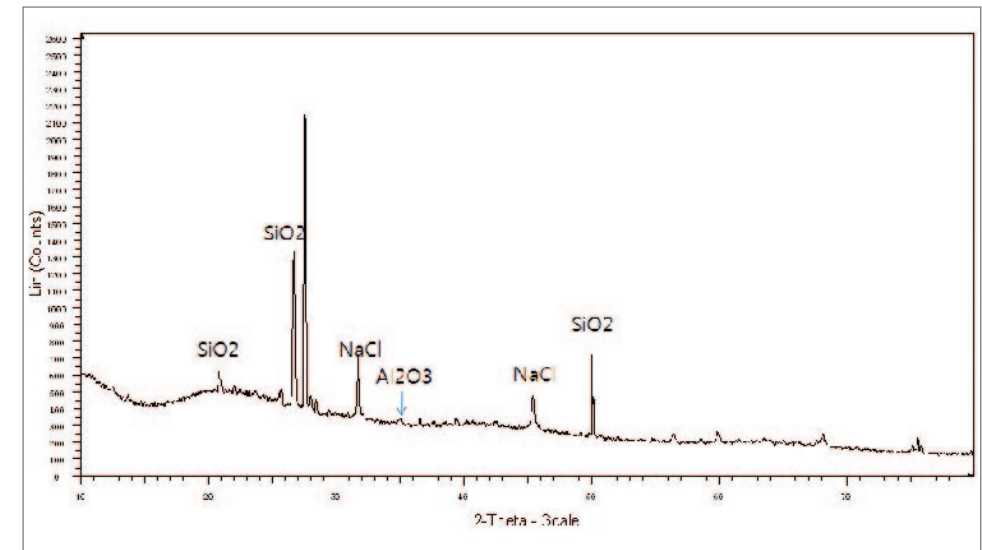


<Figure Appendix V-4-2> EDS results of the adhered material(propulsion section and motor)

The XRD results confirmed that silicon oxide( $\text{SiO}_2$ ) and salt( $\text{NaCl}$ ) crystals were present. The peak positions of the two samples were reasonably similar. Although the peak size was almost negligible, an aluminum oxide( $\text{Al}_2\text{O}_3$ ) crystal peak was also observed(See <Figure Appendix V-4-3>).



Sample 1

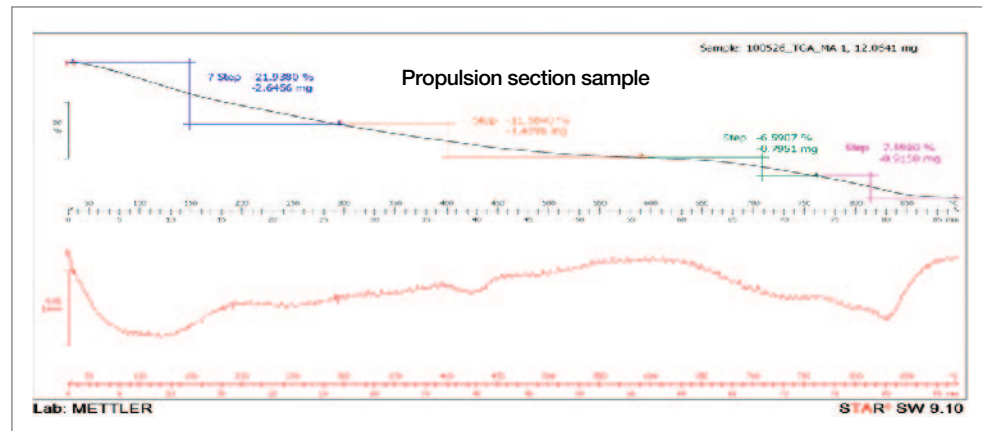


Sample 2

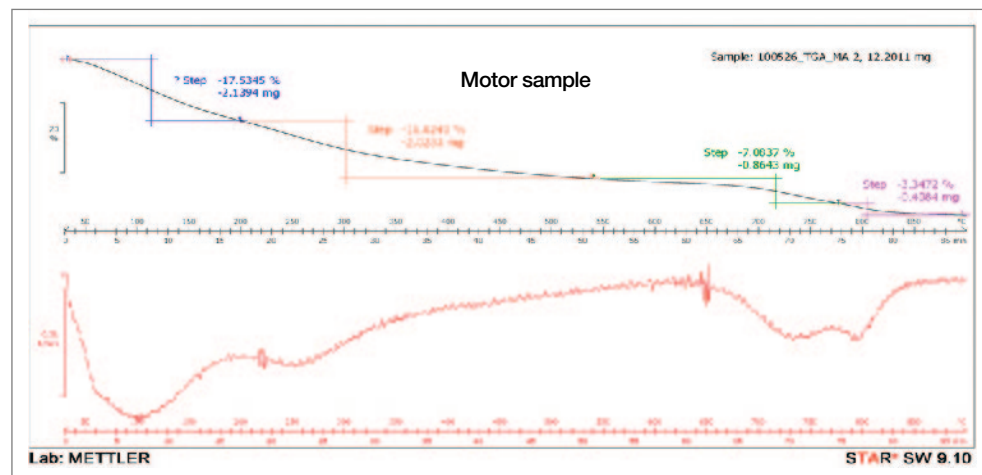
<Figure Appendix V-4-3> XRD results of the adhered material(propulsion section and motor)

Combining the EDS results with the XRD ones, the main component of the adhered material was oxides of aluminum, the majority of which was in amorphous form. These results concurred with those of stern samples.

The results of CHNS elemental analysis for identifying combustible elements showed that nitrogen was hardly found, and the contents of carbon, hydrogen, and sulfur were 0.40~0.86wt.%, 3.29~3.34wt.%, and 5.60~6.61wt.%, respectively. These results were similar to those of hull samples. In the TGA pyrolysis performed under the same analysis conditions with the hull samples, the results were similar to those of hull samples as well(See <Figure Appendix V-4-4>).



Sample 1



Sample 1

<Figure Appendix V-4-4> TGA results of the adhered material(propulsion section and motor)

As a summary of all the analysis results, the adhered materials from the propulsion section and the motor of the torpedo were the same type of material, and the adhered material consisted of mainly amorphous oxides of aluminum with a small amount of sulfur or sulfur compounds along with salt and silica. The composition is shown in <Table Appendix V-4-2>.

As will be discussed in the conclusion section, it was assessed that the adhered material was a product of underwater explosive with a substantial portion of aluminum.

Component	Content(% weight)	Remarks
Al <sub>x</sub> O <sub>y</sub>	53.9 ~ 54.3	Contains small portion of silicon dioxide
Water	29.6 ~ 30.1	
Sulfur	5.6 ~ 6.6	
Carbon	0.4 ~ 0.9	
Salt	8.6 ~ 10.1	

<Table Appendix V-4-2> Composition of the adhered material(propulsion section and motor)

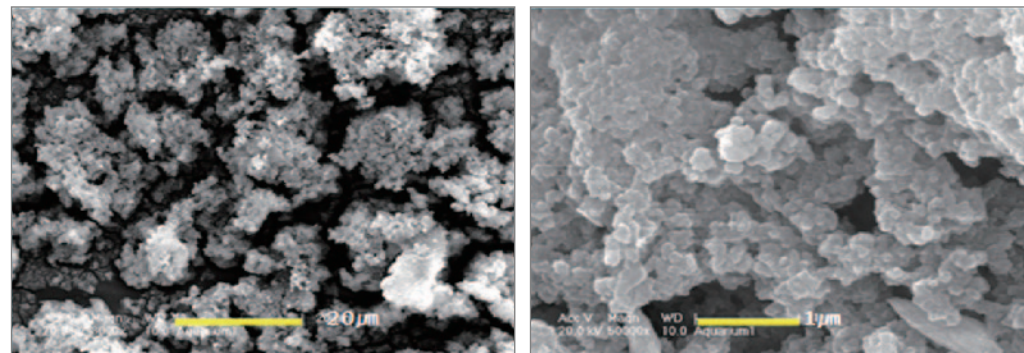
## 5. Fifth Analysis(Material Acquired from Small-scale UNDEX Experiment)

The analysis conducted small-scale UNDEX experiments in order to compare the adsorbed material found on the hull and torpedo with the explosion products from an underwater explosive formulation containing aluminum.

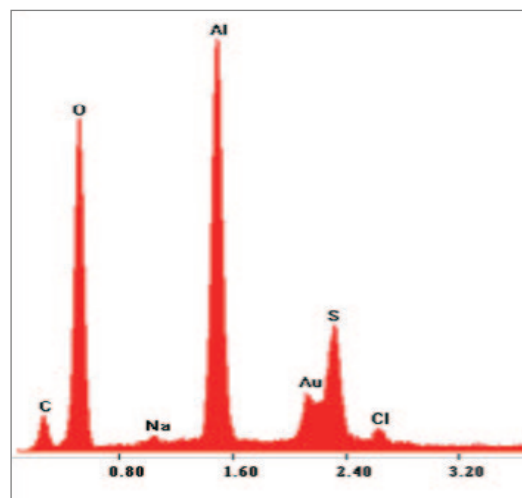
A water tank of 2m length × 1.5m width × 1.5m height was used with transparent polycarbonate window on the front side, and it was filled with 4.5 tons of sea water. An aluminum plate was installed on top of the tank in order to collect the samples, and detonated 15 grams of HBX-3 explosive(TNT 29%, RDX 36%, Al 35%) in the center of the tank. The propagation of the shockwave and the expansion-contraction-elevation processes of the bubble were observed through a high-speed camera. After the explosion, a small amount of explosion products(a few milligrams) was adsorbed on the plate. Since adsorbed samples were too small, the XRD analysis, which requires a relatively larger amount of samples, was conducted using the aluminium plate itself with explosion products adsorbed on

its surface. For the EDS analysis, the adsorbed material was extracted from the plate.

The adsorbed samples were agglomerates of fine particles. The sizes of the fine particles were less than a micrometer (See <Figure Appendix V-5-1>). According to the EDS results shown in <Figure Appendix V-5-2>, the samples obtained from small-scale UNDEX experiment consisted of carbon, oxygen, sodium, magnesium, aluminum, silicon, sulfur, and chlorine. The results were almost identical to the compositions from the hull and torpedo samples.

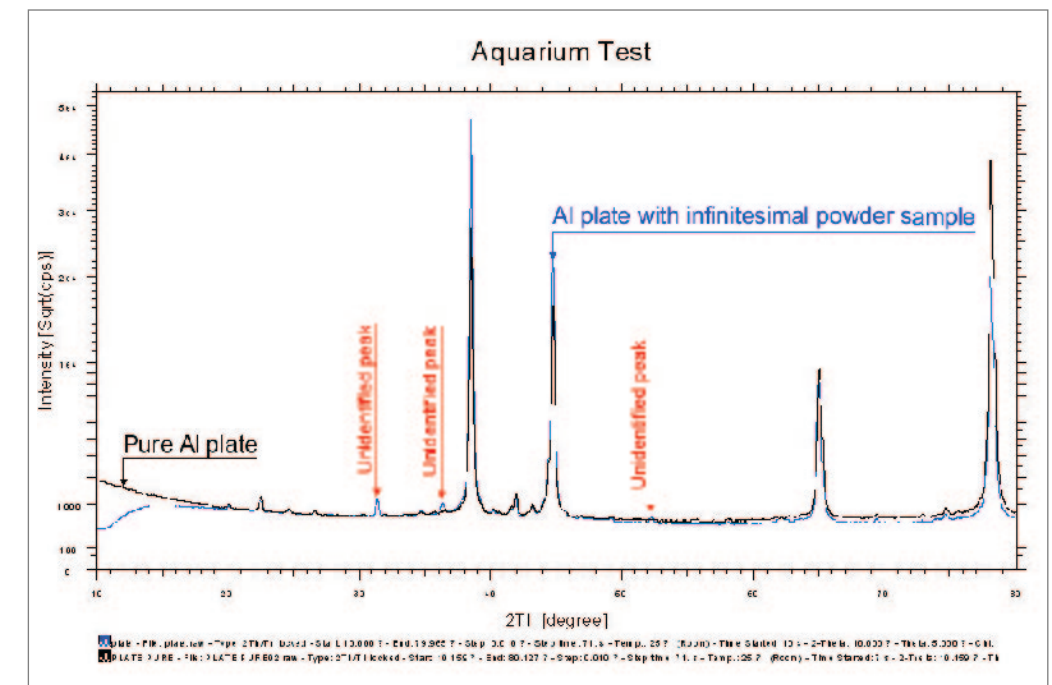


<Figure Appendix V-5-1> SEM images of the explosion products

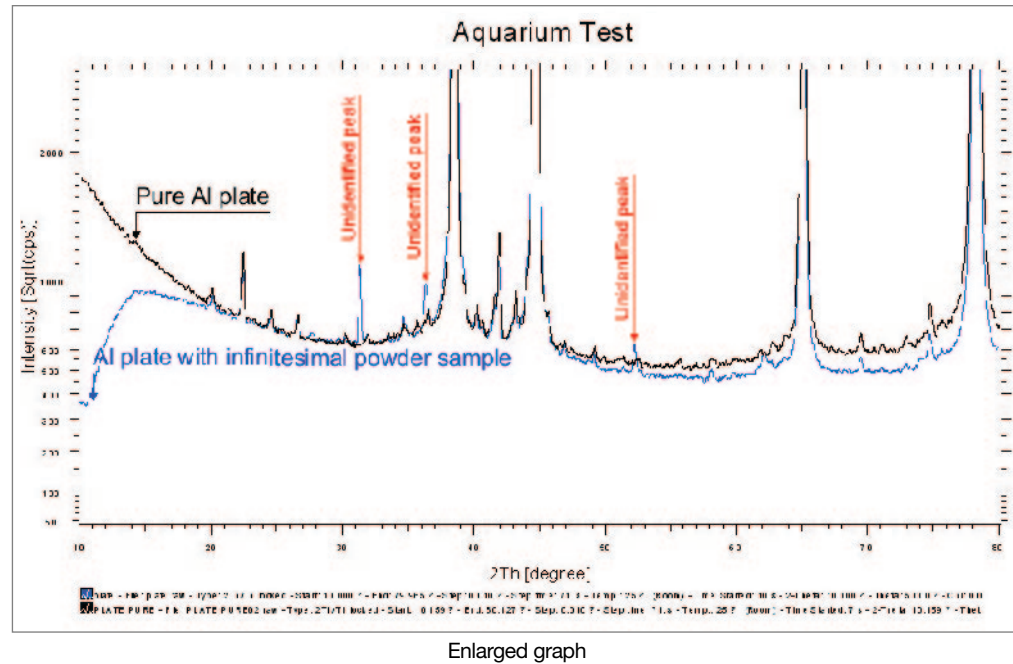


<Figure Appendix V-5-2> EDS analysis of UNDEX sample

Since XRD analysis was conducted using the aluminum plate with a small amount of underwater explosion products adsorbed on the surface, the aluminum crystal peak became apparent while the peaks of other substances were relatively weak in comparison. In <Figure Appendix V-5-3>, the XRD result of the explosion products adhered to an aluminum plate was depicted along with the one of the aluminum plate only. When the weak peaks were magnified, crystalline aluminum oxide was rarely observed. This happened because nearly all of the oxides of aluminum were found in amorphous form, which did not appear in the XRD analysis. Other weak peaks were identified to be irrelevant to the aluminum oxide. Through these analysis results, it was found that underwater explosive formulations containing aluminum powder produced amorphous oxides of aluminum upon explosion, as were also found in the hull and torpedo samples. However, the compositions of the explosion products may vary depending on the composition of underwater explosive formulations, amount of explosives, and condition of explosion.



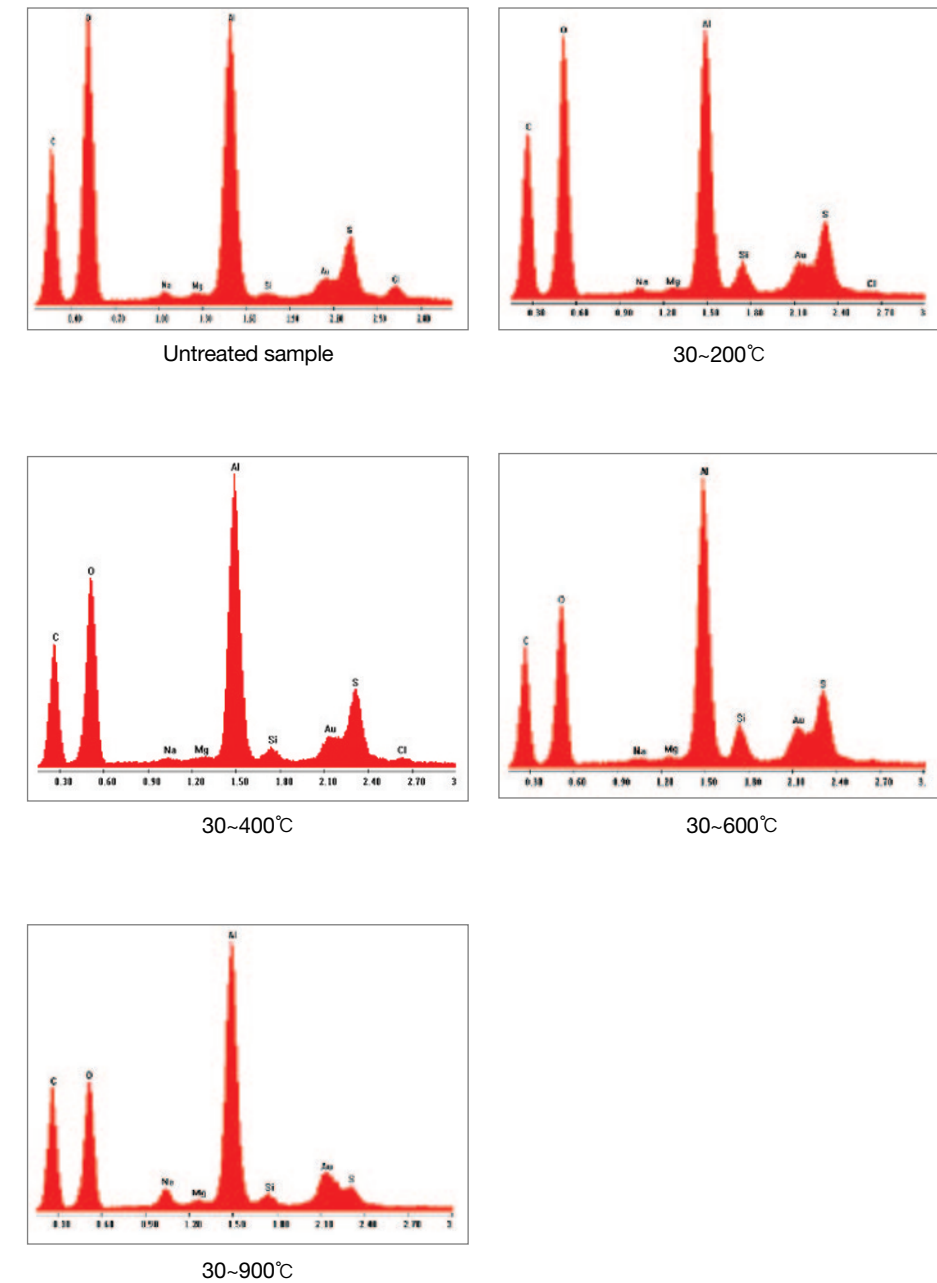
Original graph



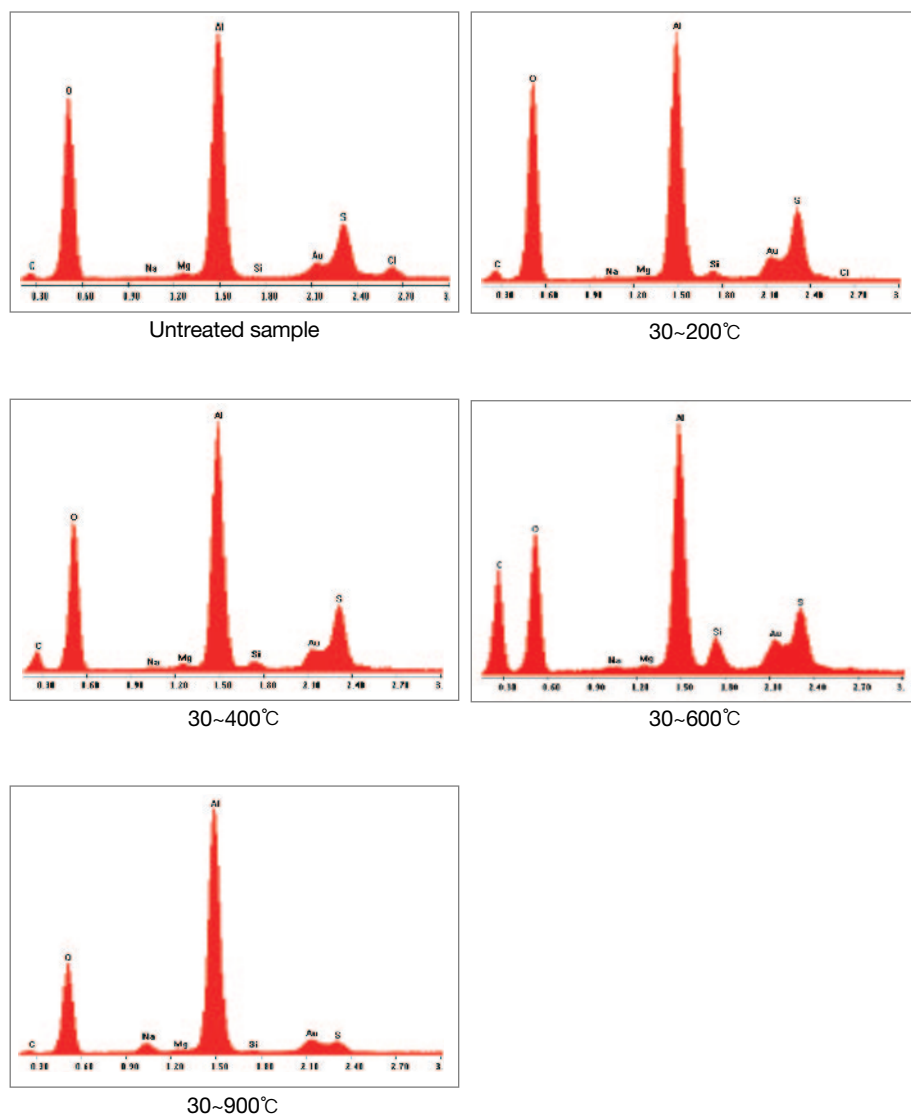
〈Figure Appendix V-5-3〉 XRD results of the explosion products

## 6. Thermal Characteristics and Microstructure of the Adhered Material

The analysis pyrolyzed the adhered material at different temperature ranges(30~200℃, 30~400℃, 30~600℃, 30~900℃) under nitrogen atmosphere and subsequently performed the EDS analysis with pyrolyzed products in order to comprehend thermal characteristics of the adhered material. The analysis areas for the EDS analysis were 0.25mm×0.20mm, or 0.50mm×0.40mm(See 〈Figure Appendix V-6-1〉). In addition, the team also performed a spot analysis with the agglomerate of particles(See 〈Figure Appendix V-6-2〉) and compared with the area analyses. When two different sets of EDS results were compared, the difference of carbon compositions was attributed to the adhesive tape used in the area analysis. Accordingly, the oxygen composition was also changed slightly.



〈Figure Appendix V-6-1〉 Change of elemental composition of adhered materials in EDS area analysis with different heat treatment



〈Figure Appendix V-6-2〉 Change of elemental composition of adhered materials in EDS spot analysis with different heat treatment

As was shown in two figures, mainly the oxygen content was decreased between 30 and 600 °C. Upon further increase of the temperature, carbon and sulfur disappeared.

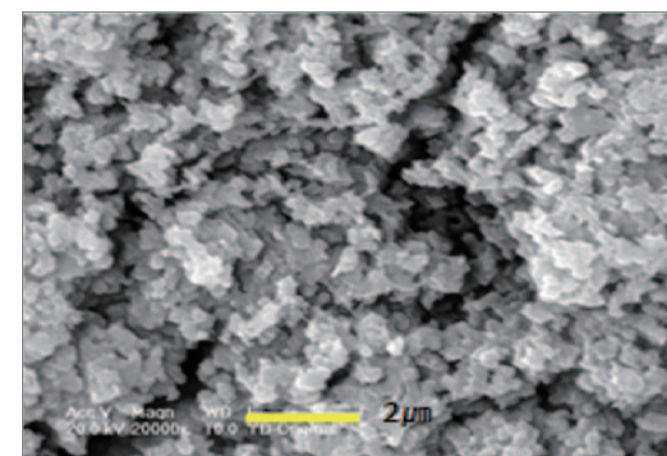
In 〈Table Appendix V-6-1〉, compositions of oxygen and aluminum are summarized in both area and spot analyses in different temperature ranges. Elemental composition was calculated by considering the oxygen content in silica. Oxygen/aluminum ratio of the sample pyrolyzed from 30 to 200 °C was quite similar with that of the unpyrolyzed sample.

This happened due to the evaporation of the moisture in the treatment of samples including vacuum at the EDS analysis of the unpyrolyzed sample. TGA analysis showed that approximately 50% of the moisture evaporated in the temperature range of 30 to 200 °C. Further increase of the pyrolysis temperature prompted the oxygen content to diminish due to the evaporation of the moisture entrapped in micro pores(See 〈Figure Appendix V-6-3〉) and/or strongly interacted with the adhered material.

Generally, it is known that EDS analysis on a mixture of ununiform particles cannot give an accurate quantitative information on the element composition. In this regard, 〈Table Appendix V-6-1〉 shows the qualitative trend of change in oxygen and aluminum composition with heat-treatment temperature.

Sample Name	Area Analysis		Spot Analysis	
	O(Atom %)	Al(Atom %)	O(Atom %)	Al(Atom %)
Raw sample	72.90	27.10	68.24	31.76
30~200°C	71.29	28.71	69.31	30.69
30~400°C	65.93	34.07	64.42	35.58
30~600°C	61.05	39.95	61.39	39.61
30~900°C	60.57	39.43	56.80	43.20

〈Table Appendix V-6-1〉 Change of O/Al composition ratio in EDS analysis with different heat treatment

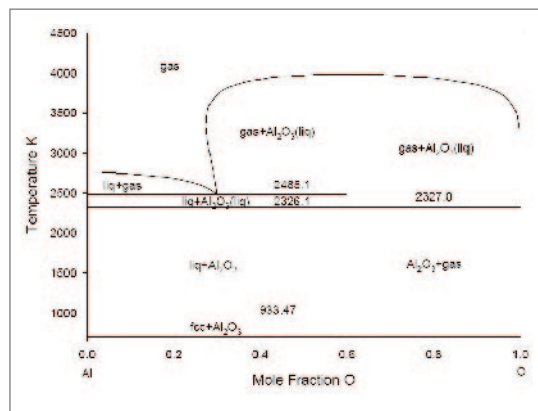


〈Figure Appendix V-6-3〉 Microstructure of the adhered material

## 7. Amorphous aluminum oxide

As mentioned previously, pure aluminum becomes covered with a very thin (several nm) film of amorphous aluminum oxide in a short time upon production. This amorphous aluminum oxide film is too dense for oxygen to penetrate, and prevents further oxidation inside the film. However, when it is exposed to the moisture, alkalies, or acids for a long time, it undergoes further oxidation to form a white product, the main compositions of which are aluminum hydroxide ( $\text{Al}(\text{OH})_3$ , bayerite), boehmite ( $\text{AlO}(\text{OH})$ ), and aluminum oxide ( $\text{Al}_2\text{O}_3$ ). This corrosion product is not in amorphous form, but rather in a crystalline form. There have been numerous reports that corrosion products become crystalline oxides of aluminum when aluminum is corroded by sea water or salinity in the shore.

To produce amorphous aluminum oxide ( $\text{Al}_x\text{O}_y$ ), aluminum oxide should be liquid when produced, and be cooled rapidly. It is impossible to make amorphous by cooling the solid. <Figure Appendix V-7-1> illustrates the phase diagram of aluminum oxide according to the change of composition ratio between aluminum oxide and oxygen, and shows that  $\text{Al}_2\text{O}_3$  exists as liquid above  $2325.1^\circ\text{C}$  and stays as solid below  $2325.1^\circ\text{C}$ . Thus, to be amorphous, aluminum oxide should be liquified at the temperature of higher than  $2325.1^\circ\text{C}$  and cooled rapidly.



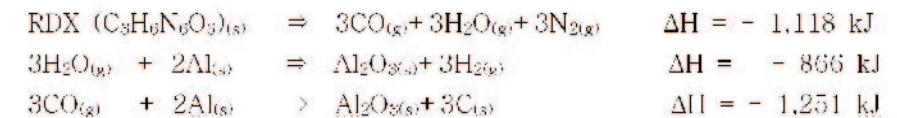
<Figure Appendix V-7-1> AL-O Binary Phase Diagram<sup>17)</sup>

17) Yajun Liu, "The Kinetics of Incongruent Reduction Between Sapphire and Mg-Al Melts" Phd Thesis, Georgia Institute of Technology, 2006.

Besides the condition mentioned above, aluminum oxide becomes amorphous if it is not able to form proper crystalline lattices by reacting between aluminum and oxygen with improper stoichiometry.

Thus, amorphous aluminum oxide ( $\text{Al}_x\text{O}_y$ ) is produced by either explosions or plasma reactions, which accompany rapid oxidation, high temperature heating, and rapid cooling.

Aluminum oxide is usually incorporated to underwater explosive formulations to augment bubble energy by using high combustion energy of aluminum. Explosion reactions take place in less than 10 microseconds at the temperature of higher than  $3,000^\circ\text{C}$  and the pressure above 200,000 atm. During an explosion, aluminum powder reacts with the oxygen in the explosion products, and is subsequently converted to aluminum oxides generating a large quantity of heat. The chemical reaction scheme to form aluminum oxide from explosion is shown as below. This aluminum oxide produced is cooled at a rate of several tens to hundreds thousand degrees per second less than several tens milliseconds.

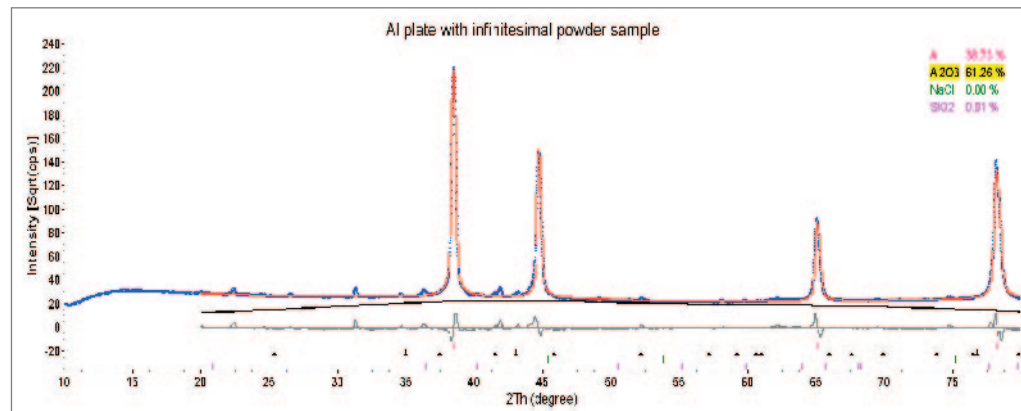
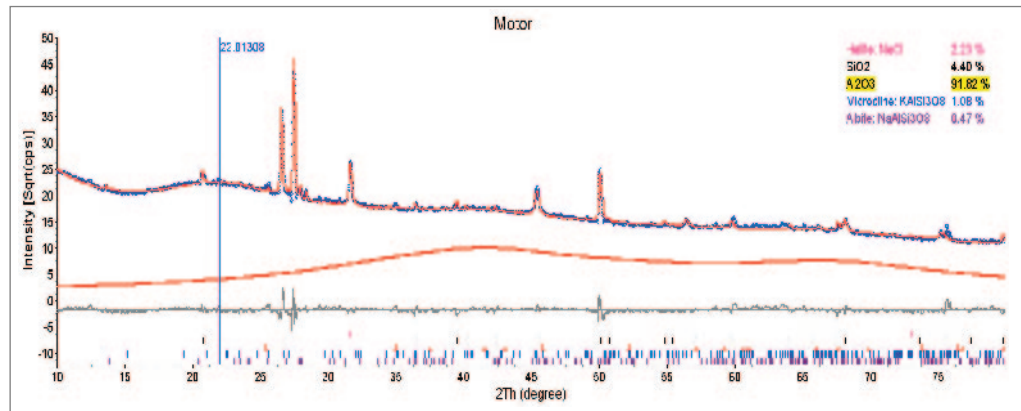
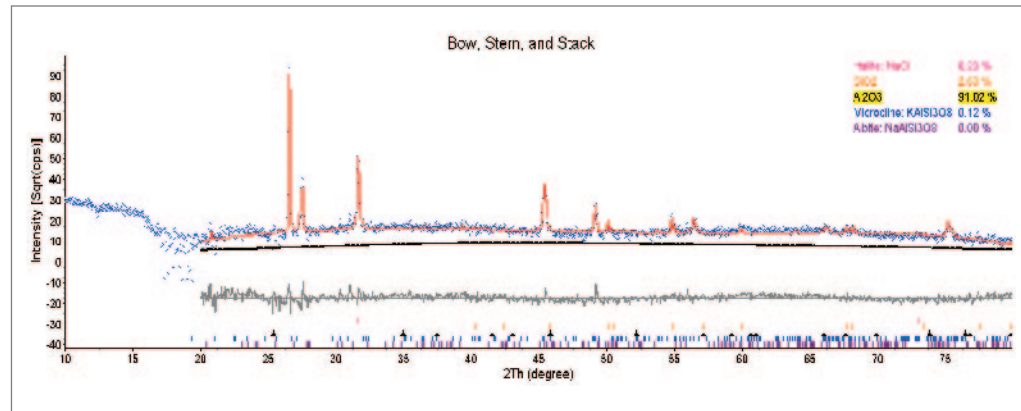


Aluminum oxide which is produced as a component of explosion products from aluminum based explosive formulations is known to be amorphous. As explained previously, producing amorphous aluminum oxide by explosion is attributed to the reaction between aluminum and oxygen with improper stoichiometry in an extremely fast oxidation (explosion), and/or the formation of improper crystalline lattices in a rapid cooling process from liquid to solid.

In order to identify whether aluminum oxide of the adhered material was amorphous, a detailed XRD analysis was performed with the TOPAS program<sup>18)</sup> and pyrolysis experiments of the adhered material.

According to the detailed XRD analysis with the TOPAS program, the adhered materials from both the hull of ROKS Cheonan and torpedo propulsion section were composed of more than 90% of amorphous aluminum oxide. In addition, explosion products of UNDEX experiments were also analyzed to have mostly amorphous aluminum oxide, except crystalline ones from the aluminum plate (See <Figure Appendix V-7-2>).

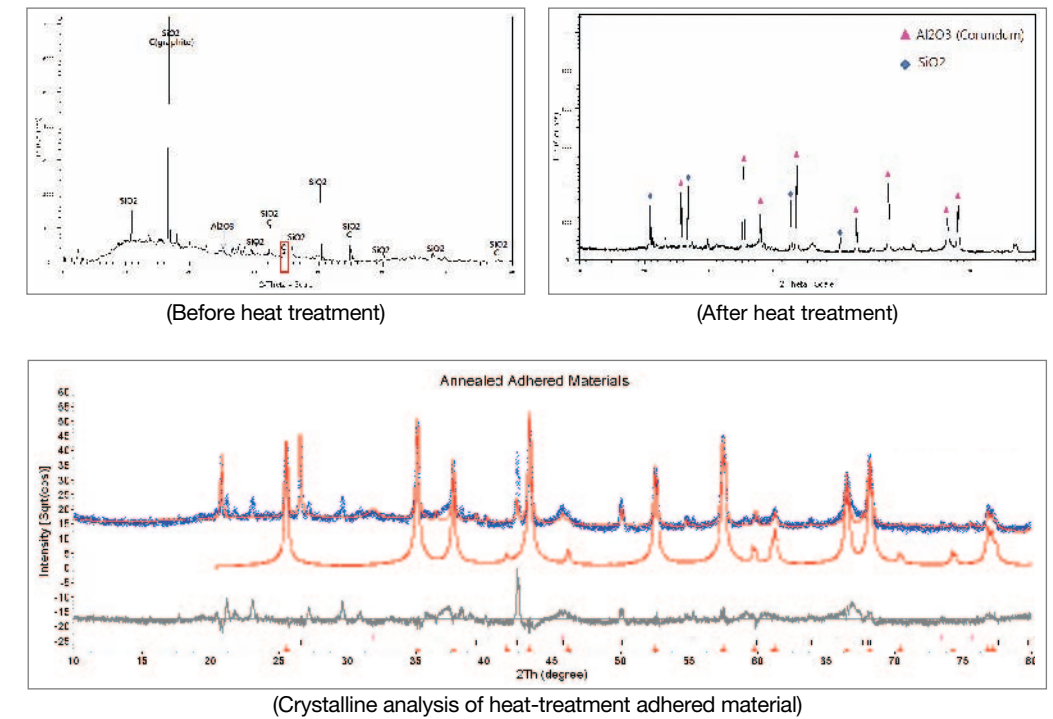
18) TOPAS program: Stands for Total Pattern Analysis Solution, and is a software used to analyze the X-ray diffraction data.



〈Figure Appendix V-7-2〉 Analysis of amorphous Al<sub>2</sub>O<sub>3</sub> content

In general, amorphous materials are usually transformed to crystalline ones by heat treatment at an appropriate temperature below the melting point. If a crystalline aluminum oxide is found in heat-treated material, in which no crystalline aluminum oxide nor crystalline aluminum was found originally, the material should have an amorphous aluminum oxide as an ingredient in it. To comprehend this, the adhered material collected from the hull of ROKS Cheonan was heated to 1,200 °C for 30 min. and cooled slowly in an ambient condition. The change of crystallinity before and after the heat treatment was compared.

The XRD results depicted in 〈Figure Appendix V-7-3〉 showed that the main component of the adhered material before the heat treatment was silica (including a small amount of graphite), and crystalline aluminum oxide (Al<sub>2</sub>O<sub>3</sub>) was produced and graphite disappeared after the heat treatment. Thus, the adhered material should be produced by either rapid oxidation or rapid cooling.



〈Figure Appendix V-7-3〉 XRD results of the adhered material before and after heat treatment

## 8. Analysis Result

White powders adhered on the hull and the parts of the torpedo were confirmed to be explosion products formed by the detonation of an underwater explosive formulation with aluminum. They were not corrosion products of aluminum.

The following provides findings that can rule out the possibility of the adsorbed materials as corrosion products of aluminum from ROKS Cheonan or the torpedo motor. The adhered materials were:

- Adhered in large amounts to non-aluminum surface as well.
- Adhered not firmly, and could be detached easily.
- Were not combined closely, and easily disintegrated.
- Mainly composed of amorphous aluminum oxides.
- In amorphous form, and white corrosion product of aluminum is normally crystalline.

In addition, reasons supporting the adhered material as explosion formulation are listed as follows:

- The major component of adhered material was amorphous aluminum oxide, and appeared not to be originating from ROKS Cheonan herself.
- No scientific reasons for the formation of amorphous aluminum oxide underwater were found.
- Graphite was detected as well.
- Amorphous aluminum oxide is produced when aluminized explosives explode.<sup>19)</sup>
- Amorphous carbon, graphite, and diamond are produced upon explosion of most explosives.

.....  
19) R. R. McGuire. et. al., 'Detonation Chemistry: An Investigation of Fluorine as An Oxidizing Moiety in Explosives', Lawrence Livermore Laboratory, AD A119092, N00014-77-F-0053, July 7, 1982.

## Appendix VI. Stability Analysis Result

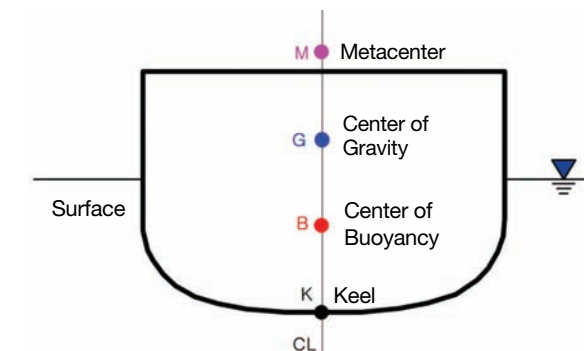
### 1. Objective

Analysis on stability was conducted in order to assess the warship design qualification of ROKS Cheonan equivalent class of corvette in perspective of a stability standard, and to technically clarify the details in sinking of the stern and bow after the separation.

Standard assessment of the stability design was conducted under several conditions: a normal operation before damage, and damage conditions with 2~4 adjacent compartments being flooded. The damage addressed here only implies flooding on the damaged regions while maintaining the longitudinal strength of the hull without separation. This assumption to assess the stability also applies to an ordinary merchant vessel as well as the warships.

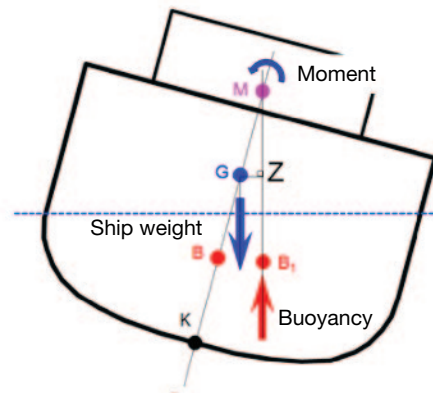
However, ROKS Cheonan was split and separated centering around the gas turbine room, and the stern sank rapidly while the bow sank after being capsized 90 degrees to the starboard side. In order to technically examine the conditions that can cause the sinking, the stability analysis on each of the bow and stern after the separation was also conducted.

### 2. Overview on Ship Stability



〈Figure Appendix VI-2-1〉 Stability factors

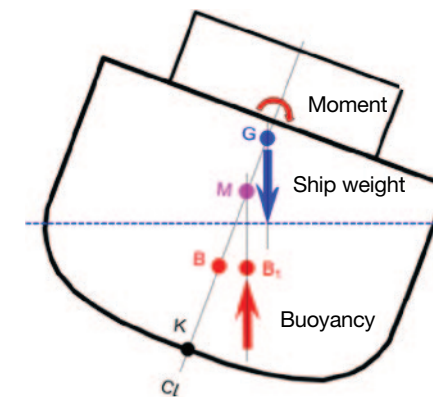
Major factors that influence the stability analysis include the center of gravity(G), center of buoyancy(B), and metacenter(M) as displayed in <Figure Appendix VI-2-1>. When both points G and B lie on a vertical line, the ship is balanced, hence in equilibrium. Ships are usually symmetrical in weight and geometrical shape, and thus points G and B lie on a vertical line that passes through the keel.



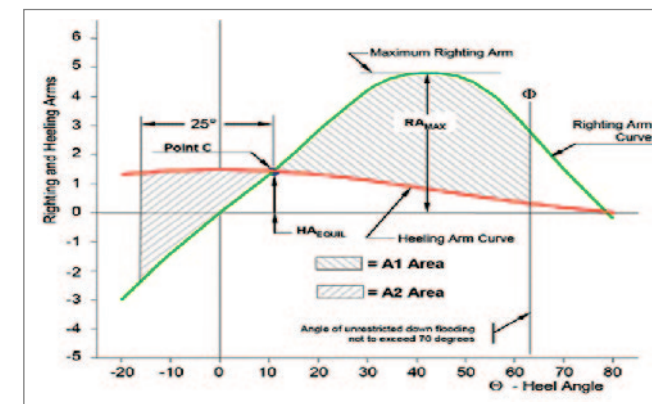
<Figure Appendix VI-2-2> Positive(+) stability

As shown in <Figure Appendix VI-2-2>, when a ship inclines to a transverse angle, the center of buoyancy moves to B1, the vertical line before the tilt(line through K-B-G) and the vertical line through B1 after the inclination cross each other at the point defined as the metacenter(point M on the Figures Appendix VI-2-1 and VI-2-2). If point M is located above point G as shown in <Figure Appendix VI-2-2>, the moments produced by gravity and buoyancy in an inclined state would move in the opposite direction from the inclining direction, and thus the ship would be stabilized. This is defined as having a positive stability( $GM > 0$ ). On the other hand, as displayed in <Figure Appendix VI-2-3> if M is located below G in a tilted state, the moment generated by gravity and buoyancy will move in the inclining direction, causing the ship to capsize. In this condition, the ship is “unstable” and this state is defined as a negative stability( $GM < 0$ ). Therefore, the position and distance of points G and M along a vertical line become a critical factor in determining static stability of a ship. The magnitude of the moment to stabilize a ship is described as the length of the line, GZ, shown in <Figure Appendix VI-2-2>. This is defined as the righting arm, and it is possible to draw a curved shape depending on the inclination angle of a ship. Meanwhile, a ship could be heeled due to the effects of wind and wave. After estimating

the heeling moment(The heeling arm is defined as the heeling moment divided by the displacement of the ship) by the wind pressure and wave along with the list angle, and overlapping with the righting curve addressed earlier, the curve shown in <Figure Appendix VI-2-4> can be obtained. The area A1 represents the stabilizing energy and A2 represents the capsizing energy; when  $A1/A2$  is larger than 1, the ship is assessed to have a dynamic stability.



<Figure Appendix VI-2-3> Negative(-) stability

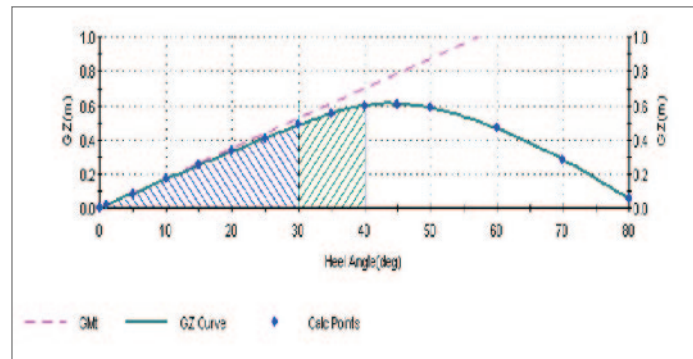


<Figure Appendix VI-2-4> The righting arm curve overlapped with the heeling arm curve, displaying a dynamic stability of a vessel

### 3. Stability Before the Damage

#### 1) Static Stability

The stability arm curve representing the static stability of ROKS Cheonan is computed as shown in <Figure Appendix VI-3-1>.



<Figure Appendix VI-3-1> The righting arm curve of ROKS Cheonan prior to the damage

Category	US Navy	UK Navy	Merchant vessel	ROKS Cheonan	
Area of shaded region under righting arm curve	0° ~ 30°	None	≥ 0.080 m · rad	≥ 0.055 m · rad	0.18
	0° ~ 40°	None	≥ 0.133 m · rad	≥ 0.090 m · rad	0.30
	30° ~ 40°	None	≥ 0.048 m · rad	≥ 0.030 m · rad	0.12
Max righting arm curve angle	None	Above 30°	Above 25°	45°	
GM(horizontal metacenter height)	None	0.3m	0.15m	Appx. 1.0m	

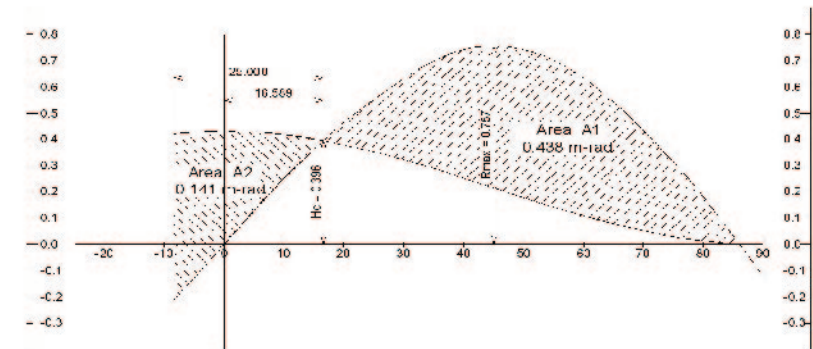
<Table Appendix VI-3-1> Static stability analysis result of ROKS Cheonan before the damage

A comparison between the static stability of ROKS Cheonan with the standards of UK Navy and merchant vessel is summarized in <Table Appendix VI-3-1>(Note: static stability standard is not established in the US Navy Standard). Through this result, it can be assessed that the static stability level of ROKS Cheonan before the damage was well above than that of a merchant vessel and twice as stable compared to the UK Navy stan-

dard. Prior to the damage, the hull stability was maximized at the heeling angle of 45°, and could endure the heeling angle of up to 80°.

#### 2) Dynamic Stability

The righting arm curve overlapped with the heeling arm curve displaying the dynamic stability of ROKS Cheonan is depicted in <Figure Appendix VI-3-2>.



<Figure Appendix VI-3-2> The righting arm curve and the heeling arm curve

Category	US Navy design standard	UK Navy design standard	Merchant vessel design standard	Result on ROKS Cheonan
Wind speed(Knots)	90 knots	90 knots	50 knots	90 knots
Capsizing force vs. stability ratio(A1/A2)	Above 1.4	Above 1.4	Above 1.0	3.1

<Table Appendix VI-3-2> Dynamic stability analysis result prior to the damage

<Table Appendix VI-3-2> summarizes the dynamic stability of ROKS Cheonan before the damage in comparison with US, UK Navy and merchant vessels. The result indicates that the stability level of ROKS Cheonan prior to the damage was well above the standards for a merchant vessel and was competitive enough in comparison to the US and UK Navy standards.

## 4. Stability Analysis of ROKS Cheonan after the Damage

### 1) Damage Stability Standard

〈Table Appendix VI-4-1〉 displays the damage stability standard applied to ROKS Cheonan in comparison with merchant vessels. ROKS Cheonan is designed to survive against up to 30 knots of beam wind with two compartments being flooded. In the analysis, the result with two flooded compartments amply suffices the stability standard, but in order to measure the maximum stability, a further analysis of stability with three and four inundated compartments was conducted.

Category	Type	Dynamic stability standard	Damaged compartments(standard)
Passenger	-	Wind speed 25 knots	2 Compartments
Chemical liquid transportation	-	-	2 Compartments
Gas transportation	LNG	-	2 Compartments
	LPG	-	1 Compartment
Oil tanker	Length 150m & above	-	2 Compartments
	Length shorter than 150m	-	1 Compartment
Corvette class standard	-	Wind speed 30 knots	2 Compartments

〈Table Appendix VI-4-1〉 Damage stability standards in different types of ships

A number of damage conditions were considered to assess the damage stability of ROKS Cheonan under flooding. For the cases with damages in two compartments, the most hazardous conditions were considered in terms of stability: Case 1 assumes flooding of the gas turbine and diesel engine rooms, and Case 2 supposes simultaneous flooding of the diesel engine room with 1 adjacent aft compartment. For the cases of three compartments flooded, Case 3 presumes simultaneous flooding of the diesel engine room and 2 adjacent aft compartments, and Case 4 assumes inundation in the gas turbine, diesel engine and 1 adjacent aft compartment. For the cases of extreme condition with 4 compartments flooded, Case 5 supposes that four aft compartments including the diesel engine room were

flooded, while the steering gear room remains intact, and Case 6 included the steering gear room as one of the four flooded compartments.

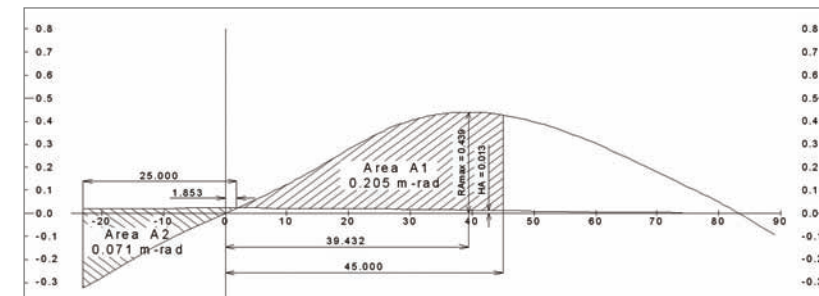
### 2) Damage Stability Assessment with 2 Compartments Flooded

#### (1) Case 1: 2 Compartments Damaged(Diesel Engine Room and Gas Turbine Room Flooded)

As shown in 〈Figure Appendix VI-4-1〉, it is possible to stay afloat with the diesel engine room and gas turbine room flooded. The stability curve for this case is shown in 〈Figure Appendix VI-4-2〉, and the results are summarized in 〈Table Appendix VI-4-2〉. The standards such as initial inclining angle, capsizing force vs. stability ratio(A1/A2), stability(A1), maximum residual righting arm(RA<sub>max</sub>-HA), and the margin line are all satisfied after the damage. Hence, the stability level with the diesel engine and gas turbine room inundated suffices the standards.



〈Figure Appendix VI-4-1〉 Buoyancy level with 2 compartments flooded(Case 1)



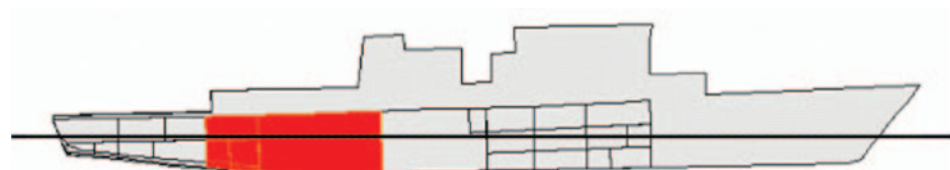
〈Figure Appendix VI-4-2〉 Dynamic stability curve with the damage

Category	Design standard	ROKS Cheonan	Result
Initial inclining angle after the damage	Below 15°	0°	Sufficient
Capsizing force vs. stability ratio(A1/A2)	Below 1.4	2.887	Sufficient
Stability(A1)	Above 0.024 m · rad	0.205 m · rad	Sufficient
Max residual righting arm(RAmax-HA)	Above 0.075m	0.192m	Sufficient
Margin line <sup>20)</sup>	Located above waterline	1.545m	Sufficient

〈Table Appendix VI-4-2〉 Stability analysis results of Case 1

### (2) Case 2: 2 Compartments Damaged(Diesel Engine Room & 1 Aft Compartment Flooded)

The buoyancy level estimation result with the diesel engine room and one adjacent aft compartment flooded is depicted in 〈Figure Appendix VI-4-3〉, and it indicates that buoyancy is achieved. The stability estimation results are summarized in 〈Table Appendix VI-4-3〉. The standards such as initial inclining angle after the damage, capsizing force vs. stability ratio(A1/A2), stability(A1), maximum residual righting arm(RAmax-HA), and the margin line are all met. Therefore, the stability level of flooding in the diesel engine room and one adjacent aft compartment satisfies the design standards.



〈Figure Appendix VI-4-3〉 Buoyancy level with 2 compartments flooded(Case 2)

Category	Design standard	ROKS Cheonan	Result
Initial inclining angle after damage	Below 15°	0°	Sufficient

20) Margin line: 76mm line below the main deck side, and must be above waterline.

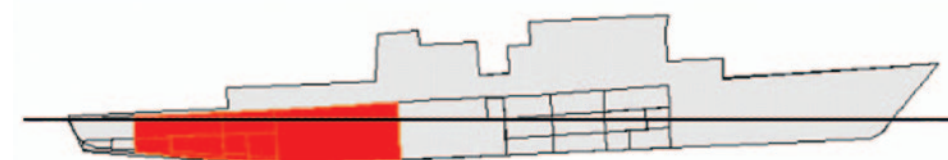
Capsizing force vs. stability ratio(A1/A2)	Above 1.4	2.913	Sufficient
Stability(A1)	Above 0.024 m · rad	0.201 m · rad	Sufficient
Max residual righting arm(RAmax-HA)	Above 0.075m	0.424m	Sufficient
Margin line	Located above waterline	1.689m	Sufficient

〈Table Appendix VI-4-3〉 Stability analysis results of Case 2

### 3) Damage Stability Assessment with 3 Compartments Flooded

#### (1) Case 3: 3 Compartments Damaged(Diesel Engine Room & 2 Aft Compartments)

As the design standard for ROKS Cheonan upon inundation of two compartments was sufficiently fulfilled, analysis on stability and buoyancy level was conducted for conditions where three compartments flooded including the diesel engine room and 2 adjacent aft compartments. The result on buoyancy level is displayed on 〈Figure Appendix VI-4-4〉, and buoyancy would be maintained with the main deck hatch closed. The stability computation results are as shown in 〈Table Appendix VI-4-4〉. The initial inclining angle after the damage, capsizing force vs. stability ratio(A1/A2), stability(A1), and the maximum residual righting arm(RAmax-HA) are sufficiently contented. The margin line standard was assessed to be unfulfilled, but this only indicates that the aft end of the stern shown in 〈Figure Appendix VI-4-4〉, may submerge a little and gradual flooding would occur if the main deck hatch remained open, but if it was closed, buoyancy would be maintained without additional flooding. Therefore, it can be concluded that while a partial submerging of the stern could occur, the stability is still retained, hence, it is possible for the buoyancy level to be stably maintained for an extended period of time.



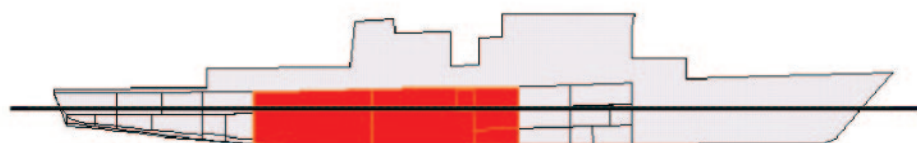
〈Figure Appendix VI-4-4〉 Buoyancy level with three compartments flooded(Case 3)

Category	Design standard	ROKS Cheonan	Result
Initial inclining angle after damage	Below 15°	0°	Sufficient
Capsizing force vs. stability ratio(A1/A2)	Above 1.4	3.040	Sufficient
Stability(A1)	Above 0.024 m · rad	0.076 m · rad	Sufficient
Max residual righting arm(RA <sub>max</sub> -HA)	Above 0.075m	0.163m	Sufficient
Margin line	Located above waterline	-0.627m	Insufficient

〈Table Appendix VI-4-4〉 Stability analysis results of Case 3

## (2) Case 4: 3 Compartments Damaged(Diesel Engine Room, Gas Turbine Room, 1 Compartment in front of the Gas Turbine Room)

As one of the cases beyond the design standard(two compartments flooded), analyses of stability and buoyancy level were conducted with an assumption of three compartments flooded including the machinery room, gas turbine room and one compartment in front of the gas turbine room. The result of buoyancy level calculation is depicted in 〈Figure Appendix VI-4-5〉, and it shows buoyancy could be maintained. The calculated stability results are summarized in 〈Table Appendix VI-4-5〉. The initial inclining angle after the damage, capsizing force vs. stability ratio(A1/A2), stability(A1), max residual righting arm(RA<sub>max</sub>-HA), and the margin line standards are sufficiently satisfied. Consequently, with three compartments(diesel engine room, gas turbine room, and one compartment in front of the gas turbine room) flooded, the stability level remains stable.



〈Figure Appendix VI-4-5〉 Buoyancy level with 3 compartments flooded(Case 4)

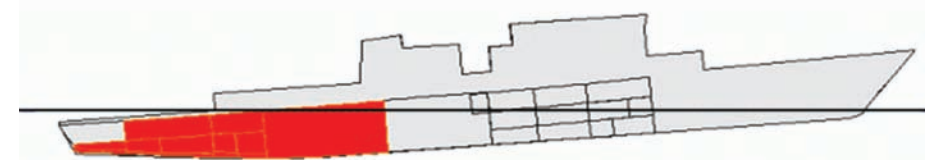
Category	Design standard	ROKS Cheonan	Result
Initial inclining angle after damage	Below 15°	0°	Sufficient
Capsize vs. stability ratio(A1/A2)	Above 1.4	2.724	Sufficient
Stability(A1)	Above 0.024m · rad	0.158m · rad	Sufficient
Max residual righting arm(RA <sub>max</sub> -HA)	Above 0.075m	0.318m	Sufficient
Margin line	Located above waterline	1.048m	Sufficient

〈Table Appendix VI-4-5〉 Stability analysis results of Case 4

## 4) Damage Stability Assessment with 4 Compartments Flooded

### (1) Case 5: 4 Compartments Damaged(4 Aft Compartments including the Diesel Engine Room Flooded, except the Steering Gear Room)

As one of the cases which are way beyond the design standard(2 compartments flooded), analyses of stability and buoyancy level were conducted supposing four compartments flooded(without steering gear room), including the diesel engine room. The calculation result on the buoyancy level is shown to 〈Figure Appendix VI-4-6〉. It indicates that the buoyancy is achieved if the main deck hatch was closed. The stability computation results are summarized in 〈Table Appendix VI-4-6〉. The initial inclining angle after the damage, capsizing force vs. stability ratio(A1/A2), stability(A1), maximum residual righting arm(RA<sub>max</sub>-HA) are sufficient to qualify the standards, therefore, stability would be maintained. The margin line standard is assessed to be insufficient, but this indicates that while the aft end of the stern shown in 〈Figure Appendix VI-4-6〉 may submerge due to gradual flooding if the main deck hatch remained open, but buoyancy could be achieved if it was closed. To summarize, a partial submerging of the stern could occur, but stability is still retained, hence, buoyancy level will be maintained for a long duration of time.



〈Figure Appendix VI-4-6〉 Buoyancy level with four compartments flooded(Case 5)

Category	Design standard	ROKS Cheonan	Result
Initial inclining angle after damage	Below 15°	0°	Sufficient
Capsize vs. stability ratio(A1/A2)	Above 1.4	2.871	Sufficient
Stability(A1)	Above 0.024 m · rad	0.089 m · rad	Sufficient
Max residual righting arm(RAmax-HA)	Above 0.075m	0.187m	Sufficient
Margin line	Located above waterline	-0.758m	Insufficient

〈Table Appendix VI-4-6〉 Stability analysis results of Case 5

## (2) Case 6: 4 Compartments Damaged(4 Aft Compartments including the Diesel Engine and Steering Gear Room Flooded)

As one of the cases well beyond the design standard(two compartments flooded), analyses on stability and buoyancy level were conducted with four compartments flooded including the diesel engine room and steering gear room. The stability computation results are summarized in 〈Table Appendix VI-4-7〉. Despite the fact that the initial inclining angle level was satisfied, capsizing force vs. stability ratio(A1/A2), stability(A1), maximum



〈Figure Appendix VI-4-7〉 Buoyancy level with four compartments flooded(Case 6)

Category	Design standard	ROKS Cheonan	Result
Initial inclining angle after damage	Below 15°	0°	Sufficient
Capsize vs. stability ratio(A1/A2)	Above 1.4	2.871	Sufficient
Stability(A1)	Above 0.024 m · rad	0.089 m · rad	Sufficient
Max residual righting arm(RAmax-HA)	Above 0.075m	0.187m	Sufficient
Margin line	Located above waterline	-0.758m	Insufficient

〈Table Appendix VI-4-7〉 Stability analysis results of Case 6

residual righting arm(RAmax-HA), and the margin line levels were all turned out to be insufficient. Hence, the hull would lose its buoyancy level and completely sink with the time passing.

## 5. Stability of the Bow and Stern after Separation

An ordinary stability design for a vessel analyzes the stability prior and posterior to the damage, while the damage dealt here only implies flooding, not a separation. However, ROKS Cheonan was split and separated centering around the gas turbine room, after which the stern sunk shortly, and lastly the bow sunk after being capsized in 90 degrees to the starboard side. In order to technically specify the circumstances regarding the sinking, stabilities after the separation of the bow and stern was also analyzed.

### 1) Stability of the Bow and Stern Immediately After Separation

The stability characteristics of the bow and stern after the separation of the ship are listed in 〈Table Appendix VI-5-1〉. G' in the table indicates the new center of gravity to which the original center G has migrated according to the volume change of loaded fluids(e.g.: fuel). Therefore, the stability assessment index  $G'M = KM - KG - GG'$ .

In 〈Table Appendix VI-5-1〉, the G'M of the bow section is calculated to be a negative value of -0.02m. Thus, any minuscule external force such as wind or wave to the sep-

Category	Bow section	Stern section
Displacement	664 tons	559 tons
KG	4.347m	3.515m
KM	4.425m	5.903m
KB	2.420m	2.346m
GG'	0.098m	0.036m
G'M	-0.020m	2.35m

〈Table Appendix VI-5-1〉 Initial stabilities of the bow and stern after the separation

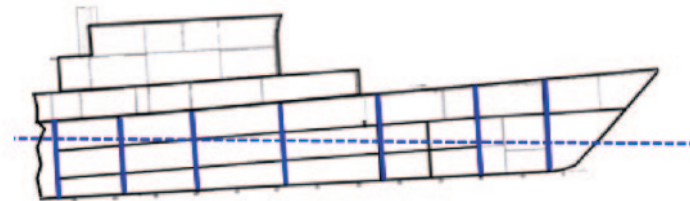
arated bow could cause the ship to lose its stability and thus capsize. The capsizing direction would correspond to the direction of the external force. In conclusion, the bow section loses its stability after the separation, due to the elevated center of gravity.

The G'M of the stern section is calculated to be 2.35m. Hence, the stern section is estimated not to have capsized immediately after the separation.

## 2) Buoyancy Assessments of the Bow and Stern after Separation

### (1) Buoyancy Assessment of the Bow

Right after the separation, the buoyancy level of the bow section before the capsizing is analyzed and displayed in <Figure Appendix VI-5-1>. Since there was no stability on the bow section with the GM value of -0.02m, it is assessed that the ship would have capsized to the starboard direction as the explosion force was exerted from the portside bottom. It is analyzed that the separated bow, having seven compartments, would have experienced gradual flooding. Therefore, it would have been able to maintain buoyancy for some period of time while being capsized; however, due to continued influx of seawater through the entrance and the ventilator, the ship sank eventually.

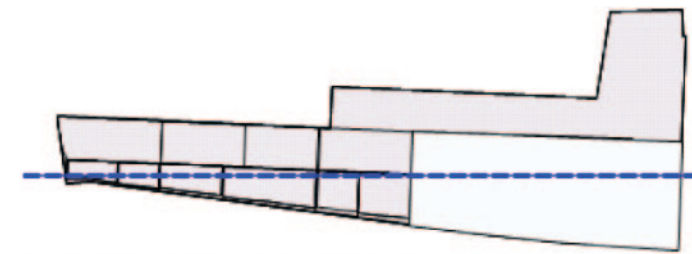


<Figure Appendix VI-5-1> Estimation of the bow buoyancy level immediately after the separation

### (2) Buoyancy Assessment of the Stern

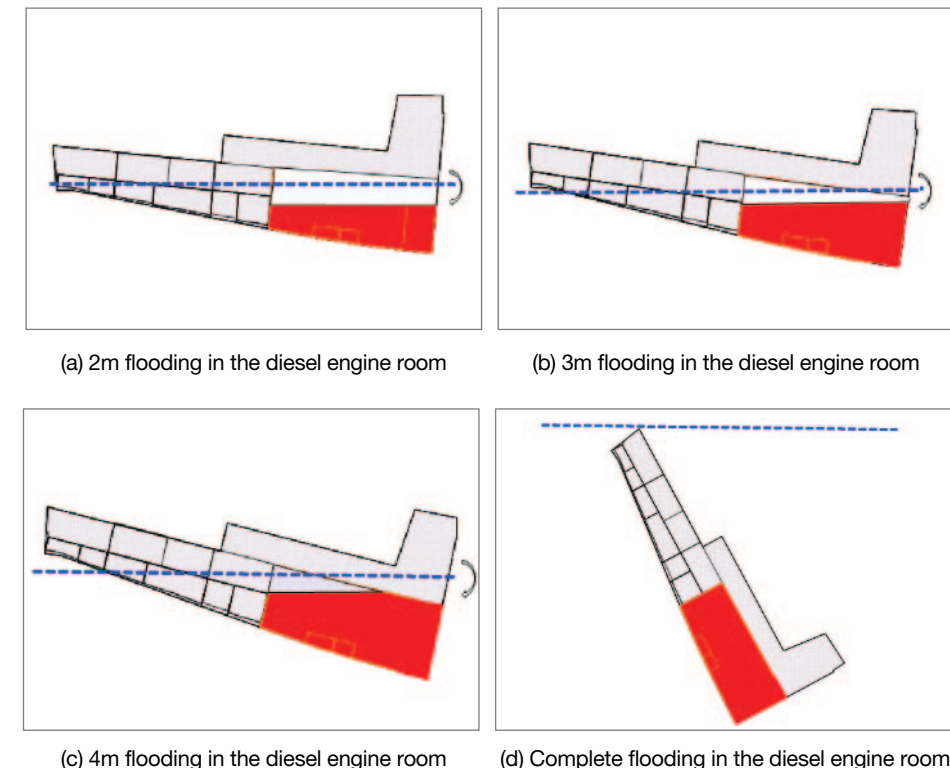
The buoyancy level of the stern section immediately after the separation is estimated and displayed in <Figure Appendix VI-5-2>. With GM value of 2.35m, it is estimated that its stability was retained with no capsizing.

The separated stern section consisted of four watertight compartments, and especially it contained the diesel engine room occupying 40% of the stern volume; thus, flooding of the diesel engine room would have had a significant impact on the buoyancy



<Figure Appendix VI-5-2> Estimation of the stern buoyancy level immediately after the separation

level of the stern. First, the posture and buoyancy level of the ship were analyzed in accordance with different flooding conditions in the diesel engine room to substantiate the sinking process of the stern. If compartments other than the damaged diesel engine room were completely sealed, buoyancy retention would have been possible until the damaged diesel engine room was flooded up to 4m, and in case of complete flooding in the diesel engine room, the ship would have sunk. The buoyancy level estimations on each of the conditions are depicted in <Figure Appendix VI-5-3>.



<Figure Appendix VI-5-3> Buoyancy level estimations with each flooding condition in the diesel engine room

The details of the time and posture regarding the sinking of the stern have also been analyzed. The actual damage status of the stern was taken into consideration during the analysis. The initial inflow of seawater to the diesel engine room is depicted in (Figure Appendix VI-5-4). It commenced from the watertight bulkhead between the diesel engine room and gas turbine room through the crater created by the splitting of the shaft connecting the gas turbine and reduction gear, as well as from the hatch on the upper portion of the diesel engine room used for installing diesel engine on the main deck and generator on the stack. The second inflow occurred from the opened watertight doors along the main passageway; the doors were open since ROKS Cheonan was under normal operating condition. Eventually, the overflow of seawater propagated from the diesel engine room to the

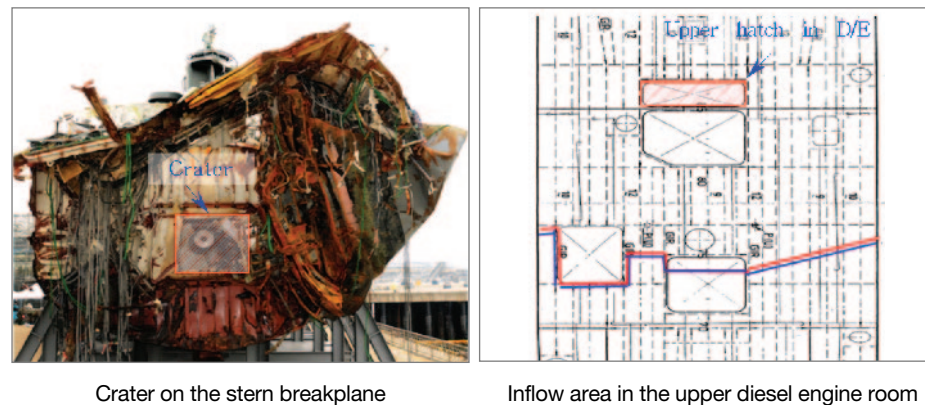


(Figure Appendix VI-5-4) Crater on the stern breakplane & the main deck hatch

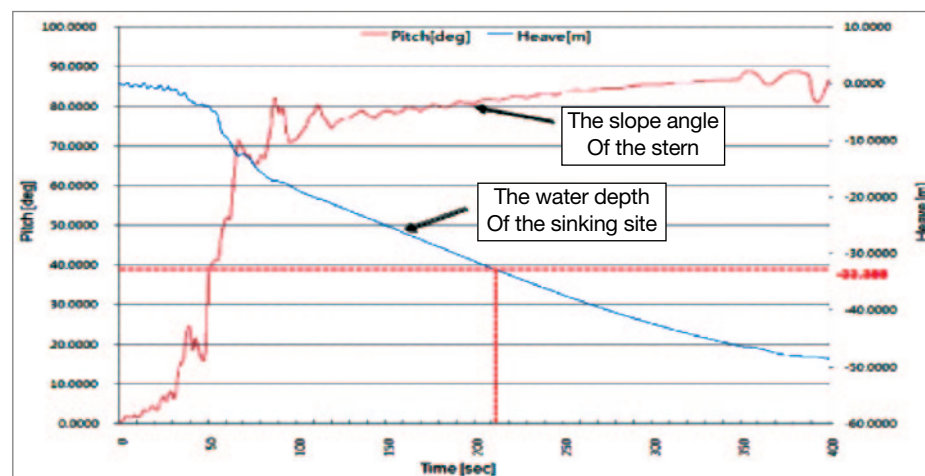


(Figure Appendix VI-5-5) Sinking time estimation of the stern

aft compartments.

A time elapse analysis of the stern sinking is shown in (Figure Appendix VI-5-5). Since 90 seconds after the separation of the hull, as the diesel engine room became flooded, the ship inclined in 80 degree angle, and from 210 seconds, more than the length of the stern section, 33.4m, had submerged. Although differences may exist in flooding volume due to the equipped structures in the machinery room, a complete sinking would have occurred at least after 200 to 250 seconds.

### 3) Sub-conclusion

The stability design standard of ROKS Cheonan prior to the damage was much stricter than that of a merchant vessel at the time of its construction, and was assessed to possess basic stability twice as strong compared to the merchant vessel standard. As for protection from damages, it was designed to endure two, three, and even four compartments flooded as long as the steering gear room remains intact.

In regard of the separation centering around the gas turbine room as a center, it is analyzed that the buoyancy level of the stern would have been maintained as long as the bulkhead between the gas turbine room and diesel engine room is not damaged and kept watertight; however, in the actual incident, rapid inflow occurred through the crater on the watertight bulkhead between the diesel engine room and gas turbine room as well as around the stack on the main deck and the upper diesel engine room, leading the ship to sink completely 200 - 250 seconds after the separation.

The separated bow would have lost its stability immediately due to the negative stability ( $GM < 0$ ). After the split, any minuscule external force such as wind or wave would have been sufficient to capsize the bow. It would have been capsized toward the starboard direction as a result of the external force exerted on the portside. However, considering the bow was divided into seven compartments it would have been able to maintain buoyancy for a significant duration of time after the separation, followed by capsize, and sinking because of the continuous inflow of seawater through the entrance and ventilator.

## Appendix VII. Basic Hull Strength Analysis Result

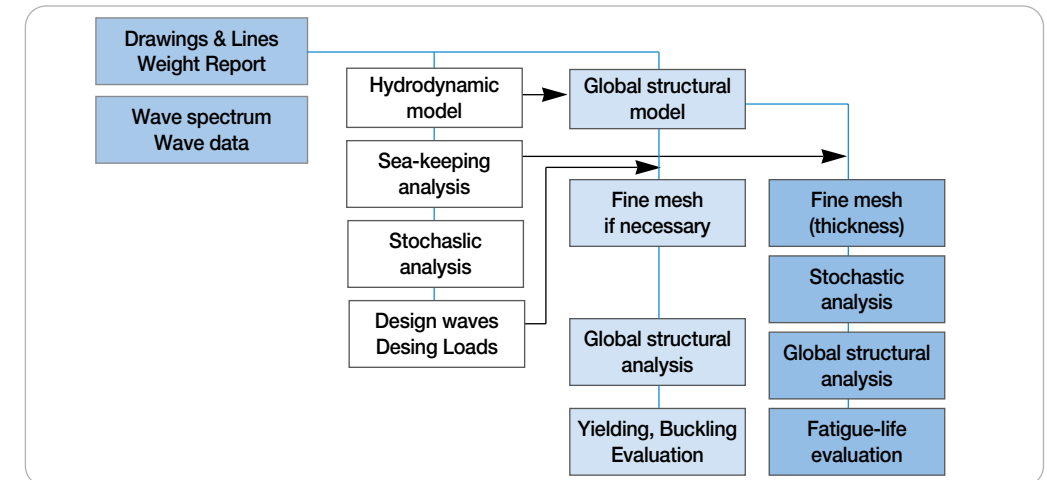
### 1. Objective

At the time of its design, ROKS Cheonan was designed based on the structural design standard of US Navy, Structural Design Manual for Naval Surface Ship(1974). However, the structural safety of ROK Navy vessels nowadays are being validated in accordance with the direct strength analysis which is based upon the shipbuilding design technology of ROK. By carrying out the direct strength analysis on the structure of a ROKS Cheonan class warship, which was designed in accordance with US Navy standard of 1974, the structural stability of ROKS Cheonan was assessed on the basis of contemporary standard. The verification of basic structural safety is a fundamental procedure which comes before the damage analysis, and is conducted in order to evaluate the basic strength which is required to execute a destruction factor analysis.

### 2. Flow Chart of Direct Strength Analysis

The direct strength analysis calculates the motion and load of a ship against waves, estimates with the most probable extreme load which a ship could undergo within its lifetime of 25 to 30 years by a stochastic and statistical method, and then determines the design wave for generating the extreme load. It then conducts a structural analysis by loading a 3D structure model for the whole ship, and evaluates the structural safety(See <Figure Appendix VII-2-1>).

As demonstrated in <Figure Appendix VII-2-1>, the most recent direct strength analysis procedure includes fatigue life evaluation. However, since the direct strength analysis of ROKS Cheonan was conducted not for a designing purpose, but for analysis of damage factors, and because fatigue failure already turned out not to be the cause of the sinking, the fatigue life evaluation was excluded from the analysis.

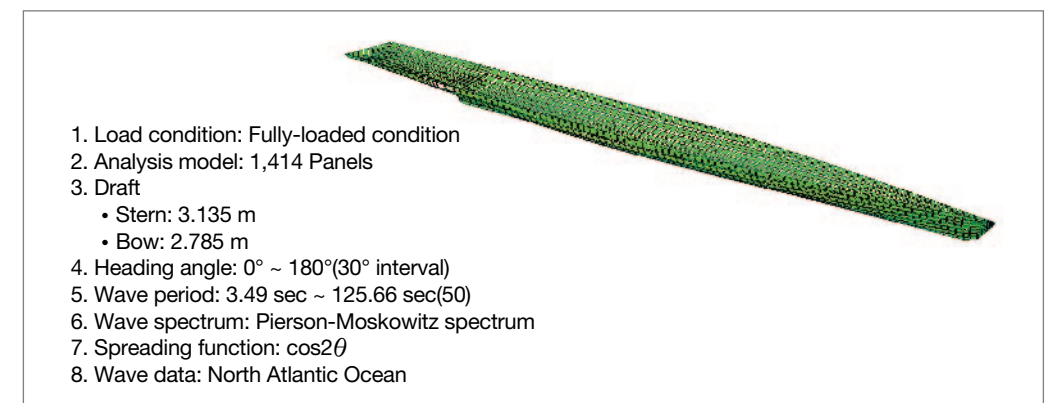


<Figure Appendix VII-2-1> Direct strength analysis flow chart

### 3. Hydrodynamic Analysis

#### 1) Hydrodynamic Analysis Modeling

The analysis model for the wave load estimation of ROKS Cheonan includes a detailed modeling of the hull section below the waterplane to effectively delineate the shape of the ship and pressure distribution. <Figure Appendix VII-3-1> illustrates the 3D model and the load condition used for the wave load estimation. Additionally, the loads were distributed along the hull under an assumption of a fully-loaded condition.



<Figure Appendix VII-3-1> 3D hydrodynamic analysis model and load condition

## 2) Design Wave Selection

The design waves for basic strength analysis were selected as shown in <Table Appendix VII-3-1>, and these design waves assume the most intensive loading that the ship may experience with a probability of  $10^{-8}$ , while operating on the most severely conditioned sea, Northern Atlantic Ocean, during 25~30 years of its navigation.

- Design wave maximizing wave vertical bending moment affecting the center of the ship.
- Design wave maximizing wave horizontal bending moment affecting the center of the ship.
- Design wave maximizing torsion moment affecting the center of the ship.
- Design wave maximizing vertical acceleration at the bow.
- Design wave maximizing pressure on the center waterplane of the ship.

Design load	Heading angle	Wave length	Design value	Design wave height
Vertical bending moment	180°	65.37m	83,824kN·m	10.60m
Horizontal bending moment	120°	43.81m	18,722kN·m	4.53m
Torsion moment	60°	65.37m	13,757kN	8.55m
Vertical acceleration	120°	48.75m	14.71m/sec <sup>2</sup>	6.92m
Pressure	90°	34.24m	75.92kPa	6.67m

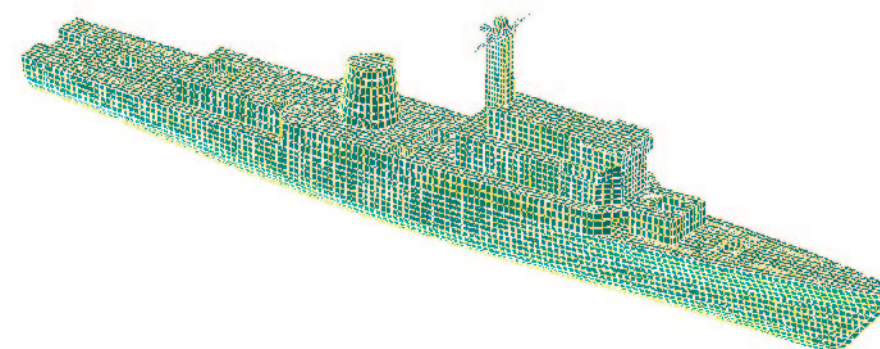
<Table Appendix VII-3-1> Design wave estimation results of ROKS Cheonan to conduct the direct strength analysis

## 4. Structural Analysis

### 1) Structural Analysis and Allowable Stress Standard

The range of finite element model for structural analysis included every structure on the ship such as the superstructures, the stack, and the mast set up along the full width and length of the ship. The evaluation of the main hull structure, which was composed of mild steel, was based on the allowable stress standard employed in the ROK Navy design/con-

struction standard. The structural analysis result on the superstructures, which are composed of aluminium, was based on the allowable stress standard from Korean Register of Shipping in its rules for a high speed craft.



<Figure Appendix VII-4-1> 3D structural analysis model

Mild Steel	Yield Stress(σ <sub>Y</sub> )	Allowable stress(σ <sub>e</sub> )	AL 5083, H116	Yield Stress(σ <sub>Y</sub> )	Allowable stress(σ <sub>e</sub> )
Longi. Member	235 MPa	200 MPa	Longi. Member	215 MPa	127 MPa
Trans. Member	235 MPa	177 MPa	Trans. Member	215 MPa	

<Table Appendix VII-4-1> Allowable stress of main hull structure

<Table Appendix VII-4-2> Allowable strength of superstructure

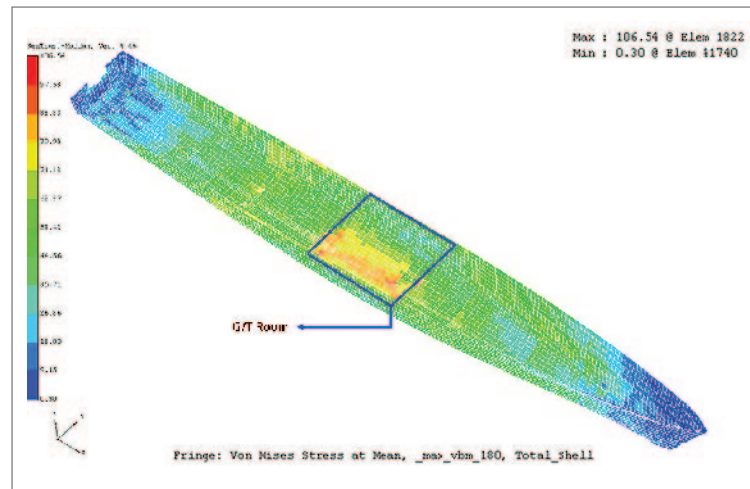
### 2) Structural Analysis Result and Evaluation

The direct strength analysis was carried out for each design wave(ones that maximize the vertical bending moment, horizontal bending moment, torsion moment, and the vertical acceleration respectively) which generates maximum loadings, using the maximum values of allowable stress for each structural member. The result of the direct strength analysis for every design wave showed that the vertical bending moment was the dominating load factor for ROKS Cheonan. Consequently, only the results of vertical bending moments are provided below.

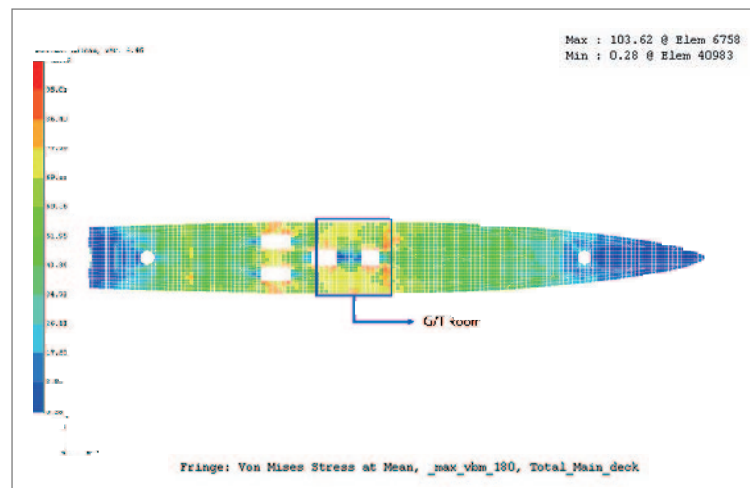
#### (1) Yield Strength Assessment

The analysis results for the main structures, including the shell and main deck, are pro-

vided in <Figure Appendix VII-4-2> and <Figure Appendix VII-4-3>. <Table Appendix VII-4-3> compares the maximum generated stress on the major longitudinal members such as main deck, shell plate as well as the bulkheads, web frames, and the superstructures with the allowable stress. As described in <Table Appendix VII-4-3>, the stress generated on every structural member is below their allowable stress levels. Especially, the stress on the major structural members is, at maximum, around 50% of the standard values, well sufficing the yield strength assessment standard.



<Figure Appendix VII-4-2> Structural analysis result of the shell plates



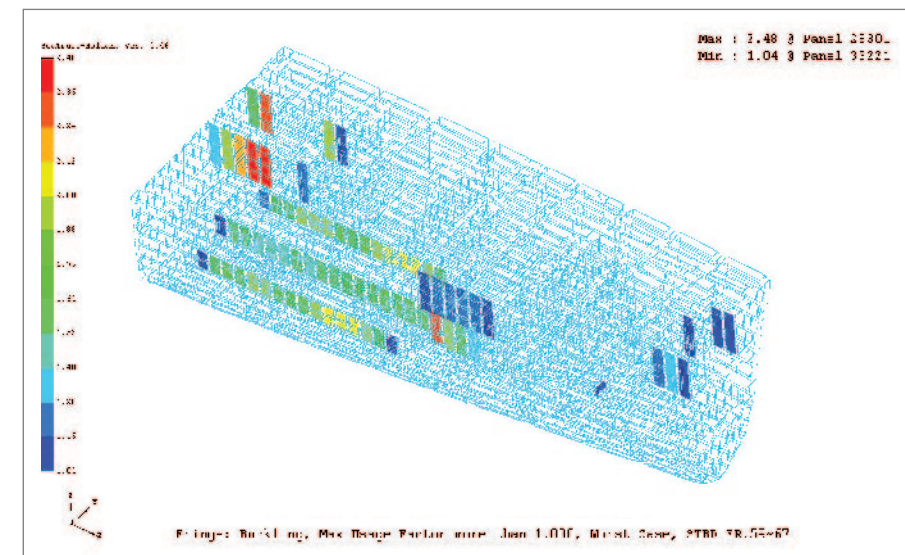
<Figure Appendix VII-4-3> Structural analysis of the main deck

Members	Material	Allowable stress(MPa)	Possible maximum stress(MPa)	Remarks
O-2 Deck	AL <sup>21)</sup>	127	20.0	16% Sufficient
O-1 Deck	AL	127	77.6	61% Sufficient
Main deck	MS <sup>22)</sup>	200	103.62	52% Sufficient
1st Platform deck	MS	200	42.14	21% Sufficient
2nd Platform deck	MS	200	44.84	22% Sufficient
Shell	MS	200	106.54	53% Sufficient
FR. 39 BHD	MS	177	52.8	30% Sufficient
FR. 77 Web frame	MS	177	152	86% Sufficient

<Table Appendix VII-4-3> Stress evaluation of each structural member

## (2) Buckling Strength Assessment

For the buckling strength assessment of ROKS Cheonan, an analysis method based on the ship design/construction standard(steel) was applied. The representative buckling strength assessment results on the compressive stress and the breaking stress affecting plates of major structural members(derived by using stress estimates from hull structure analysis) are listed in <Figure Appendix VII-4-4>, <Figure Appendix VII-4-5> and <Figure Appendix



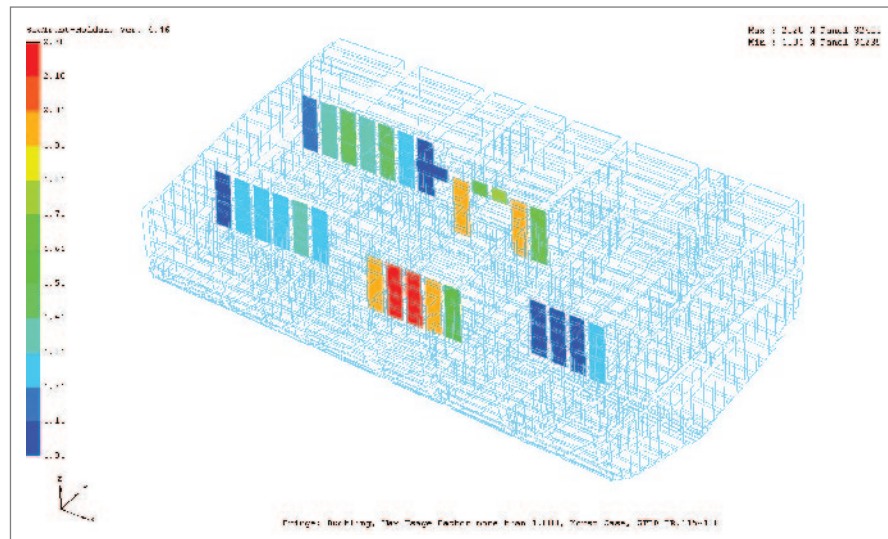
<Figure Appendix VII-4-4> Buckling strength assessment result: FR. 27 ~ FR. 67

21) AL: Aluminum.  
22) MS: Mild Steel.

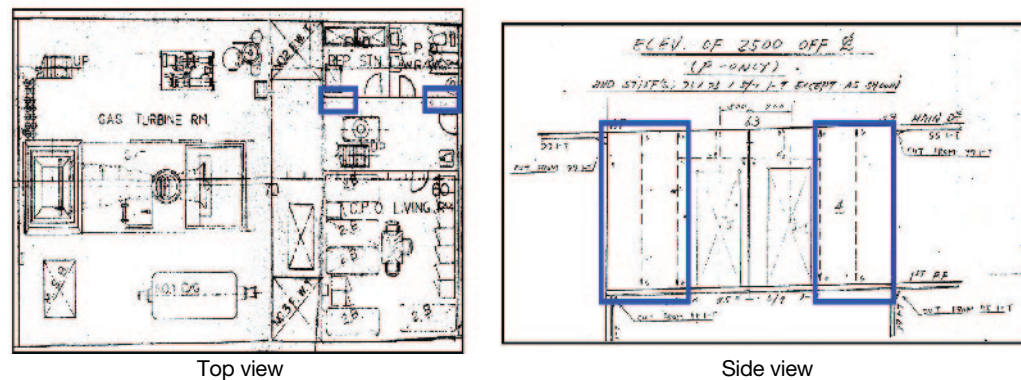
VII-4-6). Based on the result of the analysis, while there was no possibility of buckling at the central region of the hull, one at partial longitudinal bulkhead was assessed possible. However, these bulkheads are structures for sectioning each compartment, and therefore, do not affect the hull girder strength. An example of longitudinal bulkhead for sectioning compartments is provided in <Figure Appendix VII-4-6>.

## 5. Analysis Result

Based on the result of the direct strength analysis regarding the maximum design waves (wave height 10.6m), with extreme loads on the hull, and during the ship lifetime of 25-30 years, it was found that ROKS Cheonan sufficiently satisfies the yield strength standard. Although there is a possibility of buckling in some bulkheads on the stern and the bow, these partial bulkheads are sectioning members, and hence would not affect the hull girder strength as non-resistant bulkheads. Therefore, excluding the possibility of extraordinary conditions such as an external attack, it is analyzed that ROKS Cheonan possessed sufficient structural strength.



<Figure Appendix VII-4-5> Buckling strength assessment result: FR.106 ~ FR.130



<Figure Appendix VII-4-6> Location and shape of partial longitudinal bulkhead(example)

Joint Investigation Report  
**On the Attack Against ROK Ship Cheonan**

Copyright © 2010 by the Ministry of National Defense  
of the Republic of Korea

Published by Myungjin Publication Inc.

The first print date of the first edition\_ September 10, 2010

Sales Contact\_ (Tel.) 82-2-326-0026

ISBN 978-89-7677-711-9 03300

Price written on the back cover.

Damaged copies can be exchanged with new ones.